Evaluation of Microwell based Systems and Miniature Bioreactors for Rapid Cell Culture Bioprocess Development and Scale-up

Thesis submitted for the degree of
Doctor of Philosophy

by
Mohd Helmi Sani

The Advanced Centre for Biochemical Engineering
Department of Biochemical Engineering
University College London

2016

DECLARATION

I, Mohd Helmi Sani, confirm that the work presented in this thesis is my own. Where information has been derived from other sources, I confirm that this has been indicated in the thesis.

Signature

This dissertation is dedicated to my wonderful wife, Suhaida, who always motivates and inspired me during my study.

To my parents, mother-in-law, daughter and son.

Thank you.

ACKNOWLEDGEMENTS

First and foremost, praise to Allah S.W.T for His Gracious and Blessing. I would like to extend my heartiest gratitude and appreciation to my principal supervisor, Dr. Frank Baganz for his ideas, time, and assistance that enabled me to accomplish this thesis efficiently. I am also deeply indebted to Dr. Martina Micheletti, secondary supervisor for this project for her ideas and opinions at all times.

My special gratitude goes to all the lab members of Mammalian Cell Culture who always provide hands and knowledge, especially to Ana Catarina Pinto, Lourdes Velez-Suberbie, Douglas Marsh, Daria Popova, Richard Tarrant, and countless others. Besides that, I would like to thank my Colonnade's office mates, Alex Chatel, Chris Longster, Fernanda Masri, Asma Ahmad, Jennifer Man, and Kate Lawrence for the coffee break, the lunchtime chat and friendship, as well as those who are directly or indirectly involved in this research at the Department of Biochemical Engineering, University College London.

I also would like to express gratitude to the government of Malaysia for awarding me the Skim Latihan Akademik IPTA/Universiti Teknologi Malaysia (SLAI/UTM) scholarship for my Ph.D at the Department of Biochemical Engineering, University College London.

Last but not least, my thanks and love to my amazing wife, Suhaida Mustapha who always supported and encouraged me in my study, my adorable daughter and son, Nur Syauqina Damia and Muhammad Harith Imad, my parents, parents-in-laws and families in Malaysia and fellow friends in the United Kingdom who always motivated me throughout my years at University College London, U.K. Thank you for the support and contributions in order of making this thesis a successful accomplishment.

ABSTRACT

The increased use of antibodies for human therapy has driven rational approaches to accelerate bioprocess development in producing cost effective and highly productive antibodies. The potential of microwell based systems and miniature bioreactors (MBR) to mimic the scalability and operations of conventional bench reactors are seen as an alternative. This study has investigated the microtitre plate (MTP), micro-Matrix and MBR (HEL-BioXplore) as scale-down mimic for rapid and accurate reproduction of Chinese hamster ovary (CHO) cell growth and product yields in bench scale stirred tank reactors. A microtitre plate with sandwich lid CR1524a (for slow growing animal cells) was found to be suitable for CHO cell cultivation. An evaluation of feeding approaches in MTP showed that bolus addition resulted in 9.19 x 10^6 cell mL^{-1} and 38 % higher IgG titres compared to addition of FeedBeads. In order to enable scale translation, the engineering parameters for the MBR were characterised with regard to mixing time, volumetric oxygen transfer coefficient and power input. The MBR system was fitted with either direct driven impeller or magnetically driven impeller with singular hole impeller or horseshoe sparger. The combination of the direct driven impeller and horseshoe type sparger with bolus addition was selected as the best configuration and produced 8.89 x 10^6 cell mL^{-1} and 0.84 gL^{-1} IgG titres. Additionally, a prototype micro-Matrix system was characterised for its performance in a cell culture process. The micro-Matrix with controlled aeration and continuous feeding supported a cell concentration of 8.67 x 10^6 cell mL^{-1} and viability >90 % after 264 hours. Furthermore, scale translations of the studied systems were evaluated at the matched mixing time of 6 s with conventional lab scale 5L stirred tank reactors (STR). The scale-up studies demonstrated that the miniature systems were able to mimic the performance of the conventional bench reactors. Results from the scale-up studies between the MTP, MBR and STR with bolus feeding addition showed a comparable viable cell concentration of 9.30 x 10^6 cell mL^{-1}, 9.56 x 10^6 cell mL^{-1} and 10.04 x 10^6 cell mL^{-1} and IgG titres of 0.92, 0.69 and 0.83 gL^{-1} respectively. Whereas, scale translation studies between micro-Matrix and MBR with continuous feeding gave equivalent viable cell concentration with 11.1 x 10^6 cell mL^{-1} and 9.76 x 10^6 cell mL^{-1} and IgG titres of 0.50 gL^{-1} and 0.64 gL^{-1} respectively. Overall, the miniature bioreactors evaluated have the potential for cell screening and optimisation studies which could generate early data for bioprocess development.

TABLE OF CONTENTS

LIST OF FIGURES

LIST OF TABLES

LIST OF ABBREVIATIONS AND SYMBOLS

Abbreviation	Description
AGT	Advanced granulation technology
BHK	Baby hamster kidney
CD CHO	Chemical defined Chinese hamster ovary
CFD	Computational fluid dynamic
CHO	Chinese hamster ovary
cIVC	Cumulative integral viable cell
CO_2	Carbon dioxide
dCO_2	Dissolved carbon dioxide
DHFR	Dihydrofolate reductase
Dir/HS	Direct driven/horseshoe sparger
Dir/SH	Direct driven/singular hole sparger
DMSO	dimethyl sulfoxide
DNA	Deoxyribonucleic acid
DO	Dissolved oxygen
DoE	Design of experiment
DOT	Dissolved oxygen tension
DSW	Deep square well
EU	European Union
GS	Glutamine synthetase
H	Homogeneity index
HCL	Hydrochloric acid
HEK-293	Human embryonic kidney
HEL	Hazard Evaluation Laboratory
HT	High throughput
Ig	Immunoglobulin
IVCC	Integral viable cell concentrations
KOH	Potassium hydroxide
mAbs	Monoclonal antibodies
Mag/HS	Magnetic driven/horseshoe sparger
Mag/SH	Magnetic driven/singular hole
MBR	Miniature bioreactor

MSX	Methionine sulphoximine
MTP	Microtitre plates
MTX	Methotrexate
NS0	Mouse myeloma
OSR	Orbital shaken reactor
OTR	Oxygen transfer rate
OUR	Oxygen uptake rate
P.I.D	Proportional integral derivative
pCO_2	Partial pressure carbon dioxide
PER-C6	Human-retina-derived
QbD	Quality by design
q_{gluc}	Specific glucose consumption
q_p	Specific product formation
RO	Reverse osmosis
Rpm	Rotational per minutes
Rps	Rotational per seconds
SDR	Sensor dish reader
SRW	Standard round well
STR	Stirred tank reactor
TAP	The Automation Partnership
UHTS	Ultra high-throughput screening
UK	United Kingdom
US$	United States dollar
USA	United States of America
USD	Ultra scale-down
v/v	volume per unit volume
VCC	Viable cell concentrations
vvm	volume per volume per minute
µM	micro Molar

Symbol	Description	Unit
$\bar{\varepsilon}_{T_g}$	Total energy dissipation rate in gassed bioreactor	Wm^{-3}
C_A^*	Dissolved O_2 concentration saturation	mol m^{-3}
C_L	Dissolved O_2 concentration in the liquid	mol m^{-3}
N_A	Rate of mass transfer	-
N_P	Dimensionless impeller power number	-
°C	temperature in degree centigrade	-
a	the specific contact area	-
D_i	Impeller diameter	m
D_T	Tank diameter	m
g	gravitational acceleration	ms^{-2}
gL^{-1}	gram per litre	-
h^{-1}	per hour	-
k_L	mass transfer coefficient	-
k_La	volumetric oxygen transfer coefficient	h^{-1}
L	litre	-
mL	millilitre	-
$mmoL^{-1}$	milimolar per litre	-
N	Impeller rotational speed (rps)	
N_i	stirrer speed (rps)	s^{-1}
P	power	Watt
P/V	power per unit volume	Wm^{-3}
pH_f	pH during final time measurement	
pHi	pH during initial time measurement	
pHt	pH during measured time	
Re	Reynolds numbers	-
Re_i	Impeller Reynolds numbers	-
T_m	mixing time	s
µL	microlitre	-
ρ	fluid density	kgm^{-3}
τ_p	probe response time	s

Chapter 1 Introduction

1.1 Overview of therapeutic antibody production

The past twenty years have seen increasingly rapid advances of therapeutic antibody production for the pharmaceutical markets (Walsh, 2014). Biopharmaceuticals from therapeutic antibodies has seen an increase in its growth and sales over the past four years (Aggarwal, 2014). Ever since the Food and Drugs Administration (FDA) approved an early mAbs (Rituximab) in 1997, progression of monoclonal antibodies (mAbs) has advanced with 17 novel biologics approved annually over four-year in the United States and Europe markets (Walsh, 2014). Moreover, in the year 2012, monoclonal antibodies were recorded as the highest selling biopharmaceuticals with total revenue of $24.6 billion in the United States's biotechnology sector (Aggarwal, 2014). Monoclonal antibodies produced significant results on the treatment of different types of cancer and anti-inflammatory disorders such as non-Hodgkin lymphoma and rheumatoid arthritis (Shukla and Thömmes, 2010). Currently, there are six blockbuster therapeutic mAbs products that commercially available in the pharmaceutical market: Avastin, Herceptin, Remicade, Rituxan, Humira and Erbitux (Butler and Meneses-Acosta, 2012).

The majority of novel therapeutic antibodies are produced from the mammalian cell expression system and continue to be dominated by the mAbs based product (Kelley, 2007). Mammalian cells are the preferred host for complex therapeutic antibodies production because of its capacity for proper protein folding, assembly and post-translational modification such as glycosylation patterns (Chadd and Chamow, 2001; Wurm, 2004; Warnock and Al-Rubeai, 2006). In addition, Chinese hamster ovary (CHO) cell are the most widely and most favoured cell lines for derivation of mAbs because of its good growth kinetic, high concentration of protein expression and easily adapted in suspension culture (Kelley, 2007). According to Browne and Al-Rubeai (2009), CHO cell line is known to have stable cell line and better clone selection compared to other mammalian cell lines. At present, majority of CHO cell manufacturing cultivation modes of operation is by means of fed-batch or perfusion culture rather than batch culture to maximise the product formation and cell viability (Hu and Aunins, 1997). Additionally, the production of commercial mAbs has

revolutionised drastically from lab scale bioreactor (10 L) up to commercial manufacturing production (20,000 L) with several biotechnology companies reported the product titres can yield to 5 – 10 gL^{-1} (Wurm, 2004; Kelley, 2007). These improvements have made the mammalian cell as the major platform for the production of monoclonal antibodies for biopharmaceuticals production.

1.2 Antibodies

Antibody is immune type glycoproteins that belong to the immunoglobulin super family. The antibody is a Y-shaped protein molecule synthesized by lymphocytes in vertebrates in response to detection of foreign substances. These immune molecules are formed from four polypeptides consisting of two identical heavy chains and two identical light chains (Figure 1.1) by disulphide bonds that comprised of homology regions of amino acid sequences (Jefferis, 2007). Each antibody is highly specific and binds to particular antigens (antibody generating substance). There are five different types of antibodies that are grouped into different isotypes based on their heavy chains; IgA, IgD, IgE, IgG and IgM. These five types of antibodies are based on the constant region structure and immune function (Jefferis, 2007).

Moreover, therapeutic antibodies are produced by recombinant DNA technology and classified according to their sequence source; murine only, chimeric, humanized and human only (Chadd and Chamow, 2001). Figure 1.2 shows the schematic classification of antibodies according to their sequence source. A murine antibody was extracted from mouse cell and is regarded as foreign sources by the host body which able to draw out its own antibody reaction (Chadd and Chamow, 2001).

By contrast, a chimeric antibody is the result of the construction of the animal (murine) antigen binding variable domain to the human constant domain. While, humanised antibody means the antibody that have more than 90 % of human sequences with murine complementarily-determining regions. Human only antibody means that it has human antibodies with 100 % sequences. The first human only antibody was successfully developed in the 1990s (Chadd and Chamow, 2001).

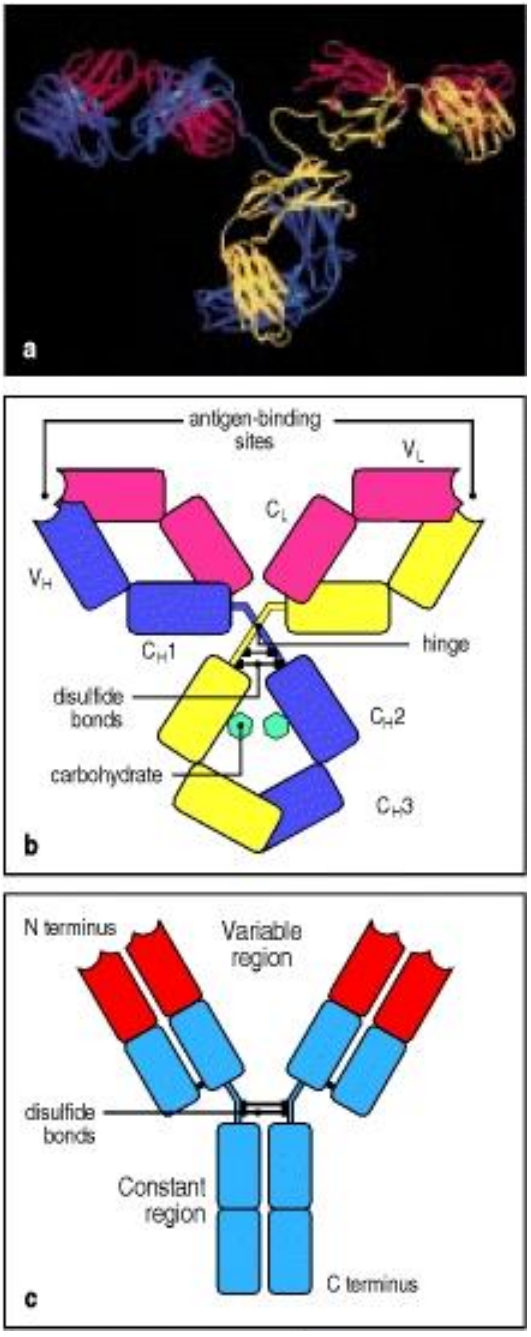

Figure 1.1: Structure of typical antibodies molecules (a) the X-ray crystallographic structure of an IgG antibody. (b) a schematic illustration of the antibody structure with the four chain: two identical heavy chains and two identical light chains (c) a simplified schematic illustration of an antibody molecule. Image adapted from (Janeway, 2001).

Currently, many antibody products in clinical development are fully humanised. Advanced technologies for antibody development in partnership from big pharmaceutical companies has enabled a new generation of human antibody. Moreover, the expectation in the medical and regulatory community is that companies will use the best approach for their product to achieve humanization (Jones *et al.*, 2007).

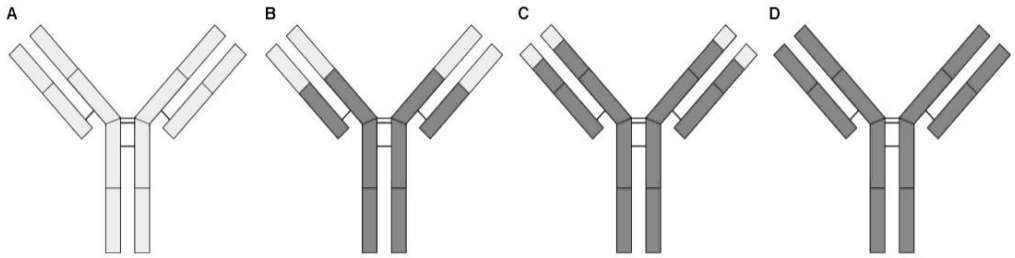

Figure 1.2: Schematic classification of antibodies according to their complementary sequence source. A: murine, B: chimeric, C: humanised, D: human. Image adapted from (Velez Suberbie, 2013).

1.2.1 Monoclonal antibodies

Monoclonal antibodies accounted for a quarter of all new drugs in the market with profits of approximately US$100 billion annually (Aggarwal, 2014). Walsh (2014) reported that over the past four years, mAbs recorded the highest number of approval with 17 from 54 biologics approved in the United States and European Union (EU; Brussel). The importance of monoclonal antibodies (mAbs) has encouraged the researchers to find alternatives for cost effective and promising cell lines that able to yield high quality protein (Griffin *et al.*, 2007; Matasci *et al.*, 2008) Several factors such as media composition development and optimisation, different feeding strategies, extended fed-batch process and engineering characterisation of operating condition in bioreactors have contributed to the improvement of product titres of mAbs (Kelley, 2007; Walsh, 2014).

Conventionally, there are two expression systems suitable for mAbs production; mammalian and non-mammalian based expression systems. Walsh (2014) reported the progression of mAbs manufacturing platforms derived from the mammalian based expression have 60 % approval over non-mammalian system. Besides that, there are several factors that need to be evaluated for manufacturing mAbs including; antibody structure, expression systems, productivity, ease of purification and material costs (Chadd and Chamow, 2001). In addition, for antibody products to be effective, mAbs must be synthesized in biologically active form, with proper folding and post translational modification (Jayapal *et al.*,2007).

1.3 Mammalian cell

As of today, bacterial and mammalian based expression systems are the main expression systems used for producing therapeutic antibodies. However, the latter is the better option because of its similarity in biochemical properties to the naturally occurring human forms such as post-translational modification and glycosylation patterns (Butler, 2005; Warnock and Al-Rubeai, 2006; Matasci *et al.*, 2008). Apart from that, mammalian cell lines have become the preferred host system because of its high specific productivity, cell stability and reproducibility. Basically, there are five mammalian cell hosts which are commonly used for protein production; Chinese hamster ovary cell (CHO), mouse myeloma (NS0), baby hamster kidney (BHK), human embryonic kidney (HEK-293) and human-retina-derived (PER-C6) (Butler, 2005). Chinese hamster ovary cell is the most preferred host because CHO cell have well characterised platform technologies which permit for stable transfection, amplification and choices of high producer clones compared to other cell types such as microbial or plant (Butler, 2005). Besides that, the production of antibodies from mammalian cell culture has improved extensively in recent years (Wurm, 2004). Contemporary mammalian cell culture processes can yield antibody concentration up to 5 - 10 gL^{-1} (Butler, 2005). This is resulted from development in expression technology and process optimisation of upstream technologies at cell culture stage (Birch and Racher, 2006).

1.3.1 Chinese hamster ovary cell

Chinese hamster ovary (CHO) cell is known as the predominant host cell for the production of biopharmaceuticals. Chinese hamster ovary cell was originated from a primary culture of ovarian cells from Chinese hamster (*Cricetulus griseus*) and initially used in protein production as an immortalised cell (Puck, 1985). CHO cell was favoured because of its ability to adapt and grow well in suspension culture and able to scale up in a large scale culture (Wurm, 2004; Warnock and Rubeai, 2006). Furthermore, CHO cell lines can reach maximum cell densities of 2 x 10^7 cells mL^{-1} in fed batch cultures (Warnock and Rubeai, 2006). Basically, there are two expression vector system most commonly used for the production of therapeutics antibodies: glutamine synthetase (GS) gene expression system and dihydrofolate reductase (DHFR) gene. For successful gene expression, GS and DHFR vectors must have a strong promoter that can initiate expression of the antibody gene (Birch and Racher, 2006).

Glutamine synthetase (GS) synthesise glutamine from glutamate and ammonium, with the latter being an undesirable waste product of the cells (Wurm, 2004). Figure 1.3 shows the relationship between the glutamine and glutamate in the GS gene expression system. The inhibition of GS is achieved with the addition of methionine sulphoximine (MSX). On the other hand, DHFR expression system, a recombinant protein can be amplified by the use of folate analogue methotrexate (MTX) to inhibit the function of DHFR, an essential metabolic enzyme. After exposure of MTX, the majority of cells dead, but the surviving cells which contain several hundred to a few thousand copies of the integrated plasmid embedded in chromosomes and elongated. (Wurm, 2004; Birch and Racher, 2006).

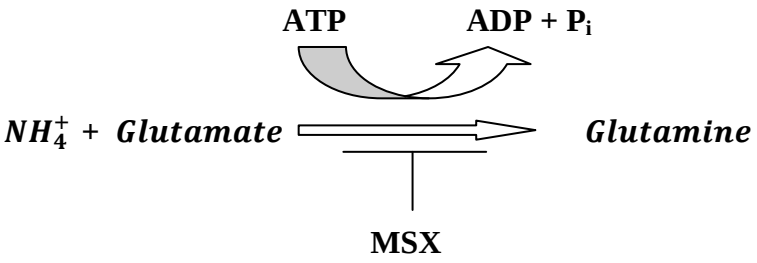

Figure 1.3:Glutamine synthetase (GS) gene expression system in CHO cells.

1.3.2 CHO cell metabolism

Glucose and glutamine are the major carbon and energy sources for CHO cells. Glycolysis and glutaminolysis are the key metabolic pathways in mammalian cells (Quek *et al*., 2010). Both pathways are vital for CHO cell growth and metabolism (see Figure 1.4). Chinese hamster ovary cells consume glucose for energy production and generate lactate as metabolic by-product through the glycolysis pathway (Li *et al*., 2012). In glycolytic process, excess glucose via pyruvate is reduced to lactate by lactate dehydrogenase A (LDA) before being metabolised in the tricarboxylic acid (TCA) cycle. This process has a negative impact on the energy yield which can be achieved by glucose (Altamirano *et al.,* 2013).

Lactate accumulation in CHO cell metabolism has resulted in lower cell growth in batch and fed-batch cultivation and reduced productivity (Li *et al.,* 2010; Gagnon *et al.,* 2011). Therefore, several strategies have been attempted previously to limit lactate accumulation such as genetically modified metabolic pathways (Paredes *et al.,* 1999) and improved operating conditions of bioreactor through media optimisation and feeding strategies. However, lactate consumption by the cells is more profound compared to secretion which resulted in attempts to reduce the initial glucose concentration (Zhou *et al.,* 1995; 1997), alternatively feeding galactose (Altamirano *et al.,* 2006), or directly feeding lactate (Li *et al.,* 2012).

In CHO cell bioreactor processes, several parameters such as pH, temperature and dissolved oxygen influence the cell growth and metabolism. Gagnon *et al*. (2011) showed that by controlling the culture pH by feeding glucose lactate accumulation can be suppressed. They suggested that suppressing the pathway through cellular engineering can alter the cellular metabolism which subsequently altered the lactate production. Furthermore, Kuwae *et al.* (2005) showed that cells cultured at lower pH can reduce lactate accumulation in culture. They suggested that cells between pH 6.6 to 7.2 will reduce peak lactate concentration by 70 %.

By contrast in the glutaminolysis pathway, CHO cells assimilate nitrogen for biomass synthesis and release mainly ammonium as by-product (Altamirano *et al*., 2006; Fan *et al*., 2015). Ammonium can build up in medium and cell cytoplasm through the chemical decomposition and metabolism of glutamine (Chen and

Harcum, 2005). Accumulation of this by-product from the unbalanced nutrient supply for cell activities may inhibit the cell growth (Fan *et al*., 2015) and negatively affect the protein glycosylation thus altering the product quality (Chen and Harcum, 2005). Therefore, many strategies have been developed to overcome the toxic effects of ammonium on CHO cell culture. Research has focused on reducing the ammonium level by substituting glutamine with pyruvate (Genzel *et al.,* 2005) or substituting glutamine by glutamate (Altamirano *et al.,* 2000; 2004). Besides that, deZengotita *et al.* (2002) demonstrated the use of selected amino acids such as glycine, threonine and glycine beta could protect hybridoma and CHO cells from elevated carbon dioxide and osmolality levels.

By understanding the interplay between these pathways on the cell growth, cell metabolism and glycosylation at metabolic levels will benefit bioprocess optimisation of antibody productivity in CHO cell cultivations.

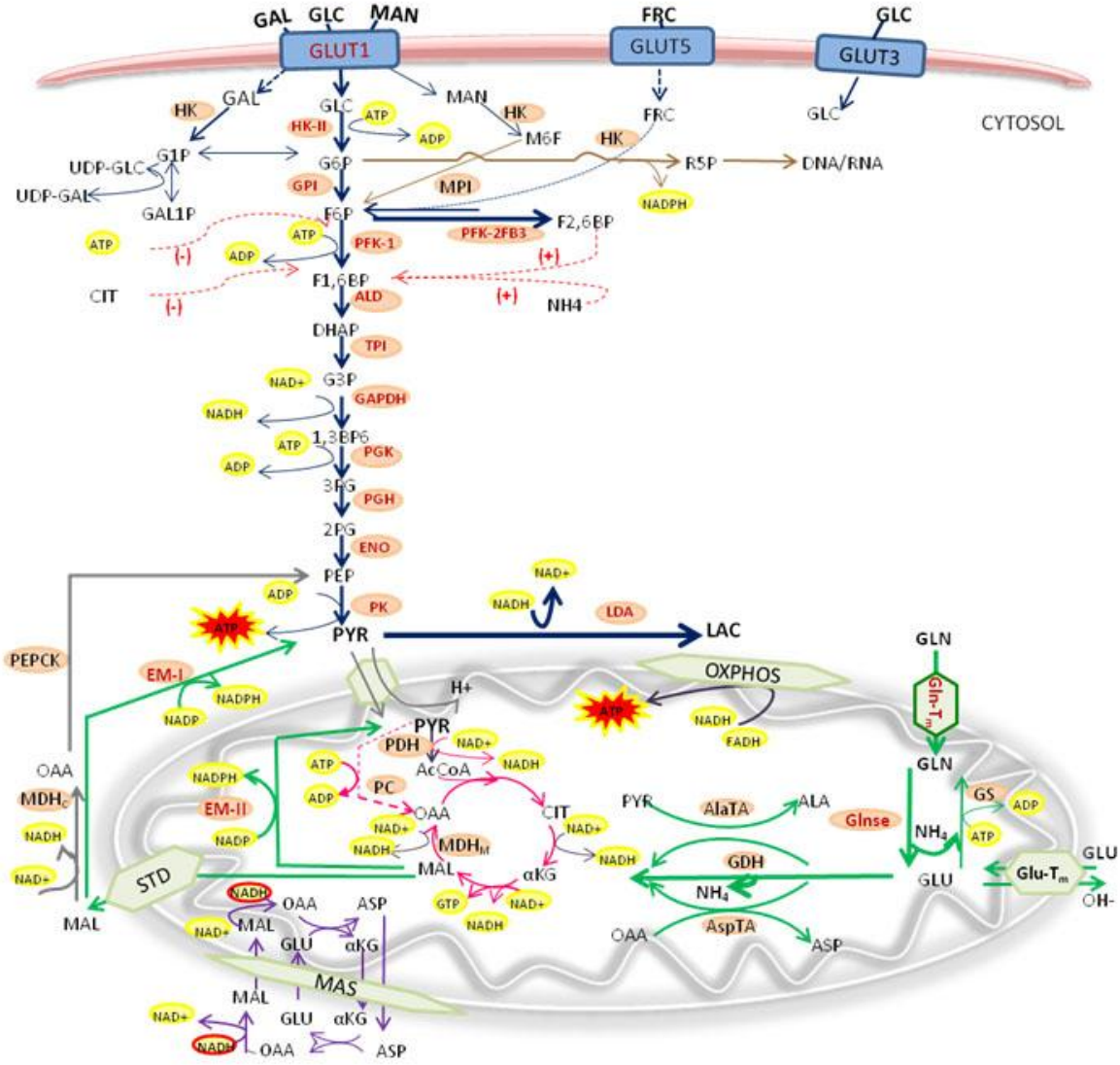

Figure 1.4: Schematic diagram of glycolysis and glutaminolysis pathways for CHO cell metabolism. Legend: Blue arrows: Glycolysis pathway, Green arrows: Glutaminolysis pathway (images adapted from Altamirano *et al.*, 2013).

1.3.3 Production of therapeutic antibodies from CHO cell

Chinese hamster ovary cell is the most utilised mammalian cell type for therapeutic antibodies in bioprocess development. Even though CHO cell is slow growth and very sensitive to a wide range of environmental changes, its versatility and high in productivity makes CHO cell the best candidate for protein production. On the contrary, protein production from CHO cell is very challenging process development. The development of improved cell culture processes might be critical as several parameters such as medium formulation, feeding strategies and engineering parameters need to be characterised (Butler, 2005).

Today, most of the large scale cell cultures are performed in chemically defined serum free media (Wurm, 2004). Medium formulation plays important roles in production process and cell line development. CHO cell lines have been adapted to serum free suspension culture. Serum free media are more favourable because of the more defined composition and the feeding strategy has a profound impact on cell growth and biologic products (Wen, 2009). Besides that, serum free media eliminates the risk of contaminants such as viruses, mycoplasma and prions from animal-derived products that might have negative impacts on end products used by humans (Schröder *et al.,* 2004). Moreover, the advantage of serum free medium is the absence of animal materials; therefore the cells do not easily attach to a solid substrate that make the cells grow well in suspension (Wen, 2009).

One of the main concerns of using CHO cell lines is their susceptibility to shears or hydrodynamic stress (Nienow, 2006). The lack of cell wall makes the mammalian cell more shears sensitive that can give detrimental effect toward the cell growth and viability. Cells that continuously received hydrodynamic stress can give lethal effects which subsequently entered a programmable death sequence (apoptosis) (Chisti, 2001; Nienow, 2006). These lethal effects not only give detrimental effect toward the cell growth, viability and size, but will disrupt the cell during the downstream process.

Although significant progress has been made to improve protein production and quality, mammalian cell culture remains costly, laborious and time-consuming process (Browne and Al-Rubeai, 2009). Economic concerns and time constraint are the major critical factors to generate high producer cell lines and processes for protein production (Griffin *et al.*, 2007). It is therefore common practice to develop a model of the production process in a small scale reactor, where lower costs, ease of handling and higher throughput are possible. The usage of microtitre plates (MTP) and miniature bioreactors are more common in terms of screening the cells before being transferred to the large scale culture for bioprocess development.

1.4 Cell culture bioprocess development

Over the years, various options have been considered to accelerate the bioprocess development of biopharmaceuticals. For the past decade, microbial systems have been the major interest for the development of high throughput bioprocess system (Duetz and Witholt, 2004; Ferreira-Torres *et al.*, 2005). Research has focused on a different aspect of parallelism and engineering characterization of the microtitre plates such as quantification and modelling of oxygen mass transfer rates (Hermann *et al.*, 2003; Doig *et al.*, 2005), mixing time (Nealon *et al.*, 2006) and pH control in microtitre plates (Elmahdi *et al.*, 2003). In the case of miniature bioreactors similar studies on oxygen transfer and power input have been conducted for microbial fermentation processes (Betts *et al.*, 2006; Gill *et al.*, 2008b).

1.4.1 Conventional bioprocess development

Traditionally, the development of mammalian cell lines cultivation required a large set of shake flasks for screening the cell culture for experimental conditions prior to pilot scale cultivation (Amanullah *et al.*, 2010). However, this system has long development times, laborious, as well as limited throughput. For improvement, various designs of microbioreactors and miniature bioreactor systems has been developed, including shaken microtitre plates (MTPs) (Duetz and Witholt, 2004; Duetz, 2007; Barrett *et al.*, 2010; Chen *et al.*, 2009), miniature stirred bioreactor

(Betts *et al.*, 2006; Harms *et al.*, 2006) and other miniature devices such as micro-24 micro reactor (Betts *et al*., 2014). Although each miniature bioreactors is designed to fulfil the requirement of bioprocess development, there usually is a trade off in terms of productivity and throughput (Doig *et al.*, 2006). Figure 1.5 shows the conventional bioprocess development sequence.

Studies using microwell based systems and miniature bioreactors for the high throughput bioprocess development of mammalian cell culture are very minimal (Girard *et al.*, 2001). To date, researchers have investigated the potential of shaken microtitre plates (Micheletti *et al*., 2006; Chen *et al*., 2009; Barrett *et al*., 2010; Silk *et al*., 2010) and mixed minibioreactor (Diao *et al.*, 2008) for development and optimisation of mammalian cells. Several researchers has quantified engineering parameters such as liquid phase mixing time, solid suspension and the energy dissipation rate (Nealon *et al*., 2006; Micheletti *et al*., 2006; Barrett *et al*., 2010).

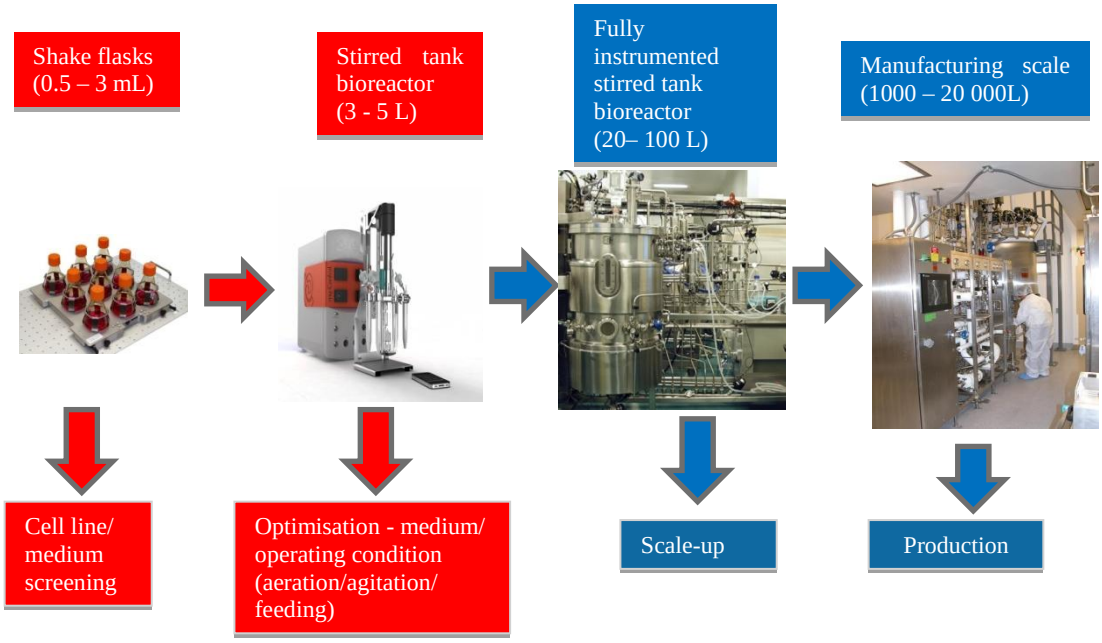

Figure 1.5: Conventional bioprocess development sequence.

1.4.2 Advanced process development sequence

The increased use of monoclonal antibodies as a human therapy is driving the search for rational approaches to establish highly productive and cost effective processes (Li *et al.*, 2010). Advancement of high throughput (HT) technology over the past 10 years in bioprocessing industries is seen as a significant alternative for the conventional process development (Lye *et al*., 2003). High throughput technology is a new platform of bioprocess development that gives flexibility at the early research stage with minimal usage of materials. High throughput can offer a miniaturised system that amenable to automation (Micheletti *et al*., 2006; Barrett *et al*., 2010). Currently, the majority of high throughput studies are focused on microwell based systems (Micheletti and Lye, 2006). Additionally, the microwell based systems have the ability to run parallel cultivations simultaneously and have the potential to mimic quantitatively laboratory and pilot scale bioreactors (Lye *et al.*, 2003; Kumar *et al.*, 2004).

Figure 1.6 shows the advanced bioprocess development sequence. Recent introduction of micro-Matrix (Applikon Biotechnology, B.V. Deflt Holland) are solution to miniaturised, automated and high throughput bioprocessing. The micro-Matrix offers a single use, 24 independently control bioreactors in microtitre plate format which can replicate larger scale bioreactors. The ability of micro-Matrix independently controlled bioreactors which promote a solution to automatic liquid handling in microwell based systems make micro-Matrix an ideal alternative to high throughput bioprocessing.

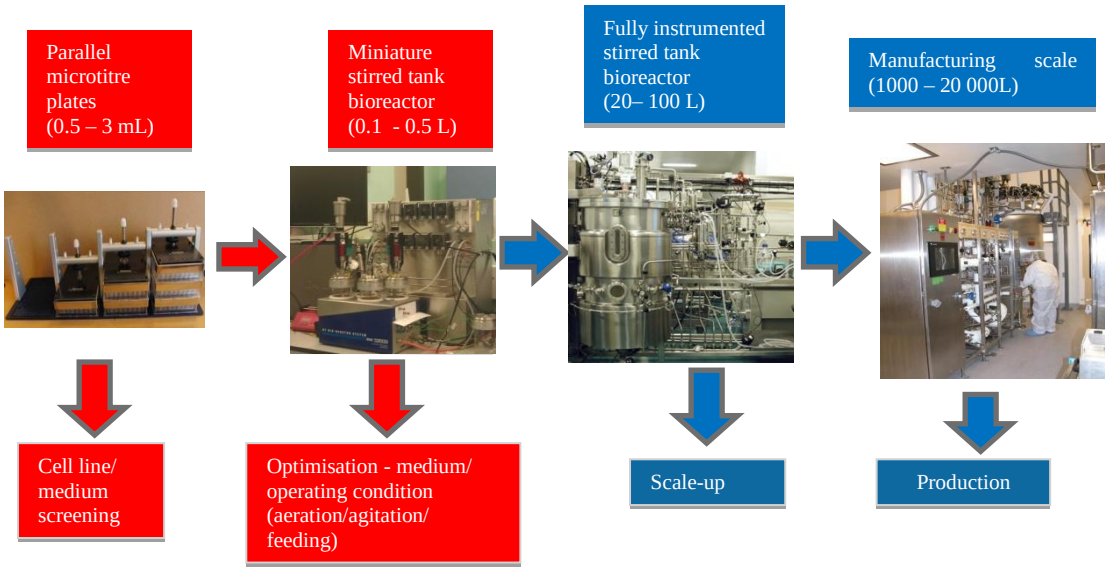

Figure 1.6: Advanced bioprocess development sequence.

1.5 Bioreactor system for therapeutic antibodies production

Bioprocess development of mammalian cell culture involved a series of bioreactor systems from small scales up to commercial scales. Figure 1.7 shows a series of bioreactor scales utilize from small scale to production scales. In this work, a series of bioreactor system was studied from microtitre plates, miniature bioreactor and lab stirred tank bioreactors. The extensive use of the microtitre plates (MTP), micro-Matrix, miniature bioreactor (HEL-BioXplore) and bench scale stirred tank reactor for bioprocess development were further discussed in the Section 1.5.1, 1.5.2, 1.5.3 and 1.5.4 respectively.

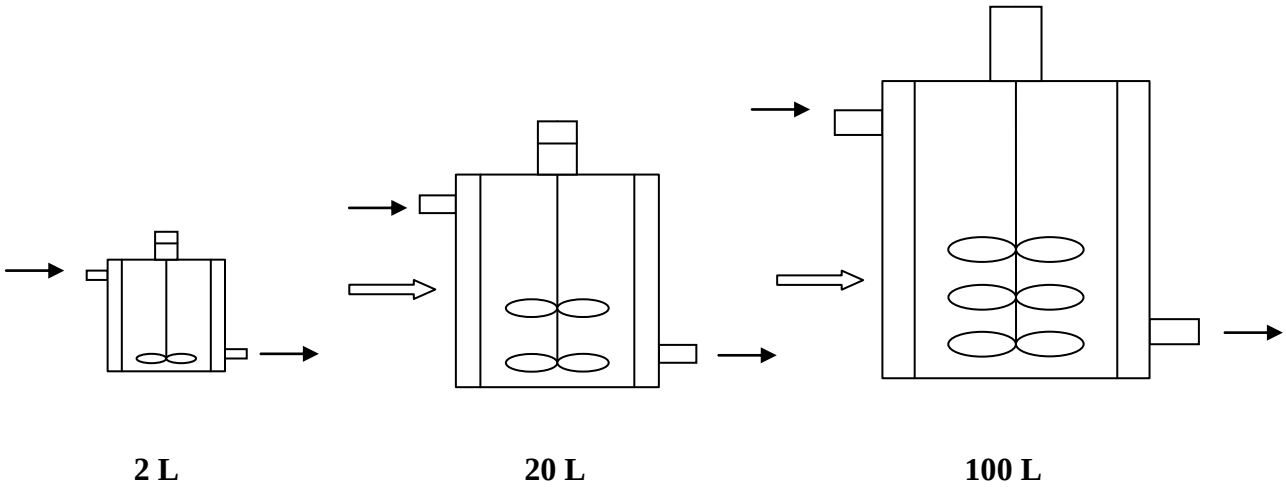

Figure 1.7: Flows of different scales of bioreactors in bioprocess development of mammalian cell cultures (adapted from Birch and Racher, 2006).

1.5.1 Microtitre plate

Microtitre plate (MTP) or microwell was invented 50 years ago by the Hungarian physician, Dr. Guyla Takatsy as a platform for diagnostic tests after a severe outbreak of influenza virus (Manns, 2003). Conventionally, microtitre plates are used for analytical methods such as medical diagnostic tests (for enzyme-linked immunosorbent assays), chemistry and biotechnology application. Microtitre plates are usually made from various plastics and polymers (polycarbonate or polypropylene), glass (borosilicate, quartz), metal (aluminium, stainless steels) (Lye *et al*., 2003, Betts and Baganz, 2006) with some new innovative plates incorporating optical-grade glass, fibre glass matting, polymer based filter membrane and specialty papers (Manns, 2003).

Microtitre plates are available in various formats typically 6, 12, 24, 96, 384 to 3456 wells per plate for ultra-high throughput screening (UHTS). The wells can be either in rectangular and cylindrical geometries with round, flat or pyramidal shaped bottoms and deep or shallow wells (Lye *et al*., 2003; Betts and Baganz, 2006). Figure

1.8 describes different type of microwell formats use in the bioprocess development experiments (Lye *et al*., 2003).

Central to this approach a number of bioprocesses experimentation using microtitre plates has been applied at the screening stage to enhance throughput. So far, there are several commercial small scale screening system available on the market with instrumented controllable micro bioreactor such as SimCell™ (Bioprocessors Corporation, Woburn, MA), Micro-24 Microreactor System (Pall Corporation, Port Washington, NY), M2P Biolector GmbH, (Aachen, Germany), Cellstation™ (Fluorometrix Corp., Stow, MA) and most recently the micro-Matrix (Applikon Biotechnology B.V., Holland).

Microtitre plates are widely used in the industry due to its cost effective, high throughput and minimum use of materials. The advantage of microtitre plates (MTPs) to perform parallel reactions at very minimal volume in small scale has made MTPs an excellent choice for the screening phase of process development in cell culture (Betts and Baganz, 2006). Studies by several researchers to understand the parameters affecting microbial cell growth in microtitre plates had provide the basis for the establishment of mammalian cell culture in microtitre plate systems (Duetz *et al*., 2000; Elmahdi *et al*., 2003; Hermann *et al*., 2003; Kensy *et al*., 2005).

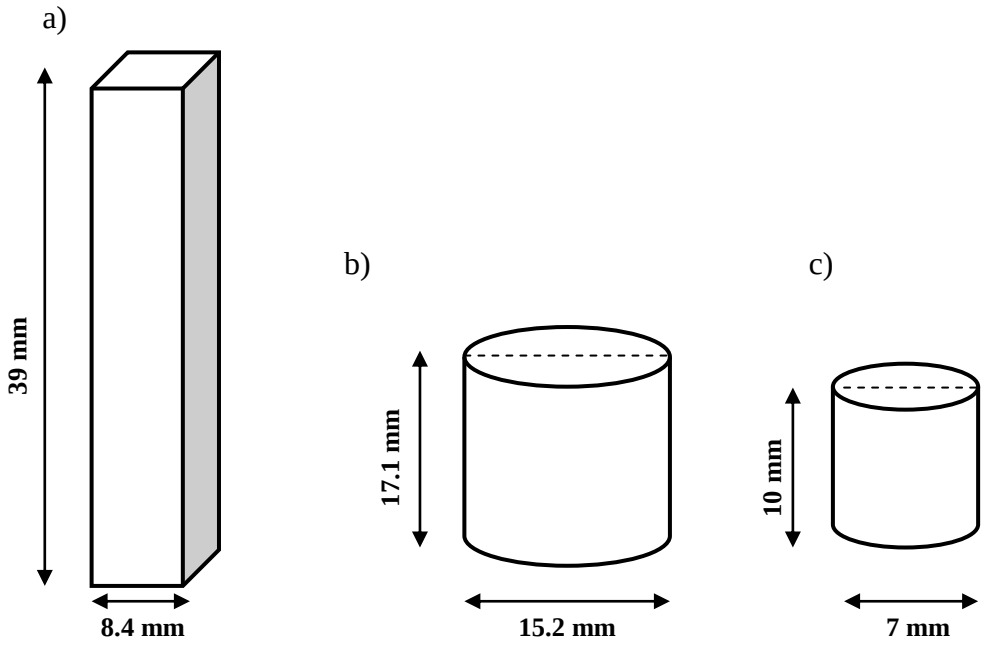

Figure 1.8: Schematic diagram of individual format of microwell based system: (a) 96-deep square well format; (b) 24-standard round well format; (c) 96-standard round well format (adapted from Lye *et al*., 2003; Barrett, 2008).

In addition to antibody production, MTPs experimentation can be used for medium formulation, selection of high producer clones and different aspects of environmental parameters in process development. Moreover, the processes that carry a large bioreactor burden can be alleviated by the use of high throughput miniature devices. In particular, microtitre plates not only reduce labour intensity and materials cost but increase the level of parallelism and throughput (Betts and Baganz, 2006).

Besides all the advantages, there are a number of challenges using these systems such as high evaporation rate and poor mixing patterns between each of the wells. Mammalian cells tend to form aggregates and accumulate at the centre in the wells, which cause difficulty with sampling and cell quantification (Wen, 2009). Mixing in the wells can be achieved by pipette aspiration, mechanically agitated stirrer bars or orbital shaking (Lye *et al*., 2003). Currently, the common method of liquid mixing in the microtitre plates is by shaking of the entire plates on shaking incubator (Micheletti and Lye, 2006). Nealon and his colleague (2006) has reported the quantification of macro mixing times in different geometries of microtitre plates in static condition with jet mixing theories (Re_j = 1000 - 3960) and liquid addition volumes (V_A = 10-859 µl). The result showed that generation of quantitative and reproducible data can be performed through efficient mixing and better understanding of the engineering environment with individual microtitre plates (Nealon *et al*., 2006).

Another key challenge for shaken microtitre plates is to provide adequate oxygen for the cells to grow. Under oxygen limitation, cell growth may become slow and eventually will affect the production of antibodies (Barrett *et al*., 2010). In order to validate oxygen transfer rate, the DOT (dissolved oxygen tension) in microtitre plates can be measured using optical sensor (Oxo-Dish OD-24, PreSens-Presicion Sensing GmbH, Regensburg, Germany). The microtitre plates were equipped with the sensor at the bottom of each well that had been immobilised by a fluorescence optode. The measurement was taken under the sensor dish reader (SDR SensorDish®) with a read out unit located in the centre below each well of a 24 well plate. Figure 1.9 shows the experimental set up of standard 24-well with sensor for measurement of pH and dissolved oxygen (Kensy *et al*., 2005). Evaporation rates in

the microtitre plates can be improved by using the Duetz system (sandwich lid) that been developed by the Duetz and co-worker (2000) for microbial systems. Silk *et al*. (2010) reported that the sandwich lid system has minimised the liquid losses to 0.6 % v/v in microtitre plates over 14 days of cultivation. This result shows that the sandwich covers developed by Duetz group are reliable and efficient in minimising the evaporation rate in the microtitre plate system.

For the past decade, microtitre plates have been broadly used as a scale-down model for mammalian cell culture process development in expressing recombinant proteins. Research showed that a variety of microtitre plates as bioreactor for mammalian cell culture process development has been reported featuring optical based sensor for high throughput cell culture (Chatterjee *et al.,* 2015). In addition, engineering characterization of liquid mixing and gas liquid mixing mass transfer in microtitre plates (Barrett *et al*., 2010) and fed batch operation of cell culture processes using bolus feeding techniques (Silk *et al*., 2010) have been described.

However, the techniques of nutrient feeding in a microtitre plates are not well established. Fed batch operation in the microtitre plates presents great challenges in liquid handling and implementation of continuous feeding (Silk *et al*., 2010). Up to now, most of the techniques that have been applied are specifically designed for microbial system such as glucose silicone elastomer discs with slow release technique (Jeude *et al.,* 2006) and enzyme controlled glucose auto delivery system (Panula-Perala *et al.,* 2008). Both of the system had shown promising result to increase the microbial cell density and product formation.

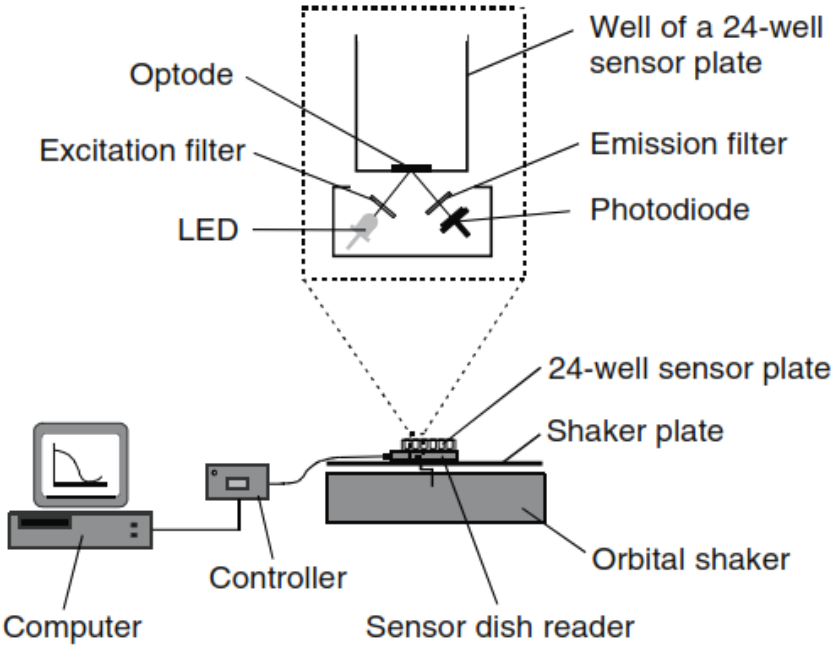

Figure 1.9: Experimental set up for 24 microtitre plates for optical measurement of pH and DO (adapted from Kensy *et al*., 2005).

By contrast, Panula-Perala *et al*. (2008) developed a novel method using an enzyme-based substrate-delivery system (EnBase™) for growth of microorganisms in microtitre plates and shake flasks. Their method 5 – 20 times higher cell densities were obtained compared to standard methods. The advantages of this enzyme delivery system are that it does not require additional sensors or liquid supply system which can minimize the contamination risks compared to bolus feeding techniques. Furthermore, the EnBase™ method is robust, easy to apply at mililitres scale down model and has the potential to control the microbial growth rate and oxygen consumption (Panula-Perala *et al*., 2008). The feeding strategies applied in the microtitre plates are summarised in the Table 1.1.

The other method is the slow release technique of glucose in shake flasks for microbial production strains (*Hansenula polymorpha*) developed by Jeude *et al*. (2006). The FeedBead® system provided a continuous delivery of glucose using silicone elastomer disks in slow release diffusion technique. However, the weakness of the system is that the release rates are high and the releases take place in a short period of time, which is not adequate for longer mammalian cell cultures (Hedge *et al*., 2012).

Hegde *et al.* (2012) have developed a continuous feeding system in shake flasks that consists of hydrogel nutrient feed. The research group developed a method of hydrogel-based nutrient delivery in the shake flasks without the need of manual feeding. They demonstrated the continuous feeding of glucose to suspension of CHO culture in shake flasks which resulted in a viable cell density increase of 23% and the lactate concentration decreased by 89% at the end of the culture. They summarized important criteria's for successful delivery system in mammalian cell cultures are: (a) the system must not have undesirable effect on growth and productivity (b) the release of the nutrient must be over a period of 5-10 days and (c) it must be possible to release other nutrient prior to addition of glucose.

Table 1.1: Different feeding strategies applied in the mammalian cell cultures.

Culture	Materials	Nutrient	Concept	Reference
CHO cells	2-Hydroxyl ethyl methacrylate [HEMA] (97% pure), ethylene glycol dimethacrylate [EGDMA] (98% pure)	Glucose/protein hydrolysate	Glucose-loaded hydrogel with controlled release	Hedge *et al*. (2012)
GS-CHO cells	CD CHO AGT (containing glucose and other nutrients)	Glucose	Bolus addition	Silk *et al*. (2010)
E.coli	Inactive polymer, starch from a gel phase (in tablet or liquid form)	Glucose	Release of glucose by enzymatic degradation of polysaccharide (EnBase™)	Panula-Perala *et al*. (2008)
Hansenula polymorpha	Polymer matrix consist of PDMS and glucose (sterile silicone elastomer discs)	Glucose	Defined kinetic of glucose released from silicone elastomer discs (FeedBeads®)	Jeude *et al*. (2006)

1.5.2 Micro-bioreactors (micro-Matrix)

The demand to reduce the development time of potential new biopharmaceuticals to the market has enabled major pharmaceutical companies developing scale-down platform technologies (Birch and Racher, 2006). These platforms are meant to be a robust framework for bioprocess development which contains all elements required to produce the biopharmaceutical products. One of the alternatives is using a scale-down models that can be relied to mimic laboratory and pilot scale bioreactors. It is predicted that using a scale-down models the growth kinetics and product expression can be optimized at miniature scale and scale-up quantitatively (Betts and Baganz, 2006).

The micro-Matrix (Applikon Biotechnology B.V., Holland) is new, small scale micro-bioreactors that have features for high throughput, parallel experiments, automated liquid handling and scalability. The system was developed in a microtitre plate format, with 24 independently controlled micro-bioreactors which can mimic the larger bioreactor unit operations. The square well cassette design is based on the deep square well (DSW) microtitre plates developed by Wouter Duetz (2007). The unique features of the cassette include the PreSens sensors at the bottom of the cassette. Figure 1.10 shows the micro-Matrix system with its square deep well plate cassette.

The cassette was deep well plates, square bottom with maximum liquid volume of 7 mL and working volume ranging from 3 – 5 mL. The cassette was covered with top plate that has a gasket seal for efficient gas transfer and gas filter bars to minimise cross contamination between cassette and cabinet. The micro-Matrix system also has the standard 25 mm orbital diameter shaking platform for mixing capability and lock features at the side of the system to hold firmly the cassette when agitated. The PreSens sensors at the bottom of the cassette have the ability to monitor temperature, pH and dissolved oxygen (PreSens-Presicion Sensing GmbH, Regensburg, Germany).

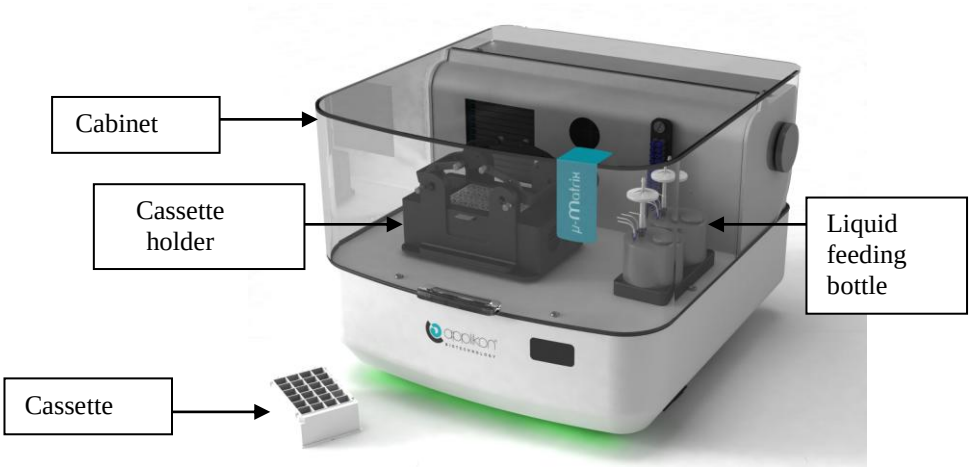

Figure 1.10: The micro-Matrix bioreactor system with 24-deep well plate cassette (adapted from the website of Applikon Biotechnology B.V. Holland).

Each individual well or bioreactor has its own control system with proportional, integral and derivative controller (P.I.D). These P.I.D enable for control of temperature, pH, and DO on individual well. Furthermore, every single well temperature control is integrated with individual Peltier element for cooling and heating. The culture pH was controlled through automated gas addition and liquid addition. For dissolved oxygen concentration, it can be controlled up to four gases (oxygen, nitrogen, carbon dioxide, or compressed air) addition per bioreactors per wells. Figure 1.11 shows the schematic diagram of one well of DWP cassette for the micro-Matrix system.

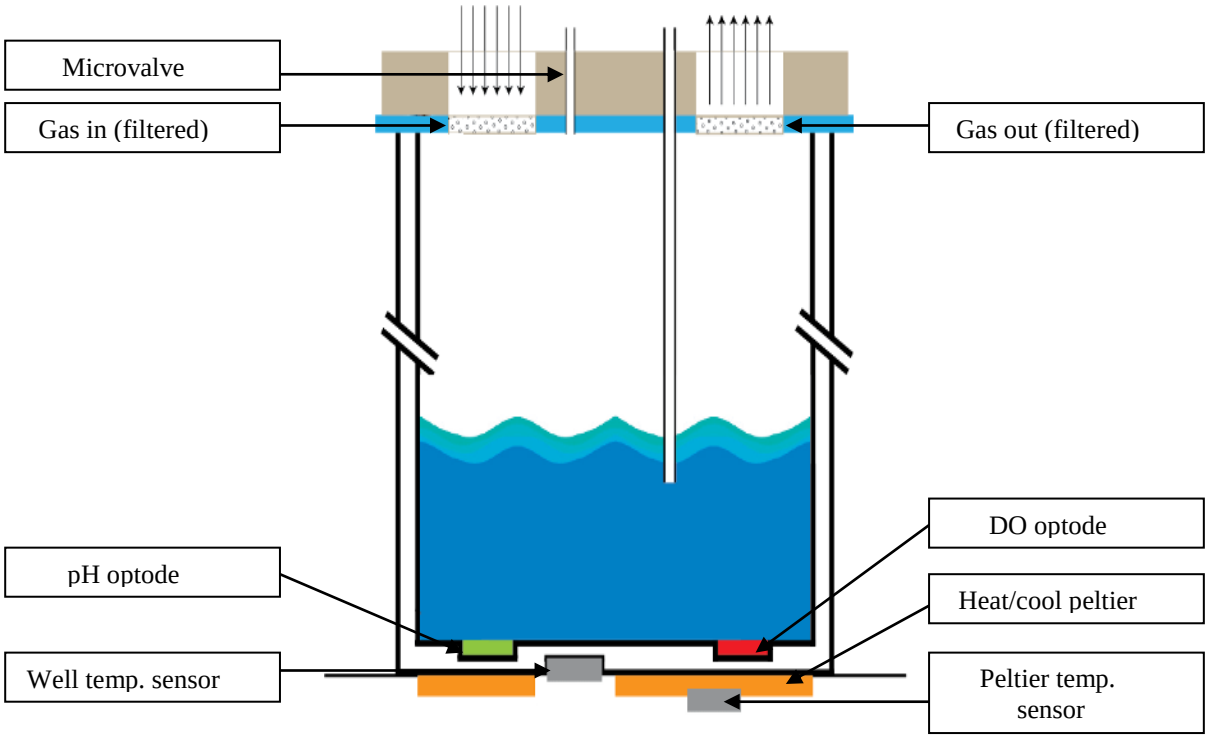

Figure 1.11: Schematic diagram of single well of the 24-DWP of the micro-Matrix system (adapted from the website of Applikon Biotechnology B.V. Holland).

1.5.3 Miniature stirred bioreactors (HEL-BioXplore)

The interest of developing miniature bioreactors for bioprocess development has progressed tremendously in the last 10 years (Betts *et al*., 2006; Gill *et al*., 2008a). Lye *et al*., (2003) described miniature bioreactor systems that facilitate parallel and automation of several fermentations simultaneously have the potential to reduce the fermentation times and costs. The capacity of miniature stirred bioreactor to monitor on-line and control the pH, dissolved oxygen and temperature could make an excellent alternative for mammalian cell culture bioprocess development. Furthermore, the engineering characteristic of miniature bioreactors has been studied in term of energy dissipation rate using computational fluid dynamic (CFD) analysis (Lamping *et al.*, 2003), k_La values (Puskeiler *et al.*, 2005), and mixing time (Betts *et al*., 2006).

The key design features of miniature bioreactors are based on the conventional stirred tank reactors to enable rapid and scalable fermentation process. Betts *et al*. (2006) have characterised the volumetric oxygen transfer and mixing time of a novel 10 mL miniature stirred bioreactor as a scale down model for microbial fermentations. One of the advantages of these reactors is their ability to monitor continuously and real time visualisation of parameters in each single bioreactor. The specific power input of the miniature bioreactor was compared with a conventional 7 L bioreactor. It was concluded that the performance using an equivalent P/V is almost similar between these two bioreactors with regard of growth and product kinetics (Betts *et al*., 2006)

Furthermore, Puskeiler *et al*. (2005) has developed a millilitre size bioreactor with a gas inducing impeller that has k_La value as high as over 0.45 s^{-1} (for 8 mL volume) agitated at 2300 rpm. The key feature of the 48 ml miniature bioreactor developed by Puskeiler *et al*. (2005) is a standalone reaction block with integrated heat exchangers. They also described the fed-batch mode of fermentation, which illustrates the potential of miniature bioreactor to achieve high levels of oxygen transfer. Moreover, the automated liquid handling and monitoring of several parameters such as pH was feasible using this miniature bioreactor block with gas inducing impellers.

Recently, Gill *et al*. (2008a) has investigated a novel miniature stirred bioreactor (Figure 1.12) and determined productivity of *Escherichia coli* and *Bacillus subtilis* fermentations which showed comparable operation of 4 autonomously controlled bioreactors. The bioreactor system has the continuous on -line monitoring, control of pH and DOT, and each bioreactor is geometrically similar to the conventional bioreactor. Table 1.2 compares several key parameters between miniature bioreactors and standard 5 L stirred tank rectors (STR). The results showed that the miniature bioreactor systems studied by Gill *et al.* (2008a) has excellent reproducibility with specific growth rates ($0.68 \pm 0.01 h^{-1}$ for *E.coli* and $0.45 \pm 0.01 h^{-1}$ for *B. subtilis*). In addition, the kinetic growth and product parameters determined from the miniature bioreactor shown are comparable with that of the conventional 5 L stirred tank bioreactor.

As reviewed above, the existing prototypes of miniature bioreactors have successfully demonstrated cultivation of the bacteria and yeast at its scaled. Nevertheless, animal cell culture cultivation using miniature stirred bioreactors are not extensively studied and well established. To date, there are only a few research of miniature reactor (< 0.5L) of stirred, suspension bioreactors published for animal cell culture.

Table 1.2: Comparison between miniature bioreactor and 5 L stirred tank reactors (adapted from Al-Ramadhani, 2015).

Parameters	UNIT	MBR	5L
Total vol.	L	0.5	5
Working vol.	L	0.3	3.5
Total ht	m	0.155	0.32
Diameter	m	0.085	0.16
Aspect ratio	H/L	1:1	1:1
No. of impellers	-	1	1
Type of impeller	-	Marine (direct driven) /magnetic driven marine	Pitched blade marine
Impeller diameter (D_I)	m	Direct-0.034 Magnetic-0.033	0.065
Impeller depth	m	Direct – 0.07	0.045
D_I:D_T	-	Direct – 0.40 Magnetic – 0.39	0.41
No. of impeller blades	-	Direct – 3 Magnetic – 4	3

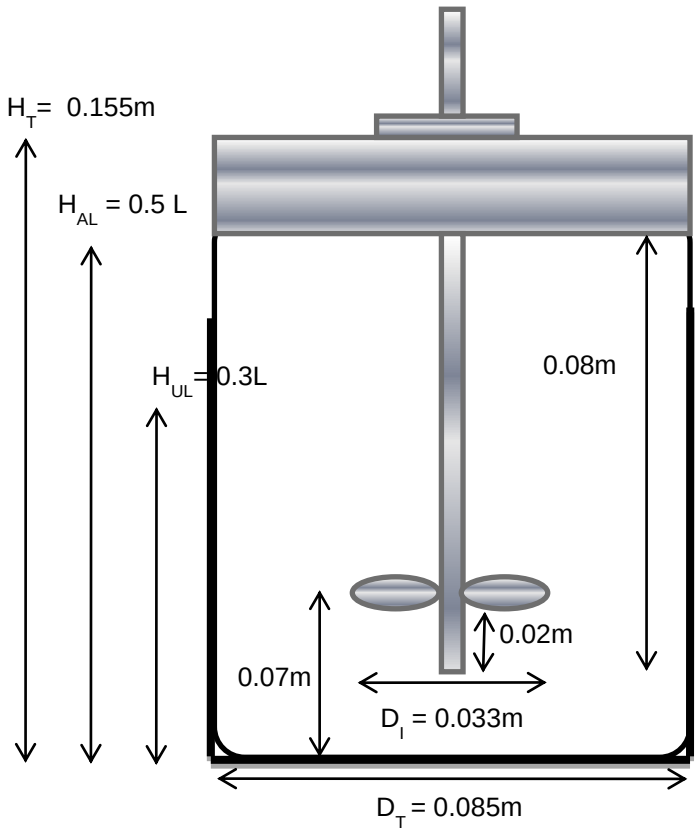

Figure 1.12: Miniature bioreactor system (HEL-BioXplore) (adapted from Gill *et al.*, 2008a,b).

The Diao research group described a mixed mini bioreactor or suspended animal cells using two wide culture chambers (U shape) that are linked by a 5 mm wide channel. In this bioreactor, the mixing is achieved by continuous transfer of the culture medium between two chambers using oscillatory regulating pressure. It has been shown that the insect cells, *Spodoptera frugiperda* grown in the bioreactor have a comparable length of lag phase and growth rate in comparison with the same insect cells in 50 mL spinner flasks. Additionally, the cells in the mixed mini bioreactor gave higher maximum cell density of $5.3 \pm 0.9 \times 10^6$ cell mL^{-1} than that of $3.4 \pm 0.4 \times 10^6$ cell mL^{-1} obtained in the 50 mL spinner flasks (Diao *et al*., 2008).

According to Betts and Baganz, (2006), the automation of miniature bioreactors is the key to high throughput capability in process development. A number of automated systems have recently been available for mammalian cell culture with automated sampling and post fermentation conditioning. Medicel Oy has designed automated small scale bioreactor that have 15 parallel fermentation systems (Medicel Explorer) with working volumes of 150 mL, independent control of pH, DO and agitation and one continuous feed. The system has been demonstrated for mammalian cell culture with good batch to batch reproducibility and comparability to shake flasks performance (Bareither and Pollard, 2011).

The Automation Partnership (TAP) (with collaboration of an industry consortium) has designed a high throughput screening tool for protein production. Besides that, TAP has also recently developed an advanced automated microscale bioreactor for cell culture, ambr^{TM} system. The system operates with twenty four disposable cell culture reactors of 10 mL working volume and uses a robotic arm for liquid handling (Bareither and Pollard, 2011). Furthermore, the development of an automated bioprocess framework robotics should be further integrated with miniaturised downstream processing for product recovery and purification (Lye *et al*., 2003).

1.5.4 Stirred tank bioreactors (STR)

A number of reactor designs have been investigated for maximising the production of antibodies from mammalian cell lines. For the past 40 years, several alternatives have been developed, but conventional stirred tank reactors (STR) have materialized as the industry's system of choice for industry production (Chu and Robinson, 2001). The advantages of stirred tank bioreactors derive from its ease of monitoring and ease of scale-up. Besides that, a stirred tank reactor not only provides a homogenous system and mixing mechanism but can monitor the operating parameters (pH, temperature, DOT concentration) efficiently. Mixing in STR is achieved by means of mechanical impellers that are attached to the motor. The typical type of impeller applied in the STR for animal cell is the marine or pitched-blade which gives an axial flow pattern in the culture (Warnock and Al-Rubeai, 2006).

Zhang *et al.* (2010) has highlighted the importance of shear and mixing operation in mammalian cell cultured with different scales and types of bioreactors. Nienow (2006) reported that the homogeneity and the pH of the culture are the important factors to be considered in large scale culture. The author reviewed the shear sensitivity due to the agitation and bubble formation during the fermentation. The largest commercial scale being employed are now up to 20 000 litres achieved by Lonza, GlaxoSmithKline, Eli Lily and Co., Johnson and Johnson and other leading biopharmaceuticals firms (Nienow, 2006). Besides that, fed-batch mode of operation gives higher cell densities with 5 -10 gL^{-1} of antibody in large scale culture (Zhang *et al*., 2010).

The drawback of using stirred tank reactors as a scale down model is the lack of throughput, large requirement of nutrients and medium, laborious work for inoculation, sampling and harvesting, and the high shear sensitivity of the mammalian cell culture.

1.6 Characterisation of scale-up process

Processes of scale-up from small scale laboratory equipment to industrial scale remain as critical parameters for mammalian cell cultivation. Design of industrial scale bioreactor is usually based on the performance of scale-down bioreactors. The successes of scale-down prototypes to mimic the larger scale reactors are significantly important to minimise the repercussion in term of reproducibility, cost effective process and stability of operations. Besides that, the optimisation of engineering characterisation of scale-down bioreactors play vital role in scale-up process includes; mixing time, oxygen mass transfer coefficient and power input (Micheletti *et al.*, 2006).

1.6.1 Mixing time

Mixing is one of the important operations in bioprocess to achieve homogeneity. Mixing of bulk liquid in a closed vessel includes the physical process of diffusion, distribution and dispersion (Doran, 1995). Mixing gives direct interaction of heat transfer, gas dispersion and blending of different component of materials in medium in a reactor vessel. Furthermore, poor mixing achieved in bioreactors can result in pH, nutrient and temperature gradients as well as poor operating parameters control (Al-Ramadhani, 2015). In a bioreactor, mixing is normally achieved by mechanical agitation of an impeller (Doran, 1995. Therefore, the selections of impeller designs are very crucial which depend on viscosity of the liquid and sensitivity of culture towards the mechanical shears (Doran, 1995).

Mixing time, T_m is defined as the duration of time required to reach 95 % homogeneity in a perfectly mixed vessel (Xing *et al*., 2009). There are two methods that commonly use to determine the mixing time in a reactor vessel; decolourisation and tracer addition method. In the decolourisation method, a fluorescent dye is used along with high speed camera to record the colour changes in the liquid. In the tracer method, a tracer is added into the bulk medium to monitor the concentration changes until it becomes homogeneous and stabilise. The tracer can be acid, base or salt concentration that can reduce the uniformities of gradient temperature, pH concentration and other properties (Xing *et al*., 2009). In order to have homogenous

distribution the probe that recorded the concentration changes is placed at several locations and height across the vessel (Velez-Suberbie *et al.*, 2013). The equation uses to determine the normalised pH time is:

$$H_t = \frac{pH_t - pH_i}{pH_f - pH_i} \tag{1.1}$$

Where, H homogeneity index

pH_t pH during measured time

pH_i pH during initial time measurement

pH_f pH during final time measurement

On the other hand, Nienow (1998) proposes the following equation where the tank height (H_T) ratio is equal to the tank diameter (D_T):

$$T_m = 5.9 \left(\overline{\varepsilon}_{T\,g}\right)^{-o.33} \left(\frac{D_i}{D_T}\right)^{-o.33} {D_T}^{0.67} \tag{1.2}$$

Where, T_m mixing time (s)

$\overline{\varepsilon}_{Tg}$ Total energy dissipation rate in gassed bioreactor (Wm^{-3})

D_i impeller diameter (m)

D_T tank diameter (m)

Production of mammalian cell culture at industrial scale is expensive and time consuming processes. Mixing of mammalian cell cultures are achieved using either marine or pitched blade impellers due to the cell shears sensitivity. These impellers designs will create a low shears and gently mix the culture without damaging the cells (Mirro and Voll, 2009). As mentioned before, scale-down prototypes are crucial to determine the design of industrial scale bioprocess. Using the scale-down experiment, a number of key engineering operating parameters could be determined for translation at production scale. Ideally, the scale-up process should be carried out as close as possible to those good conditions in a small vessel to achieve high productivity and performance (Doran, 1995). Therefore, matched mixing time seems

as the desirable option to accomplish reproducibility in the scale-up process. Moreover, Nienow (2006) described that for a successful and effective mixing, T_m should be as small as possible.

1.6.2 Volumetric oxygen transfer coefficient

The aeration system in a reactor must be able to maintain oxygen concentration for cells maintenance during fermentation. Oxygen uptake rate (OUR) by cells in the bioreactor is determined by the cell growth and metabolism. In aerobic fermentation, cells consumed oxygen molecules from the liquid and utilised the carbon source for growth and metabolism. In a well-mixed reactor, the oxygen transfer rate (OTR) to the liquid is determined by the mass transfer coefficient (k_L a), where, k_L is the mass transfer coefficient and a is the specific contact area (Van't Riet, 1979). Oxygen transports in reactors become the rate limiting step and control the overall mass transfer rate (Doran, 1995). Shuler and Kargi (2002) described that mass transfer rate as shown in the equation 1.3:

$$\frac{\mathrm{dCL}}{\mathrm{dT}} = k_L\, a\, (C_A{}^* - C_{AL}) \tag{1.3}$$

Where, $k_L a$ Oxygen mass transfer coefficient (h^{-1})

$C_A{}^*$ Dissolved oxygen concentration saturation (mol m^{-3})

C_{AL} Dissolved oxygen concentration in the liquid (mol m^{-3})

$k_L a$ is used to characterise the oxygen mass transfer capability in the reactors. If the $k_L a$ of a system is small, the ability of the reactor to deliver oxygen to the cells is limited and vice versa (Doran, 1995). Nienow (2006) reported that typical $k_L a$ profile for large scale mammalian cell culture in the range of 1 – 15 h^{-1} for adequate oxygen transfer rate in the media.

The mass transfer coefficient can be determined by the dynamic (Van't Riet, 1979) or static (Wise, 1951) gassing out methods. The dynamic gassing out technique is utilised during the activity of growing culture in the fermenter to lower the oxygen level prior to aeration. Normally the process is carried out during fermentation to give a more realistic assessment of fermenter's efficiency (Van't Riet, 1979). The static gassing out is a technique of lowering the oxygen concentration by gassing the liquid with nitrogen gas where the liquid is scrubbed free of oxygen. The deoxygenated liquid is aerated and the increase in the dissolved oxygen is monitored using DO probe (Wise, 1951). The following equation is typically used to determine the k_La:

$$k_L a = A\,(\varepsilon_{T_g})^{\alpha}\, v_s{}^{\beta} \tag{1.4}$$

Where, v_s the superficial gas velocity

ε_{T_g} the total energy dissipation rate in a gassed reactor

A, α, β constants

1.6.3 Power requirement

The power requirement is important in determining the efficiency of operating parameters in bioreactors such as mixing, oxygen transfer rate and k_La. In a typical mammalian cell culture stirred tank bioreactors (STRs), low power input is required to minimise the mechanical stress damage, implied on the cells due to mixing properties (Chisti, 2000). Mixing in bioreactors is usually achieved using impellers which are driven by the electrical power, and the power requirement is determined by the type or size of impellers, viscosity of the liquid and speed of the impeller (Doran, 1995; Nienow, 2006). The relationship between these variables is usually expressed in dimensionless number such as the impeller Re_i and the power number N_p:

$$Re = \frac{P}{\rho\, N_i^3\, D_i^5} \tag{1.5}$$

Where, P power input (W)

ρ fluid density (kgm^{-3})

N_i stirrer speed (rps)

D_i impeller diameter (m)

For a given impeller, Re_i values greater than 1 x 10^4 describes the turbulent flow regime, while Rei < 10 corresponds to laminar flow regime. The relationship between the Re_i and N_p could be determined experimentally for different types of impellers. Once the power number is known, the power input (W) in STRs is achieved using the following equation

$$P = N_P \, \rho N^3 {D_i}^5 \tag{1.6}$$

Where, P power input (W)

N_P dimensionless impeller power number

ρ liquid density (kgm^{-3})

N impeller rotational speed (rps)

D_i diameter of impeller (m)

1.7 Aim and objectives of thesis

This study aim was to evaluate the microwell based systems (microtitre plates (MTPs) and micro-Matrix, (Applikon Biotechnology, B.V. Holland) and miniature bioreactor (HEL-BioXplore, HEL Ltd, UK) for the rapid development of antibody (IgG) production in CHO cells. It was underpinned by a detailed analysis of the engineering environment of miniature bioreactors for rapid and accurate reproduction of Chinese hamster ovary (CHO) cell growth kinetics and product yields at larger scales specifically for fed-batch and high cell density cultivations.

Objective 1: Characterisation of microtitre plate (MTP) and evaluation of fed- batch operating strategies using MTP

Chapter 3 aims to characterise the initial CHO cell growth conditions using the 24-standard round well (24-SRW) that have sensor spots for an on-line monitoring of pH and dissolved oxygen (DO). Two different feeding strategies using bolus addition and FeedBead® system were evaluated using parallel MTP based on selected operating conditions.

Objective 2: Engineering characterisation of miniature bioreactors and evaluation of fed-batch operating strategies using MBR

Chapter 4 seeks to characterise engineering parameters of miniature bioreactors (HEL-BioXplore) for mixing time (T_m), volumetric oxygen transfer coefficient (k_La) and power requirement in MBR. Process condition from MTPs experiment was further evaluated with miniature bioreactor (HEL-BioXplore) for CHO cell growth kinetics, product yield and different feeding strategies.

Objective 3: Scale translation of different geometry of reactors at matched mixing time.

The aims were to validate scale-up conditions at the matched mixing time using laboratory scale 5 L stirred tank reactors (STR). The different designs and scales of bioreactors were compared for CHO cell growth kinetics and product yields.

Objective 4: Characterisation of a new micro-bioreactor (micro-Matrix) system for automated liquid addition and parallel control of operating parameters.

The aim was to characterise a novel, single use 24-well micro-bioreactor (micro-Matrix) for CHO cell growth and product yields. The system works on microtitre plates (MTP) footprint with automated liquid addition and parallel control of pH, temperature and dissolved oxygen (DO). The micro-Matrix was evaluated for its robustness, reproducibility and scalability of fed-batch system on bolus and continuous feeding.

Chapter 2 Materials and Methods

All experiments in this work were carried out using an adapted glutamine synthetase Chinese hamster ovary (CHO) cell line (strain CY01) expressing IgG_4 monoclonal antibody (generously provided by Lonza Biologics, Slough, UK).

2.1 Cell storage and recovery

Cells were cryostorage in liquid nitrogen using chemically defined medium (CD CHO medium, Life Technologies, Paisley, UK) containing 10 % dimethyl sulfoxide (DMSO) (Sigma-Aldrich, Gillingham, UK). For cell recovery, cells were thawed rapidly in water bath and re-suspended in 9 mL of warmed CD CHO medium, then centrifuged at 450 g for 5 minutes. The supernatant was decanted and the pellet was re-suspended in 5 mL of 20 mL warmed CD CHO medium and added back to shake flask (125 mL polycarbonate Erlenmeyer flasks with vent caps; Corning Life Sciences, New York, USA). The shake flask was incubated for 24 hours at 37°C, 5% CO_2 (Sanyo, Loughborough, UK) and agitated at 150 rpm on orbital shaker (Sartorius, Epsom, UK). After 24 hours, cells were checked for growth and viability before routinely sub-cultured.

2.2 Cell culture

2.3 Cell maintenance and media

Chinese hamster ovary (CHO) cell was routinely maintained in shake flasks (250 mL polycarbonate Erlenmeyer flasks with vent caps; Corning Life Sciences, New York, USA) at working volumes of 100 mL. Cells were cultured at 37°C and 5% CO_2 using an incubator (Sanyo, Loughborough, UK) on an orbital shaker (Sartorius, Epsom, UK). The shaking platform was set to agitate at 150 rpm. Cells were routinely sub-cultured every 3 or 4 days interval (for 25 passages) using a seed density of 0.2×10^6 viable cells ml^{-1}. These cells were sub-cultured using CD CHO medium (Life Technologies, Paisley, UK), with supplementation of 25 µM methionine sulphoximine (MSX) (Sigma-Aldrich). Methionine sulphoximine was added to the medium to maintain a selection of the recombinant gene.

2.4 Microtitre plate cultures

Experiments in chapter 2.3 use the 24-standard round well (SRW) microtitre plates. For fed-batch experiment, the CHO cells were cultured on pre-calibrated oxygen (Oxodish®) and pH (HydroDish®) sensors integrated in 24-well microtire plates (PreSens-Precision Sensing GmbH, Regensburg, Germany) for on-line monitoring of dissolved oxygen and pH respectively.

2.4.1 Batch cultures

Twenty four standard round well (24-SRW) (Ultra low attachment plates, Corning Life Sciences, New York, USA) was used in microtitre plates (MTPs) experiments. The Chinese hamster ovary cell was inoculated using MTPs at a seed density of 0.2×10^6 cells ml^{-1} with working volume of 850 µL and incubated at 37°C, 5% CO_2 using an incubator (Sanyo, Loughborough, UK). All cultures were shaken on 25 mm diameter orbital shaker (Sartorius, Epsom, UK) with rotational speeds of 220 rpm.

Chemically defined medium (CD CHO medium, Life Technologies, Paisley, UK), was used to culture the cells without the addition of methionine sulphoximine (MSX). Microtitre plates were covered with two types of sandwich covers system to minimise evaporation and contamination: CR1524 (for fast growing cells) and CR1524a (for slow growing cells) (Duetz *et al.*, 2000). The microtitre plates were held with metal clamps (Enzyscreen B.V., Holland). The sandwich lids were sterilised by autoclaving and subsequently oven dried before use.

2.4.2 Fed-batch (bolus feed)

The fed-batch CHO cell culture using microtitre plates were prepared initially, accordingly to the batch culture protocols. Briefly, all cultures was cultured with seed density of 0.2×10^6 cells mL^{-1}, working volume of 850 µL at 37°C, 5% CO_2 and shaken on orbital shaker with rotational speeds of 220 rpm. All microtitre plates were covered with sandwich cover, CR1524a (Enzyscreen B.V., Holland) to minimise evaporation and contamination (Duetz *et al.*, 2000), and held with metal clamps (Enzyscreen B.V., Holland). For on-line monitoring of dissolved oxygen and

pH, the CHO cells were cultured on pre-calibrated oxygen (Oxodish®) and pH (HydroDish®) sensors integrated in 24-well microtitre plates (PreSens-Precision Sensing GmbH, Regensburg, Germany). The 24-well with sensors was read out on the SDR SensorDish® reader.

The feeding strategy applied in this experiment was a bolus feed. Feeding of the cultures was commenced on day seven of cultivation after the glucose concentration was depleted below 2 gL^{-1} in each well. The medium used for feeding was CD CHO AGT powder (Life Technologies, Paisley, UK). The CD CHO AGT powder was made up to 10 fold concentrated feed with approximately 60 gL^{-1} glucose. The concentrated feed was added with additional glucose (Sigma-Aldrich) to make up glucose concentration to 150 gL^{-1}. One percent (v/v) of feed was fed to each well every day from day seven to maintain glucose concentration at 2 gL^{-1}. In order to minimise evaporation and changes in medium osmolality, the concentrated feed was diluted with sterilised deionised water such that liquid addition were 6 fold dilution and the concentration of nutrients per bolus shot was unchanged.

2.4.3 FeedBead®: Controlled glucose delivery

FeedBeads® (Kühner AG, Birsfelden, Switzerland) are polymer-based (silicone matrix) with embedded crystalline glucose that controlled glucose release by defined kinetic for continuous feeding in microbial cultivation of shaken systems (Jeude *et al.*, 2006). In the preliminary studies for determination of glucose concentration released from the silicone elastomer discs, FeedBeads® (diameter 6 mm) was added into a 100 mL shake flask (250 mL polycarbonate Erlenmeyer flasks with vent caps; Corning Life Sciences, New York, USA) of 12.5 mL Dulbecco's Phosphate Buffer Solution (Life Technologies, Paisley, UK). The shake flasks were incubated at 37°C, 5% CO_2 (Sanyo, Loughborough, UK) and shaken on orbital shaker (Sartorius, Epsom, UK) with rotational speeds of 150 rpm.

The glucose concentration released from silicone elastomer discs was determined by direct measurement of glucose concentration using YSI 2700 Select Bio Analyser (YSI Inc., Yellow Springs, Ohio, USA). The fed batch CHO culture in MTPs was prepared accordingly to the batch culture protocols. Briefly, all cultures was cultured

with seed density of 0.2 × 10^6 cells mL^{-1}, working volume of 850 µL at 37°C, 5% CO_2 and shaken on orbital shaker with rotational speeds of 220 rpm. All microtitre plates were covered with sandwich cover, CR1524a (Enzyscreen BV, Holland) to minimise evaporation and contamination (Duetz *et al*., 2000), and held with metal clamps (Enzyscreen B.V., Holland). The feeding strategy applied was FeedBeads® addition. One FeedBeads® silicone elastomer disc was fed to the cultures on day seven of cultivation after the glucose concentration was depleted below 2 gL^{-1} in each well. The glucose concentration released from silicone elastomer discs were determined by direct measurement of glucose concentration using YSI 2700 Select Bio Analyser (YSI Inc., Yellow Springs, Ohio, USA).

2.5 Micro-bioreactors (micro-Matrix) cultures

In this experiment, Chinese hamster ovary cell was inoculated using chemically defined medium (CD CHO medium, Life Technologies, Paisley, UK) without the addition of MSX. The cells were inoculated aseptically in the 24-deep well plate (DWP) cassette, integrated with PreSens sensors (PreSens-Precision Sensing GmbH, Regensburg, Germany) at a seed density of 0.2 × 10^6 cells ml^{-1} with working volume of 3.5 mL and incubated at 37°C, 5% CO_2 using an in-house incubator. The in-house incubator was built for controlling the temperature of the cabinet of micro-Matrix system. All cultures were shaken on built-in 25 mm diameter orbital shaker with rotational speed set at 270 and 300 rpm. The cassette was covered with the top plate that assembled with the aeration and liquid addition manifold (Figure 2.1). There was a gasket seal (on top of the cassette) and filter gas bars on the top plate to reduce the risk of cross contamination within the wells.

The temperature was controlled the at 37°C ± 0.5°C. pH was controlled at 7.1 ± 0.4 by sparging CO_2. The system was aerated using headspace aeration at a flow rate of 0.5 mL min^{-1} for the four main gaseous. For the control aeration system, DOT was control according to the standard of 30 % of air, while for the non-control aeration; it was direct sparging of 95 % compressed air and overlay with 5% CO_2. The overlay of 5 % of CO_2 is to mimic the same environment as an incubator shaker for 24-SRW. The liquid addition was added through the opening and closing of micro valve (Figure 2.2). Micro valve was calibrated accordingly using the external priming

module attached on top of the top plate. The opening and closing of the micro valve were determined by the pulse time. The pulse time was determined by finding the volume per pulse for a specific media used in cultivation. This is done by weighing the dosed liquid with certain pulsing times. Prior to inoculation, the complete top plate with aeration and liquid addition manifold and feeding bottle was sterilised at 121°C for 20 minutes.

For fed batch cultures, feeding strategy applied was either bolus fed or continuous feed. The cultures were fed to maintain glucose concentration at 2 gL^{-1}. The medium used for feeding was CD CHO AGT powder (Life Technologies, Paisley, UK). The feeding media were prepared as mentioned in the section 2.3.2.

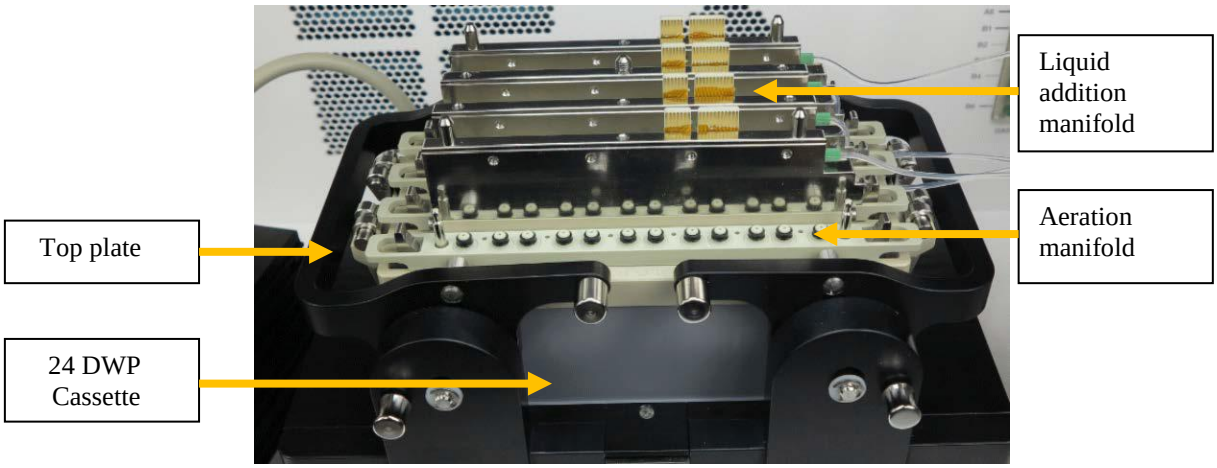

Figure 2.1: Top plate assembled with aeration and liquid addition manifold.

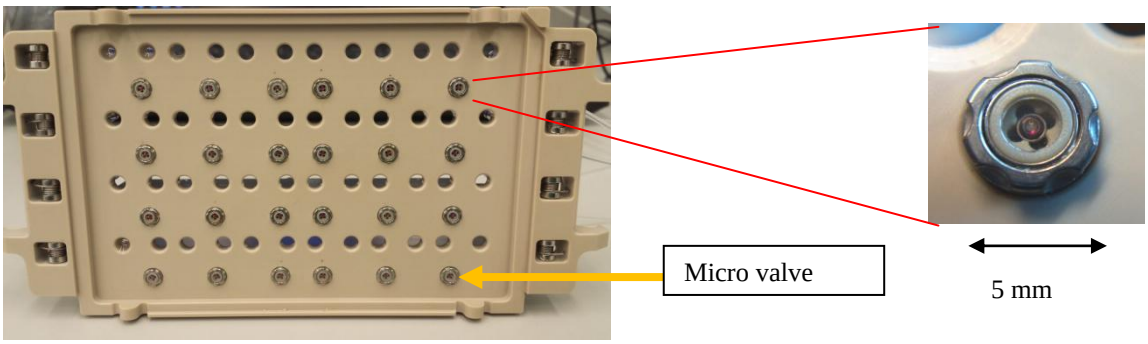

Figure 2.2: Microvalve for the liquid additions.

2.6 Miniature stirred bioreactors (HEL-Bioxplore) cultures

For miniature stirred bioreactors, it was carried out with either 2 or 4 vessels made of borosilicate glass which run in parallel. The vessels were modelled based on the lab-scale 5 L vessel with working volume 1:1 aspect ratio. The working volume of the vessel was 0.35 L. The four vessels were housed in a polyblock that control the temperature of the vessels. Figure 2.3 shows the details of the miniature stirred bioreactors used in this experiment. These vessels were sealed with stainless steel head plate and tightened with stainless steel tightening collar. The head plate accommodates the on-line probes for temperature, pH and dissolved oxygen. For pH and DOT probes, the probe used was Easyferm 120 (Hamilton, Bonaduz, Switzerland) and Oxyferm 120 FDA (Hamilton, Bonaduz, Switzerland) respectively.

The temperature was controlled using the polyblock at 37°C ± 0.5°C. pH was controlled at 7.1 ± 0.1 by sparging CO_2 or by the addition of a sodium carbonate buffer (100 mM Na_2CO_3, 100 mM $NAHCO_3$). Aeration in the bioreactor vessel was achieved either by two type of spargers; horseshoe sparger or singular hole sparger. DOT was maintained at 30% ± 1% by sparging air, oxygen or nitrogen using a standard laboratory rotameter (Cache Quality Instrumentation, Wakefield, UK) at a flow rate of 50 mL min^{-1}. Agitation was provided either by a single 3 blade marine impeller (direct driven) or 4 bladed marine impeller (magnetic bottom driven) rotating at 450 rpm and 400 rpm respectively. Prior to inoculation, the culture vessel was sterilised at 121°C for 20 minutes with 0.2 L of deionised water which was removed aseptically after the sterilisation.

CHO cells were cultured with seed density of 0.2×10^6 cells mL^{-1}. Chemically defined medium (CD CHO medium, Life Technologies, Paisley, UK), was used to culture the cells without the addition of methionine sulphoximine (MSX). For fed batch cultures, feeding strategy applied was a bolus and continuous fed. For bolus addition, the cultures were fed once a day to maintain glucose concentration at 2 gL^{-1}. For the continuous feed, the culture was continuously fed over 24 hours/day with calculated feeding regimes to maintain the glucose concentration at 2 gL^{-1}. The medium used for feeding was CD CHO AGT powder (Life Technologies, Paisley, UK). The CD CHO AGT powder was made up to 10 fold concentrated feed with approximately 60 gL^{-1} glucose. The concentrated feed was added with additional

glucose (Sigma-Aldrich) to make up glucose concentration to 150 gL^{-1}. Metabolites (glutamine, glutamate, glucose, lactate, ammonium) and osmolality were monitored daily using a NOVA Bioanalyser 400 or NOVA Bioprofile Flex (Nova Biomedical, Cheshire, UK).

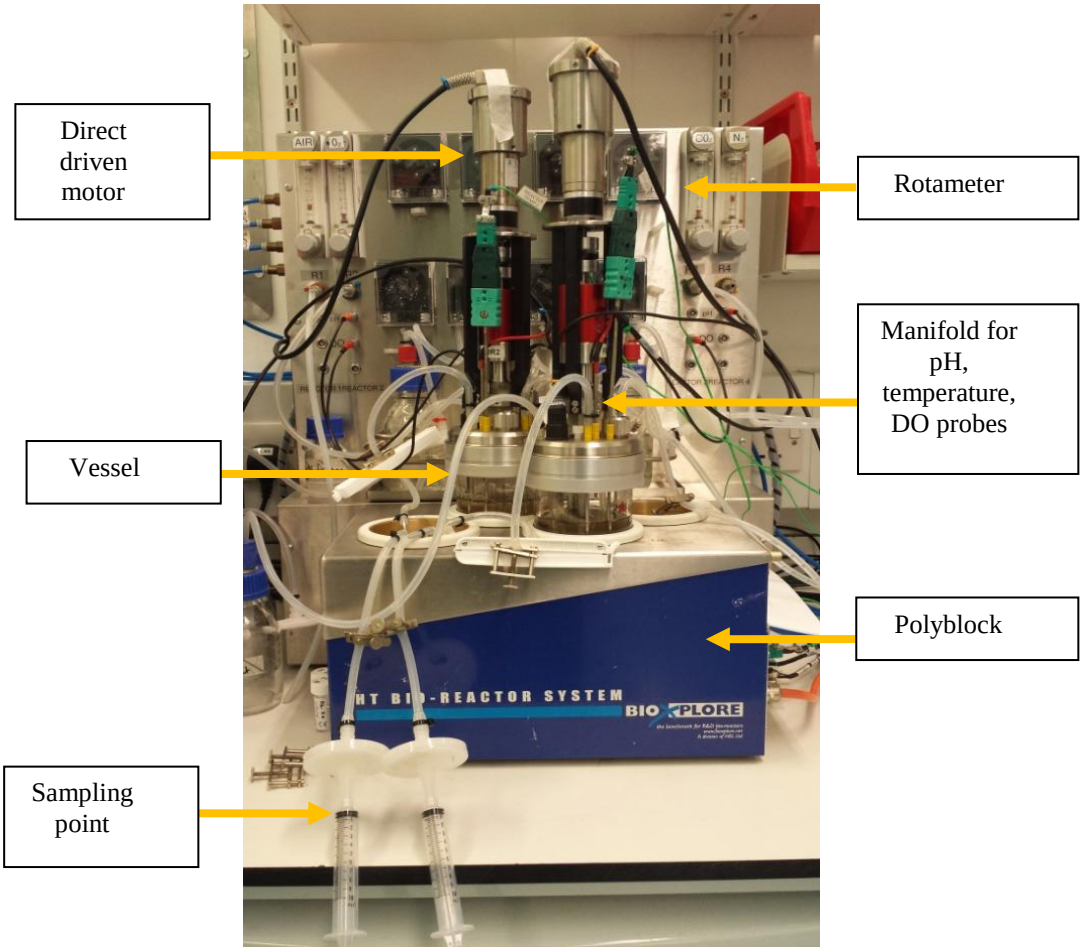

Figure 2.3: HEL-BioXplore miniature bioreactors.

2.7 Stirred tank bioreactor (STR) cultures

The experiments in this chapter were carried out with two bench top 5 L stirred tank bioreactors (Biostat B-DCU, Sartorius, Epsom, UK) run in parallel with a working volume of 3.5 L. The bioreactors consisted of borosilicate glass vessel supported with stainless steel scaffold and attached to a stainless steel head plate. The head plate accommodates the on-line probes for temperature, pH and dissolved oxygen. The operating parameters (temperature, pH, dissolved oxygen) in the bioreactors were set in a Biostat B-DCU supply tower located within the two bioreactors. The temperature was controlled using an electrical heating jacket (covered around the glass vessel) at 37°C ± 0.1°C. pH was controlled at 7.1 ± 0.1 by sparging CO_2 or by the addition of a sodium carbonate buffer (100 mM Na_2CO_3, 100 mM $NAHCO_3$).

Aeration in the bioreactor vessel was achieved via horseshoe type sparger with 5 aeration holes. DOT was maintained at 30% ± 1% by sparging air, oxygen or nitrogen using a standard laboratory rotameter at a flow rate of 100 mL min^{-1}. Agitation was provided by a single three-blade segment marine impeller rotating at 260 rpm. Prior to inoculation, the culture vessel was sterilised at 121°C for 20 minutes, with 2 L of deionised water which was removed aseptically after the sterilisation. CHO cells were cultured with seed density of 0.2×10^6 cells mL^{-1}. Chemically defined medium (CD CHO medium, Life Technologies, Paisley, UK), was used to culture the cells without the addition of methionine sulphoximine (MSX).

For fed batch cultures, feeding strategy applied was a bolus fed. The cultures were fed once a day to maintain glucose concentration at 2 gL^{-1}. The medium used for feeding was CD CHO AGT powder (Life Technologies, Paisley, UK). The CD CHO AGT powder was made up to 10 fold concentrated feed with approximately 60 gL^{-1} glucose. The concentrated feed was added with additional glucose (Sigma-Aldrich) to make up the glucose concentration to 150 gL^{-1}. Metabolites (glutamine, glutamate, glucose, lactate, ammonium), were monitored daily using a NOVA Bioanalyser 400 or NOVA Bioprofile Flex (Nova Biomedical, Cheshire, UK).

2.8 Engineering characterisation of reactors process

2.8.1 Mixing time

Mixing time was measured in the HEL-BioXplore miniature bioreactor using the pH tracer method. The experiment was conducted using the horsehoe type and singular hole sparger and two type of impellers; direct driven and magnetic driven. Different gas flow rates and impeller speeds were tested. The 500 mL reactor vessel was filled with 300 mL of RO water. Then, it was added with 2 N KOH to increase the medium pH. Once the pH has a steadied reading, a tracer of 2 N HCL was added to the medium. By using a stopwatch, the time taken for the pH reading to drop over 95 % of the pH difference was measured as the mixing time (T_m). The different pH value was considered as the corresponding mixing intensity. Figure 2.4 shows the tracer was injected opposite to the pH electrode, at 10 mm from the surface. The pH electrode was placed at 20 mm from the vessel bottom.

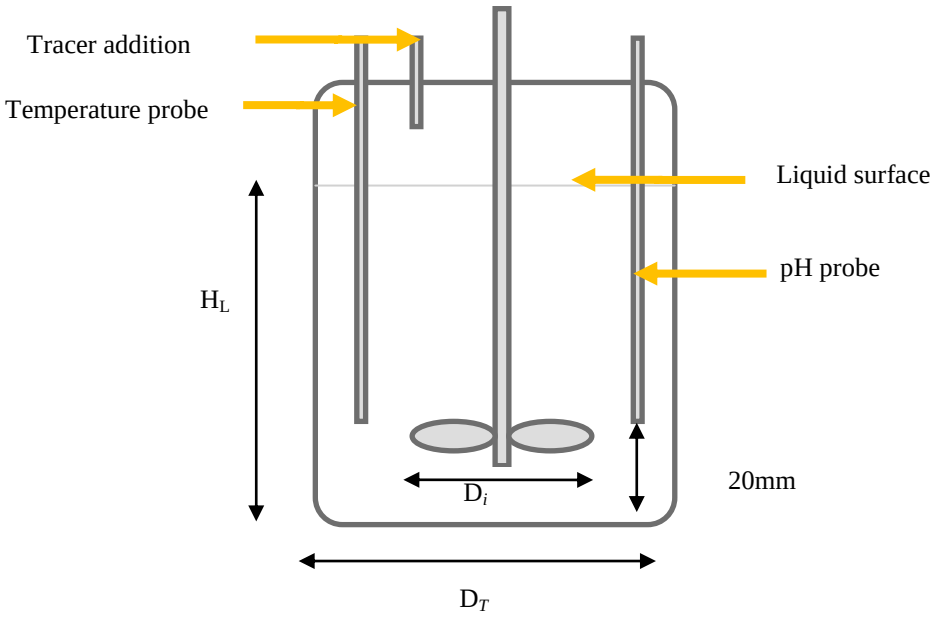

Figure 2.4: Schematic of the bioreactor set-up for mixing experiments. The tracer was manually added as bolus addition on top of the liquid surface (adapted from Xing *et al*., 2009).

The following homogeneity for mixing was considered:

$$H_t = \frac{pH_t - pH_i}{pH_f - pH_i} \tag{2.1}$$

2.8.2 Volumetric oxygen transfer coefficient

The estimation of the oxygen transfer coefficient (k_La) in bioreactor is usually determined experimentally. The oxygen mass transfer coefficient (k_La) was determined using the static gassing out method as mentioned by Wise (1951), (Lamping *et al.*, 2003) and (Betts *et al.*, 2006). Prior to experiment, the probe response time (τ_p) was measured and the DO electrode was calibrated to 100 % and 0 % air saturation by sparging air and nitrogen respectively. The experiment was carried out using the CD CHO medium. k_La was measured in a HEL-BioXplore 500 mL miniature bioreactor filled with 350 mL CD CHO medium and controlled at the operating temperature, 37°C. The 100 % oxygenated medium was lowered by sparged nitrogen until the oxygen level was totally scrubbed off from the medium (0 %). The air supply was then quickly pumped into the medium at a constant flow rate and the increase in the oxygen concentration over time was recorded. The re-oxygenation at steady state is measured between 20 % and 80 % of saturation. Different gas flow rates and impeller speeds were tested.

The oxygen mass transfer coefficient (k_La) was calculated from the oxygen mass balance equation:

$$OTR = \frac{dC}{dt} = k_L\, a\, (C^* - C_L) \tag{2.2}$$

Where,
- OTR Oxygen transfer rate (mol m^{-3} h^{-1})
- k_La Oxygen mass transfer coefficient (h^{-1})
- C* Dissolved oxygen concentration saturation (mol m^{-3})
- C_L Dissolved oxygen concentration in the liquid (mol m^{-3})

k_La is given by calculating the slope of the graph of ln (C^* - C_L) over period of time which has a gradient of k_La as described by:

$$ln\,(C^* - C_L) = -k_L\,a\;t \tag{2.3}$$

2.8.3 Power input

Power input was determined using the theoretical of ungassed power correlations. The impeller diameter for magnetic-driven impeller and direct driven impeller, a value of 0.033 m and 0.034 m was used respectively. Since, this is ungassed power correlation; volumetric gas flow rate was negligible. For theoretical calculation, the liquid was assumed to be close to water; with density of 998.2 kg m-3, viscosity of 1.003 x 10-3 Nm-2. The ungassed power equation described as:

$$P_{ug} = N_P\,\rho N^3 {D_i}^5 \tag{2.4}$$

2.9 Analytical techniques

Approximately 850 µl medium was aseptically removed from shake flask cultures, while a sacrificial well approach were used for MTP experiments (Micheletti *et al*., 2006). Evaporation of the culture was monitored throughout the experiment by gravimetric analysis. All culture data was corrected for evaporation losses using ratio between initial volume and the volume removed for analysis. Unless stated otherwise, all MTP cultures were performed in triplicate. All data was averaged and standard deviations were calculated.

2.9.1 Determination of cell number and viability

Cell number and viability were analysed using a haemocytometer (Olympus IX70, Southend-on-Sea, UK) or by automated cell counting devices, VI-Cell XR (Beckman Coulter, High Wycombe, UK) which automates the trypan blue dye exclusion

method for counting cells, with samples diluted using Dulbecco's Phosphate Buffer Solution (Sigma Aldrich) as necessary.

2.9.2 Cell size analysis

The average cell size diameter was determined using a CASY analyser (Innovatis, Bielefeld, Germany). The measurement was set up to 40 µm with a 150 µm orifice for 5 times repeat measurement. The samples were diluted using 10 mL of Casyton buffer as necessary.

2.9.3 Determination of antibody titres

The samples for IgG antibody titres analysis were centrifuged and the supernatant was stored frozen prior quantification. The quantification was determined by an Agilent 1200 High performance liquid chromatography (HPLC) (Agilent Technologies, South Queensferry, UK) and analysed using 1 mL HiTrap Protein G HP column (GE Healthcare, Buckinghamshire, UK). The gradient for HPLC was performed with a sodium phosphate buffer (10 mM NaH_2PO_4, 10 mM Na_2HPO_4, adjusted to pH 7.0) and glycine buffer (20 mM, adjusted to pH 2.8). The elution peak was measured by UV at 280 nm. The mAb concentration was determined by integrating the elution peak and using a standard curve of purified mAb.

2.9.4 Determination of metabolites

Metabolites (glucose, lactate, ammonia, glutamine, glutamtate) were measured using a NOVA 400 BioProfileVR or NOVA Bioprofile Flex automated metabolite analyser (Nova Biomedical, Cheshire, UK). Samples were diluted with deionised water as necessary.

2.10 Derived growth calculations

2.10.1 Specific growth rate and doubling time

The maximum specific growth rate (μ_{max}) was determined from the exponential growth phase by plotting the natural logarithm of viable cell concentration measured against time. It was defined by:

$$\frac{dx}{dt} = \mu x \tag{2.5}$$

$$\mu = \frac{Ln\ X_{V1} - Ln\ X_{V0}}{t_1 - t_0} \tag{2.6}$$

Where,

	Ln	Natural logarithm (Log_e)
	X_{V1}	Viable cell concentration at time 1 (cell mL^{-1})
	X_{V0}	Viable cell concentration at time 0 (cell mL^{-1})
	μ	Specific growth rate (h^{-1})
	t_1	Elapsed time at time 1 (h)
	t_0	Elapsed time at time 0 (h)

The cell doubling time is derived by integrating equation 2.6 and rearranging:

$$Ln\frac{x_1}{x_0} = \mu\ (t_1 - t_0) \tag{2.7}$$

$$t_d = \frac{Ln\ 2}{\mu} \tag{2.8}$$

Where, t_d Doubling time (h)

Ln 2 Log_e 2

μ Specific growth rate (h^{-1})

t_1 Elapsed time at time 1 (h)

t_0 Elapsed time at time 0 (h)

2.10.2 Integral viable cell concentration (IVCC)

The integral viable cell concentration (IVCC) is calculated as the average of viable cell concentration between two data points and multiplied by the time difference between the two data points:

$$IVC_i = \left(\frac{X_{V0} + X_{V1}}{2}\right) . (t_1 - t_0)$$

(2.9)

Where, X_{V1} Viable cell concentration at time 1 (cell mL^{-1})

X_{V0} Viable cell concentration at time 0 (cell mL^{-1}

t_1 Elapsed time at time 1 (h)

t_0 Elapsed time at time 0 (h)

Whilst, the cumulative integral viable cell concentration (cIVC) is calculated as follows:

$$cIVC = \sum IVC_i$$

(2.10)

2.10.3 Average specific antibody production (q_p)

The average specific antibody production (q_p) was measured for product formation (IgG) concentration over culture cumulative cell time. The calculation was determined by dividing cumulative antibody concentration by cumulative integral viable cell concentration.

$$q_p = \left(\frac{[IgG]}{\left(\frac{X_{V0} + X_{V1}}{2}\right) . (t_1 - t_0)} \right) \tag{2.11}$$

Where, X_{V1} Viable cell concentration at time 1 (cell mL^{-1})

X_{V0} Viable cell concentration at time 0 (cell mL^{-1})

t_1 Elapsed time at time 1 (h)

t_0 Elapsed time at time 0 (h)

2.10.4 Specific glucose consumption (q_{glc})

The specific glucose consumption (q_{gluc}) is a calculation of measured glucose consumption over elapsed time in cell culture. q_{gluc} is determined by plotting of linear slope of cumulative glucose consumption cq_{glc} (pg L^{-1}) measured over the cumulative integral viable cell concentration cIVC (cells d mL^{-1}):

$$q_{glc_i=} \left([glucose_i] - [glucose_{i-1}] + [glucose_{feed}] \right) \tag{2.12}$$

$$cq_{glc} = \sum q_{glci\,i}$$

2.11 Statistical analysis

The data were analysed by paired t-test analysis and the differences were considered significant when P value was < 0.05.

Chapter 3 Characterisation of microtitre plates (MTPs) and evaluation of fed-batch operating strategies

3.1 Introduction

Productions of biopharmaceuticals are complicated processes which involve long bioprocess development times, are laborious and costly (Li *et al.*, 2010). In order to reduce the materials and cost, several alternatives have been considered to accelerate the process development of biopharmaceuticals (Micheletti *et al.*, 2006). Microtitre plates (MTP) experimentation which focused on principles of parallelism and high throughput is seen as excellent options (Lye *et al.*, 2003; Micheletti *et al.*, 2006). Moreover, MTPs are designed to fulfil the bioprocess development requirements for selection and screening of high producer clones, medium formulation and feeding strategies (Betts and Baganz, 2006).

Previous works have demonstrated the performance of microtitre plate (24-SRW) in the suspension culture of hybridoma cell line (Barrett *et al.*, 2010). Additionally, Silk *et al.* (2010) have established the bolus feeding strategy for GS-CHO cells in shaken MTPs. In this chapter, the preliminary studies of Chinese hamster ovary (CHO) cell growth profile using the 24-standard round well (24-SRW) was characterised. The initial experiment focused on the characterisation of sandwich covers (CR1524 and CR1524a) for cell growth and viability, metabolites concentration (glucose, lactate, and ammonium), osmolality and IgG antibody production. For fed batch operations, dissolved oxygen and pH was monitored using the pre-calibrated oxygen (Oxodish®) and pH (HydroDish®) sensors integrated in 24-well microtitre plates (PreSens-Precision Sensing GmbH, Regensburg, Germany). Moreover, different types of feeding strategies were applied in MTPs was further investigated for enhanced growth and productivity.

Chapter aims and objectives:

- To reproduce the growth profile and product formation of mAb producing CHO cell line (CY01) in microtitre plates (24-SRW) (Silk, 2014).

- To investigate the capability of on-line monitoring of dissolved oxygen and pH using PreSens pre-calibrated sensors integrated in 24-well microtitre plates of fed-batch mode of operation.
- To investigate two types of fed-batch mode applied in the microtitre plates (24-SRW) culture of CHO cells.

3.2 Parallel microtitre plate (MTPs) of CHO cell in batch mode

The preliminary experiments compared the initial growth conditions of CHO cell in the batch cultures with two types of commercial sandwich covers: CR1524 (for fast growing cells) and CR1524a (for slow growing cells). The former consists of a stainless steel foil (0.2 mm) with pinhole to control the headspace aeration rate and evaporation (Duetz *et al.*, 2000). On contrary, CR1524a covers have 5 layers to seal the MTP which are (a) stainless steel lid for rigidity, (b) microfiber filter (c) an ePTFE filter (0.3 micron) (d) a stainless steel foil with pinhole (e) silicone layer of 96 holes to hermetically seal the MTP. According to Silk *et al.* (2010) two important criteria for successful microtitre plate experimentations were to maintain sterility and control of evaporation rate. The exchange of headspace air was 1.1 mL min^{-1} and 0.25 mL min^{-1} for CR1524 and CR1524a respectively. Whilst, the evaporation rate measured at 30°C with 50 % humidity was 30 µL $well^{-1}$ day^{-1} and 6 µL $well^{-1}$ day^{-1} for CR1524 and CR1524a respectively (Duetz, 2007).

The initial work by Silk (2014) shows the drawback of Breatheasy membrane (Diversified Biotechnology) to seal the MTPs. The evaporation rate for shaken MTPs using the Breatheasy membrane with fill volume of 0.8 µL was found at rate of 38 % (120 rpm) and 41 % (180 rpm) volume loss after 144 hours. Silk (2014) further explored the feasibility of sandwich cover by Enzyscreen to overcome the evaporation problem. The sandwich cover CR1524 was used and the evaporation rate measured was 24 µL $well^{-1}$ day^{-1} compared to 50 µL $well^{-1}$ day^{-1} for Breatheasy membrane. Table 3.1 summarised the evaporation rate observed during the MTP batch experiment. The evaporation rate obtained in this work is comparable with Silk *et al*. (2010) and Enzycreen B.V. Holland.

Besides that, the shaking diameter use in this work was 25 mm compared to 20 mm (Silk, 2004) which may gave effect on oxygen transfer rate (OTR) capacity in MTP. According to (Maier and Buchs, 2001), OTRmax can be increased by 0.04 % if the system has the similar condition but different shaking diameter.

Table 3.1: Comparison of absolute evaporation rate during batch CHO cells.

Culture vessel	Sterile covers	Cell type	Evaporation rate (µL well^{-1} day^{-1})	Reference
24-SRW	Breatheasy (Diversified Biotech)	Hybridoma cell line (VPM8)	10% losses from initial fill volume at 37°C	Barrett *et al*. (2010)
24-SRW	Breatheasy (Diversified Biotech)	CHO-S (MedImmune)	50 at 37°C	Silk *et al*. (2010)
24-SRW	CR1524 (Enzyscreen)	GS-CHO (MedImmune)	24 at 37°C	Silk *et al*. (2010)
24-SRW	CR1524a (Enzyscreen)	GS-CHO (Lonza Biologic)	8 at 37°C	This work
24-SRW	CR1524a (Enzycreen)	n/a	6 at 30°C	Enzycreen

3.2.1 Growth kinetics and antibody productivity

The initial growth rate of batch CHO cells cultured in MTP for both sandwich covers was very similar. Sandwich cover CR1524 gave considerably higher viable cell concentration (VCC) than the MTP culture with CR1524a cover (Figure 3.1 A). MTP culture with CR1524 cover had VCC of 8.51± 0.181 x 10^6 cell mL^{-1} and MTP culture with CR1524a cover had VCC of 7.92± 0.078 x 10^6 cell mL^{-1}. The paired t-test was performed to determine the viability of CHO cell culture in the two MTPs system. There was no significant difference between the VCC of CR1524 cultures with the CR1524a cultures (p-value 0.18). The peak VCC obtained in this experiment was notably higher compared with VCC produced by Silk (2014) with 4.40 x 10^6 cell mL^{-1} on day 8 with the similar sandwich cover CR1524.

The difference observed in the previous work was the agitation speed at 180 rpm compared to 220 rpm optimised agitation speed (data not shown) applied in this work. Duetz, (2007) noted that high rotational speed would likely support growth in culture due to enhanced mixing. In terms of CHO cell viability in batch cultures, MTP with sandwich cover CR1524a shows high cell viability over a considerably longer time (until day 12 of culture) than MTP with sandwich cover CR1524 (Figure 3.1 B). The extra silicone layer provided with the CR1524a had prolonged the cell viability as it provide better sterility and hermetically seal the MTPs.

A higher IgG antibody production (Figure 3.1 C) was observed in the MTP with CR1524a cover (for slow growing cells) with 0.86 gL^{-1} compared to MTP with CR1524 cover (for fast growing cells) with 0.55 gL^{-1} at the end of culture. The higher antibody production might due to the longer time of fermentation that occurs in the MTP with CR1524a with 12 days of cultivation than 9 days for MTP culture with CR1524. Apart from that, cell specific productivity (q_p) gave comparable results when plotted for product formation with IVCC (Figure 3.2). The CR1524a gave the highest q_p with 26.1 pg $cell^{-1}$ d^{-1} compared to CR1524 with 17.2 pg $cell^{-1}$ d^{-1} correspondingly.

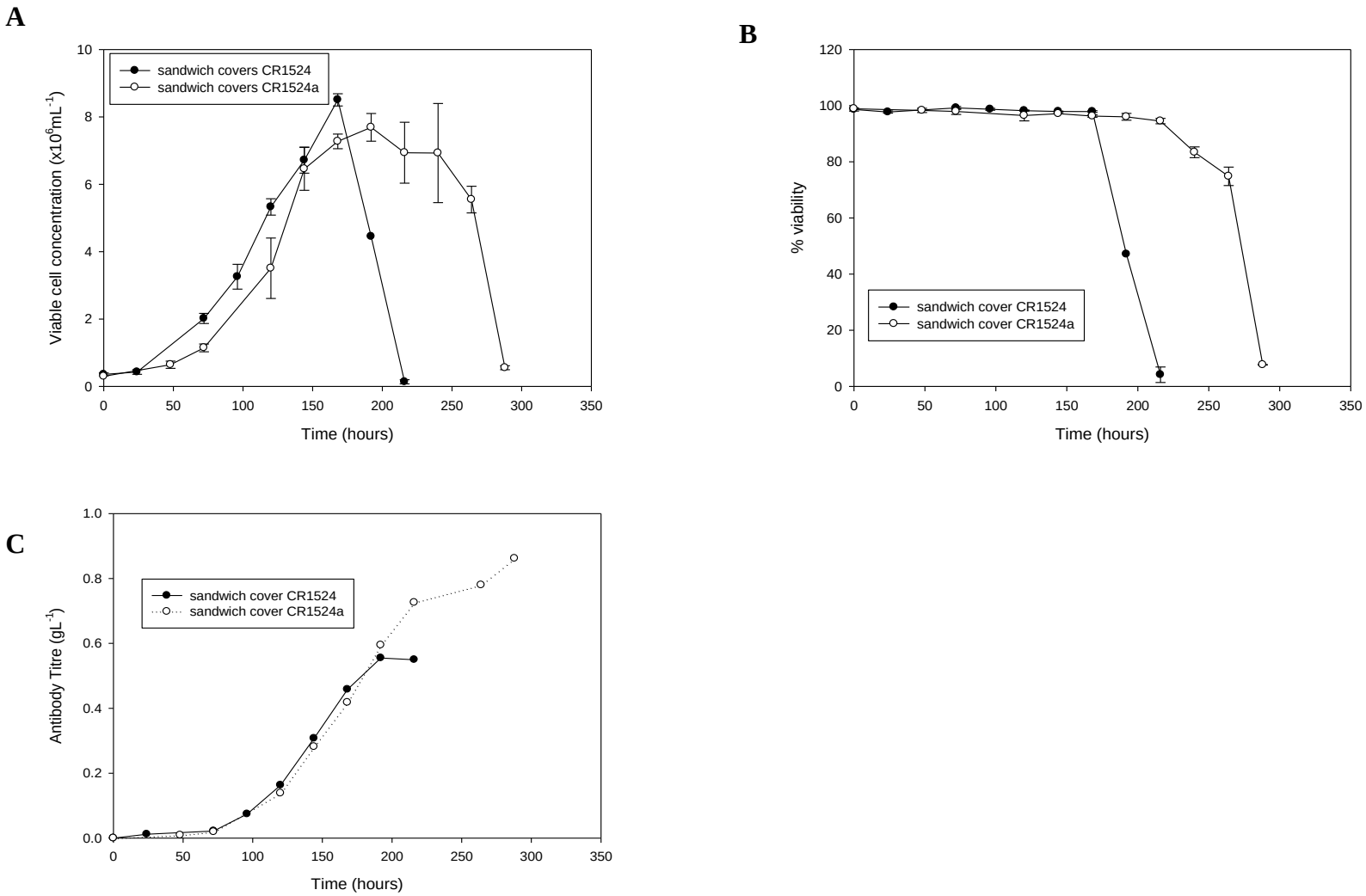

Figure 3.1: CHO growth kinetics in batch culture for shaken 24-SRW microtitre plates (MTP) with two different sandwich covers: CR1524 (for fast grow cells) (●) and CR1524a (for slow grow cells) (○); A: Viable cell concentration; B: Cells viability; C: IgG antibody titre. Error bars represent one standard deviation about the mean (n = 3).

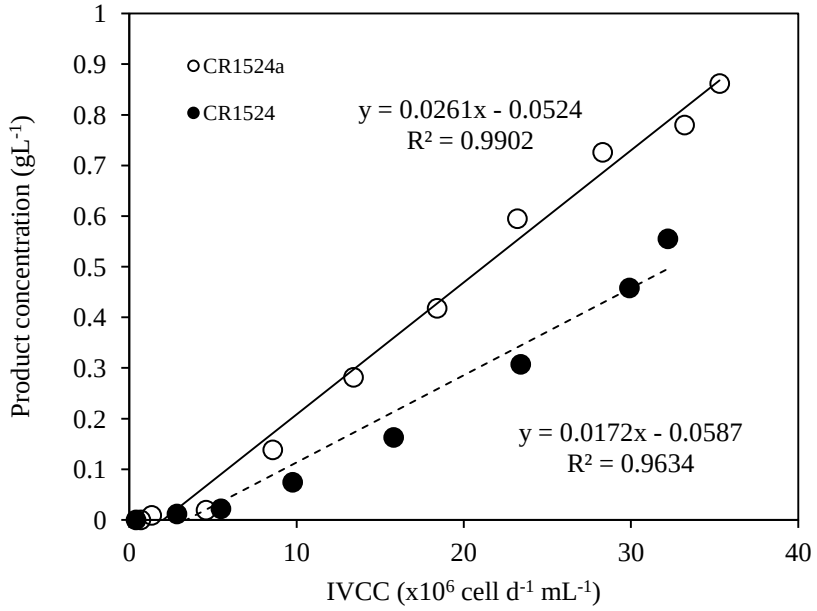

Figure 3.2: Comparison plots of product formation vs IVCC for the two covers with trend line, solid line (○) represents CR1524a and dashed line (●) represents CR1524.

3.2.2 Metabolites analysis

Glucose is known as the major carbon source employed in the CHO cell line fermentation (Altamirano *et al*., 2000). For batch culture, glucose was utilise rapidly by CHO cells metabolism making the culture inefficient and subsequently increase the accumulation of by-product of lactate and ammonium (Altamirano *et al*., 2000). The concentration of glucose in both 24-SRW MTP with sandwich covers (CR1524 and CR1524a) dropped below 2 gL^{-1} after seven days (168 hours) of culture with very similar uptake rates (Figure 3.3 A). Result showed that the glucose exhaustion had affected the CHO viable cell concentration. The cells were observed entering the death phase as glucose was no longer available.

By contrast, the lactate concentration in the 24-SRW MTPs showed variation between the two sandwich covers. For MTP with CR1524 cover, the highest lactate concentration was observed on day 9 with 4.59 gL^{-1}, while MTP with CR1524a the lactate production peaked on day 5 with 2.29 gL^{-1} (Figure 3.3 B). The higher maximum lactate concentration in MTP with CR1524 cover is

probably because the cells were in the death phase and not consumed the lactic acid secreted, which led to poorer cell viability and increase in pH (Gagnon *et al.*, 2011). Besides that, there is the possibility of a lactate metabolic shift by the cells due to unavailability of primary carbon sources. In animal cell metabolism, glucose might be synthesised from lactate during the initial conversion of lactate through pyruvate, catalysed by lactate dehydrogenase (LDH) (Tsao *et al.*, 2005). The consumption of lactate reduces its own accumulation, thus alleviating the adverse effect on cell viability. This explanation is in agreement with research using metabolic flux analysis on lactate consumption (Altamirano *et al.*, 2006) and feeding lactate directly (Li *et al.*, 2012) for improvement of CHO cell metabolism.

Ammonia concentration was observed to vary between the two MTPs (Figure 3.4 A). Microtitre plates (MTP) with cover CR1524 showed higher ammonia concentration compared to MTP with cover CR1524a. Microtitre plates with cover CR1524 ammonia concentration peaked on day 9 of cultivation with 8.02 $mmolL^{-1}$, whilst microtitre plates with cover CR1524a peaked on day 12 with 3.84 $mmolL^{-1}$. The elevated concentration of ammonia suggests that increased osmolality had shift the metabolism to favour formation of by-products such as ammonia and lactate (Zhu *et al.*, 2005).

The dramatic reduction in viable cell concentration (Figure 3.1 A) was observed during the growth phase as a result of high levels of osmolality (450 – 650 mOSm Kg^{-1}). The highest osmolality concentration was observed in cultures using sandwich cover CR1524 with 624.3 mOSm Kg^{-1}, while those with cover CR1524a reached a value of 498.6 mOSm Kg^{-1} (Figure 3.4 B). Zhu *et al.*, (2005) also showed that high osmolality appeared to accelerate the cell death and led to rapid decrease in viable cell concentration. Furthermore, the results suggest that increased osmolality are the consequence of the high lactate production rate (Figure 3.3 B) in the culture.

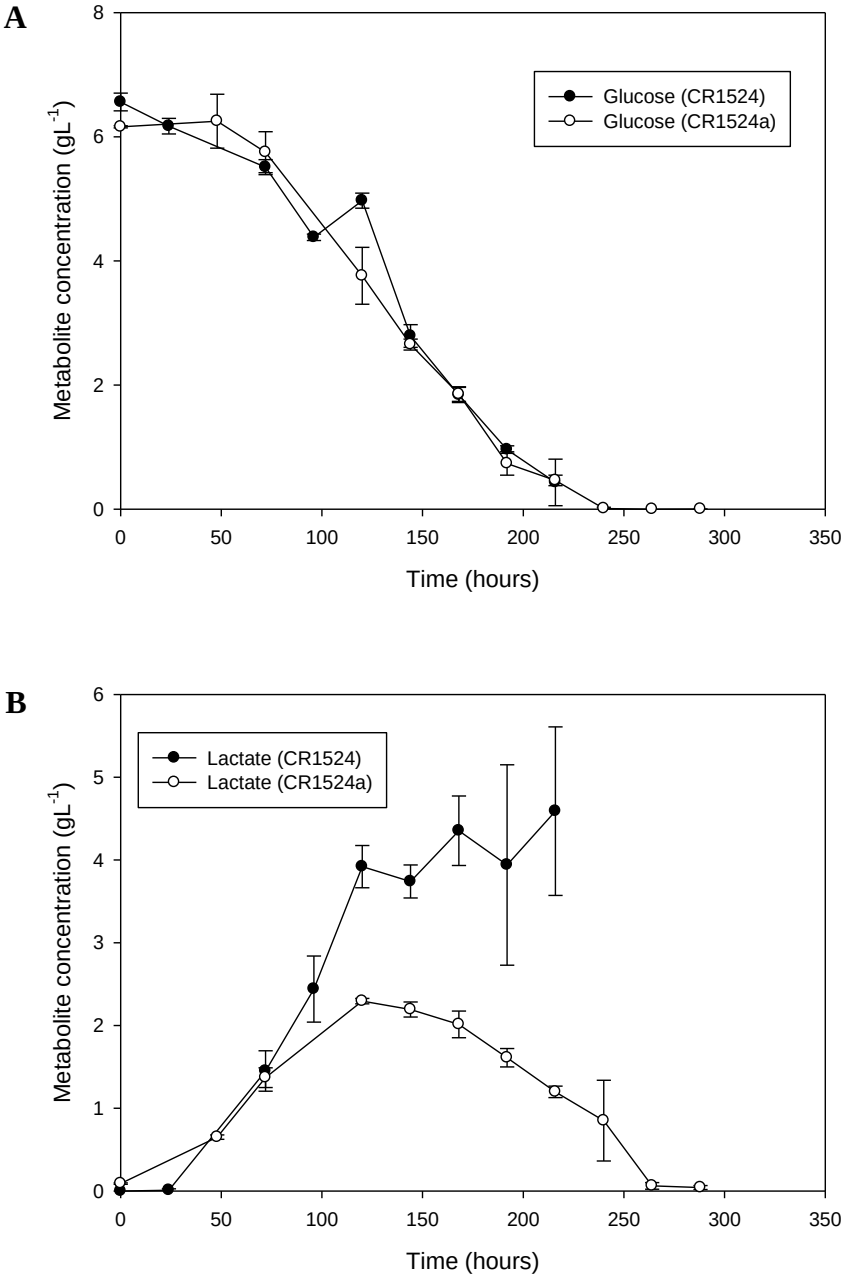

Figure 3.3: CHO metabolites concentration in batch culture for shaken 24-SRW microtitre plates (MTP) with two different sandwich covers: CR1524 (for fast grow cells) (●) and CR1524a (for slow grow cells) (○). A: Glucose concentration and B: Lactate concentration. Error bars represent one standard deviation about the mean (n = 3).

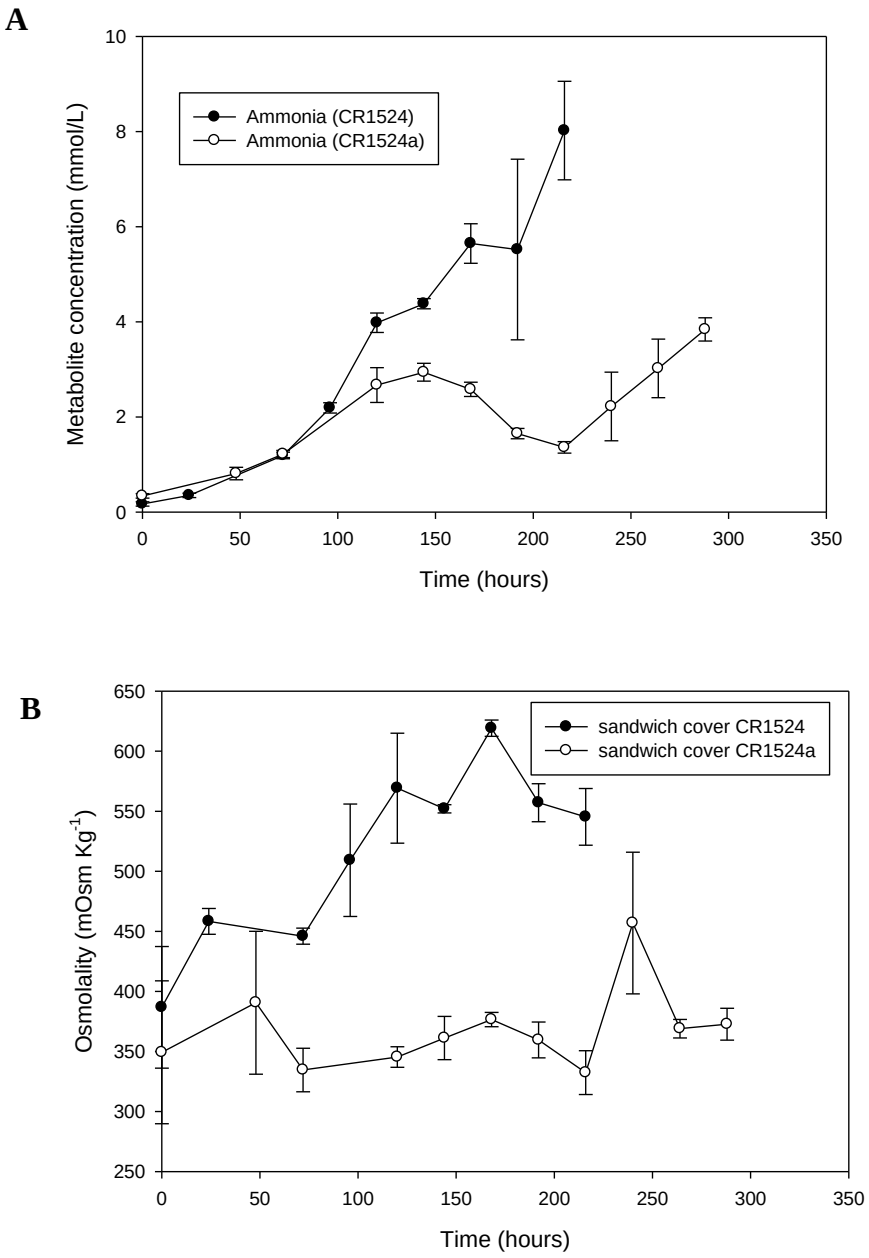

Figure 3.4: CHO ammonium and osmolality concentration in batch culture for shaken 24-SRW microtitre plates (MTP) with two different sandwich covers: CR1524 (for fast grow cells) (●) and CR1524a (for slow grow cells) (○). A: Ammonium and B: Osmolality. Error bars represent one standard deviation about the mean (n = 3).

3.3 Parallel microtitre plates (MTPs) of CHO cell in fed-batch mode

3.3.1 Growth kinetics and antibody productivity

The preliminary fed-batch mode experiments were done to compare the initial growth condition of CHO cells with two types of sandwich covers: CR1524 (for fast growing animal cells) and CR1524a (for slow growing animal cells). The sandwich covers were important for CHO cell cultured in MTP to minimise the liquid losses throughout the cultivation. Both covers provided efficient sterile condition for the 24-SRW MTP as no microbial contamination was observed over few experiments. The feeding strategy applied was daily bolus feed addition in each well for 6 days until day 13.

The growth profile for cultures with either cover was comparable (Figure 3.5). Both cultures had a prolonged exponential phase but reached the peak viable cell concentration at different days. Peak viable cell concentration was higher in the MTP with sandwich cover CR1524 (for fast growing cells) (9.01×10^6 cell mL^{-1} on day 8) than MTP with sandwich cover CR1524a (for slow growing cells) (8.71×10^6 cell mL^{-1} on day 7) (Figure 3.5 A). Even though, the viable cell concentration (VCC) was higher in culture using CR1524, the cell viability was extremely poor compared to culture using CR1524a. At the end of experiment on day 14, the cultures in MTPs with sandwich cover CR1524a had a viability of 82.5% compared to cultures in MTP with CR1524 a viability of 1.2% (Figure 3.5 B). Besides that, the low percentage viability might be due to the high rate of water loss (high evaporation rate) from each well that occurs during cultivation. This is attributed to the low evaporation rate measured through the CR1524a cover with 8 µl $well^{-1}$ day^{-1} compared to 30 µl $well^{-1}$ day^{-1} for CR1524 cover (Duetz, 2007).

The titres of IgG antibody production was found higher compared to the batch culture system. The fed-batch culture MTP with CR1524 and CR1524a cover

gave final IgG titres of approximately 1.30 gL^{-1} and 1.25 gL^{-1} respectively (Figure 3.6). The slightly higher IgG titre antibody production in MTP with CR1524 could be due to evaporation of wells leading to increased culture osmolality as discussed by Barrett *et al*. (2010) and Silk *et al*. (2010). They discussed that higher osmolality in culture might contributed to the higher final antibody titres in MTP. Silk *et al*., (2010) reported that final IgG in 24-SRW was 1.5 gL^{-1} with final osmolality of 506 $mOsmKg^{-1}$. Furthermore, high specific antibody production at elevated osmolality was well documented in other literature (Takagi *et al*., 2000).

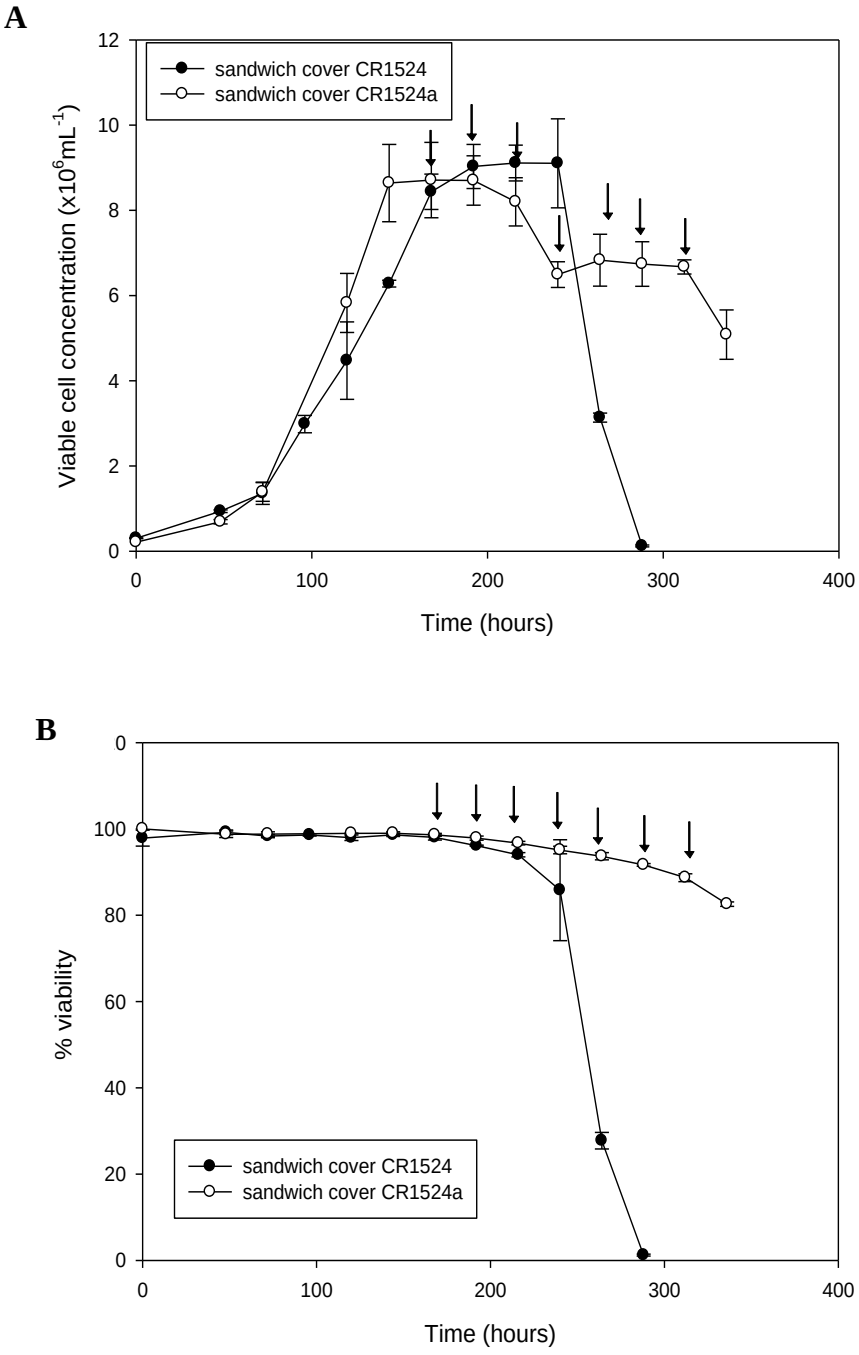

Figure 3.5: CHO growth kinetics in fed-batch mode for shaken 24-SRW microtitre plates (MTP) with two different sandwich covers: CR1524 (for fast grow cells) (●) and CR1524a (for slow grow cells) (○); A: Viable cell concentration and B: Cells viability. Arrows (↓) stand for feed addition every day from day 7 of cultivation. Error bars represent one standard deviation about the mean (n = 3).

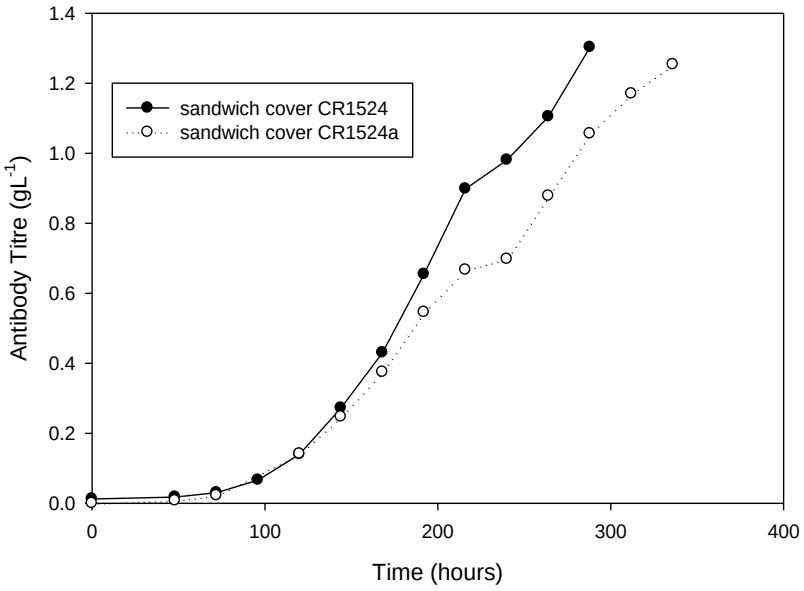

Figure 3.6: IgG antibody production of CHO cell fed-batch mode for shaken 24-SRW microtitre plates (MTP) with two different sandwich covers: CR1524 (for fast grow cells) (●) and CR1524a (for slow grow cells) (○).

3.3.2 Metabolites analysis

The glucose concentration in fed-batch cultures (Figure 3.7 A) using both covers dropped below 2 gL^{-1} after seven days of experiment. From the time when the glucose was nearly exhausted, the culture was bolus fed every day to maintain the concentration approximately at 2 gL^{-1}. The feeding strategy was seen to extend the culture growth and cell viability until fourteen days in MTPs with CR1524a. In contrast, the glucose concentration in the MTP with CR1524 was seen to increase rapidly after the bolus feed was applied. The sharp increase in glucose concentration in the MTP with CR1524 cover consequently had an impact on the lactate concentration and osmolality of the culture. Besides that, the large increase in glucose concentration was due to the unused glucose in the culture. In terms of lactate concentration (Figure 3.7 B), the culture in MTP with CR1524a showed a significant lower lactate and osmolality concentration (Figure 3.8 B)

compared to MTP culture with CR1524. According to Gagnon *et al*., (2011), the consumption of lactic acid by the CHO cells resulted in a decrease of osmolality, which is favourable as the nutrient feed can be supplemented directly without increasing the osmolality towards an inhibitory level. Once the glucose concentration is depleted, the cells will convert pyruvate generated from glucose metabolism to form lactic acid and thus lowering the pH and triggering the glucose addition to the microwells. In fed-batch mode, this sequence was repeated and continued for the duration in culture. The net result is effective control of lactate throughout the cultivation at low level (Gagnon *et al*., 2011).

Ammonia is seen as metabolic by-product of the culture. Ammonia concentration in the fed-batch cultures for both MTPs with CR1524 and CR1524a (Figure 3.8 A) cover showed that osmolality had significant effect toward ammonia production. Ammonia concentration in MTP with cover CR1524 reached the highest concentration (14.2 $mmolL^{-1}$) on day 8 of cultivation. In contrast, ammonia production in MTP with cover CR1524a is constant in the range (2 – 4 $mmolL^{-1}$) over 14 days of cultivation. The high concentration of ammonia had resulting in lower cell numbers and reduced growth rates as reported by Genzel *et al*. (2005).

There is a significant difference in osmolality (Figure 3.8 B) between the two fed batch cultures. The microtitre plate (MTP) with CR1524 had a higher osmolality of 866.3 mOsm Kg^{-1}, while MTP with CR1524a had an osmolality of 499.2 mOsm Kg^{-1}. The high osmolality observed in the MTP with CR1524 cover is likely due to the unused glucose supplemented with the concentrated feed. The high osmolality had a detrimental impact on the viable cell concentration and cell viability (Figure 3.5 A, B). Although elevated osmolality led to lower viability and viable cell concentration, the antibody titre was not affected as observed in Figure 3.6.

Even though both covers show promising results in term of cell growth kinetics and product formation, CR1524a was chosen as an ideal sandwich lid cover for MTPs. Besides that, some differences in growth parameters were observed between the two covers; peak cell density, maximum specific growth rate, specific glucose consumption rate and specific product formation rate. Table 3.1 summarise the differences of growth parameters in MTPs for both sandwich lid covers. The cumulative integral viable cell concentration was 4.61 x 10^8 cell d^{-1} L^{-1} (CR1524) and 5.30 x 10^8 cell d^{-1} L^{-1} (CR1524a). The maximum specific growth rate was slightly higher for the slow growth covers CR1524a (0.014 $h^{-1)}$ compared to CR1524 (0.012 h^{-1}). However, the specific antibody production rate was lower with CR1524a at 12.9 pg $cell^{-1}$ d^{-1} compared with CR1524 with 18.8 pg $cell^{-1}$ d^{-1}.

Table 3.2: Cell culture parameters in MTPs for CR1524 and CR1524a sandwich covers.

Sandwich lid cover	**CR1524**	**CR1524a**
Peak cell concentration (x 10^6 cell mL^{-1})	9.01 ± 0.52	8.75 ± 0.31
Cumulative integral viable cell concentration (x 10^8 cell d^{-1} L^{-1})	4.61	5.30
μmax (h^{-1})	0.012	0.014
IgG antibody titre (gL^{-1})	1.30 ± 0.02	1.25 ± 0.03
q_P (pg $cell^{-1}$ d^{-1})	18.8	12.95
***q_{glc} (pg $cell^{-1}$ d^{-1})**	90.2	88.4

*q_{glc} were calculated during exponential phase before feeding was initiated.
The data represents 3 replicate of MTPs for 24-SRW ± s.d.

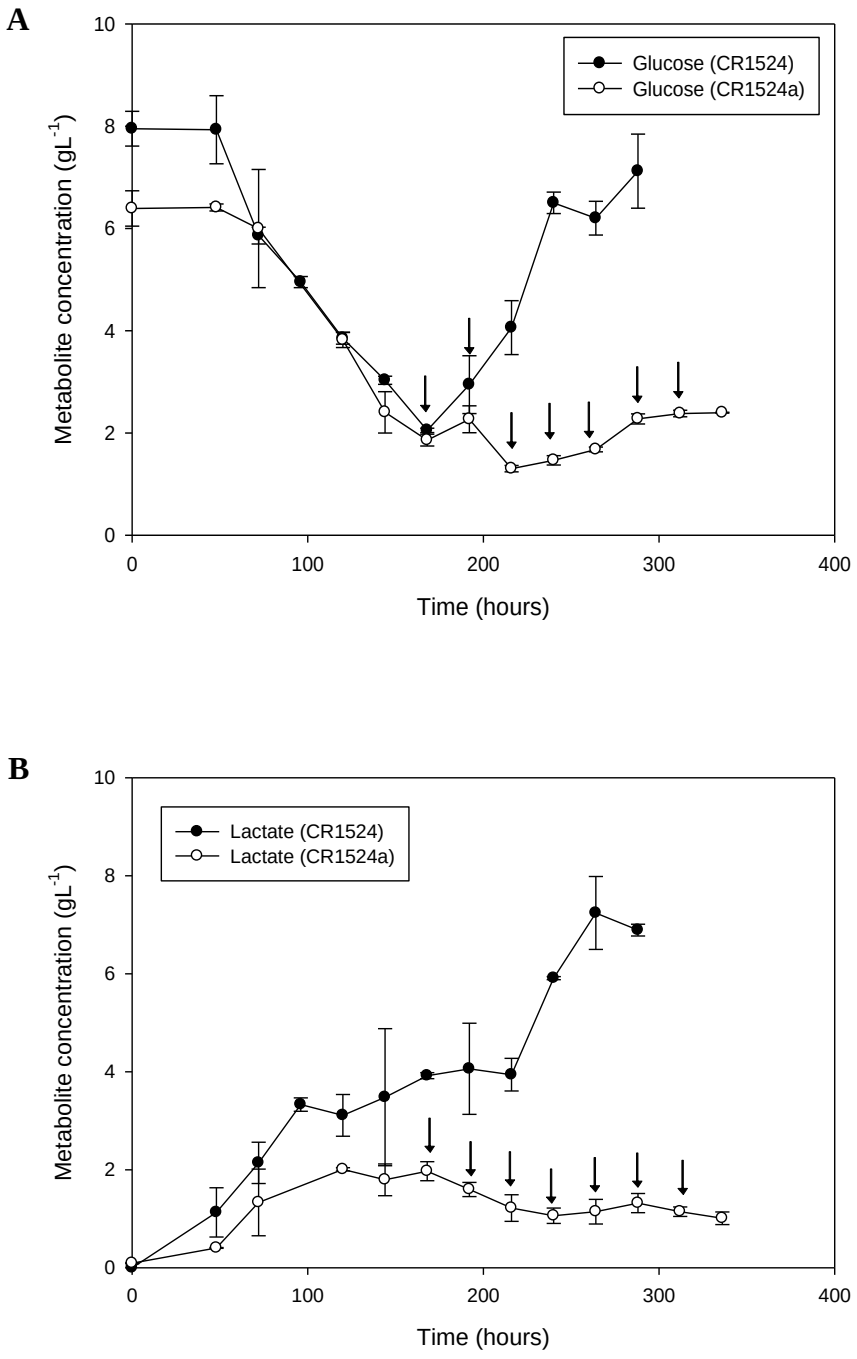

Figure 3.7: CHO metabolites concentration in fed-batch mode for shaken 24-SRW microtitre plates (MTP) with two different sandwich covers: CR1524 (for fast grow cells) (●) and CR1524a (for slow grow cells) (○): A: Glucose concentration and B: Lactate concentration. Arrows (↓) stand for feed addition every day from day 7 of cultivation. Error bars represent one standard deviation about the mean (n = 3).

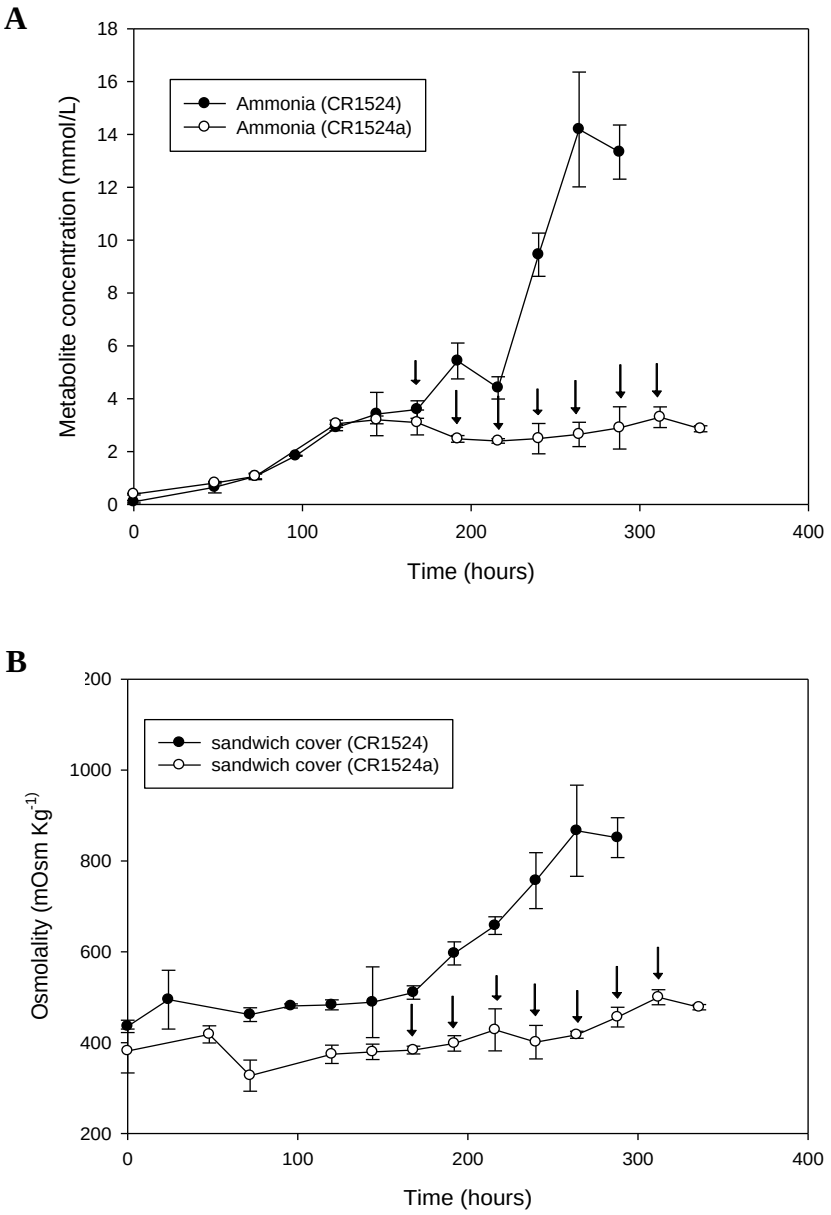

Figure 3.8: CHO growth kinetics in fed-batch mode for shaken 24-SRW microtitre plates (MTP) with two different sandwich covers: CR1524 (for fast grow cells) (●) and CR1524a (for slow grow cells) (○): A: Ammonia concentration and B: Osmolality. Error bars represent one standard deviation about the mean (n = 3).

3.3.3 Particle size distribution in fed-batch mode

Figure 3.9 shows the particle size distribution (PSD) profile of fed-batch mode for MTP cultures with the two covers. The particles size at the start of the cultivation were observed between 14 and 20 µm (viable cells) and reduced to smaller size ~ 10 µm when the cells entering the death phase (non-viable). Cultures with either cover (CR1524a and CR1524) show no significant difference of particle size during the cultivation as seen on day 0 and day 7. The impact of growth conditions on particle size was clearly seen toward the end of cultivation on day 10 after the cell started entering death phase. The graph on day 14 depicts the effect of cell death as particles size shift to the left hand side of the plot with smaller particle size and fewer cell counts (Figure 3.9 B). Besides that, several factors such as nutrient limitation and accumulation of by-products (lactate and ammonia) contributed to changes in PSD cell population profile which causing cell death (Velez-Suberbie *et al.*, 2013).

3.4 Monitoring of process parameters

Recent development in disposable optical sensor has shown the effectiveness of scale-down system for continuous monitoring the DO and pH (Deshpande *et al.*, 2004; Kensy *et al.*, 2005). The advantages of disposable optical sensors over traditional electrochemical method are non-invasive, high sensitivity, ease of miniaturisation, and free of electromagnetic inference (Chatterjee *et al.*, 2015). This advent has made small scale as system of choice for early design data experiment. PreSens-Presicion Sensing GmbH has developed a smart measurement method which has optical sensor, non-invasive, disposable, and pre-calibrated MTPs. The sensor located on the bottom of modified 24-SRW MTP to monitor the pH and DO. The pH (HydroDish®) and DO (OxoDish®) MTPs have the ability for on-line and continuously monitor the culture and visualise it in real-time. The sensor spot for HydroDish®contain luminescence dye at the bottom of the plate. It is excited by SensorDish® reader placed below the MTPs and its lifetime detected by the luminescence dyes. The lifetime of the dye depend on the

oxygen partial pressure (HydroDish®) (PreSens-Presicion Sensing GmbH, Regensburg, Germany).

Figure 3.10 A, B shows the process monitoring of the MTP PreSens sensors with 24-wells on the SensorDish® reader for 14 days fed-batch experiment. The fluctuation that observed in the graph depicts the daily bolus feed that commenced on day 7 of experiment. During the bolus addition, the software was paused for a while and the MTP were aseptically fed with 1 % feeding media under laminar flow cabinet. The system was quickly resumed after each well was completely fed. As observed in Figure 3.10 A, the initial pH measurement of the culture was ~ 9.0 ± 0.5 for 24-well. The high initial pH in the culture because of the CO_2 gradual release from the media which was previously kept in equilibrium with 5 % CO_2 incubator (Genzel *et al.*, 2005; Ge *et al.*, 2006) The culture pH was gradually reduced to acidic condition ~pH 6.5 after 72 hours due to the excessive CO_2 release as the cell growth. As the cell started to enter the exponential phase, the pH started to increase to more alkaline condition which was more favourable with the cell growth rate. Besides that, the lactate and ammonium also started to accumulate after the feeding commence which likely to increase pH at the end of fermentation (Genzel *et al*., 2005).

Figure 3.10 B illustrates the DO measurement for the HydroDish® for fed-batch experiment. The measurement was in the range of ~80 % - ~95 % for 14 days experiment. The sandwich cover CR1524a which mentioned earlier has subsequently maintained the amount of dissolved oxygen required by cell for cell growth and metabolism process. The slightly high oxygen level at the end of the experiment was due to the cells started to undergo apoptosis and oxygen consumption began to deplete. Moreover, the lack of nutrients and energy for metabolism also contributed to the high DO at the death phase (Ge *et al*., 2006).

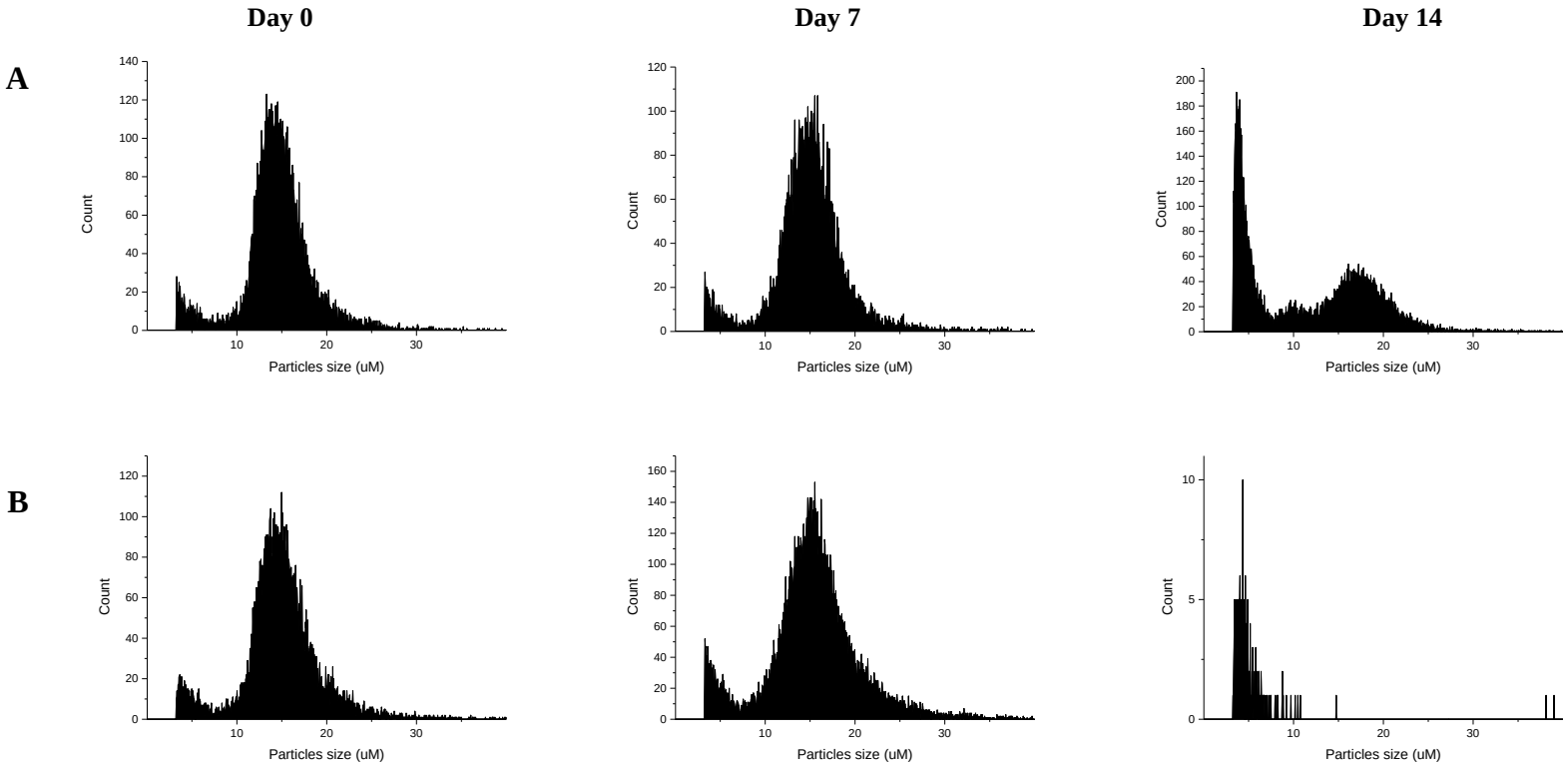

Figure 3.9: Comparison of particle size distribution of CHO cell fed-batch culture on day 0, day 7 and day 14. A: MTPs with CR1524a B: MTPs with CR1524. The measurement was done for 5 replicates using a CASY analyser.

A

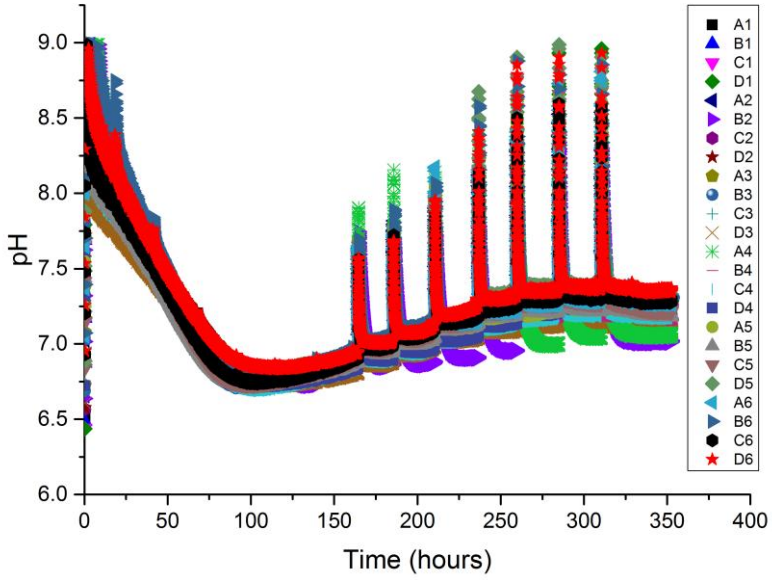

B

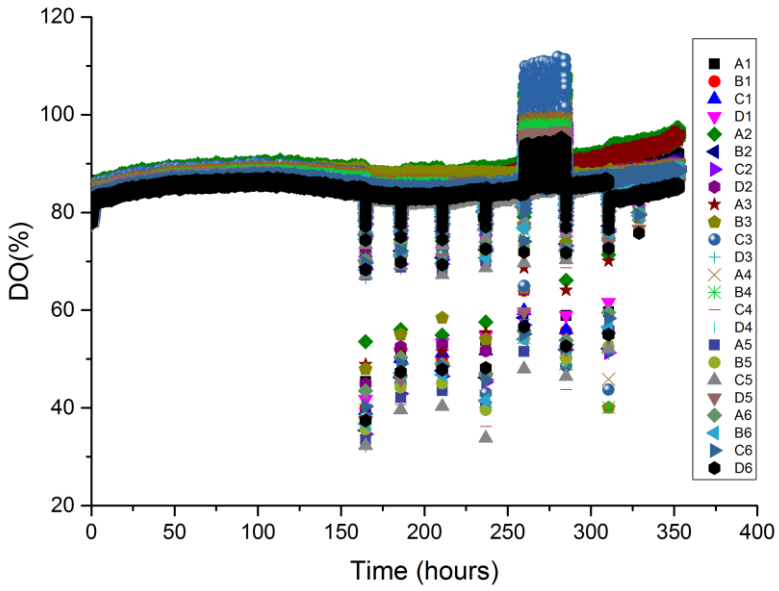

Figure 3.10: PreSens on-line data of 24-SRW. A: HydroDish for pH measurement B: OxoDish for dissolved oxygen measurement.

3.5 FeedBead®: Controlled glucose delivery by slow release technology

FeedBead® is a commercially available glucose feed for application in microtitre plate and shakes flasks culture. The principle of the FeedBead® was to continuously supply nutrients by slow release technology. One of the advantages of FeedBead® is to provide substrate limited fed-batch culture without the need for additional tubing or pumps. Notably, the single addition of FeedBead® in cultures minimise the labour intensity and contamination risks during manual feeding. The crystalline glucose was embedded inside the silicone matrix and slowly released into the culture with defined kinetics during fermentation. FeedBead® is a method developed by Jeude *et al*. (2006) to enhance the feeding strategy for *Hansenula polymorpha* shake flasks fermentations. The system provides a novel continuous feeding strategy using slow release diffusion technique in shake flasks cultures and able to produce 23.4 gL^{-1} dry cell weight of *H. polymorpha* (Jeude *et al.*, 2006).

In this study, the aim was to apply FeedBead® for CHO cell cultivation, while addressing the question whether application of FeedBead® has an impact on process performance for growth and product formation. The ability of FeedBead® to provide continuous feed to the cultures was seen as a novel technique in small scale CHO culture. For the initial study, the glucose release kinetics from the elastomer discs was determined by adding a single, two or three discs to each well with culture medium. All measurements were performed threefold. The course of relative glucose release from the silicone elastomer discs is depicted in Figure 3.11 A. For all glucose discs added, it shows rapid glucose release kinetics in the first 6 hours decreased when the crystalline glucose was almost depleted in the discs.

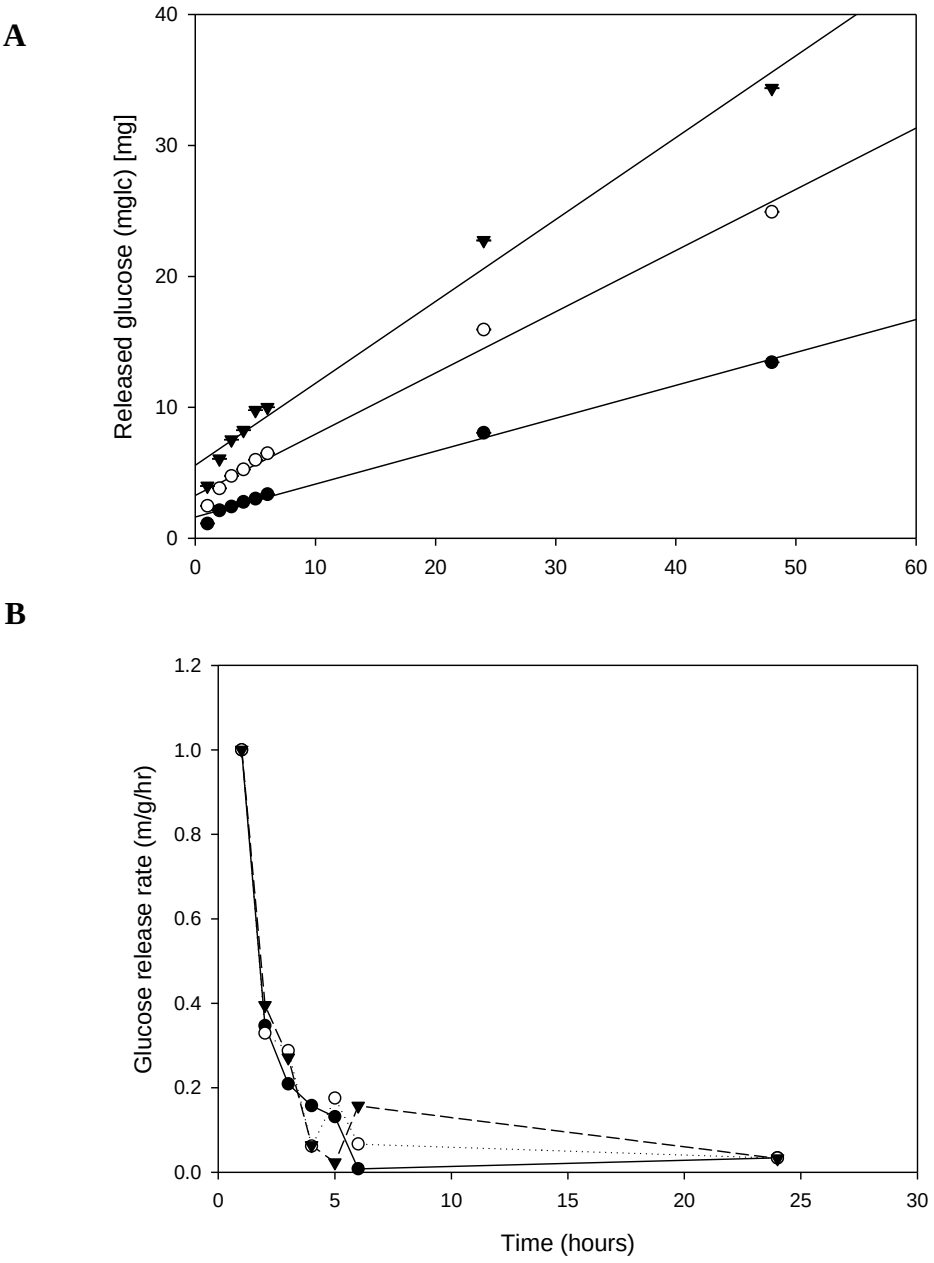

Figure 3.11: FeedBead® release kinetics in shake flasks experiment; A: relative glucose released from elastomer discs B: Glucose release rate per hour. The number of bead added into the shake flasks indicated with; one FeedBeads® (●), two FeedBeads®(○), three FeedBeads® (▼).

The absolute glucose release is shown in Figure 3.11 B. For glucose release rate, there was no significant difference between the theoretical and experimental results. The glucose released rate was in the range of 0.04 – 1.0 $mghr^{-1}$ for one, two or three bead added into the MTPs. The release rate showed that the concentration of the glucose should be adequate to support glucose uptake by cell during fermentation based on the assumption that uptake rate of 4.16 x 10^{-6} $mghr^{-1}$ by CHO cells. The assumption was made from the previous experiment in Section 3.3.2, whereby specific glucose consumption rate by CHO cell was around 90 pg $cell^{-1}$ d^{-1}.

3.6 Evaluation of two types of feeding strategies for CHO cell culture in 24 standard round well (24-SRW)

3.6.1 Growth kinetics and antibody productivity

In terms of CHO growth, the viable cell concentration (VCC) cultures was found to be higher with bolus fed (9.19 x 10^6 cells mL^{-1}) compared to FeedBeads® (8.30 x 10^6 cells mL^{-1}) (Figure 3.13 A). Both of the cultures reached nutrient starvation after 7 days of experiment and the glucose concentration was observed to decrease below 2 gL^{-1}. Normally, CHO cells culture required glucose concentration at the average of minimal amount 2 $gL^{-1}d^{-1}$ for prolong survival, productivity and cell maintenance growth (Barrett *et al*., 2010; Silk *et al*., 2010). Low nutrient concentrations will eventually lead to the cell death and decrease CHO cells viability.

In terms of CHO cell viability the bolus fed cultures showed enhanced cell viability with 82.5% compared to the FeedBeads® where no viable cells were found at the end of experiment (Figure 3.13 A). This is attributed to the supplementation of nutrients in the fed-batch cultures that commenced on day 7 of the experiment. For FeedBeads® addition, it shows that the high concentration of glucose released in the culture had damaging effects on the cells. On day 10, it shows that cell viability has decreased to 1.4%. This high glucose concentration not only will reduce the viable cell concentration, but eventually could lead to a doubling in the medium osmolality due to liquid losses over the course of the batch culture (Silk *et al*., 2010).

The microtitre plate feeding performed using an established bolus addition with diluted glucose was found to replace the water loss and minimise changes in medium osmolality in the microtitre plates. Another main factor for low viability might be due to high evaporation rate in the microtitre plates. Each bolus addition comprised of diluted glucose with a concentration of 150 gL^{-1}. The diluted feed added to the culture was found to replace the water loss and minimise changes in medium osmolality in the microtitre plates. Besides that, the feed addition proved to replace the depleted glucose concentration in the cultures due to cellular uptake and metabolism.

Final antibody titre for bolus fed and FeedBeads® were 1.25 gL^{-1} and 0.77 gL^{-1} (Figure 3.13 B). The higher IgG titre measured in bolus fed cultures is thought to be a consequences of raised final culture osmolality of 478 $mOsmKg^{-1}$ compared to 373 $mOsmKg^{-1}$ in batch culture. The result of increased antibody productivity as culture osmolality increases are well documented for CHO cells (Takagi *et al.*, 2000). In contrast, the lower IgG titer in the FeedBeads® culture is likely the consequence of cell death after 10 days of culture. As the cell entered the death phase, the accumulation of lactate and ammonium increased. Furthermore, at this rate, cell started to entered programmable death (apoptosis) and glucose uptake by cell gradually slowing down (Li *et al*., 2010). The introduction of FeedBead® was found not suitable as the glucose released rates are high and glucose uptake rate by cell was very slow. Figure 3.12 describes the glucose consumption rate by CHO cell and glucose release rate by FeedBead®. Based on the graph, high release rates can be seen in the MTP after 24 hours addition. It was predicted that after 168 hours of FeedBead® addition, the glucose concentration will increase to 23 gL^{-1}. This is in agreement with (Hegde *et al.*, 2012) regarding the short period of glucose release within 2 days in mammalian culture, contrasted with high release rates of glucose observed in FeedBead®. Furthermore, the size of the bead (6 mm) was quite big to accommodate the well with diameter of 15.2 mm. The bead added during the fed-batch mode has disrupted the mixing of the culture during experiment. As CHO cells have no cell wall and shear sensitive is very high, the continuous collisions that occur during mixing might gave detrimental impact on the cell growth. Table 3.3 shows cell parameters in the different feeding strategy applied for fed-batch mode experiment. The major different observed in the production of antibody with bolus fed has better production compared to FeedBead®.

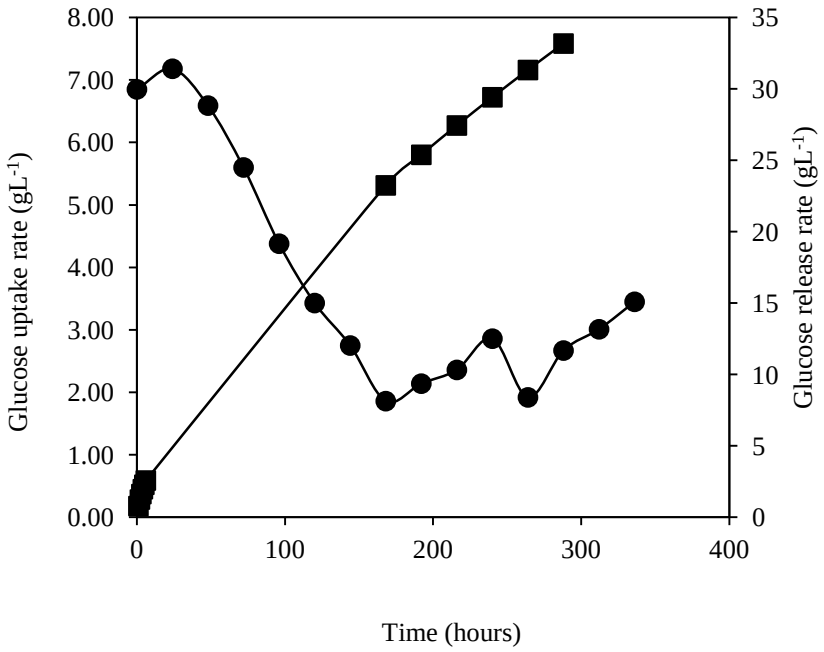

Figure 3.12: Glucose uptake rate by fed-batch CHO cell for the MTP in comparison with glucose release by FeedBead®. Glucose uptake rate (●), glucose release rate (■).

Table 3.3: Cell culture parameters in fed-batch mode for bolus fed and FeedBead®

Feeding strategy	**Bolus fed**	**FeedBead®**
Peak cell concentration (x 10^6 cell mL^{-1})	9.19 ± 1.24	8.30 ± 0.40
Cumulative integral viable cell concentration (x 10^8 cell d^{-1} mL^{-1})	5.40	3.30
μmax (h^{-1})	0.028	0.018
IgG antibody titre (gL^{-1})	1.25 ± 0.04	0.77 ± 0.08
q_P (pg $cell^{-1}$ d^{-1})	14.3	16.5
***q_{glc} (pg $cell^{-1}$ d^{-1})**	92.1	78.4

*q_{glc} were calculated during exponential phase before feeding was initiated.
The data represents 3 replicate of MTPs for 24-SRW ± s.d.

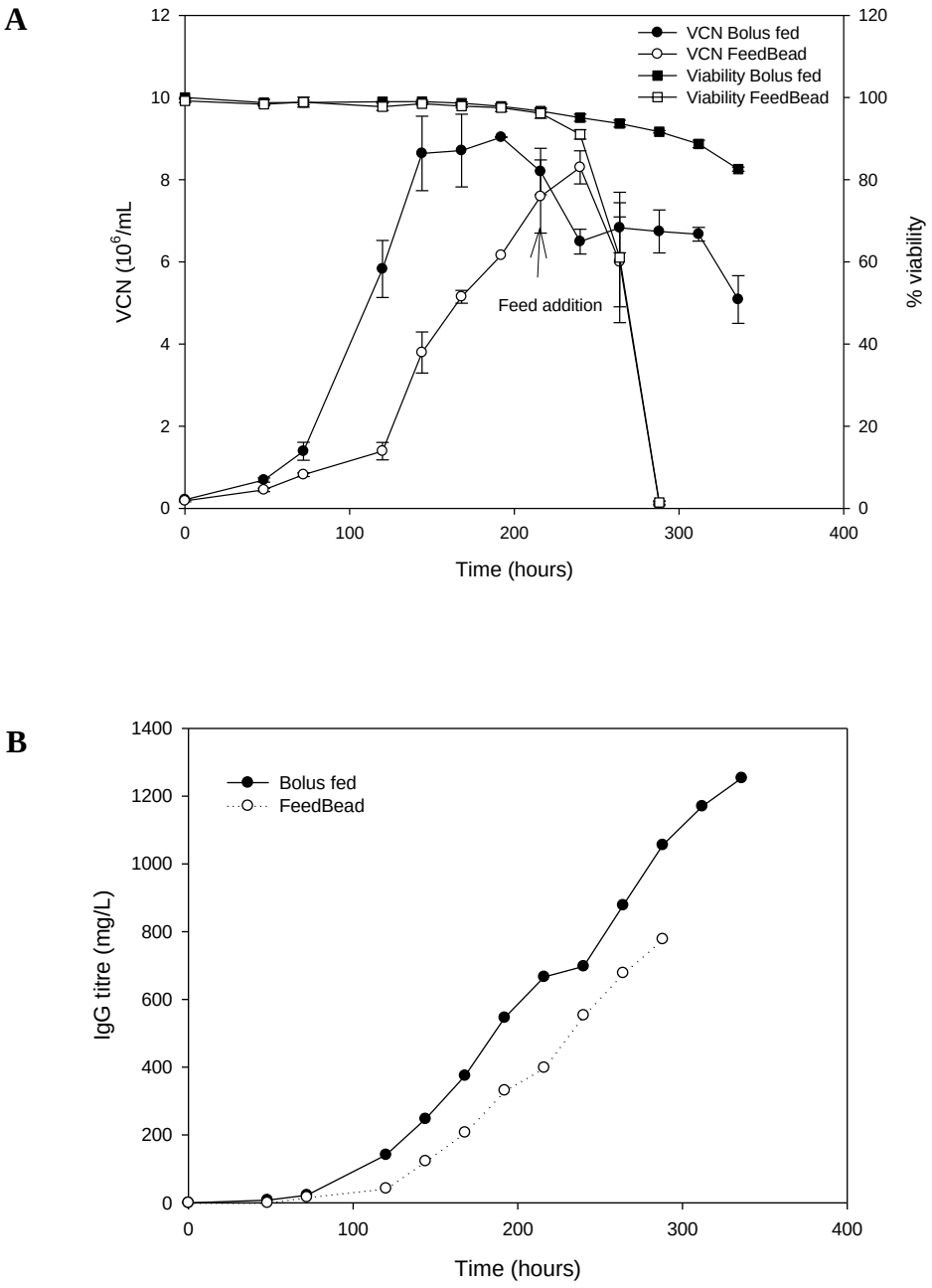

Figure 3.13: CHO growth kinetics for shaken 24-Standard Round Well (24-SRW) plates with CR1524a sandwich covers. A: viable cell concentration; bolus fed (●) FeedBeads® (○) and percentage cells viability; bolus fed (■) FeedBeads® (□) and B: IgG antibody concentration; bolus fed (●) FeedBeads® (○). Error bars represent one standard deviation about the mean (*n*=3). Arrows (↓) stand for feed addition every day from day 7 of cultivation.

3.6.2 Metabolites analysis

Glucose and lactate concentration profiles for the bolus and FeedBeads® cultures are shown in Figure 3.14A. Initially the glucose concentration in the cultures was approximately 7 gL^{-1} (±1.0 gL^{-1}). The glucose concentration in the microtitre plates dropped below 2 gL^{-1} after day 7 (168 hours) of the experiment. In the fed-batch cultures, the feed supplemented through either bolus fed or FeedBeads® was shown to compensate the depleted glucose.

After the initial addition of the FeedBeads® discs into the culture, the glucose concentration increased sharply to 10 gL^{-1}. The high concentration of glucose could not be fully utilised by the CHO cells. The high residual glucose level in the culture is ultimately decreasing the cell viability. One of the limitations of FeedBeads® system for cell culture is the high glucose release rate that eventually gives detrimental effects towards the cells. Besides, the large transient of glucose becomes highly toxic that increases the level of osmolality and metabolite concentrations in the culture (Wong *et al.*, 2005).

As for lactate (Figure 3.14 A), the concentrations for both cultures are seen to increase up to 2 gL^{-1} on day 7 of the experiment. As for FeedBeads® culture, the lactate concentration keeps on increasing until the final day of the cultivation. Lactate accumulation is generated from the glucose metabolism in glycolysis pathway. The principle is once the glucose concentration is depleted, the cells will convert pyruvate generated from glucose metabolism to lactic acid and thus lowering the pH which will trigger the glucose addition to the microtitre plates. In fed-batch mode, this sequence is repeated and continued for the duration of fed-batch culture. The net result is effective control of lactate production throughout the cultivation at low level (Gagnon *et al*., 2011).

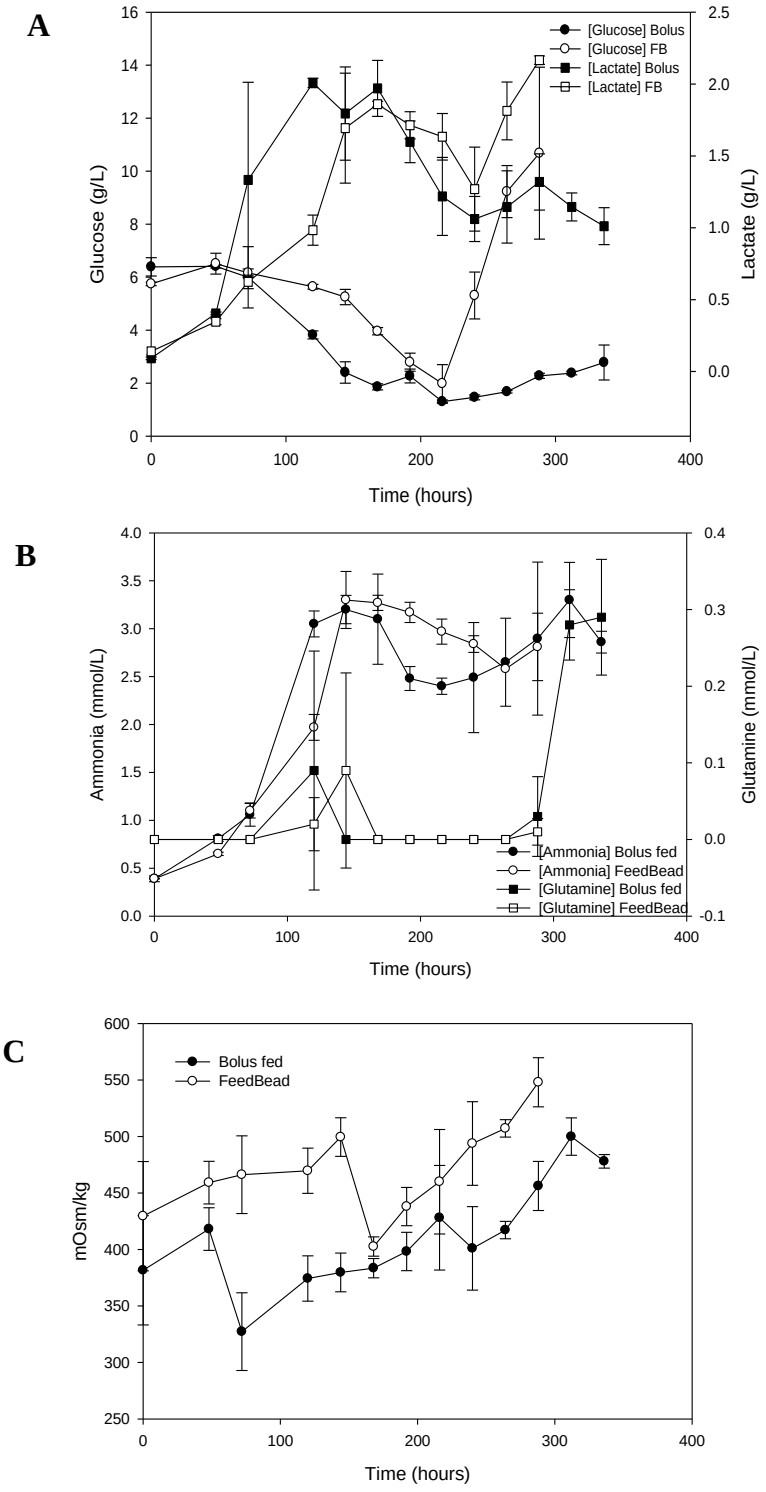

Figure 3.14: Metabolites concentration in the microtitre plate over 14 days of cultivation. A: glucose concentration; bolus fed (●) FeedBead® (○) and lactate concentration; bolus fed (■) FeedBead® (□) B: ammonium; bolus fed (●) FeedBead® (○) and glutamine; bolus fed (■) FeedBead® (□) C: osmolality; bolus fed (●) FeedBead® (○). Error bars represent one standard deviation about the about the mean (n=3).

The accumulation of ammonium (Figure 3.14 B) was seen in both feeding strategies of the microtitre plate systems. The bolus fed and FeedBead® system peaked in the range of 2.50 – 3.50 $mmolL^{-1}$ throughout the feeding phase. By contrast, there were no differences observed for the glutamine production in both systems (Figure 3.14 B). As for the osmolality concentration (Figure 3.14 C), both of the feeding strategies applied had elevated osmolality (400 – 550 $mOsmKg^{-1}$) concentration which indicated the high evaporation rates observed in the microtitre plate system as agreed by literatures (Barrett *et al*., 2010; Silk *et al*., 2010).

3.7 Conclusion

The application of microtitre plates for high throughput and parallel cultivation enables to generate early quantitative bioprocess information; reduce the costs of medium requirements; and reduce the overall costs of experimentation. In addition, bioprocess development using shaken microtitre plates offer the potential to speed up delivery of new drugs to market and increasing patient's benefits. The bolus feeding techniques employed in the microtitres are able to provide the cells with glucose after glucose starvation. Consequently, utilization of diluted feed in the fed-batch of CHO culture significantly lowered the concentration of lactate in the culture after 14 days of experiment. The peak viable cell concentration for MTP with bolus feed was 9.19 x 10^6 cells mL^{-1}, while FeedBead® was 8.30 x 10^6 cells mL^{-1}. MTP with bolus feed able to enhance viability to 82.5 % compared to FeedBead® with 1.4 % at the end of culture. The final antibody production in bolus feed was 63.4 % over than FeedBead®. FeedBeads® application was found not suitable for the CHO cell culture in microtitre plates as the glucose release rates are very high compared to the glucose uptake rate by cells. Moreover, FeedBeads® system increased the residual glucose concentration that led to metabolic waste. Overall, this work has shown that cell culture performed in the shaken microtitre plate is able to provide a basis for bioprocess data that is quantitative and reproducible.

Chapter 4 Characterisation of miniaturised stirred bioreactors and evaluation of fed-batch operating strategies

4.1 Introduction

Conventional large scale stirred tank reactors are commonly the main system used in biopharmaceutical industry for production of therapeutic antibodies (Warnock and Al-Rubeai, 2006). However, large scale STR systems have limitations of performing process development and optimisation in cell culture. In order to reduce this bottleneck, pharmaceutical companies have validated scale-down models to mimic the performance of their pilot or manufacturing scale bioreactors (Li *et al.*, 2010; Bareither *et al.*, 2013). The alternative is to develop miniaturised systems that have parallel reactors, high throughput and have the comparable key engineering parameters as conventional large scale reactors.

Design and engineering characterisation of these miniaturised stirred bioreactors are important to determine that the growth kinetics and product formation are equivalent when it is being scaled-down. These MBR are predicted to simulate analogous process performances as their large scale counterpart. The MBRs size usually varies from 0.5 L to 5 L (Nienow, 2006). Previously, Gill *et al.* (2008) have developed a 0.1 L MBR for microbial fermentation. A recent study focused on adapting this MBR design to mammalian cell culture including the optimisation of the gas delivery system and demonstration of fed-batch operation with CHO cells using the 0.5 L MBR (Al-Ramadhani, 2015). In this study, the engineering characterisation of the miniaturised stirred bioreactor with design modification was further investigated. Moreover, batch and fed-batch mode studies were applied to a CHO cell system and growth profiles and IgG productivity determined.

Chapter aims and objectives:

- To characterise the engineering parameters of the HEL-BioXplore MBR for liquid mixing time and oxygen transfer capacity.
- To apply existing correlation to predict the power requirement in mixing of the HEL-BioXplore MBR.

- To investigate the growth profile and product formation of mAb producing CHO cell line (CY01) in the HEL-BioXplore reactors.
- To investigate fed-batch strategies applied to the HEL-BioXplore reactors for CHO cell line cultivation.

4.2 Engineering characterisation of miniaturised stirred bioreactors

Engineering characterisation is the important factor to determine the performance of a bioreactor. Detailed engineering characterisation such as mixing time (T_m), volumetric oxygen transfer coefficient (k_La) and power input is the initial work to be studied to understand the performance of a bioreactor. Besides that, engineering characterisation is imperative for determination of key engineering parameter in bioreactor for accurate prediction of scale translation. By characterising the system over the typical operating range, it is possible to set a benchmark for choosing the parameter for scale translation.

The MBR system used in this chapter is a commercially available HEL-BioXplore. This system has two modes of agitation for liquid mixing; a direct driven impeller or a magnetic driven impeller. Both are marine type impellers which will produce mainly axial flow in the medium. Axial flow is usually used for low shear rate animal cell culture (Chisti, 2000; Marks, 2003; Nienow, 2006). Additionally, the vessel of the reactor was housed in a polyblock which has two functions; to control the temperature and to drive the magnetic impeller as described in Figure 2.3 in Section 2.5. The detailed engineering characterisation of the system for mixing time (T_m) and volumetric mass transfer coefficient (k_La) are described in Section 4.3 and 4.4, whilst theoretical consideration of power input requirement are discussed in Section 4.5.

4.3 Mixing time

Homogenous mixing in stirred bioreactors is a crucial operation for mammalian cell cultivation. The bioreactor must provide cells to access of all substrates through proper aeration and agitation to create an optimal environment in cell cultivation (Doran, 1995). For mammalian cell cultivation in a stirred bioreactor, hydrodynamic shear and bubble damage are traditionally the major problem due to the shear sensitivity of mammalian cells (Chisti, 2001; Marks, 2003). Mammalian cells which lack a cell wall have a high shear sensitivity compared to microbial cells. Therefore, mixing in stirred bioreactor for mammalian cells is usually kept at a minimum force of aeration and agitation to avoid shear damage to cells (Zhang *et al.*, 2010). These authors added that usually mixing force in mammalian cell culture is 100 times less than that in microbial fermentation. Furthermore, for a successful cell growth performance mixing time should be optimised and minimised as much as possible to avoid any changes of operating conditions such as pH and temperature (Doran, 1995). Given the importance of mixing in mammalian cultivation, mixing time was measured as function of operating conditions in the miniaturised stirred bioreactor.

4.3.1 pH tracer method

Mixing times were evaluated in the miniaturised stirred bioreactor for both agitation systems with working volume of 0.3 L. The method selected for the mixing time studies was the pH tracer technique. As described in Section 2.7.1, the pH tracer approach was selected over the decolourisation method because base such as sodium hydroxide is routinely added to maintain pH in commercial cell bio processing. Therefore, it is advantageous to measure the mixing time using the tracer (base) that is added regularly in a production process to mimic the actual cell cultivation conditions (Xing *et al.*, 2009). In theory, as $t \rightarrow \infty$, the liquid inside the bioreactor is completely homogenous. The *H* value will reach steady state which is equal to 1.0. Conversely, in practice, 95 % degree of mixing is considered to determine the mixing time. Thus, 5 % *H* deviation from final homogenisation ($H = 1.0$) was adopted as standard value (Xing *et al*., 2009). The raw data from the pH probe were normalised according to Equation 4.1.

$$H = \frac{pH_t - pH_i}{pH_f - pH_t} \tag{4.1}$$

Where, H homogeneity index/normalised pH

pH_t pH during measured time

pH_i pH during initial time of measurement

pH_f pH during final time of measurement

Figure 4.1 shows a representative normalised pH curve using the direct driven impeller as it approached the ±5 % region for variation of agitation rate (200 rpm, 300 rpm, 400 rpm and 500 rpm). The figure of the normalised pH shows that the 5 % *H* deviation was achieved as *H* reach steady state and is equal to 1.0. The regions of homogeneity are in the range of 5 s to 30 s for all agitation rates tested.

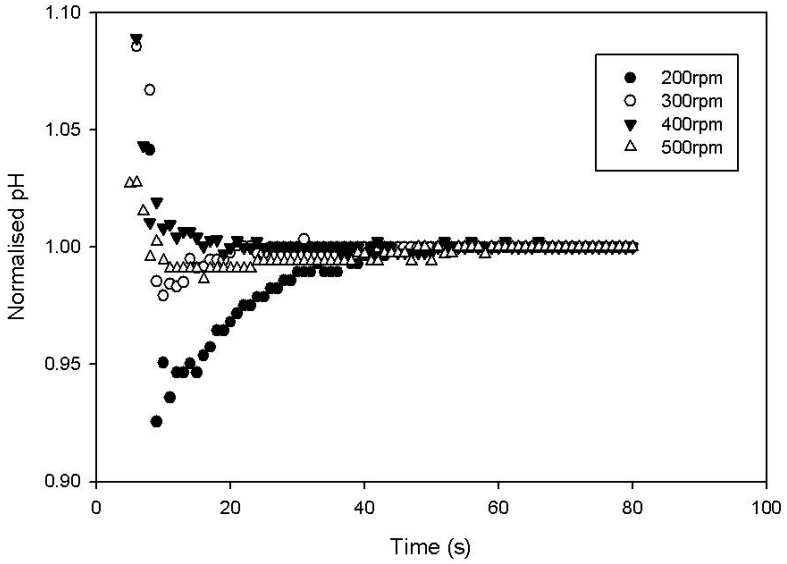

Figure 4.1: A normalised pH curve as it approaches the 5 % region in the bioreactor for different agitation rates (●) 200 rpm, (○) 300 rpm, (▼) 400 rpm, (Δ) 500 rpm.

The mixing time study was further explored for both impeller systems with two types of flow rate; 0 cm^3 min^{-1} (non-aerated) and 100 cm^3 min^{-1} (aerated). Figure 4.2, shows that mixing time is inversely proportional to agitation rate. As expected, mixing time using the direct driven impeller with flow rate of 100 cm^3 min^{-1} resulted in faster mixing time compared to non-aerated reactor (0 cm^3 min^{-1}). Figure 4.2 A represents the mixing time for the direct driven impeller at flow rates of 100 cm^3 min^{-1} and 0 cm^3 min^{-1} varying from 4 – 12 s, and 5 – 15 s respectively. Similarly, Figure 4.2 B illustrates the mixing time for the magnetic-driven impeller shared the similar pattern as direct driven impeller with faster mixing time measured with 100 cm^3 min^{-1} flow rate. The measured mixing time for 100 cm^3 min^{-1} flow rate was between 5 – 13 s, and 0 cm^3 min^{-1} was measured at 5 -14 s. The findings are consistent with large scale STR as aeration promotes better gas distribution in the liquid and are known to decrease the mixing time (Nienow, 2006). Besides that, the presence of bubbles (aerated) in the fluid mixing is known to facilitate better fluid flow in the reactor (Betts, 2015).

Since the flow rate of 100 cm^3 min^{-1} promotes better mixing time measurement in the miniaturised bioreactor, different gas delivery modes were studied to see the effect of the aeration system on mixing time. The three types of gas delivery modes were headspace aeration, singular hole sparger and horseshoe type sparger. Similarly, the presence of gas flow inside the reactor improved the mixing time. Figure 4.3 depicts that mixing time is inversely proportional to agitation rate for the three types of gas delivery modes. The average mixing time measured was 3.3 – 14.0 s. Figure 4.3 A shows the mixing time for the direct driven impeller with horseshoe sparger, singular hole sparger and headspace aeration varying from 3.3 – 9.3 s, 3.6 – 9.6 s and 4.3 – 12.3 s respectively. By contrast, Figure 4.3 B illustrates the magnetic driven impeller with the same sparging configurations varying from 4 – 10.3 s, 4.6 – 12.3 s, and 5.4 – 14 s correspondingly. The headspace aeration for both impellers produced the slowest mixing time. This is resulted from the small headspace and low airflow rate which make the mixing in the headspace produced slowest time.

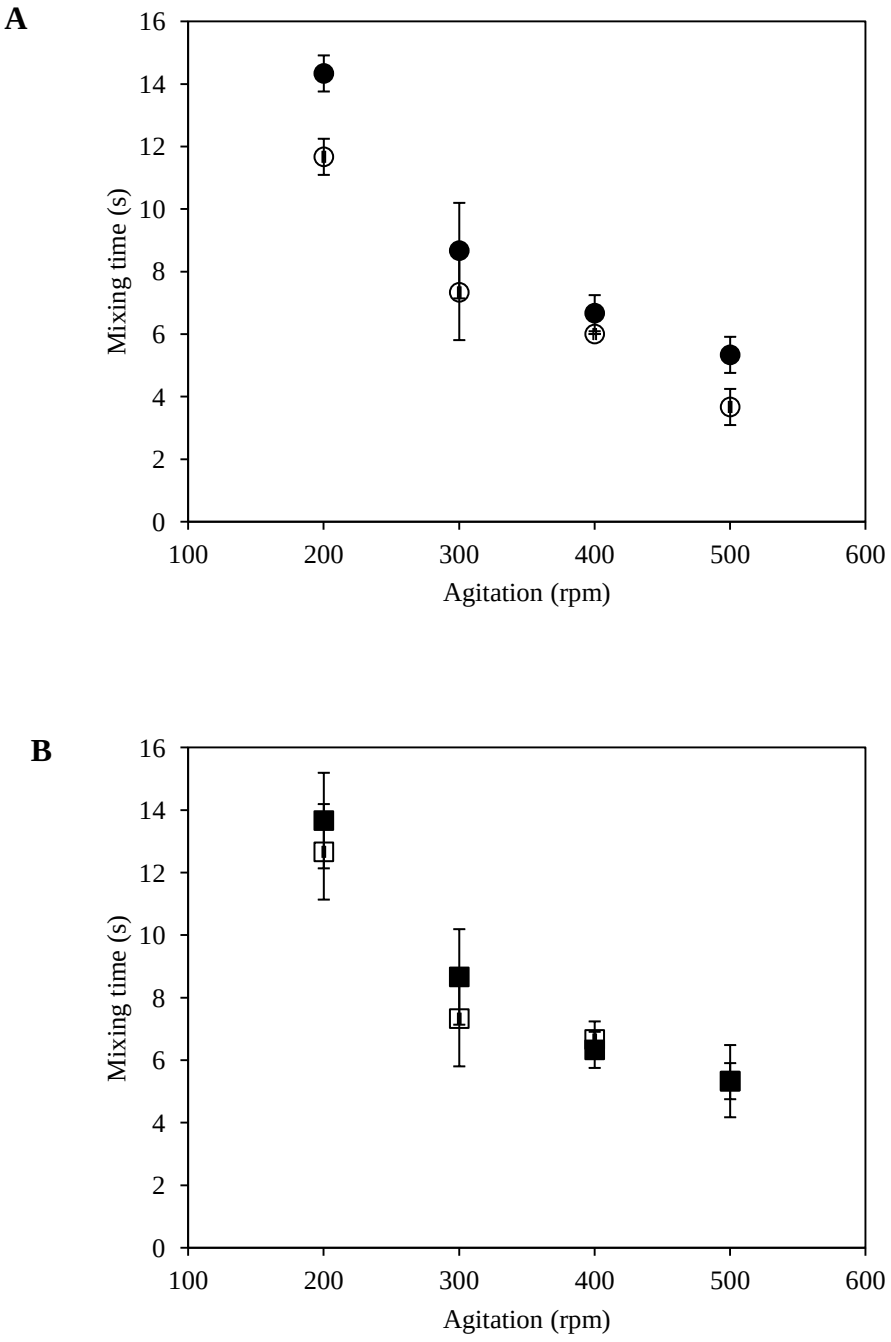

Figure 4.2: Mixing time for different agitation rate with variation of impeller A: Direct driven impeller with (●) 0 cm^3min^{-1}, (○) 100 $cm^3 min^{-1}$ and B: Magnetic driven impeller with (■) 0 cm^3min^{-1}, (□) 100 $cm^3 min^{-}$. Error bars represent one standard deviation about the mean (n=3).

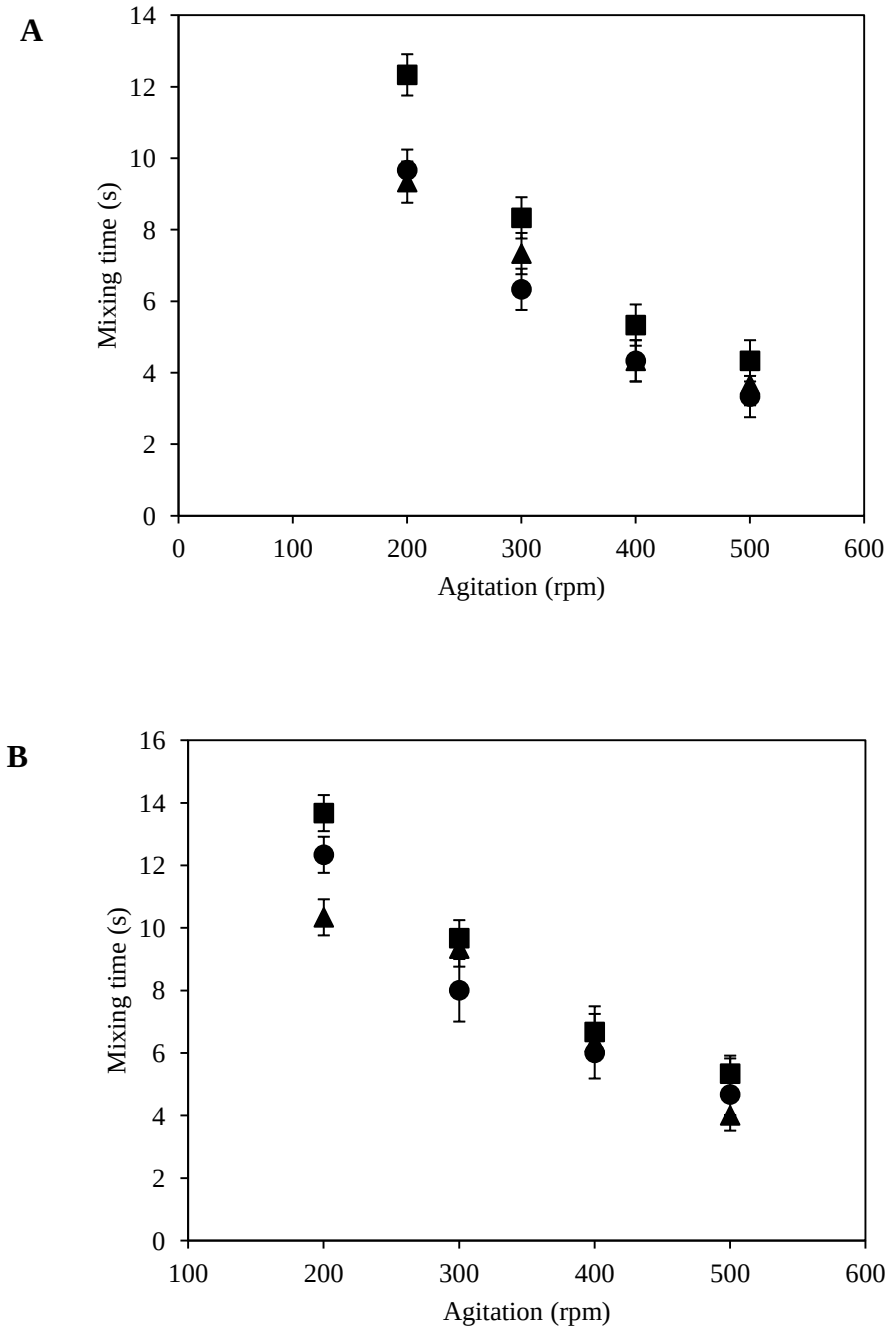

Figure 4.3: Mixing time for different agitation rate with variation of gas delivery mode for A: Direct driven impeller with (■) headspace aeration, (●) singular hole sparger and (▲) horseshoe sparger B: Magnetic driven impeller with (■) headspace aeration, (●) singular hole sparger and (▲) horseshoe sparger. Error bars represent one standard deviation about the mean (n=3).

However, these findings of the current study do not support the previous research by Al-Ramadhani (2015). He reported that gas mixing in the headspace is quicker using small headspace, but at higher gas flow rate. Overall, the direct driven impeller with horseshoe sparger was seen as excellent option for fluid mixing in MBR compared to the other system due to the fastest mixing time (Figure 4.3 A). In addition, the mixing times obtained in this experiment were comparable with recent literature values for CHO cell cultivation as summarised in Table 4.1. From the table, it can be seen that both mixing time methods are applicable for different geometries of STR bioreactors.

Table 4.1: Comparison of mixing times obtained using CHO cells for different small scale bioreactors.

Type of CHO cell	Configuration of reactor	Method of mixing time study	Mixing time (s)	Literature
GS-CHO (Medimmune)	5 L STR (Sartorius)	Decolourisation	6 ± 0.6	Silk., (2014)
***dhfr*-CHO DG44 (GSK)**	3 L STR (Applikon)	Decolourisation	4 – 13	Betts., (2015)
GS-CHO (LonzaBiologics)	0.5 L MBR (HEL-BioXplore)	Decolourisation pH tracer	3 – 15 7 – 20	AlRamadhani., (2015)
GS-CHO (LonzaBiologics)	0.5 L MBR (HEL-BioXplore)	pH tracer	3 – 14	This study

4.3.2 Mixing time correlation

Mixing time is a useful parameter to measure the mixing efficiency in a reactor and homogeneity of a fluid when agitated by impeller. As discussed previously, mixing time is measured as the time required for a liquid to become homogenous after injection of tracer at a fixed point in the reactor (Doran, 1995). These mixing time values vary depending on the geometry of the reactor. Nienow (1997) has proposed

an equation to predict the mixing time in a reactor, where; the tank height H_T and tank diameter D_T are in 1:1 ratio.

$$t_m = 5.9\left(\overline{\varepsilon}_{T\,g}\right)^{-o.33}\left(\frac{D_i}{D_T}\right)^{-o.33} {D_T}^{0.67} \tag{4.2}$$

This equation was used to compare the mixing time of predicted and experimental values. Based on Figure 4.4, the predicted values vary between the two types of impeller system. For the magnetic driven impeller, the predicted and experimental values showed no significant difference using the same working volume. The mixing time achieved is 4.7 – 12.3 s and 4.3 – 11.0 s for experimental and predicted values respectively. These values suggest that the correlation accurately predicted the mixing time in the reactor with the magnetic driven impeller. Whilst, mixing time for direct driven impeller shows that experimental values are lower compared to the predicted values. Nevertheless, the predicted value with the direct driven impeller shared the same trend of increased agitation rate will rapidly decrease the measured mixing time in the system. The results showed that the Nienow (1997) correlation is applicable for both types of impeller using a similar working volume.

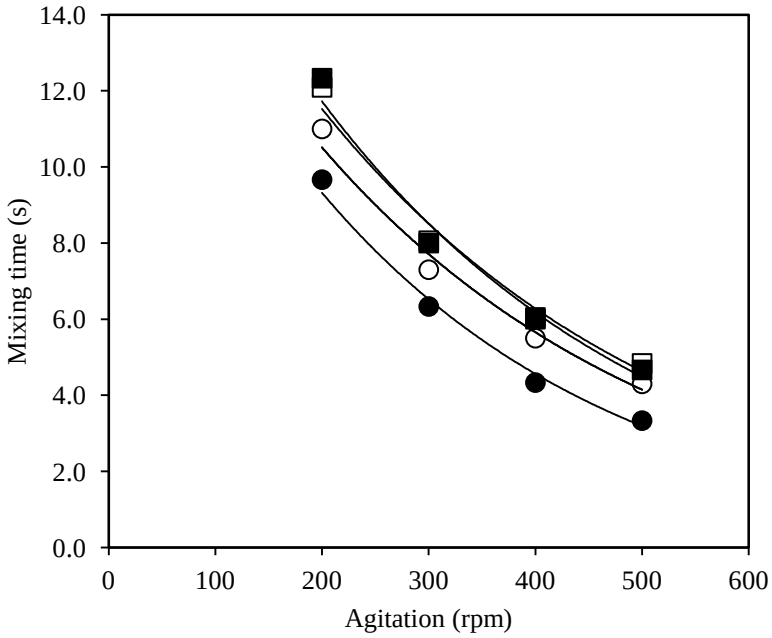

Figure 4.4: Comparison of experimental mixing time and Nienow (1998) correlation, direct driven impeller with (●) experimental, (○) Nienow correlation and magnetic driven impeller with (■) experimental, (□) Nienow correlation.

4.4 Volumetric oxygen transfer coefficient

Oxygen requirement is vital in bioprocessing involving aerobic fermentation primarily in microbial (Garcia-Ochoa and Gomez, 2009) and mammalian cell culture (Nienow, 2006; Nienow, 2015). Cells in aerobic culture usually take up oxygen from the liquid. For mammalian cells, adequate amount of oxygen transfer from gas to liquid is needed to support cell growth and product formation (Marks, 2003). An expression for rate of oxygen transfer from gas to liquid is given by Equation 2.2, where k_L is the liquid-phase mass transfer coefficient and *a* is the gas-liquid interfacial area per unit volume, C_{AL} is the oxygen concentration in the medium and C^*_{AL} is the oxygen concentration in the equilibrium concentration (Doran, 1995). Practically, the k_La profile should be determined in the MBR involving aerobic mammalian cell cultivation particularly for high cell density. Furthermore, k_La is an important parameter in scale translation of different geometry of bioreactors (Gill *et al*., 2008).

4.4.1 Static gassing out method

k_La was measured experimentally using the static gassing out method as described in Section 2.7.2. k_La was investigated in this section as function for impeller agitation in a non-coalescing liquid. The experiments were conducted in the culture media of CD-CHO with 37°C operating temperature to represent the actual culture condition. k_La was determined by gassing out the oxygen with nitrogen gas (de-oxygenation) and re-oxygenated with compressed air/oxygen before measuring DOT value as function of time using a DO probe.

The DOT-time profiles generated during the experiment were used to calculate k_La values using equation 2.2. The probe response time (τ_p) was measured at 24 ± 1 s. The probe response time measured was equivalent to that found by Gill *et al*., (2008) at 18 ± 2 s. As mentioned previously, two types of impeller and two different spargers were use in the MBR for this study. For the DOT-time profile, the DOT % measurement was taken for re-oxygenation between 20 % to 80 % to minimise the amount of time required for the experiment. The DOT-time profile of magnetic driven impeller is represented in Appendix A1, whilst the DOT-time profile of direct

driven impeller is represented in Appendix A2. The profiles show rate of re-oxygenation of culture media in the MBR for magnetic driven impeller with two different spargers. The rate increased proportionally for both spargers with variation of agitation rate in the range of 200 rpm to 500 rpm.

For the k_La, results showed a discrepancy between the configuration of bioreactors with two different impellers and spargers as depicted in Figure 4.5. The graph shows that the k_La values obtained in the MBR ranging from 5.9 h^{-1} to 12.5 h^{-1} as function of agitation rate/impeller speed. Since the k_La values achieved were > 1.0 h^{-1}, it can be assumed that oxygen is not the limiting factor in the bioreactors. Figure 4.5 A illustrates the increasing trends of k_La values for both spargers in the magnetic-driven impeller. For both spargers, the graph shown that the k_La values are directly proportional with the agitation rate. The k_La values for singular hole sparger with 5.9 – 9.0 h^{-1}, whereas horseshoe sparger with 7.7 – 8.5 h^{-1}. While, for the direct driven impeller, the k_La values showed inconsistency between the two spargers (Figure 4.5 B). The significant differences were seen in the horseshoe type sparger with decreasing k_La values from 7.3 – 7 h^{-1} with the increasing agitation rate.

However, the experimental k_La values were equivalent to the reported k_La for different type of bioreactors used for mammalian cells. Xing *et al*. (2009) determined k_La values for 5 L and 20 L Applikon STR ranging from 2.8 – 7.6 h^{-1} and 2.1 – 6.9 h^{-1} respectively. Tissot *et al.* (2010) reported k_La values lower than 15 h^{-1} (3.5- 11 h^{-1}) using a small scale orbital shaken reactor (OSR) of 0.25 L to 0.5 L and a shaking frequency of 110 rpm. The results obtained in this study using different impeller and spargers are within the range of reported system.

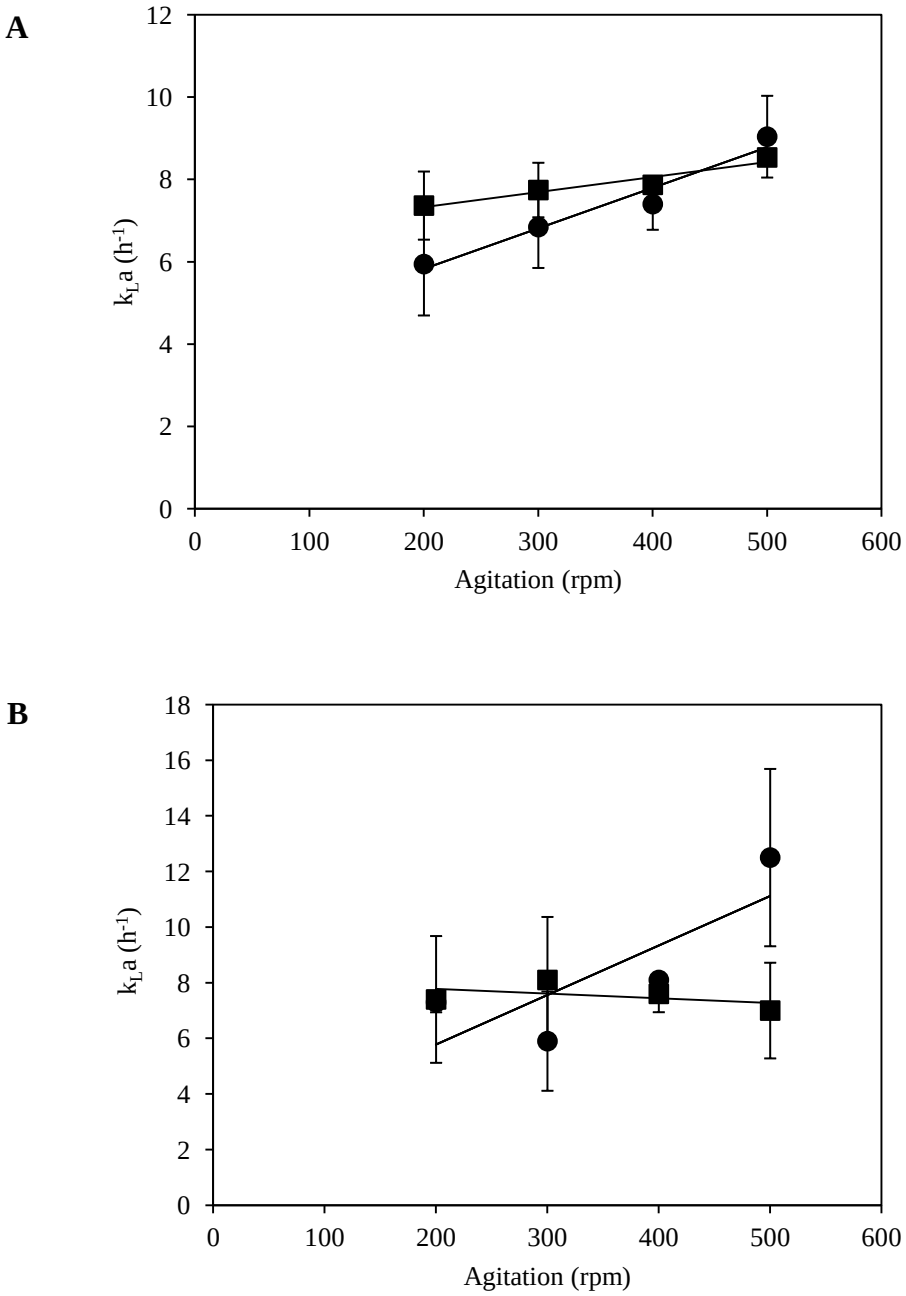

Figure 4.5: k_La profile in the MBR as function of agitation rate with flow rate of 0.33 vvm for A: Magnetic driven impeller (●) singular hole sparger and (■) horseshoe type sparger B: Direct driven impeller (●) singular hole sparger and (■) horseshoe type sparger. Error bars represent one standard deviation about the mean (n = 3).

4.4.2 Volumetric oxygen transfer coefficient correlation

The k_La correlation for the MBR was determined and compared with the predicted values as reported by other literatures. The proposed correlation by Gill *et al*. (2008) and Van't Riet (1979) for non-coalescing and coalescing media was applied for k_La prediction. This correlation was selected because the MBR and methods used in this experiment have a similar geometry and operating parameters as described by Gill *et al*. (2008). However, the correlation suggested by Gill *et al*. (2008) was predicted for microbial fermentation. The general equation for the k_La prediction is as follows, where the constant and exponents are vary between the three correlation as shown in table 4.2

$$k_L a = A\ (\varepsilon_{T_g})^{\alpha}\ {v_s}^{\beta} \tag{4.3}$$

Table 4.2: The proposed constant and exponents for equation 4.3 using three different correlations.

Literature	A	α	β
Gill *et al*. (2008)	0.224	0.35	0.52
van't Riet (non-coalescing) (1979)	0.002	0.7	0.2
van't Riet (coalescing) (1979)	0.026	0.4	0.5

Figure 4.6 shows the predicted k_La in comparison with predicted total energy dissipation rate. The experimental k_La values were equivalent to the predicted values using the correlation by Gill *et al*. (2008). The k_La produced from Gill correlation illustrates increasing trends with high k_La values. The predicted values for direct driven impeller were 7.3 – 16.3 h^{-1} (Figure 4.6 A) while magnetic-driven impeller was 6.4 – 17.1 h^{-1} (Figure 4.6 B). Furthermore, the consistent k_La for agitation rates of 400 – 500 rpm suggested that it could be the optimum agitation rate to supply oxygen to the MBR. By contrast the k_La values obtained from van't Riet correlations show low k_La values ranging from 0.12– 1.94 h^{-1} for direct driven impeller and 0.28 – 1.83 h^{-1} for magnetic-driven impeller.

Besides that, the total energy dissipated in the MBR are higher using the direct driven impeller compared to magnetic driven impeller by > 10 % due to the higher energy required to drive the motor. The highest total energy dissipated from the vessel was observed in the direct driven impeller with 9.3 x 10^3 Wm^{-3} (Figure 4.6 A). Meanwhile, lowest energy dissipated was observed from the magnetic-driven impeller with 5.1 x 10^4 Wm^{-3} (Figure 4.6 B). For a typical animal cell cultured in stirred tank reactor, the average energy dissipated rate was 1 x 10^3 Wm^{-3} (Godoy-Silva *et al.*, 2010). These authors added that energy dissipated above 10^7 Wm^{-3} will begin to lyse the cells which will affect the cell viability. Computational fluid dynamics can be used to determine the energy dissipation rate (EDR) as described by Velez Suberbie *et al.* (2013). These authors reported the maximum EDR from computational fluid dynamic simulation was higher compared to the reported EDR from mammalian STR.

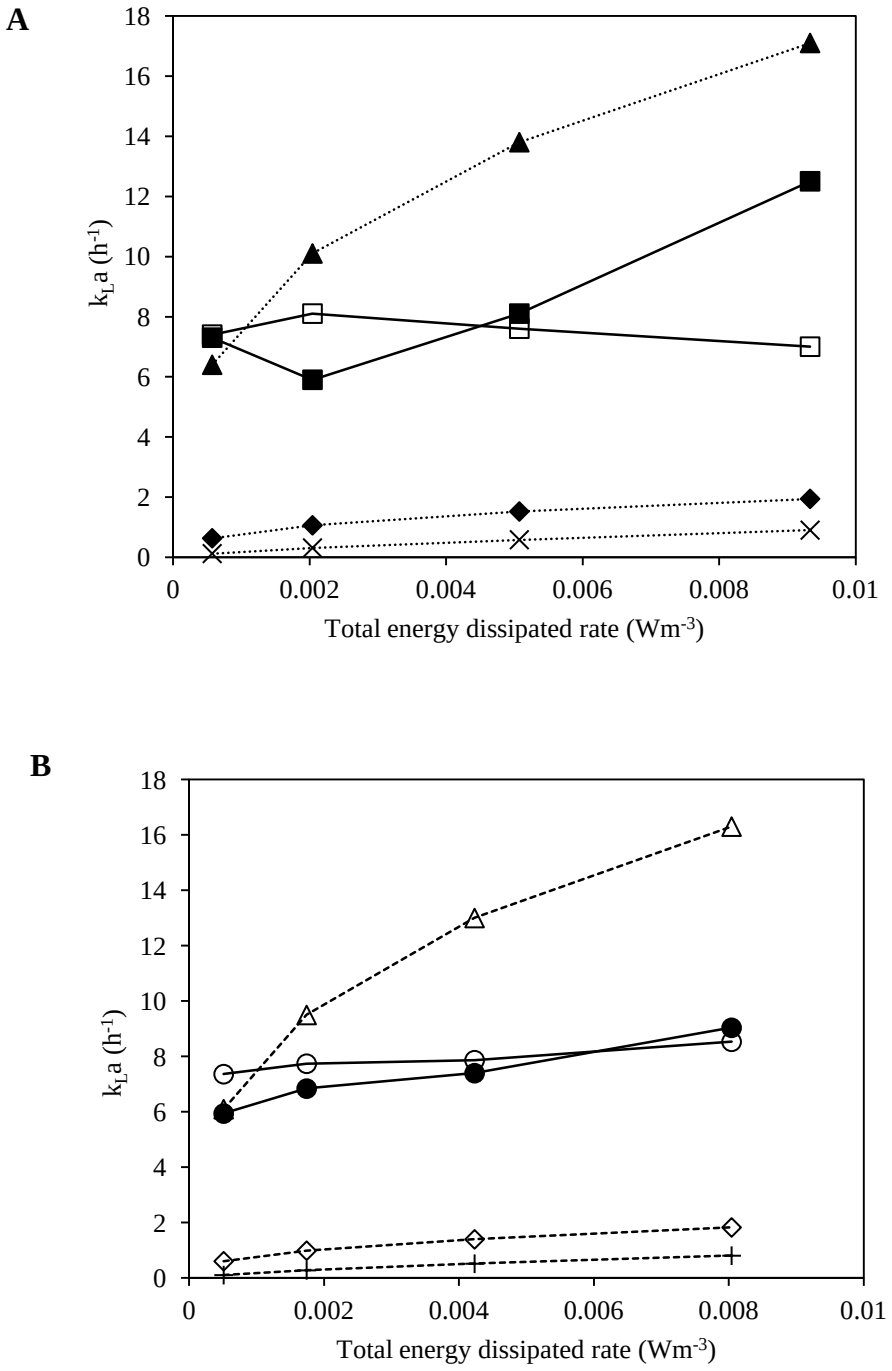

Figure 4.6: k_La profile in the MBR as function of total energy dissipated compared with the proposed correlation for A: Direct driven impeller, Gill *et al*. (2008) (-▲-), van't Riet coalescing (-♦-),van't Riet non-coalescing (-x-), direct_singular (-□-), direct_horseshoe (-■-). B: Magnetic driven impeller, Gill *et al*. (2008) (-Δ-), van't Riet coalescing (◊),van't Riet non-coalescing (-+-), magnetic_singular (-○-), magnetic horseshoe (-●-).

4.5 Power requirement for mixing

Conventionally, in a stirred tank bioreactor the impeller is driven by the electrical power. The power required usually depends on the resistance of fluid when agitated by an impeller. The gassed power input was not determined because of the system gas flow and agitation is relatively low for animal cells (Amanullah *et al.*, 2004; Nienow, 2006). The sparged aeration gave insignificant effect on power input, therefore gassed power input ($P_{g)}$ can be assumed equal to ungassed power input (P_{ug}). The ungassed power consumption can be easily predicted using equation 2.4 and depends on variables such as stirrer speed, impeller diameter, geometry of reactor and properties of the fluid (Doran, 1995). These variables are usually expressed as dimensionless numbers such as the impeller Reynolds number Re_i. Reynolds number are closely related with the power number of an impeller P_o and is defined as

$$P_O = \frac{P}{\rho {N_i}^3 {D_i}^5} \tag{4.4}$$

Power number and impeller Reynolds number represent a ratio of inertial to viscous force. Within the reactor at low agitation rate P_o is inversely proportional to Re and usually in the laminar flow (Re < 10), whereas at high agitation rate the P_o is constant with Re and described as turbulent flow (Re > 10000) (Doran, 1995). Table 4.3 shows the calculated impeller Reynolds number for the two impeller systems used in the MBR. The calculated impeller Reynolds number for both impeller systems gave Re > 4000. The Re number in the MBR shows that both impeller systems have the transition flow conditions. The transition flow lies between the laminar and turbulent flow. Doran (1995), described that there is gradual transition from laminar to turbulent flow in stirred reactor and usually depends on the system geometry. The direct driven impeller system has a greater Re than the magnetic driven impeller system due to the fact that it has greater impeller diameter. This is in agreement with the literature (Marks, 2003; Nienow, 2006) reported that small changes in impeller diameter have large effect on power requirement. Furthermore, both the magnetic and direct driven impeller are marine impellers which promote to axial flow in the system. Axial flow will produce parallel current to the axis of the impeller and lower shear rate compared to radial flow (Marks, 2003). Figure 4.7 shows the predicted

power number for both of the impellers. The direct driven impeller has higher power number of 0.26 – 1.29, compared to magnetic-driven with 0.06 – 0.95. The low power numbers obtained from both impellers are vital to minimise the mechanical damages on cell, hence will produce low mixing time (Varley and Birch, 1999). It is predicted that the P_o of impeller reduced as it moves towards the turbulent flow in the system, Re > 4000.

Table 4.3: Calculated values of impeller Reynolds number for the direct driven and magnetic driven impeller in MBR.

Impeller Reynolds number, Re_i	**N (s^{-1})**				
	3.3	**5.0**	**6.7**	**8.3**	**10.0**
Direct driven	4286	6494	8702	10780	12988
Magnetic driven	4037	6117	8198	10155	12235

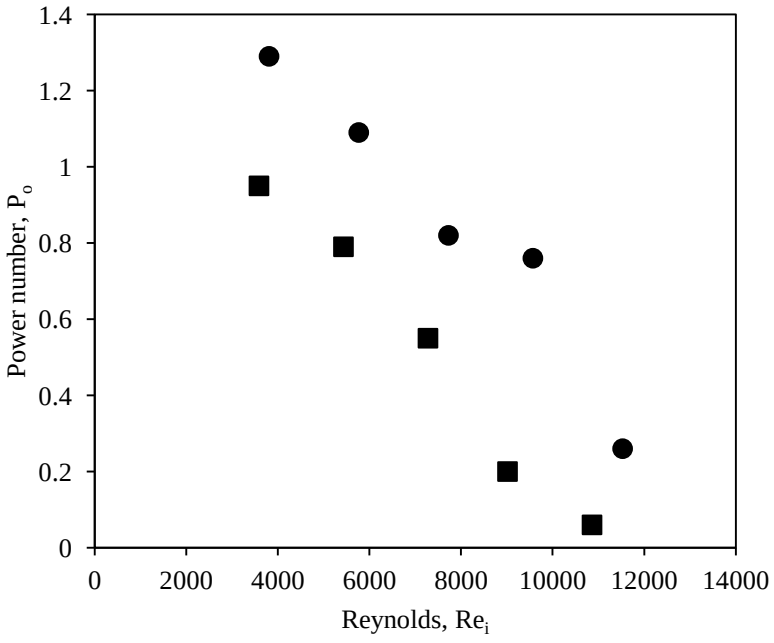

Figure 4.7: Power number for both impeller in MBR in function of Re_i for; direct driven impeller (●), magnetic driven impeller (■).

4.5.1 Predicted power input

The predicted power input in the MBR was calculated for function of impeller types at varying agitation rate. Figure 4.8 shows that the power input increased exponentially with the agitation rate. The calculated power input is in the range of 1.7 – 54.5 Wm^{-3}. These predicted values are consistent with low mechanical power input applied in agitated animal cell culture (Chisti, 2000). Furthermore, low power input is required in animal cell culture to prevent from damaging the cells because animal cell lack of cell wall (Chisti, 2000; Chisti, 2001; Nienow, 2006). Moreover, the power inputs shown in Figure 4.8 are in agreement with data by Heath and Kiss (2007) and Nienow (2006) as values 10 - 1000 Wm^{-3} are practically used in mammalian cell bioreactors. Additionally, the impeller tip speed for direct driven impeller was 0.35 – 0.88 ms^{-1}, while magnetic-driven was 0.34 – 0.86 ms^{-1} (data not shown). Both of the impellers tip speed observed was below 1.5 ms^{-1}, which reported will promote to shear damage in cells (Al-Rubeai *et al.*, 1995).

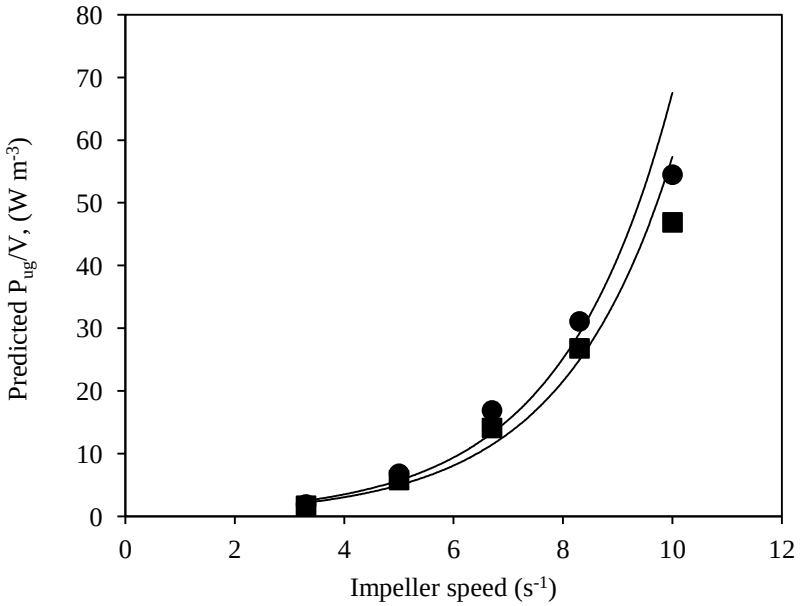

Figure 4.8: Calculated power input in MBR in function of impeller speed for; direct driven impeller (●), magnetic driven impeller (■).

4.6 Design modification of miniature stirred bioreactor

The engineering characterisation suggested that the miniature stirred bioreactor has the potential for high cell density cultivation. This study evaluates the performance of the MBR as a scale-down bioreactor for mammalian cell cultivation. This section also details CHO cell growth profile and product formation using parallel MBR fitted with different type of agitation and aeration systems. The agitation system applied was direct driven impeller and magnetic driven impeller, whilst aeration system chosen was horseshoe sparger and singular hole sparger.

4.7 Effect of different type of impeller and sparger in batch mode

The preliminary study was aimed at comparing the CHO growth kinetics in batch mode for different configuration as mentioned in Section 4.6. The four MBR configurations were: direct driven impeller with horseshoe sparger (DirHS), direct with singular hole (DirSH), magnetic driven impeller with horseshoe sparger (MagHS) and magnetic with singular hole (MagSH). The experiments were done in parallel for the same impeller type configuration. The selected operating parameter for impeller speed was based on matched mixing time of a 5L STR used for scale translation experiments (see chapter 5). With the basis of matched T_m of ~6 s, the calculated impeller speed selected for the MBR was 400 rpm (magnetic driven) and 450 rpm (direct driven). The studies were carried out as described in the Section 2.5.

4.7.1 Growth kinetics and antibody production

The growth rate trends of batch CHO cells cultured in the MBR using four different configurations (DirHS, DirSH, MagHS, and MagSH) were shown to be very similar and exhibited a good reproducibility from day 0 until day 6 (Figure 4.9 A). The peak viable cell concentration for MBR with DirHS was the highest with 7.06 x 10^6 cell mL^{-1} on day 8. The main differences between these configurations were in the cell viability. The MBR with MagHS showed a considerable longer stationary phase compared to other configurations and achieved higher cell viability of 67 % on day 11 (Figure 4.9 B). On the contrary, cell viability for both impeller systems with singular hole sparger dropped abruptly after day 7 of cultivation. The sudden drop of

cell viability in MBR is probably due to the glucose limitation, which is main carbon source in CHO cell fermentation. For batch cultivation, glucose is not added and the exhaustion of glucose was seen as the problem to extend cell growth in culture. The variation of derived growth parameters in MBR with different configurations are listed in Table 4.4. Some differences in growth parameter were observed; maximum specific growth rate, cumulative integral viable cell (cIVC) and specific product formation were higher in the MBR with DirHS.

For final antibody production (Figure 4.9 C), there was some variability between the four configurations. Both of the impellers with singular hole sparger produced low product formation. This is in agreement with Al-Ramadhani (2015), which reported of significant variability and low product formation from the MBR system using headspace aeration. He added that the variability in the product concentration trends might be due to the human error while preparing the samples for HPLC analysis. Results show that MBR with DirHS reached 0.40 gL^{-1} compared to other configuration with ~0.20 gL^{-1} at the end of culture. Although the MBR system is well controlled (DOT, pH, temperature), based on the q_p, most of the configurations have lower specific product formation of less than 10 pg $cell^{-1}$ d^{-1}. Nowadays, it is expected that the product formation should reached 1 -5 gL^{-1} or 20 pg $cell^{-1}$ day^{-1} in volumetric for controlled bioreactors (Wurm, 2004; Birch and Racher, 2006; Huang *et al.*, 2010).

Table 4.4: Derived growth parameters of CHO cell in MBR in batch mode with different impeller and sparger configurations.

Impeller/Sparger	**Dir/HS**	**Dir/SH**	**Mag/HS**	**Mag/SH**
Peak cell concentration (x 10^6 cell mL^{-1})	7.06	6.76	6.42	6.39
cIVC (x 10^8 cell d^{-1} mL^{-1})	3.62	2.35	3.33	3.39
μmax (h^{-1})	0.021	0.019	0.018	0.017
IgG antibody titre (gL^{-1})	0.40	0.20	0.21	0.20
q_P (pg $cell^{-1}$ d^{-1})	7.3	5.7	4.3	3.8
q_{glc} (pg $cell^{-1}$ d^{-1})	71	63	69	71

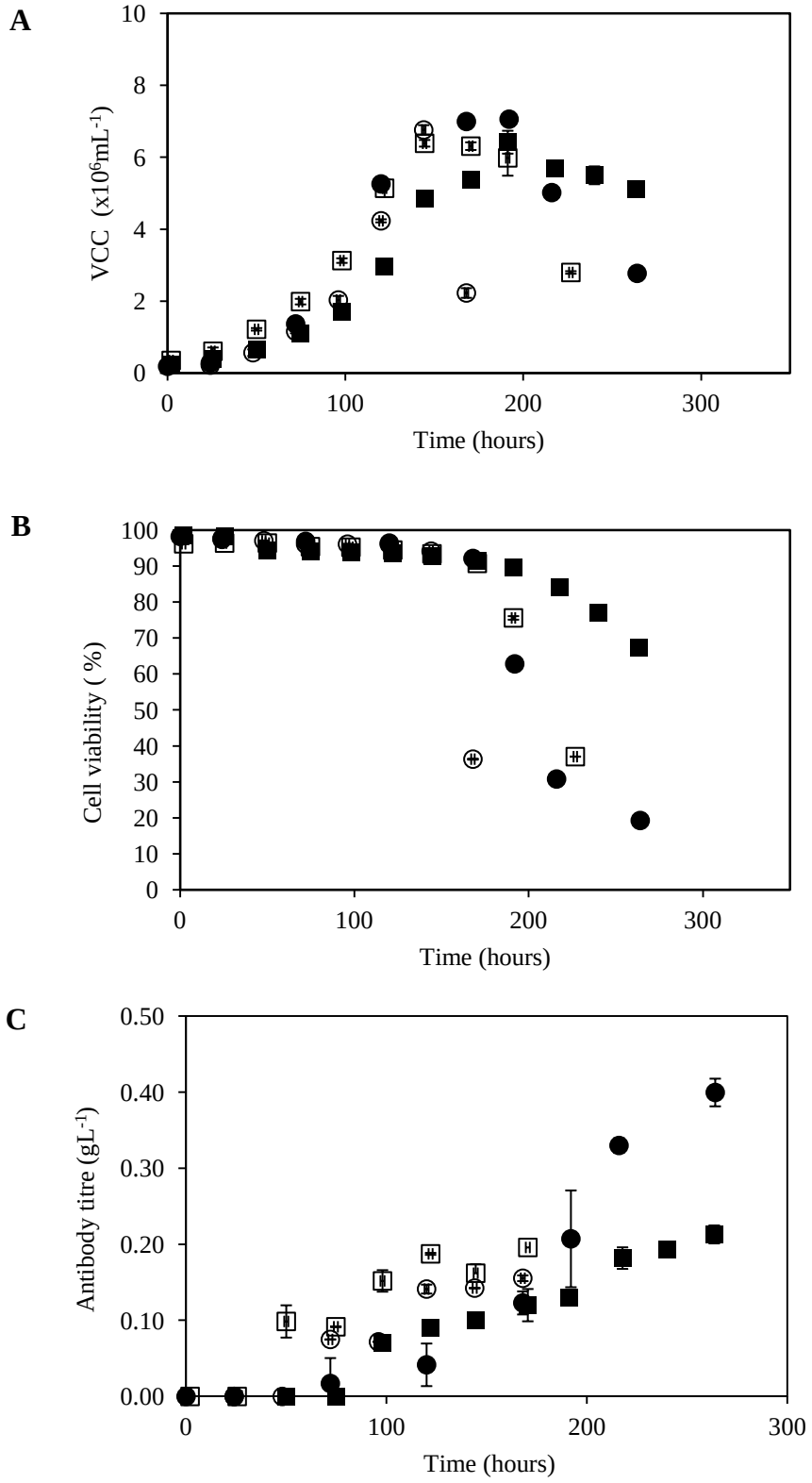

Figure 4.9: CHO growth kinetics in batch culture for HEL-BioXplore MBR with two different impellers and spargers: direct driven with horseshoe (●), direct driven with singular hole (○), magnetic driven with horseshoe (■), magnetic driven with singular hole (□) A: viable cell concentration; B: cells viability; C: IgG antibody titre. Error bars represent one standard deviation about the mean (n = 3).

4.7.2 Metabolites analysis

The metabolites and osmolality profiles for CHO cells in the MBR with different configurations are shown in Figure 4.10. It can be seen clearly that there were significant difference in the profiles. From the profiles, it shows that some of the metabolites data points (glutamine, glutamate, and ammonium) are not available due to a technical fault with the metabolite analyser. At the start of the fermentation, the glucose concentration was similar for all MBR cultures and within the range of 6 -7 gL^{-1}. As the CHO cells started to grow and entering the exponential phase, the glucose consumption increased as expected. The largest glucose consumption was observed in the MBR with DirSH (Figure 4.10 A). The cells in this reactor consumed the main carbon source available fastest and the effect can be seen in the cell viability (Figure 4.10 A), where the viable cell concentration dropped massively after 7 days cultivation.

For lactate accumulation (Figure 4.10 B), the MBR with DirSH also accumulated the highest lactate concentration as a result of the greater glucose consumption. This is in agreement with findings by Sheikh *et al.* (2005) and Velez-Suberbie *et al.* (2013) that fast glucose consumption by the cells will lead to more by-product in the medium. The lactate production also had an impact on the medium osmolality as seen in Figure 4.10 C, where MBR with DirSH reached the maximum of 385 $mOsmkg^{-1}$. The medium osmolality profile was seen increasing for all the MBR cultures (300 - 400 $mOsmkg^{-1}$) apart from for MBR with DirHS. Another by-product ammonium is highest for the MBR with MagHS at 6.0 $mmolL^{-1}$ (Figure 4.10 E). The greater ammonium concentration also will eventually increase the medium osmolality as seen in Figure 4.10 C. As for glutamine profile (Figure 4.10 D), there was large variation of glutamine produced throughout the cultivation. The cell line used is GS-CHO which supposedly does not produce any glutamine and is grown in glutamine free medium. However, glutamine can be synthesised by glutamate and ammonium as explained in Section 1.3.1. The glutamate profile (Figure 4.10 F) illustrates a similar pattern for all MBR cultures except for the MBR with DirSH. The glutamate concentration in the MBR with DirSH was observed initially with lower concentration with 2.5 $mmolL^{-1}$, whilst the other three configurations with 3.5 – 4.2 $mmolL^{-1}$.

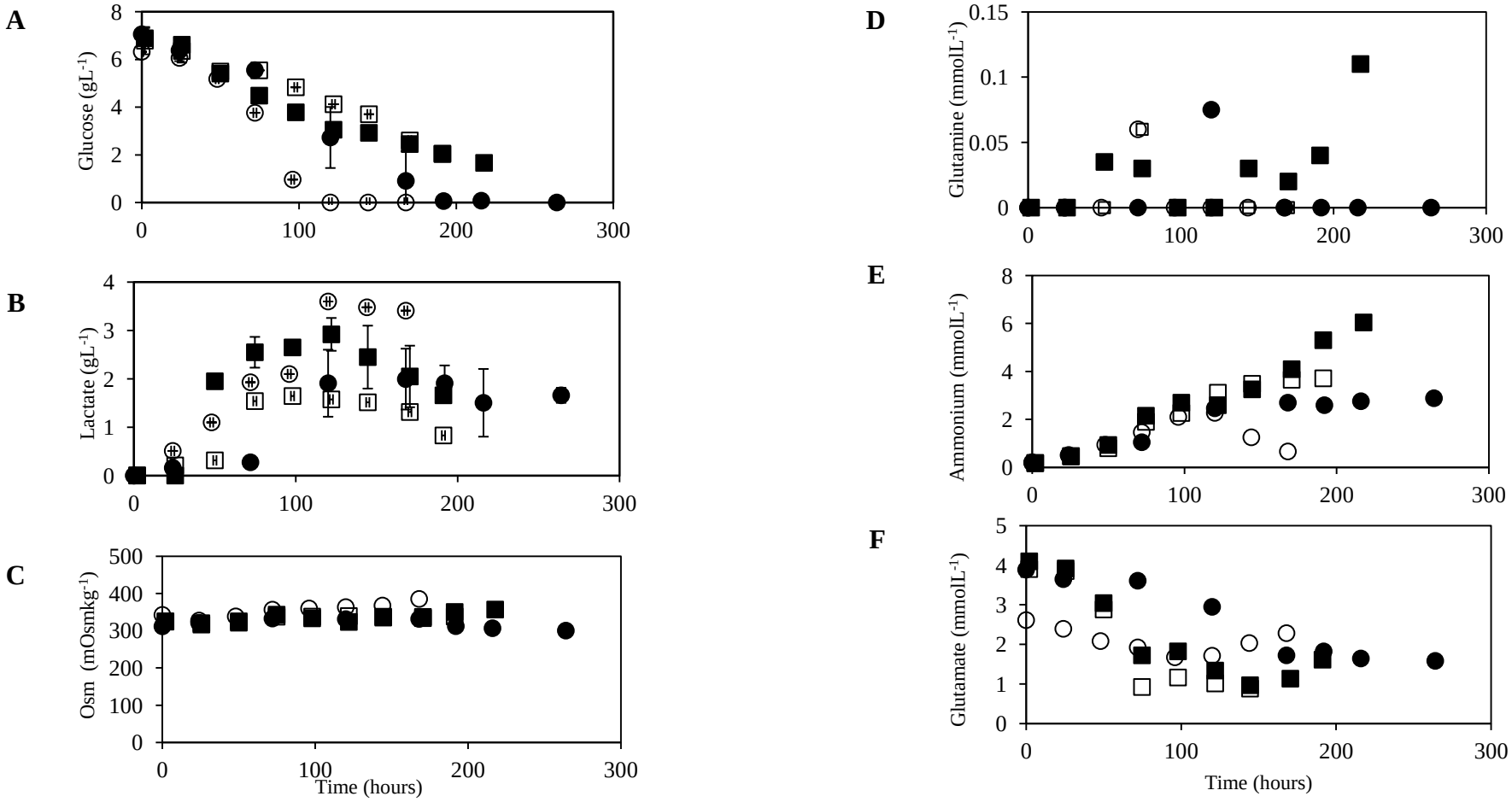

Figure 4.10: CHO metabolites concentration and osmolarity in batch culture for HEL-BioXplore MBR with two different impellers and spargers: direct driven with horseshoe (-●-), direct driven with singular hole (-○-), magnetic driven with horseshoe (-■-), magnetic driven with singular hole (-□-) A: glucose concentration; B: lactate concentration; C: osmolarity, D: glutamine concentration, E: ammonium concentration, F: glutamate concentration. (Note: missing data points due to faulty NOVA Flex to measure metabolites during the analysis).

4.8 Effect of different type of impeller in fed-batch mode

From the batch culture experiment, it was clearly seen that both MBR systems with singular hole sparger were not producing good results in terms of viable cell concentration and product formation. The MBR gas delivery mode was set up for intermittent sparging due to the low demand of oxygen in the early period of CHO cell growth. However, problems arise when using the singular hole sparger with the intermittent sparging, where large bubble formation are produced in the medium. As consequences, the large bubbles that intermittently formed had given negative effect on the cell growth as seen in Figure 4.11 A. Although the difference is minor, we chose to use the horseshoe type sparger for the fed-batch mode experiment because the geometry is similar with the standard sparger fitted in the 5 L bench STR. Furthermore, based on the engineering characterisation, the MBR with horseshoe type sparger gave shorter mixing times of ~4 - 6 s for different agitation rates, thus promoting better mixing in the MBR.

4.8.1 Growth kinetics and antibody production

All experiments were done in parallel using two MBRs with the same configuration of horseshoe type sparger. The studies were expected to produce similar growth and product formation in each MBR. Figure 4.11 A illustrates the CHO cell growth kinetics and percentage viability for both MBRs with horseshoe type sparger. The results showed that both MBR gave similar pattern of growth. Both of the MBR started the exponential phase on day 3 and attained peak viable cell concentration. on day 7 with 8.89± 0.39 x 10^6 cell mL^{-1} (direct driven impeller) and 7.68(± 0.33 x 10^6 cell mL^{-1} (magnetic driven impeller). The paired t-test was performed to determine the viability of CHO cell culture between the direct driven and magnetic driven impeller. The VCC of direct driven impeller cultures have no significant differences with the magnetic driven impeller cultures (p-value 0.08). This indicates that there is a positive linear relationship between the data sets obtained from the two culture system and highly correlated. The percentage viability for both MBRs demonstrated that the system with proper monitoring and control able to prolong the viability until the harvest point on day 14 with ~55 - 65%.

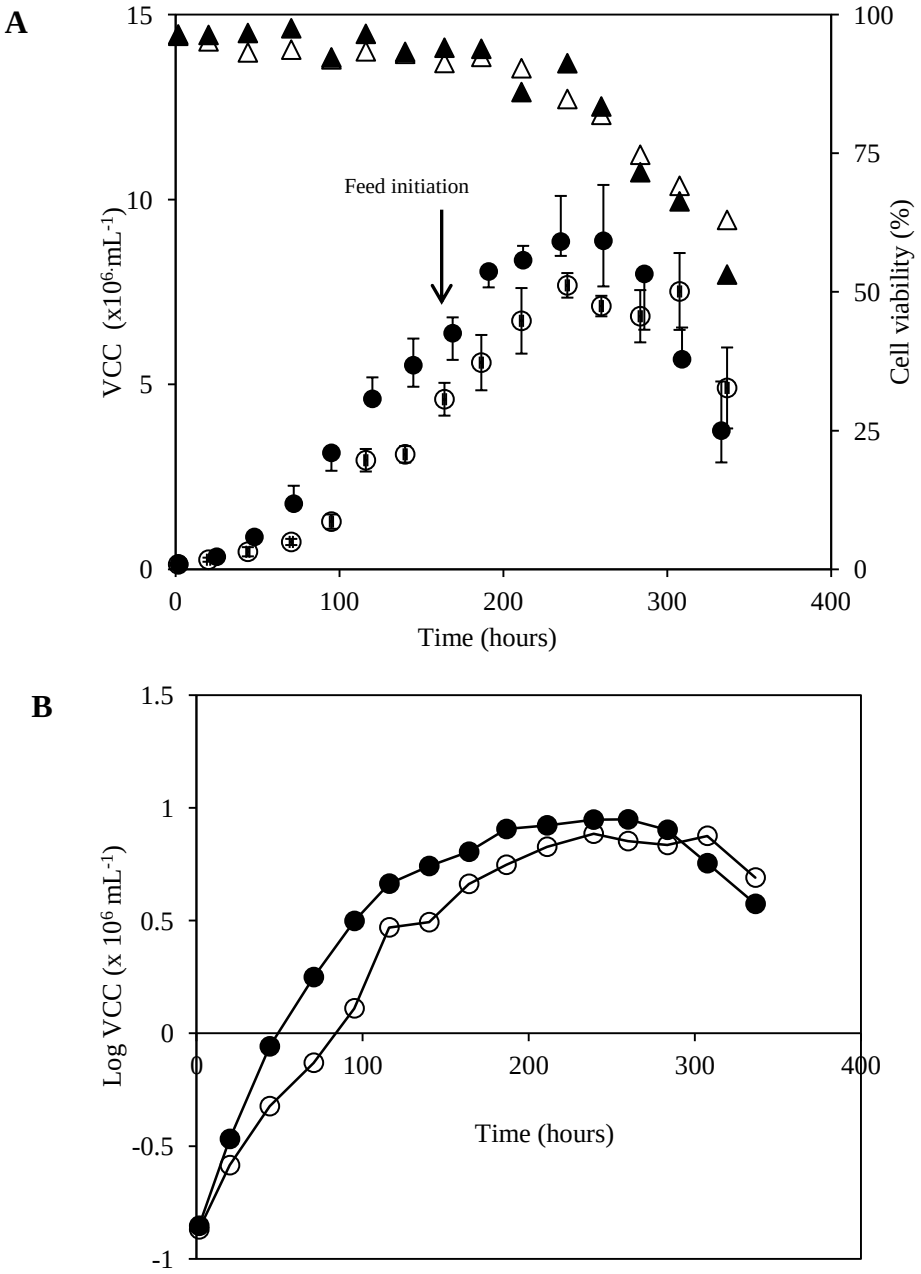

Figure 4.11: CHO growth kinetics in fed-batch culture for HEL-BioXplore MBR with two different impellers and horsehoe type sparger: direct driven (●▲), magnetic driven (○Δ) A: viable cell concentration and cells viability; B: Log VCC vs time. Arrow (↓) bolus fed addition on day 7. Error bars represent one standard deviation about the mean (n = 2).

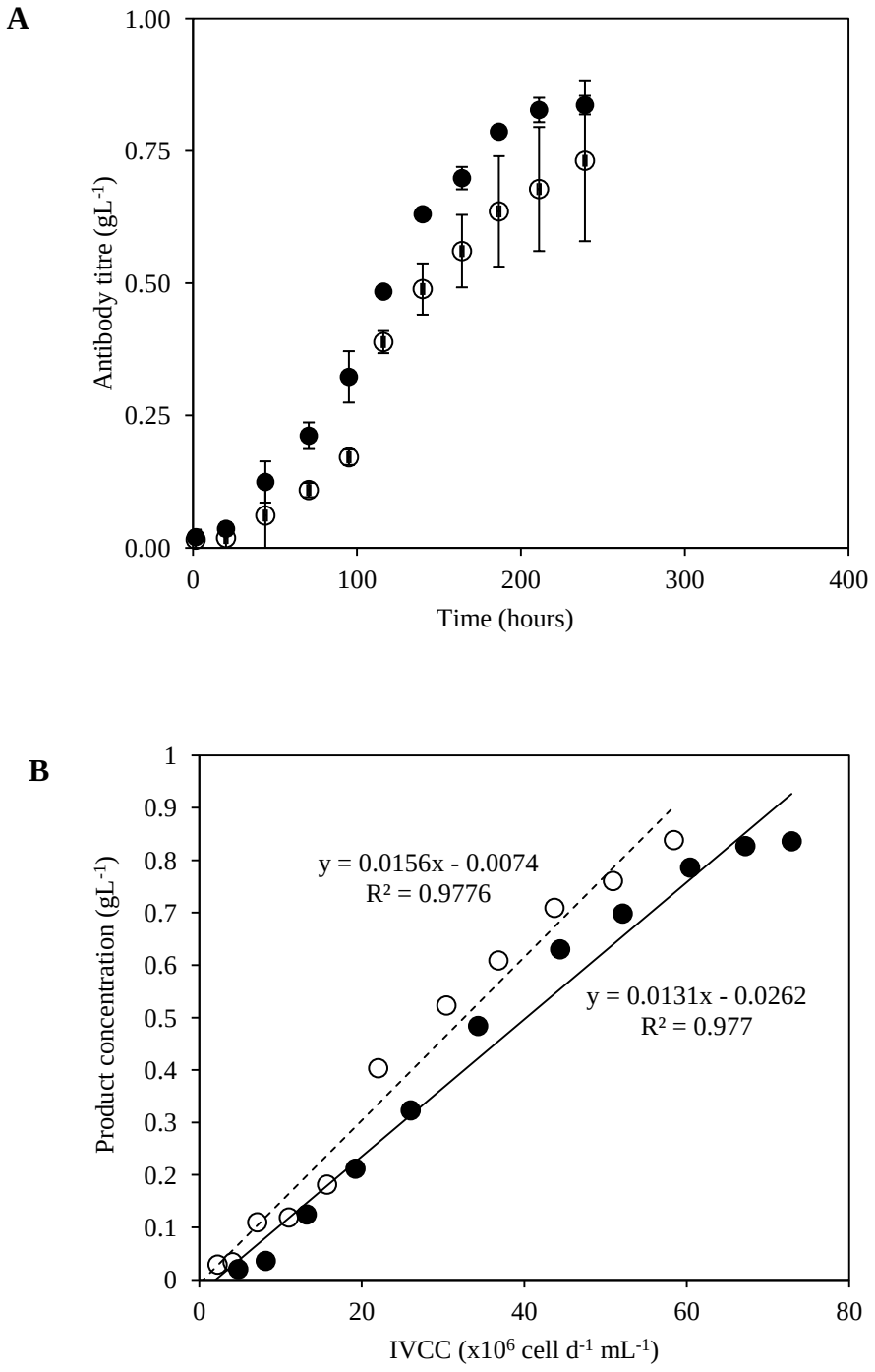

Figure 4.12: Product titre formation and IVCC in fed-batch culture for HEL-BioXplore MBR with two different impellers and horsehoe type sparger: direct driven (●), magnetic driven (○) A: IgG formation B: IgG antibody titre vs IVCC. Solid line shows the direct sparger, while dashed line shows the magnetic driven.

The derived growth parameters from this study are shown in Table 4.5. The major difference was observed in the maximum specific growth rate. The MBR with magnetic driven impeller had a higher μmax with 0.026 h^{-1} compared with MBR with direct driven impeller with 0.019 h^{-1}. Nonetheless, the cumulative integral viable cell concentration depicted a higher cIVC in the culture using the direct driven impeller compared with the magnetic driven impeller system yielding 4.96 x 10^6 cell d^{-1} mL^{-1} and 4.00 x 10^6 cell d^{-1} mL^{-1} respectively. Besides that, the maximum antibody production (Figure 4.12 B) achieved in the MBR with direct driven impeller is higher by 13 % with 0.84 gL^{-1} on day 14 compared to MBR with magnetic driven impeller system. The probability values of approximately 0.95 (95%) shows that both of the systems are reproducible. Both of the MBR shows good reproducibility based on the standard deviation of <±0.4 for cell concentration and <±0.1 for IgG concentration.

Table 4.5: Derived growth parameters of CHO cells in MBR in fed- batch mode with direct driven and magnetic driven impeller fitted with horseshoe type sparger.

.

Impeller/ Sparger	**Direct/ Horseshoe**	**Magnetic/ Horseshoe**
Peak cell concentration (x 10^6 cell mL^{-1})	8.89±0.39	7.68±0.33
cIVC (x 10^8 cell d^{-1} mL^{-1})	4.06	2.84
μmax (h^{-1})	0.019	0.026
IgG antibody titre (gL^{-1})	0.84±0.01	0.73±0.1
q_P (pg cell^{-1} d^{-1})	13.3	15.1
q_{glc} (pg cell^{-1} d^{-1})	51.5	50.1

*q_{glc} were calculated during exponential phase before feeding was initiated.
The data represents 2 replicas of MBR ± s.d.

4.8.2 Metabolites concentration

Generally, the CD-CHO medium used in the cultivation provided an initial glucose concentration of around 6 – 7 gL^{-1}. The high glucose concentration is needed in the initial stage of CHO cell fermentation to support high glucose demand. As the cells started to grow, the glucose is being consumed and it becomes limited. For fed-batch mode studies, 1 % of CD-CHO AGT was added on day 7 to prevent glucose limitation. The daily amount of glucose added to the MBR was sufficient to support the CHO cell growth until the end of fermentation. Figure 4.13 A shows the glucose consumption in the MBR with direct and magnetic driven impeller fitted with horseshoe sparger. Glucose consumption followed the similar decreasing pattern as expected in fed-batch mode for both MBRs. Glucose consumption rate observed was quite high at the beginning of the cultivation, especially during the exponential stage. As seen in Figure 4.13 A, the bolus addition of feed, was able to maintain the glucose concentration within a range of 1 – 3 gL^{-1} in the culture medium. This concentration was in agreement with several literature reports (Silk, 2014; Al-Ramadhani, 2015) suggesting that 1- 2gL^{-1} is needed to support the growth of CHO cells. The low residual glucose concentration is likely to enhance the cell growth and reduce the by-product formation (Butler, 2005).

By contrast, the lactate formation in MBR with direct driven impeller (Figure 4.13B was elevated to 4 gL^{-1}. Additonally, the high lactate concentration in the medium had an impact on the cell growth as seen in Figure 4.11 A, where the viable cell concentration quickly dropped after 260 hours. There was no stationary phase observed in this culture. As reported by Lao and Toth (1997), the combination of high lactate and osmolarity concentration had an adverse effect on cell growth and metabolism. The osmolarity also increased in the MBR with direct driven impeller to 540.8 $mOsmkg^{-1}$ as the lactate accumulation became greater in the medium (Figure 4.13 C).

Ammonium was the other waste product that has an inhibitory effect on product synthesis in mammalian cell cultivation (Ozturk and Palsson, 1991; Lao and Toth, 1997; Chen and Harcum, 2005). The effect of elevated ammonium levels in the MBR with direct driven impeller (Figure 4.13 D) resulted in lower specific growth rate as illustrated in Table 4.5. Ozturk *et al*. (1991) reported that the presence of ammonium and lactate will reduce the specific growth rate by one half in such a medium. Moreover, the continuous increase of ammonium concentration subsequently accelerated the consumption of glucose (Ozturk *et al*., 1991).

For glutamine concentration the results show fluctuation in the concentration for the MBR with direct driven impeller, whilst for the MBR with magnetic driven impeller it follows the normal trend of glutamine consumption (Figure 4.13E). Glutamine is an essential amino acid for cell metabolism. Glutamine and glucose are closely related in cell growth and metabolism and exhaustion of either one will have an adverse effect on cell growth (Lao and Toth, 1997; Altamirano *et al.*, 2000). The limitation of glutamine in the MBR with direct driven impeller caused the CHO cell growth rate to decrease. The glutamate concentration profile showed a similar trend as the batch fermentation with a decrease after 182 hours before it stabilised within 0.5 – 1 $mmolL^{-1}$ until end of cultivation.

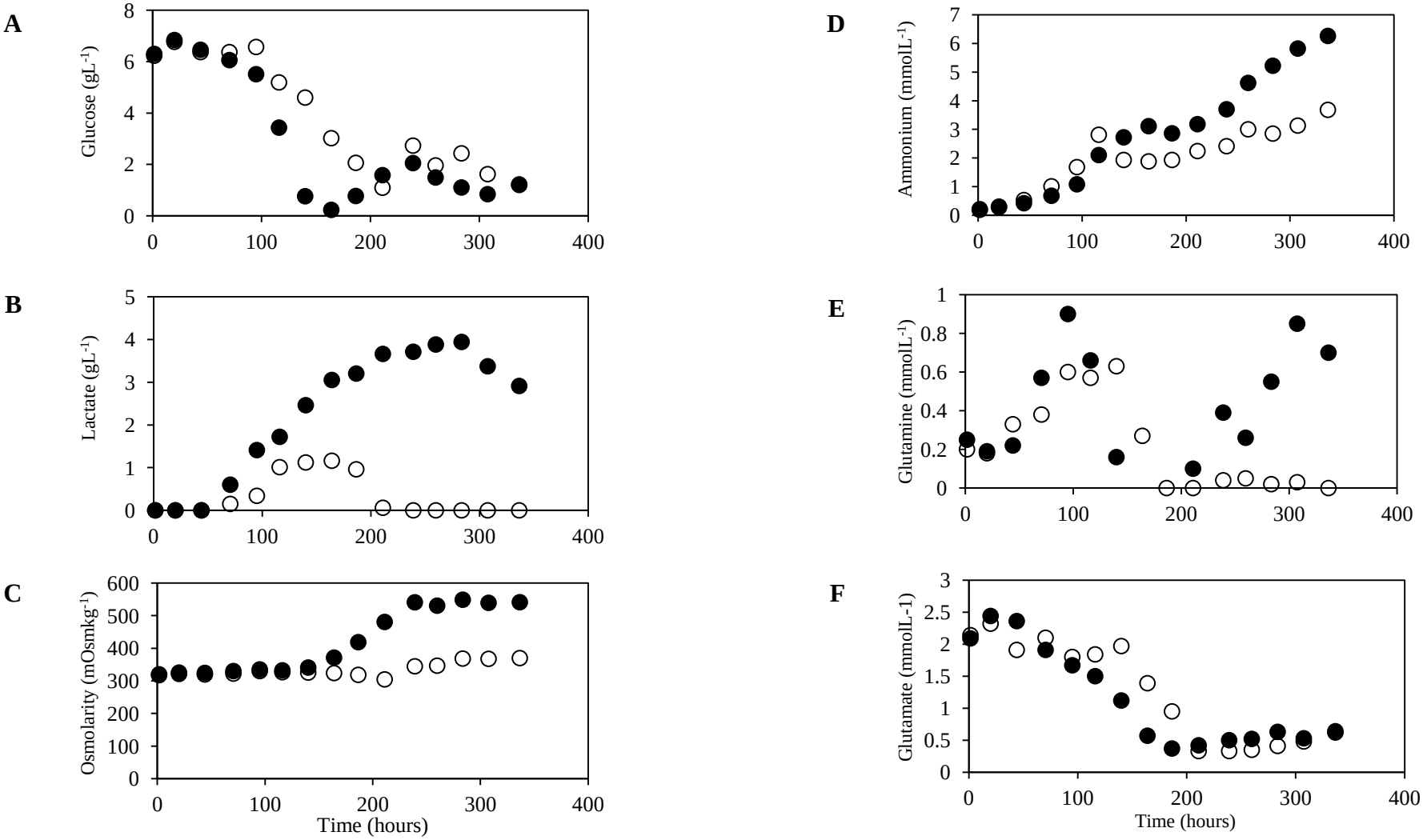

Figure 4.13: CHO metabolites concentration and osmolarity in fed-batch culture for HEL-BioXplore MBR with two different impellers with horseshoe type spargers: direct driven (●), magnetic driven (○), A: glucose concentration; B: lactate concentration; C: osmolarity, D: ammonium concentration, E: glutamine concentration, F: glutamate concentration. (Note: missing data points due to faulty NOVA Flex to measure metabolites during the analysis).

4.9 Conclusion

The chapter has presented a detailed engineering characterisation of the MBR for assessment of process performance using CHO cell culture. Mixing time (T_m) and volumetric oxygen transfer coefficient (k_La) has been characterised experimentally, whilst power input was predicted using existing engineering correlation. This system was characterised for better understanding of the MBR process performance at selected operating parameters. These engineering parameters are vital to explore the efficiency and feasibility of the MBR for high cell density cultivation especially using mammalian cells. Besides that, the characterisation is essential for scale translation studies which are described in Chapter 5.

Mixing time was characterised experimentally using the pH tracer method. The mixing time reduced significantly as the agitation rate increased in the MBR. The mixing time was measured between 3.3 – 14 s for different type of impellers and spargers as function of agitation rate. The shortest mixing time was obtained using the MBR with direct driven impeller equipped with horseshoe sparger ranging from 3.3 – 9.3 s. The mixing times measured experimentally were comparable with calculated values using the Nienow correlation of between 4.8 – 12.1 s and 4.3 – 11.0 for the direct driven and magnetic driven impeller respectively. The consistent mixing times obtained in this study showed that the correlation is suitable for the evaluated MBRs.

k_La was measured experimentally using the static gassing out technique (Wise, 1951) as described by Section 2.7.2. The studies conducted with cultivation media CD CHO at 37°C to mimic the actual fermentation condition. k_La was determined using two types of modified spargers; horseshoe type and singular hole sparger. The measured k_La obtained were 5.9 to 12.5 h^{-1} as function of agitation rate ranging from 200 rpm – 500 rpm. The k_La of the current study are consistent with values given by Xing *et al*. (2009) and Tissot *et al*. (2012) which indicated that k_La values below 15 h^{-1} are applicable for mammalian cell culture. Power input into the MBR was calculated based on equations described in Section 4.5. The power input measured was varied for two different types of impellers. As expected, direct driven impeller required more power to rotate the shaft compared with magnetic driven impeller. The

power inputs measured ranged from 1.7 – 54.5 Wm^{-3}, which is in agreement with Nienow (2006) and Heath and Kiss (2007) with power inputs from 10 – 1000 Wm^{-3} for different geometry of mammalian cell bioreactors.

Based on the findings from the engineering characterisation, batch and fed-batch mode of operation in the MBR with variation of impeller configurations were studied. Using a mixing time of 6 s for magnetic and direct driven impeller gave agitation rates of 400 rpm to 450 rpm respectively. For batch mode of operation the MBR with direct driven impeller equipped with horseshoe sparger was the best configuration in terms of cell growth (7.06×10^6 cell mL^{-1}) and IgG productivity (0.40 gL^{-1}). The findings were further explored in fed-batch mode operation of MBR with two types of impeller and horseshoe sparger.

Fed-batch mode results indicated that bolus addition of feed on day 7 enhanced the growth of CHO cell and IgG product formation. Peak viable cell concentration was 8.89×10^6 cell mL^{-1} and IgG productivity of 0.84 gL^{-1} at the end of fermentation. The significant differences observed between the two impellers were the higher lactate and ammonia concentration produced in direct driven impeller than magnetic driven impeller. Nonetheless, the higher by-product concentration reported does not affect the cell growth and reproducibility for the direct driven impeller as cIVC produced are better than magnetic driven impeller with 4.06 and 2.84×10^8 cell d^{-1} mL^{-1} respectively.

The results of this investigation show that MBR with parallel reactors produced growth kinetics and productivity that are comparable and reproducible. Furthermore, the characterised engineering parameters will serve as basis for scale translation studies using bioreactors with different geometries.

Chapter 5 Scale translation between microwell based systems and miniature bioreactors at matched mixing time

5.1 Introduction

Predictive scale-up from miniature reactors to industrial scales are essential to reproduce comparable product yields and quality (Bareither and Pollard, 2011). Moreover, scale-up is a critical step in predictive operation of a reactor to perform at optimal conditions. Nonetheless, Wurm (2004) mentioned that there are many issues that need to be scrutinized when scaling up mammalian cell cultivation from small scale to manufacturing scale. For a successful scale-up process, optimisation of miniature reactors is very important to determine the reliability of a reactor, which subsequently could save on materials and costs of bioprocess development (Micheletti and Lye, 2006). Previous studies have looked into the predictive scale-up of mammalian cell culture based on several fundamental engineering parameters for different geometries of bioreactors. Micheletti *et al*. (2006) investigated the application of 24 and 96 microtitre plates (MTP) for predictive scale-up to shake flasks based on equal energy dissipation rate. Xing *et al.* (2009) used the basis of mixing time and k_La to predict the scale translation of 5 L and 20 L stirred tank reactors (STR) to industrial scale reactor of 5000 L. Whereas, Tissot *et al.* (2010) studied the effect of k_La on different scales of orbitally shaken reactors (250 mL and 200 L) and found that k_La between 7 – 10 h^{-1} are sufficient to avoid dissolved oxygen limitation in reactors.

In this chapter, the scale translation of different geometries and scales of reactors was investigated. Cell culture performances were investigated to determine the scalability and reproducibility of microtitre plates (2 - 4 mL scale), miniature bioreactor (500 mL scale) and stirred tank bioreactor (5 L scale). The basis of the engineering characterisation of the miniature bioreactor from Chapter 4 and selected engineering parameters from previous studies for MTP (Silk, 2014) and STR (Barrett, 2008) were applied to compare the growth kinetics and productivity.

Chapter aims and objectives:

- To investigate the scale-up of fed-batch (bolus fed) of CHO cell line based on matched mixing time in 24-SRW, miniature stirred reactors and stirred tank reactors.
- To characterise a prototype micro-bioreactor (micro-Matrix) for CHO cell line growth profiles and productivity.
- To investigate the scale-up of fed-batch (continuous) of CHO cell line based on matched mixing time in micro-Matrix and miniature stirred reactors.

5.2 Fed-batch with bolus feed and matched T_m

Fed-batch culture is the most attractive choice for monoclonal antibody production due to its flexibility, reliability and productivity in reactors. Normally in fed-batch culture, bolus addition is applied to enhance the longevity and maintenance of the specific productivity of a desired protein (Altamirano *et al.*, 2000). The essential nutrients are fed in order to reduce by-product formation and improve control of environmental conditions (Bibila and Robinson, 1995). Recent studies have focused on scale-up comparison from miniature bioreactors to 5 L STR (Al-Ramadhani, 2015) and micro-24 to shake flasks and 2 L STR (Betts, 2015) using bolus addition. In this study, the fed-batch cell culture formats were selected based on predicted matched mixing time (T_m ~ 6 ± 2 s) as scale-up criterion. This is in agreement with the findings suggested by Silk (2014) which experimentally applied mixing time as scale translation criterion for small scale reactors. The literature recommended that at mixing time of 6 s with $k_La > 5\ h^{-1}$ is sufficient for oxygen transfer in reactors. Therefore, oxygen would not be the limiting factors when homogenous mixing is achieved within these conditions. The selected operating conditions for each of the reactors experimentally applied in these studies are described in Table 5.1.

Table 5.1: Selected operating parameters for cell culture cultivation based on matched mixing time.

Reactor	24-SRW (MTP)	HEL-BioXplore	Bench STR
Shaking/Stirring	220 rpm	450 rpm	260 rpm
Aeration system	Headspace	Horseshoe type sparging with flow rate of 50 mL min^{-1}	Horseshoe type sparging with flow rate of 100 mL min^{-1}
Working volume	800 μL	350 mL	3.5 L
pH/DO/Temperature control	n/a	Yes	Yes
Feeding strategy	Bolus fed	Bolus fed	Bolus fed

5.2.1 Growth kinetics and antibody productivity

The growth kinetics of CHO cell cultures in different geometries of reactors; 24-SRW (MTP), MBR, and bench 5 L STR are depicted in Figure 5.1. CHO cell growth for 24-SRW and 5 L STR shows good similarity, whilst the MBR has slower growth between 70 hours until 168 hours of cultivation (Figure 5.1 A). During this period of culture time, cells are in the exponential phase and started to proliferate. However, the peak viable cell concentration for the three reactors are comparable with 24-SRW (9.30×10^6 cell mL^{-1} on day 7), MBR (9.56×10^6 cell mL^{-1} on day 9) and 5 L STR (10.04×10^6 cell mL^{-1} on day 7) as shown in Table 5.2. The significant growth difference was observed in MBR cultures with a slower growth that only peaked on day 9. Final percentage viability of the 24-SRW and MBR were equivalent at 60 %, while 5 L STR was at 80 % after 336 hours (Figure 5.1 B). The possible explanation for this result might be that feed addition was initiated daily on day 7 until day 13.

Altamirano *et al.* (2004) suggested that addition of feed able to lengthen the cell viability as it provide extra nutrient supplement to the culture. This finding was further support the literature's suggestion that longevity of the cell culture is influenced by fed-batch of periodic addition of depleting nutrients, which subsequently would increase final protein production. The higher viability observed

in the STR on day 14 might be due to the better control and monitor of process parameters for cell cultivation in the reactor. Furthermore, the engineering parameters and bolus feeding strategies in the STR system used in this study has been characterised and optimised for mammalian cell cultivation (Barrett, 2008).

Table 5.2 summarises the derived growth parameters and yield coefficients. The yield coefficient of lactate produced over glucose consumption shows similar values between the 24-SRW and STR system. The low $Y_{lac/gluc}$ suggests that glucose is being metabolised by different pathways leading to more energetically efficient utilisation of glucose (Zhou *et al.,* 1995). However, the MBR has slightly higher value with 1.15 g g^{-1} compared to the other systems. The yield of ammonium produced over glutamine consumed shows that the MBR system has the highest yield with 1.07 mmol $mmol^{-1}$, while the 24-SRW and STR have almost identical yields with 0.98 and 0.95 mmol $mmol^{-1}$. The yield of $Y'_{NH3/Gln}$ is slightly lower to that reported in literature (1.4 – 1.7) by Zeng *et al.,* (1998) however this may be due to differences in the experimental conditions. In general, the yield coefficients determined from cultures in the three reactors are comparable with variation within the error of analysis.

Table 5.2: Derived growth parameters of fed-batch CHO cell in three different reactors formats based on matched mixing time.

Type of reactor	**24-SRW MTP**	**MBR DirHS**	**5 L STR**
Peak cell concentration (x 10^6 cell mL^{-1})	9.30± 2.43	9.56 ± 1.12	10.04 ± 0.06
CiVC (x 10^8 cell d^{-1} mL^{-1})	4.74	4.05	4.83
μmax (h^{-1})	0.024	0.018	0.018
IgG antibody titre (gL^{-1})	0.92 ±0.05	0.69 ± 0.15	0.83 ± 0.03
q_P (pg $cell^{-1}$ d^{-1})	12.2	10.2	9.7
***q_{glc} (pg $cell^{-1}$ d^{-1})**	338.7	293.3	274.5
***Y'* Lac/Gluc (g g^{-1})**	1.09	1.15	1.08
***Y'* NH_3/Gln (mmol $mmol^{-1}$)**	0.98	1.07	0.95

*q_{glc} were calculated during exponential phase before feeding was initiated.
The data represents 3 replicas of 24-SRW and 2 replicas of MBR and STR ± s.d.

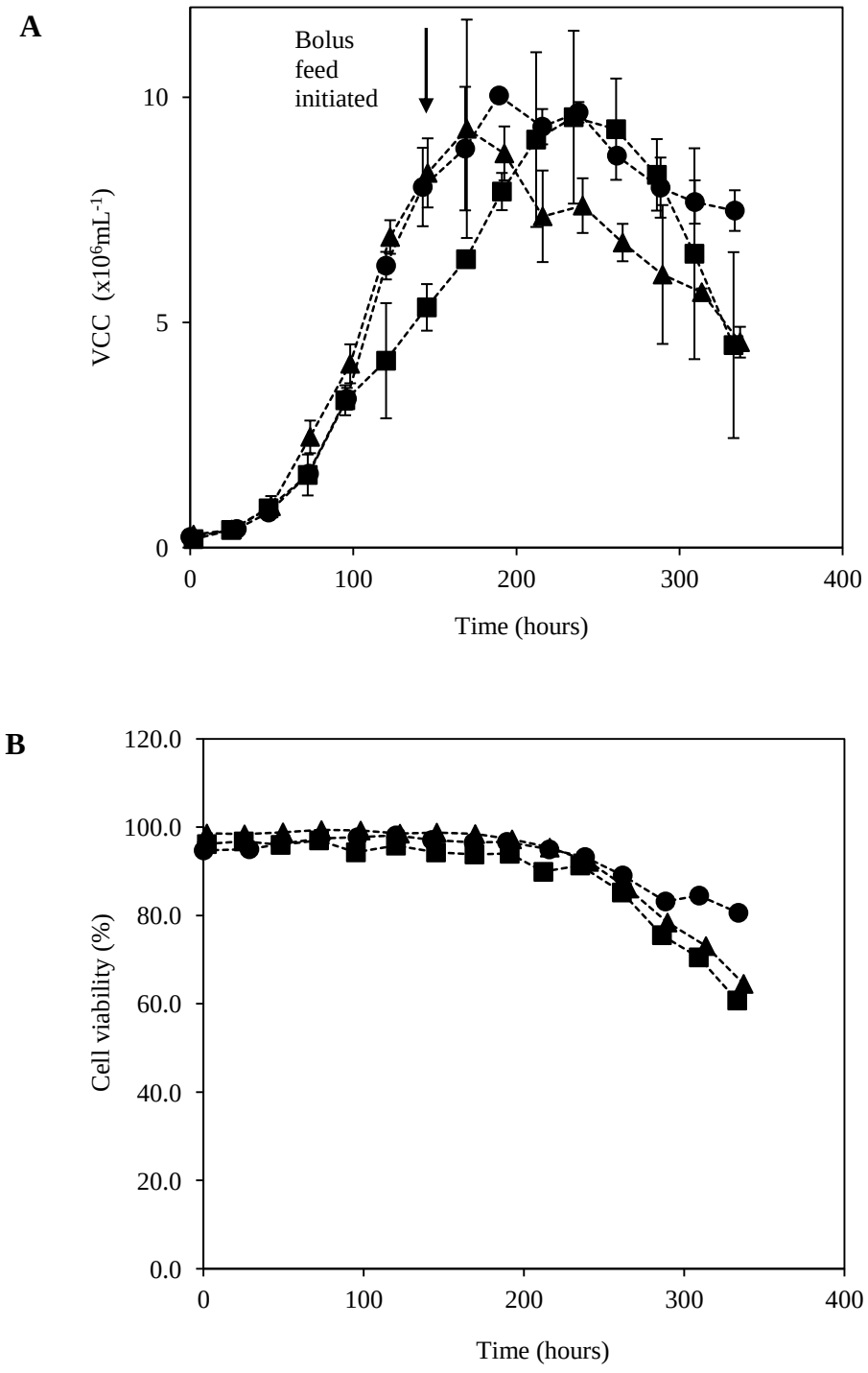

Figure 5.1: CHO growth kinetics in fed-batch cultures for three reactors: 5 L STR (●), MBR (■), 24-SRW (▲) A: Viable cell concentration; B: Cells viability. Arrow (↓) indicated bolus fed addition on day 7. Error bars represent one standard deviation about the mean (n = 2) for MBR, STR and mean (n = 3) for 24-SRW.

Apart from that, cell specific productivity (q_p) also gave similar trend when plotted for product formation with IVCC (Figure 5.3 B). The 24-SRW gave the highest q_p with 12.2 pg cell^{-1} d^{-1} compared to MBR and STR with 10.2 and 9.7 pg cell^{-1} d^{-1} correspondingly. Based on the semi-logarithmic plot of VCC vs time (Figure 5.2), the cell growth kinetics for the three reactors geometries showed similar trends. The graph indicates that 5 L STR and MBR exhibited the identical μ_{max} during the exponential stage with 0.018 h^{-1}, while 24-SRW had a higher μ_{max} with 0.024 h^{-1} at the same stage. Nevertheless, the cumulative integral VCC for the three reactors show minor disparities between the three reactors geometries with 4.0 – 4.9 x 10^6 cell d^{-1} mL^{-1} for 14 days of cultivation. As for the antibody productivity, the 24-SRW had the highest final IgG titre of 0.92 gL^{-1}, which is 10 % and 24 % higher than 5 L STR and MBR correspondingly (Figure 5.3 A). These results may be explained by the fact that the 24-SRW had a higher osmolality due to the higher relative rate of evaporation as discussed previously in Section 3.3.1. Even though osmolality was not measured for this study, it was predicted that the 24-SRW cultures have the identical trends as described in Chapter 3. The findings of the current study are consistent with Silk *et al*. (2010) who found that high osmolality may have contributed to the maximum final antibody concentration in microtitre plates. The final antibody concentrations produced in MTPs were 10 % higher compared to the shake flasks cultivations.

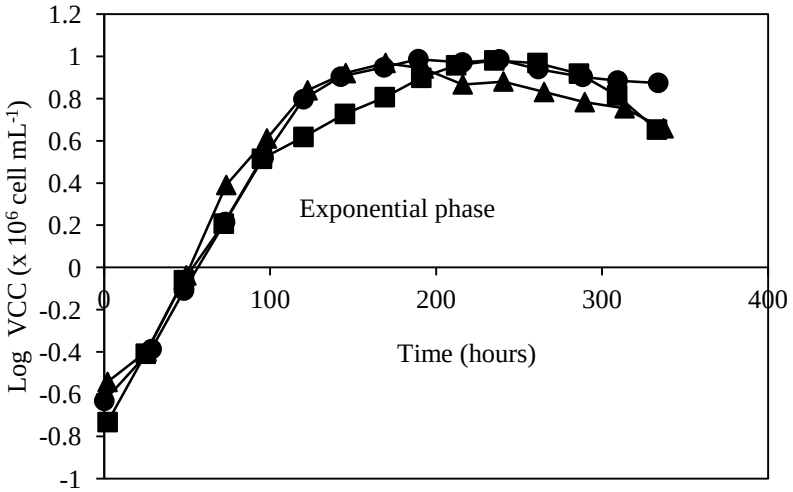

Figure 5.2: Log VCC of CHO growth kinetics in fed-batch culture for three reactors: 5 L STR (●), MBR (■), 24-SRW (▲).

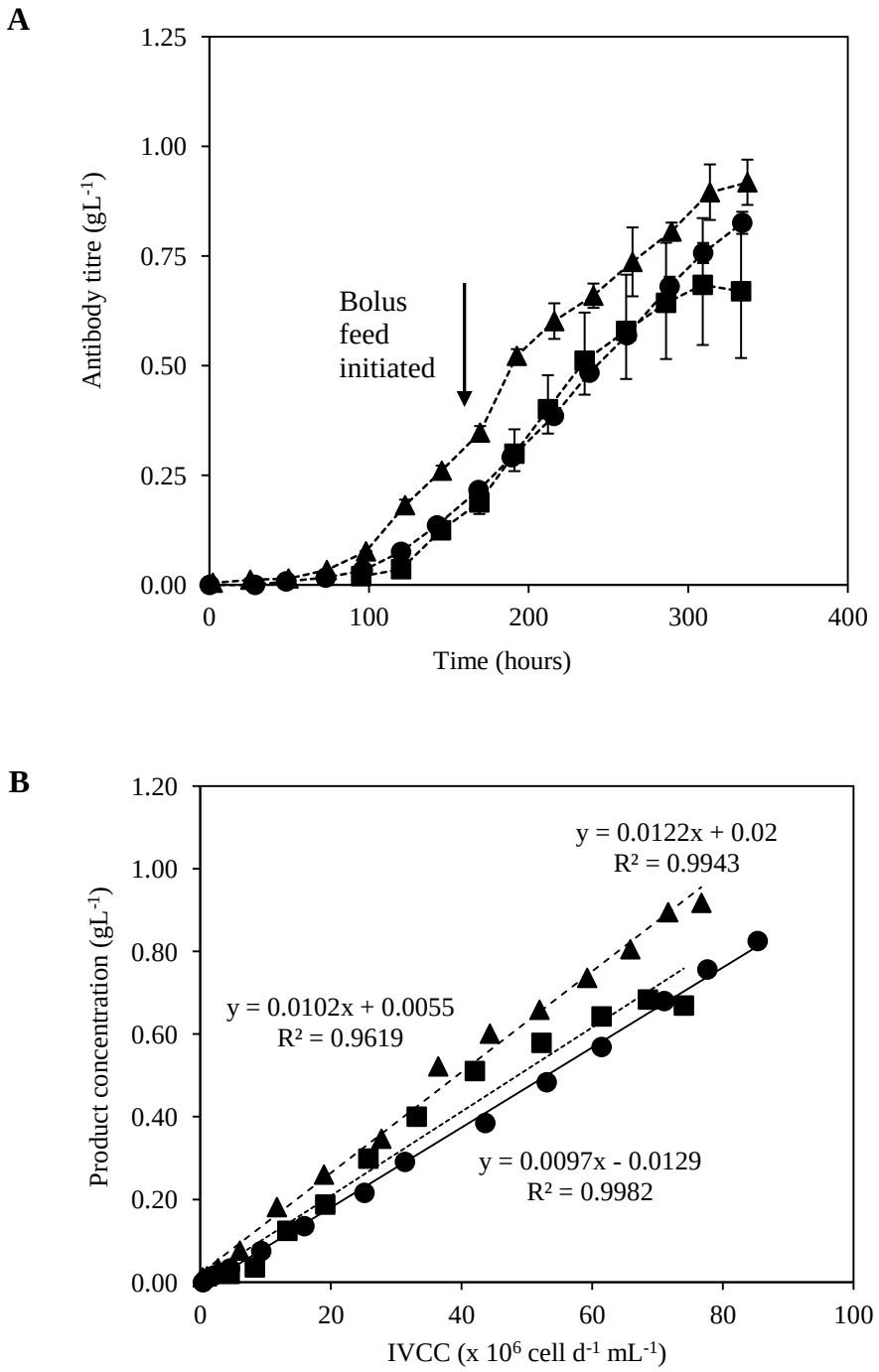

Figure 5.3: A: Antibody production in CHO growth kinetics in fed-batch culture for three reactors: 5 L STR (●), MBR (■), 24-SRW (▲). Error bars represent one standard deviation about the mean (n = 2) for MBR and STR and mean (n = 3) for 24-SRW. Arrow (↓) indicated bolus fed addition on day 7. B: Comparison plots of product formation vs IVCC for three reactors with trend line, solid line (●) represents 5 L STR, dotted line (■) represents MBR and dashed line (▲) represents 24-SRW.

5.2.2 Metabolites analysis

As previously reported in Chapter 3 and 4, starting glucose concentrations in the culture was in the range 6 – 7 gL^{-1}. Glucose consumption was almost identical for all three reactors from 0 hour until 120 hours as shown in Figure 5.4 A. During this phase, the cultures are in batch stage and no nutrient is being added as the amount of glucose available is adequate to support the cell growth and metabolism. At the same time as the glucose concentration was depleted at 168 hours, the feed was added to supplement the cultures with nutrients for cell proliferation and metabolism. At this stage, glucose concentrations were observed to be lower than 2 gL^{-1} for all reactors. Bolus fed was initiated for the three cultures on day 7 by adding 1% v/v of concentrated feed CD CHO AGT (supplemented with glucose). Since the three cultures were bolus fed daily until day 13, the glucose consumption for three reactors changed. Glucose concentration in 24-SRW are within 2 – 3 gL^{-1}, whilst in 5 L STR and MBR the concentration are within 0.5 – 2 gL^{-1}. The lower glucose concentration in MBR and STR is probably due to the higher metabolism by CHO cells as seen in the growth kinetics in Figure 5.1 A. The cell growth in MBR and STR kept increasing until 200 hours, while in 24-SRW the cell growth kinetics showed a sudden decline after bolus addition.

Lactate concentration profiles between the three reactors show a comparable production trend for 0 - 142 hours (Figure 5.4 B). Since glucose was added during the fed-batch stage, lactate was produced in MBR and STR cultures until it reached a peak of 3.54 and 2.77 gL^{-1} respectively. Surprisingly, lactate production in the 24-SRW culture dropped after the bolus addition until the later stage of culture. This finding was unexpected and suggests that there could be lactate consumption by the cells during this period. The present findings seem to be consistent with studies by Altamirano *et al.* (2004) which found that the decrease in lactate concentration during tissue plasminogen activator (t-Pa) productions was not due to dilution but actually represent lactate consumption by cells. Moreover, they noted that lactate consumption is generally taking place when glucose started to be depleted in cultures which are comparable to this study. However, the findings in our study show that the glucose supply was sufficient and maintained in range of 2 – 3 gL^{-1} during the feeding phase. Basically glucose and glutamine are the main carbon and energy sources required to support cell metabolism (Altamirano *et al.*, 2006). However, it is

observed that the glutamine consumption in CHO cells is relatively fast and not adequate for cell metabolism. The phenomenon drives the culture to a situation of nutrient depletion and accumulation of by-products (lactate and ammonium) which made the medium imbalanced and consequently inhibited the cell growth (Altamirano *et al.*, 2006). The CHO cell line cultured in this study is glutamine synthetase (GS) CHO, which does not required glutamine addition for cell metabolism (Bibila and Robinson, 1995). However, glutamine is generally available and can be synthesised from glutamate as described in Section 1.3.1. This was seen in this study with STR and MBR cultures where glutamine concentration of 2.57 mmol L^{-1} and 1.03 mmol L^{-1} correspondingly were found on day 5 of culture (Figure 5.4 C). As shown in Figure 5.4 D, glutamate consumption was similar for all three cultures, as expected.

Altamirano *et al.* (2004) also mentioned in their study, cells grown with glutamate supplementation consumed glucose more efficiently. They added that low rates of glutamate consumption are able to reduce accumulation of waste metabolite of ammonium and prolong fed-batch culture. However, the findings of the current study do not support the previous research. Ammonium concentration in three reactors cultures reached peak concentration of > 2.5 mmol L^{-1} (Figure 5.4 E) which could inhibit the cell growth and viability. The accumulation of ammonium which is a toxic metabolic by-product will create a toxic environment in the culture. Specifically, elevated ammonium levels significantly inhibit final cell densities and product formation as agreed by other studies (Chen and Harcum, 2005; Altamirano *et al.*, 2006; Gagnon *et al.*, 2011; Li *et al*., 2012). Moreover, ammonium accumulation in cell culture has a more adverse effect than lactate build up, which even at low concentration is able to inhibit cell growth and cellular productivity (Li *et al.*, 2012). Accordingly, future studies on methods to control ammonium and lactate level in culture should be emphasised. Altamirano *et al*. (2006) have studied extensively to replace glucose and glutamine with galactose and glutamate to improve the t-Pa production process. The possibility of CHO cells to consume galactoses in the absence of glucose opens up possibility of different culture strategies in fed-batch cultivation.

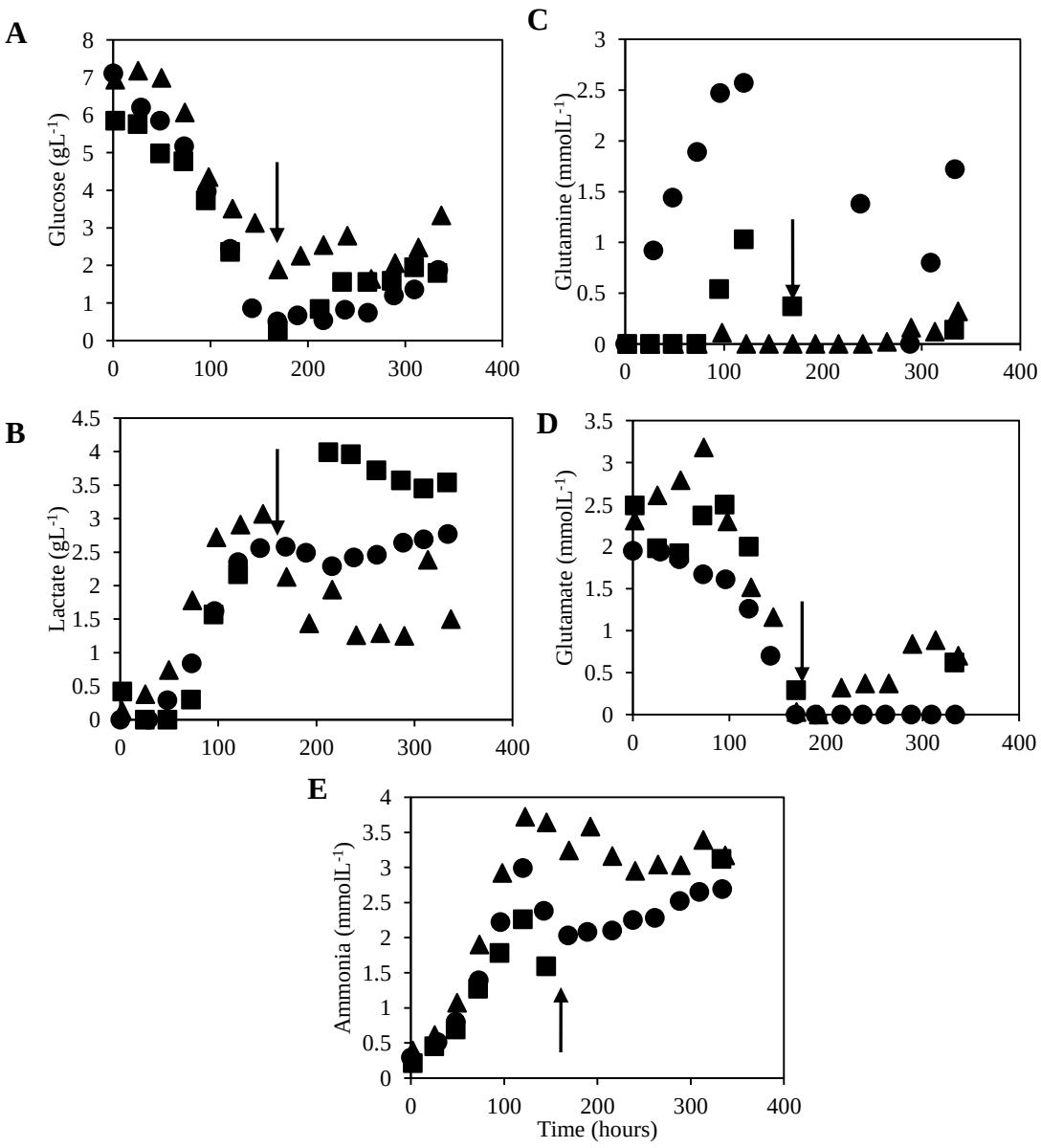

Figure 5.4: CHO metabolites concentration and osmolality in fed-batch culture for three reactors geometries; 5 L STR (●), MBR (■), 24-SRW (▲) A: glucose concentration; B: lactate concentration; C: glutamine concentration, D: glutamate concentration, E: ammonium concentration. Arrow (↓) indicated bolus fed addition on day 7. Note: missing data points due to faulty NOVA Flex to measure metabolites during the analysis.

5.3 Characterisation of a new micro-bioreactor system (micro-Matrix)

As described in Chapter 3, automation of microtitre plates is crucial to accelerate early bioprocess development of therapeutic proteins (Micheletti and Lye, 2006). Microtitre plates which are parallel and high throughput are commonly used in the screening stage of process development for cell line evaluation (Duetz *et al.*, 2000). Thus, development and innovation of microtitre plates technology has resulted in advanced microtitre plate systems that could offer automation, parallel and high throughput. The micro-Matrix by Applikon Biotechnology B.V. (Holland) is a further development of an existing micro-24 system that using the microtitre plate platform. Micro-Matrix is a micro bioreactor with a 24-deep well plate (24-DWP) cassette. The system was designed for research on early process development which could generate representative and high quality data during screening. This system enables high throughput and parallel experiments and independently controls each of the wells individually. The unique square size, deep well plate cassette is integrated with PreSens sensors (Duetz, 2007). The PreSens sensors have the ability to independently monitor the temperature, pH and dissolved oxygen (DO). Each bioreactor or well have its own proportional, integral and derivative (P.I.D) controller for pH, temperature and dissolved oxygen (DO). Individual pH control is achieved via automated gas addition and liquid addition, whilst the DO level can be controlled using up to four gas (oxygen, nitrogen, carbon dioxide, or compressed air) additions per well. The temperature control is integrated with an individual Peltier element for cooling and heating of each well. At the moment, there are no publications regarding the application of micro-Matrix for cell cultures. The finding in this study will provide the initial data using the micro-Matrix system for CHO cell cultivation.

5.4 Effect of control and non-control of aeration in the micro-Matrix with bolus feed

The preliminary studies were aimed at determining the effect of the control and non-control of aeration in micro-Matrix with bolus feed. Several operating conditions from the previous studies of 24-DWP by (Duetz, 2007) were selected to study CHO cells growth kinetics and antibody productivity. The selected operating conditions for CHO cells cultured in the micro-Matrix system in comparison with 24-SRW (MTPs) are described in Table 5.3. It shows that both systems had the same shaking diameter of 25 mm and similar headspace aeration through the filter on the top cover. The 24-SRW plate was covered with sandwich lid that had 5 layers to minimise evaporation and contamination, whereas, the micro-Matrix plate was covered with a top plate that had gas filter bars to control the gas exchanges, evaporation and contamination as described in Figure 2.1 (Section 2.4). Additionally, the significant advantage of micro-Matrix over standard 24-SRW plate is the automation interface that could monitor and control operating conditions with micro valve system for advance feeding strategies. The micro-Matrix reactor was prepared as described in Section 2.4. The reactor was aerated using headspace aeration at flow rate of 0.5 mL min^{-1} for the four main gases. For the micro-Matrix with controlled aeration, DOT was controlled according to the standard of 30 % of air, while for the non-control aeration; DOT was control through constant air flow rate. Furthermore, as direct comparison of the culture environment between the micro-Matrix and 24-SRW system, the micro-Matrix was overlayed with gas mixture of 95 % compressed air and 5% CO_2. The overlay of 5 % of CO_2 was to mimic the equivalent air environment as in the incubator shaker applied in the 24-SRW cultures.

Table 5.3: Selected operating conditions in micro-Matrix in comparison with 24-SRW system.

Reactor	micro-Matrix	24-SRW (MTP)
Type of plate	24 deep square well plate	24 standard round well
Maximum volume (mL)	7	3
Fill volume (mL)	3.5	0.85
Shaking frequency (rpm)	270	220
Shaking diameter (mm)	25	25
Feeding strategies	Bolus and continuous (micro valve)	Bolus (manual addition)
Automation	Yes	No
pH/DO/temperature control	Yes	No
Aeration	Headspace	Headspace

5.4.1 Growth kinetics and antibody production

The growth rate of the fed-batch CHO cells cultured in the micro-Matrix showed a significant distinction with the 24-SRW. The growth rates observed in micro-Matrix for control and non-control aeration were very slow, while for 24-SRW similar results as discussed comprehensively in Chapter 3 were found with 8.76 x 10^6 cell mL^{-1} (Section 3.3.1). Peak viable cell concentration for 24-SRW was the highest with 9.30 x 10^6 cell mL^{-1}, whilst micro-Matrix (control) and micro-Matrix (non-control) gave 7.80 x 10^6 cell mL^{-1} and 6.15 x 10^6 cell mL^{-1} correspondingly (Figure 5.5 A). As for the cell viability, 24-SRW and micro-Matrix (control) show good similarity with > 60% of viability on the harvest day (~336 hours). However, the micro-Matrix culture (non-control) had a very poor viability with 10 % on the harvest day (Figure 5.5 B). The possible explanation for the poor viability might be due to the accumulation of partial pressure carbon dioxide

(pCO_2). As described in Section 2.4, the micro-Matrix system was sparged with a gas mixture of 95 % air and 5 % CO_2 to mimic the condition of the standard incubator for 24-SRW cultivation. Nonetheless, the addition of 5 % CO_2 to the system had a negative effect on cell growth and viability as seen in Figure 5.5 B. Several literatures have reported a similar effect of high pCO_2 on cell growth of CHO cells (Gray *et al.*, 1996; Kimura and Miller, 1997; Zhu *et al.*, 2005). For the micro-Matrix (non-control aeration) the impact of dissolved (dCO_2) saturation from the partial pressure CO_2 over time increased as the removal of CO_2 is inadequate. This is in agreement with Gray *et al.* (1996) and Kimura and Miller-(1997) studies of the importance of CO_2 removal from the mammalian cell reactors. Additionally, from the Kimura and Miller (1997) investigation, they found that headspace aeration also contributed to the high CO_2 level to 115 mm Hg from normal level (31 – 55 mm Hg) in the 6 well plates.

The detrimental effect possibly due to dCO_2 accumulation in culture can be seen with the low specific growth rate (μ_{max}) in the micro-Matrix (non-control). The μ_{max} for non-control is 0.009 h^{-1}, while control and 24-SRW are 0.014h^{-1} and 0.019h^{-1} respectively (Figure 5.6). Moreover, product formation for both of the micro-Matrix cultures is very low with maximum titre of 0.24 – 0.30 gL^{-1} (Figure 5.7 A). The low titres obtained in the micro-Matrix are probably due to the initial dCO_2 accumulation in the wells. Derived growth parameters for cIVC and specific product formation (q_P) supports the same explanation for low product formation as described in Table 5.4. Alternatively, by-product formation of lactate and ammonium could be the cause for the low growth obtained as discussed in Section 1.3.2.

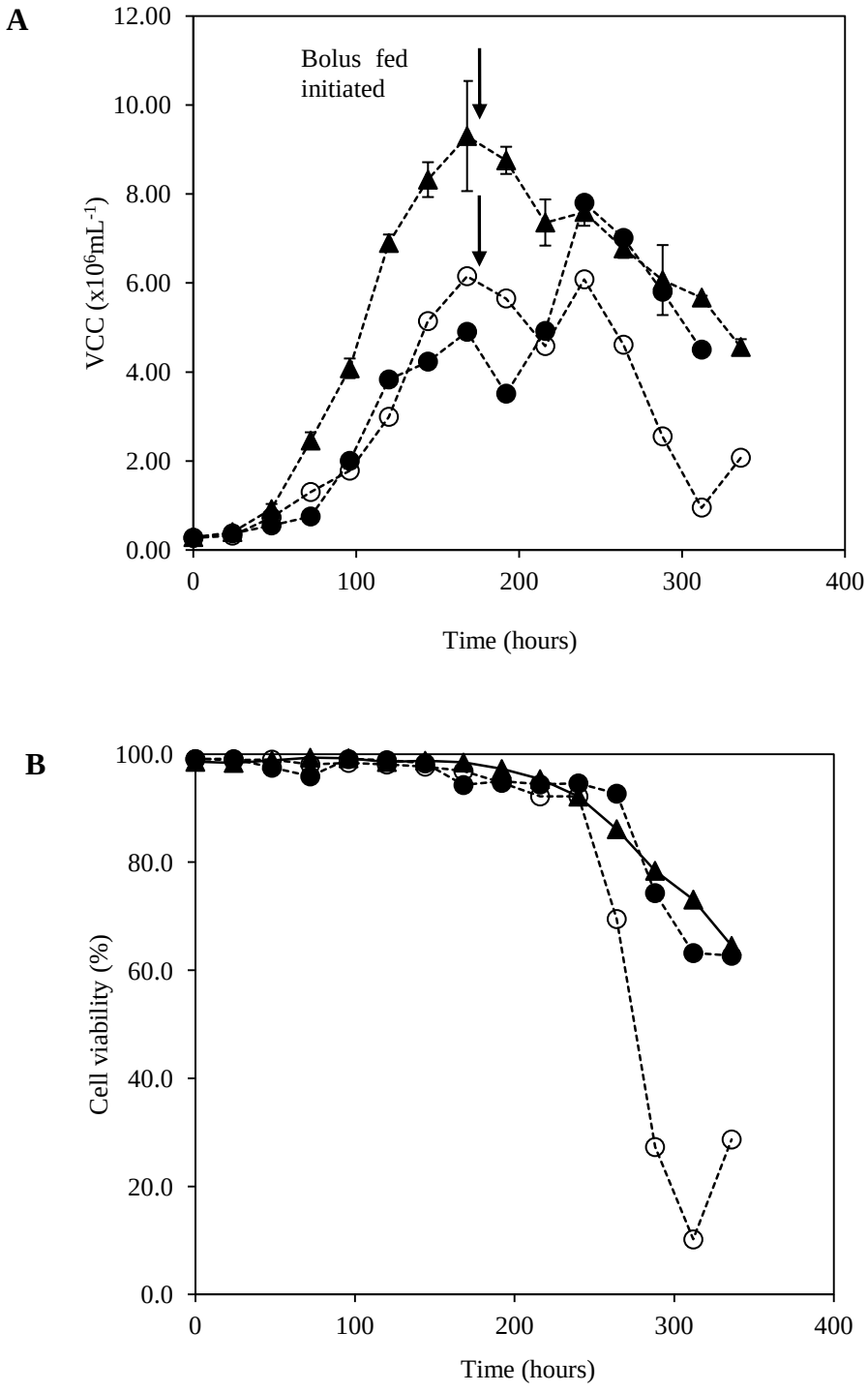

Figure 5.5:CHO growth kinetics for micro-Matrix in comparison with 24 SRW using bolus fed: micro-Matrix with control and bolus (●), micro-Matrix with non-control and bolus (○), 24-SRW (▲) A: viable cell concentration; B: cells viability. Arrow (↓) represents bolus and continuous fed addition commenced on day 7.

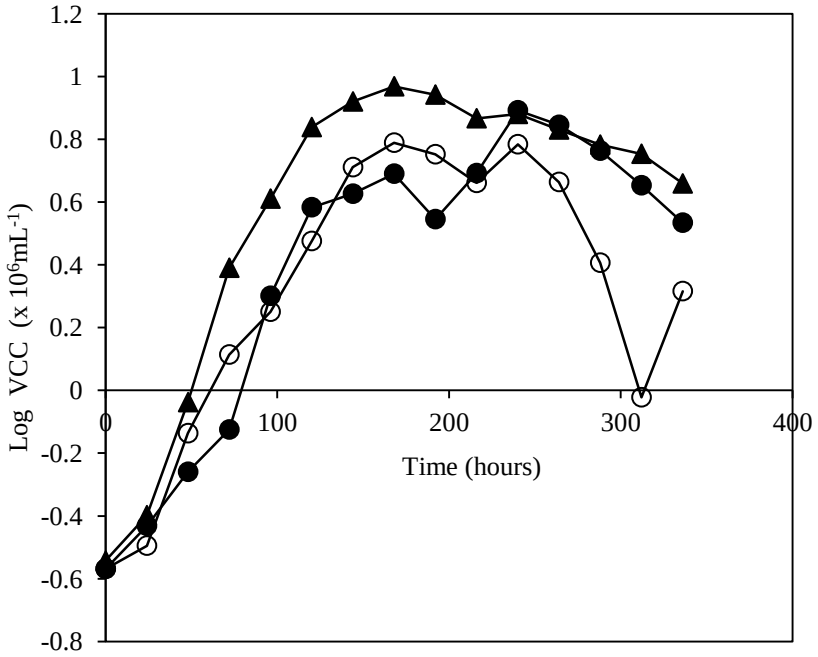

Figure 5.6: Log VCC of CHO cells growth kinetics for micro-Matrix in comparison with 24 SRW using bolus fed: micro-Matrix with control and bolus (●), micro-Matrix with non-control and bolus (○) and 24-SRW (▲).

Table 5.4: Derived growth parameters of fed-batch CHO cell in for micro-Matrix (control), micro-Matrix (non-control) and 24-SRW.

Type of reactor	**micro-Matrix (control)**	**micro-Matrix (Non-control)**	**24 MTP (SRW)**
Peak cell concentration (x 10^6 cell mL^{-1})	7.80	6.15	9.30
CiVC (x 10^8 cell d^{-1} mL^{-1})	2.85	2.80	4.77
μmax (h^{-1})	0.014	0.009	0.019
IgG antibody titre (gL^{-1})	0.30	0.24	1.0
q_P (pg cell^{-1} d^{-1})	4.9	4.6	14.5

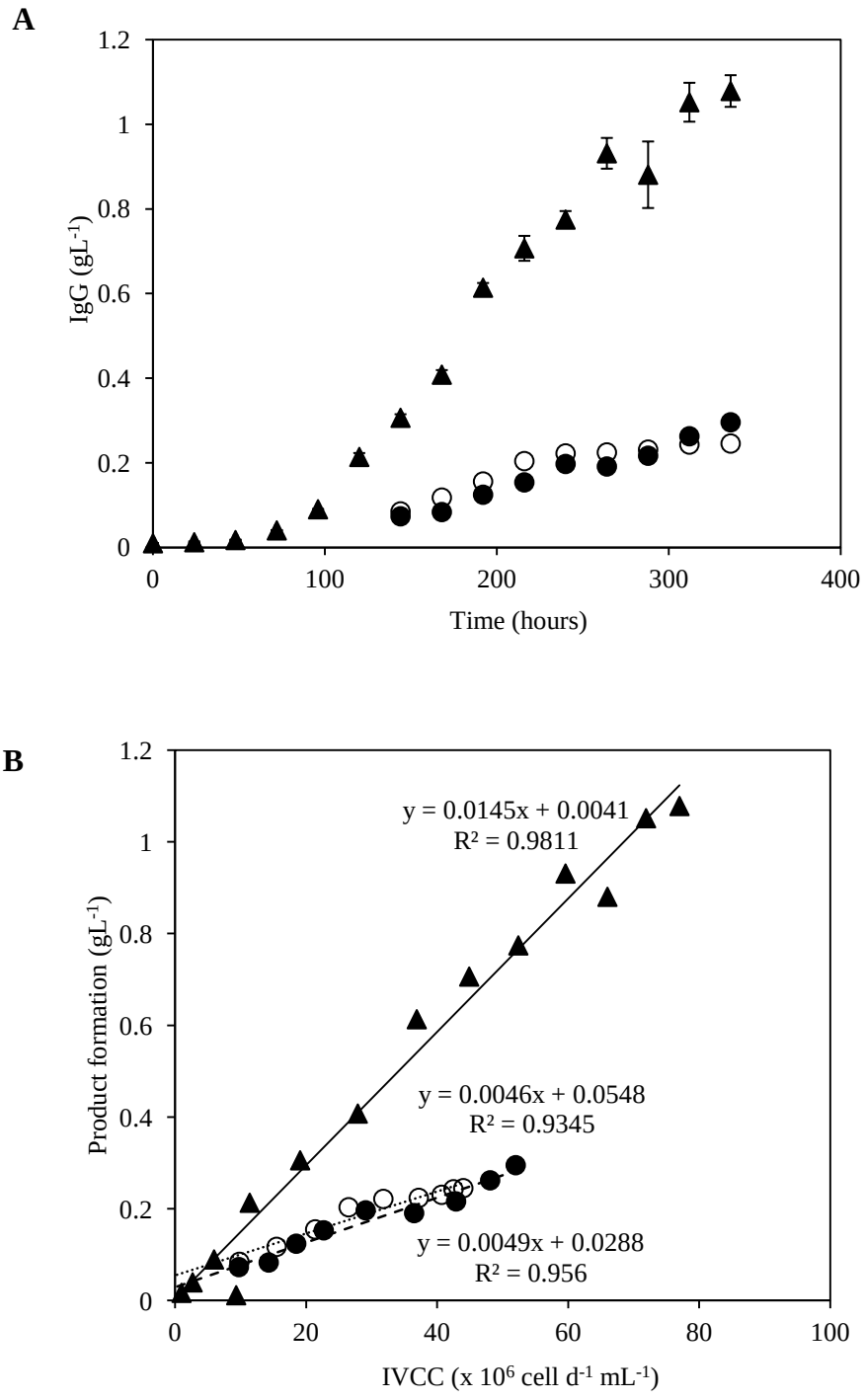

Figure 5.7: A: Antibody production CHO cells growth kinetics for micro-Matrix in comparison with 24 SRW using bolus fed: micro-Matrix with control and bolus (●), micro-Matrix with non-control and bolus (○) and 24-SRW (▲) B: Comparison plots of product formation vs IVCC for micro-Matrix and 24 SRW with trend line, solid line represents 24 SRW, dashed line represents micro-Matrix with control and bolus, and dotted line represents micro-Matrix with non-control and bolus.

5.4.2 Metabolites analysis

For glucose consumption in the micro-Matrix (control and non-control) system a good comparison with 24-SRW culture from 0 hour until 192 hours (Figure 5.8 A) was obtained. In the exponential stage, glucose was consumed at a high rate (quantify) as expected in CHO cell cultivation. After the glucose concentration decreased to about 2 gL^{-1}, it was maintained around this level by bolus feeding based on daily analysis. However, the glucose concentration in the micro-Matrix cultures was not able to be maintained around the desired concentration of ~2 gL^{-1}. The micro-Matrix system uses the micro valve technology that should provide a flow rate of 17.4 nL min^{-1} for 10 minutes.

Therefore, approximately 150 μL of glucose from a concentrated feed was added of to each well. The amount of glucose added was supposedly adequate to support the cell growth and prevent glucose starvation. This finding was unexpected and suggests that bolus feed applied in micro-Matrix failed to provide sufficient nutrients required by cells. Lactate production in the micro-Matrix and 24-SRW showed distinctive differences with large fluctuation. (Figure 5.8 B). The peak lactate concentration obtained in the micro-Matrix (non-control) with 5.25 gL^{-1}, whilst micro-Matrix (control) and 24-SRW produced 4.9 and 3.9 gL^{-1} correspondingly. Surprisingly, the fluctuation observed in the concentration is not expected as the lactate should produce exponentially with the glucose consumption. The inconsistency in the lactate production may be due to the following reasons as suggested by (Tsao *et al.*, 2005). Firstly, the inaccuracies in measuring the correct amount of glucose feed in the each wells to balance the glucose consumption and lactate production. Secondly, the cell culture volume changes in each well through the nutrient feed, pH control and sampling loss and evaporation (Tsao *et al.*, 2005).

The concentration profile of ammonia and glutamate are shown in Figure 5.9. Ammonia concentration was presumed start to accumulate for micro-Matrix and 24-SRW cultures from day 1 and peaked approximately on 300 hours and 200 hours respectively. Data analysis for ammonia from 24-SRW culture in Figure 5.4 E was referred to show that ammonia gradually increased after 24 hours cultivation. For 24-SRW, the accumulation showed a sudden drop after the bolus addition, whilst for the micro-Matrix (control) and micro-Matrix (non-control) the ammonia probably peaked at 6.8 and 6.3 mmol L^{-1} on day 14 though some intermittent data are missing due to technical problems. The high concentration of ammonia in the micro-Matrix cultures might due to low viability observed from 240 hours until 336 hours. Nonetheless, glutamate concentrations in the micro-Matrix and 24-SRW cultures decreased and stayed low during the exponential phase even when bolus feeding commenced. The low glutamate concentration is probably a consequence of the conversion of glutamate to glutamine. Since the CHO cell cultured in the system was derived from GS expression, glutamine was formed from glutamate and ammonia mainly from asparagines deamidation (Zhou *et al.*, 1997). However, due to the faulty glutamine (Gln) sensor, glutamine was not measured.

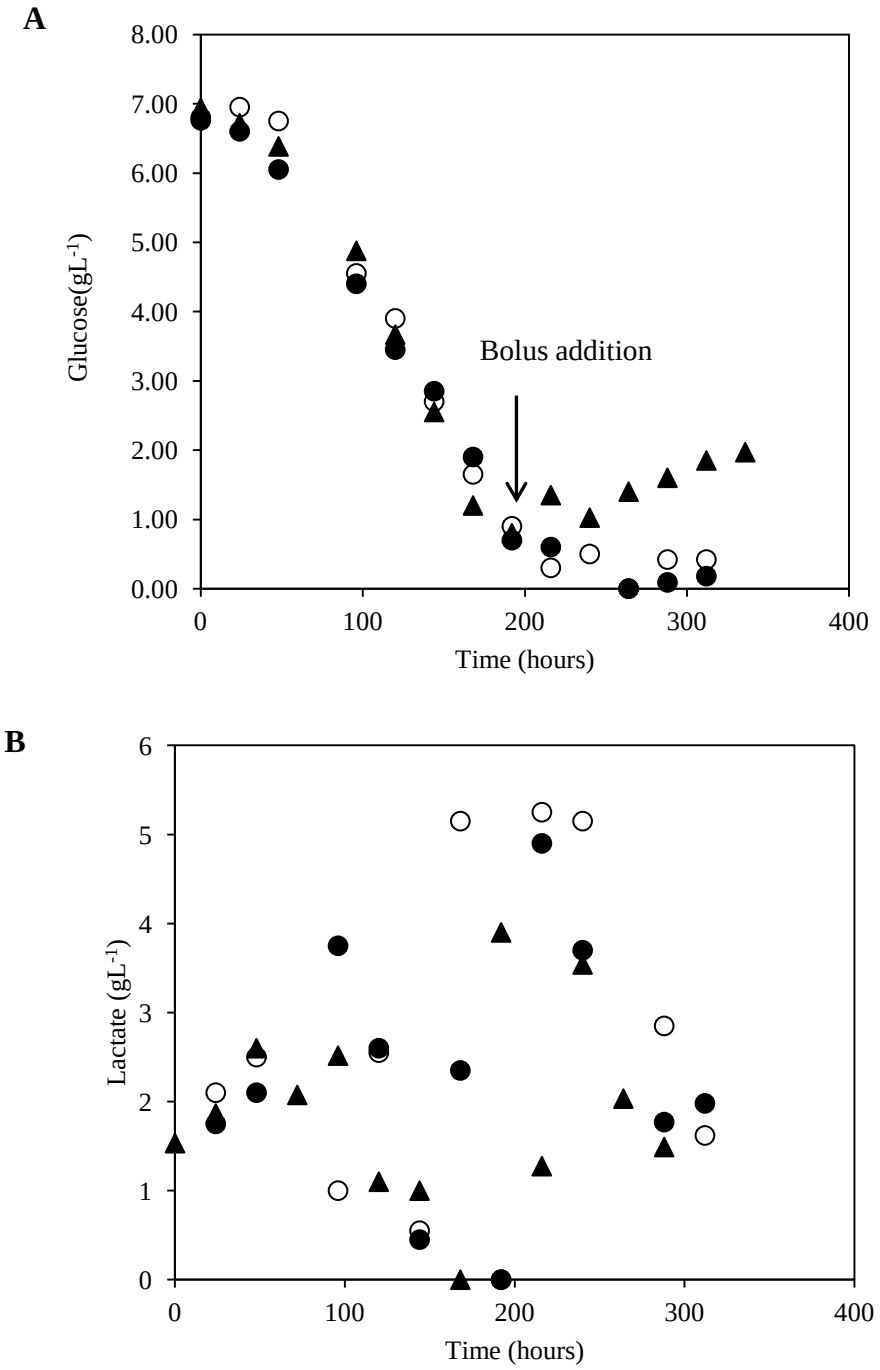

Figure 5.8: CHO metabolites concentration for micro-Matrix in comparison with 24 SRW using bolus fed: micro-Matrix with control and bolus (●), micro-Matrix with non-control and bolus (○) and 24-SRW (▲) A: Glucose concentration; B: Lactate concentration. Note: Large fluctuation of lactate concentration and missing data points due to the faulty Lac sensor and NOVA during the analysis.

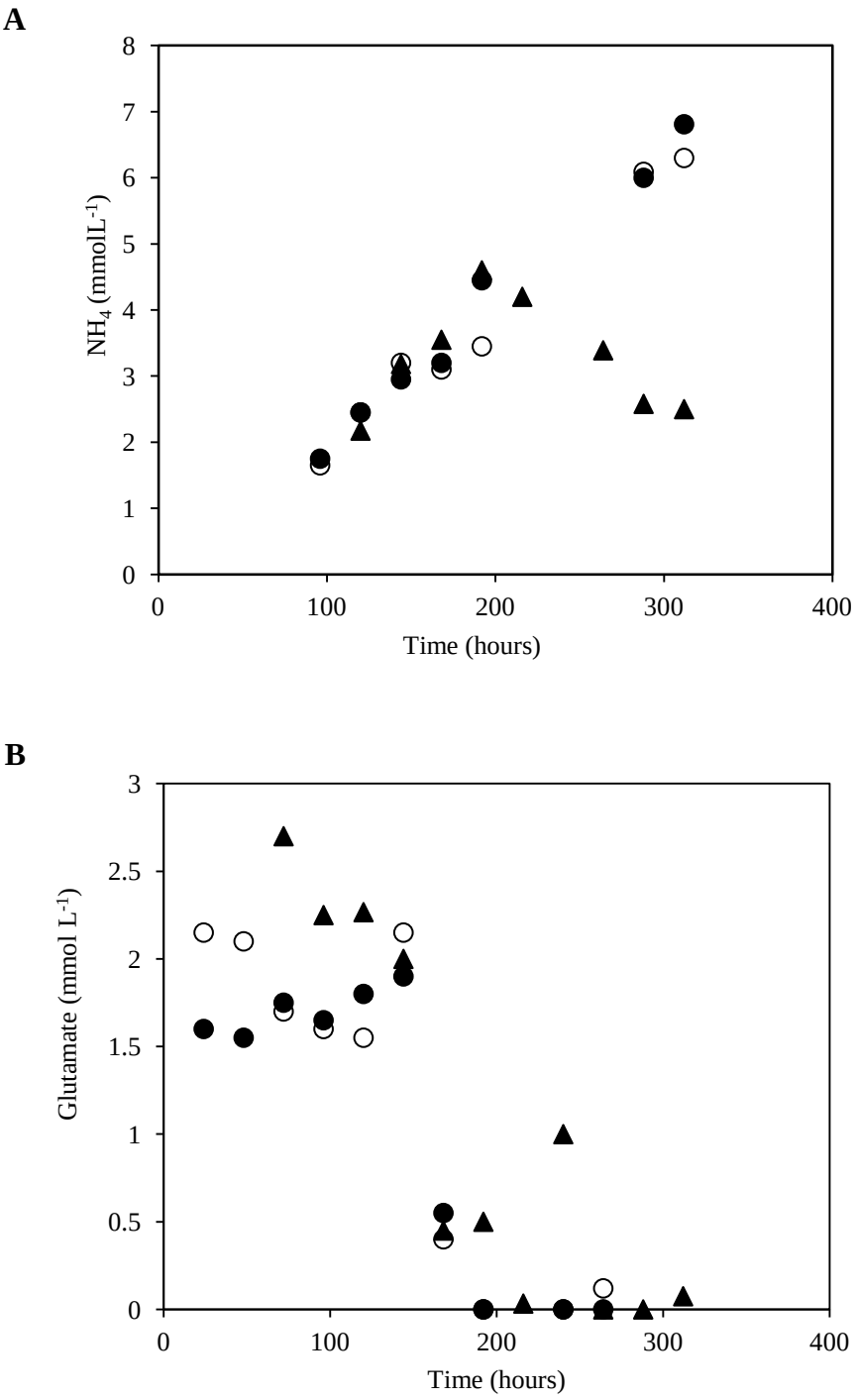

Figure 5.9: CHO metabolites concentration for micro-Matrix in comparison with 24 SRW using bolus fed: micro-Matrix with control and bolus (●), micro-Matrix with non-control and bolus (○) and 24-SRW (▲) A: Ammonium concentration, B: Glutamate concentration. Note: missing data points due to the faulty of NOVA during the analysis.

5.5 Effect of control and non-control aeration system in micro-Matrix with continuous feeding

The operating conditions for the micro-Matrix were selected using the same conditions as previously described in Table 5.3. For continuous feeding, the system was fed with CD-CHO AGT (supplemented with glucose) continuously for 6 days. The diluted feed was added continuously was at a flow rate of 104.4 nL min^{-1}. Therefore, the total feed added in the system daily was at 150 µL $well^{-1}$ d^{-1} which is sufficient for CHO cell growth and viability.

5.5.1 Growth kinetics and antibody productivity

CHO cell growth kinetics using continuous feeding in the micro-Matrix system showed a slight improvement compared to bolus fed study. In the exponential phase from 72 hours to 168 hours, the viable cell concentration showed good comparability between the control aeration and non-control aeration system (Figure 5.10 A). The viable cell concentration observed for the control aeration system peaked at 8.67 x 10^6 cell mL^{-1} after 240 hours, while that for the non-control aeration system peaked at 6.91 x 10^6 cell mL^{-1} after 216 hours. The continuous feeding applied in the micro-Matrix system increased the viable cell concentration by 10 % compared to the bolus addition for both control and non-control aeration systems. Furthermore, during the exponential phase (Figure 5.11), the maximum specific growth rate was almost equivalent for both systems with continuous feeding ranging from 0.017 – 0.018 h^{-1} as described in Table 5.5.

However, the viability of the CHO cells dropped abruptly after 264 hours (Figure 5.10 B). The lowest percentage viability was observed on 336 hours with 22.2 % and < 1 % for control and non-control aeration system respectively. The low viability observed in these cultures is probably due to the gas mixture (95 %, 5 % CO_2) that supposedly to mimic the environment of incubator for 24-SRW cultures was found not efficient for micro-Matrix. For micro-Matrix with control aeration, CO_2 gas was added to control the pH of the system. Conversely, the addition of

gas mixture of 5 % CO_2 actually increased the dCO_2 in the well which probably led to CO_2 toxicity in the cultures. Kimura and Miller, (1997) described comprehensively regarding high pCO_2 level in their study of six well plates of recombinant tPa production from CHO cells. The online pH of the micro-Matrix system dropped from 7.1 to 6.7 (data not shown). It is possible that the changes in pH also affected the protein processing and secretion of IgG as shown in Figure 5.12 A. The maximum IgG concentration obtained was very poor for both systems with 0.30 gL^{-1} and 0.26 gL^{-1} for control and non-control cultures respectively. Cell specific productivity (q_p) for both control and non-control systems is also in agreement with the IgG productivity. The q_p for the micro-Matrix is below 5 pg $cell^{-1}$ d^{-1}, which is very low for compared to 24-SRW system (14.5 pg $cell^{-1}$ d^{-1}). There are also reported literatures regarding elevated pCO_2 decreased the cell growth and protein productivity (Gray *et al.*, 1996; Kimura and Miller, 1997; Zhu *et al.*, 2005). Although osmolality was not measured experimentally, it can be predicted that the medium osmolality increased to a level that gave adverse impact on cell growth and productivity. The reason for this assumption was to the fact that high osmolality usually led to programmed cell death (apoptosis) in cultures (deZengotita *et al.*, 2002).

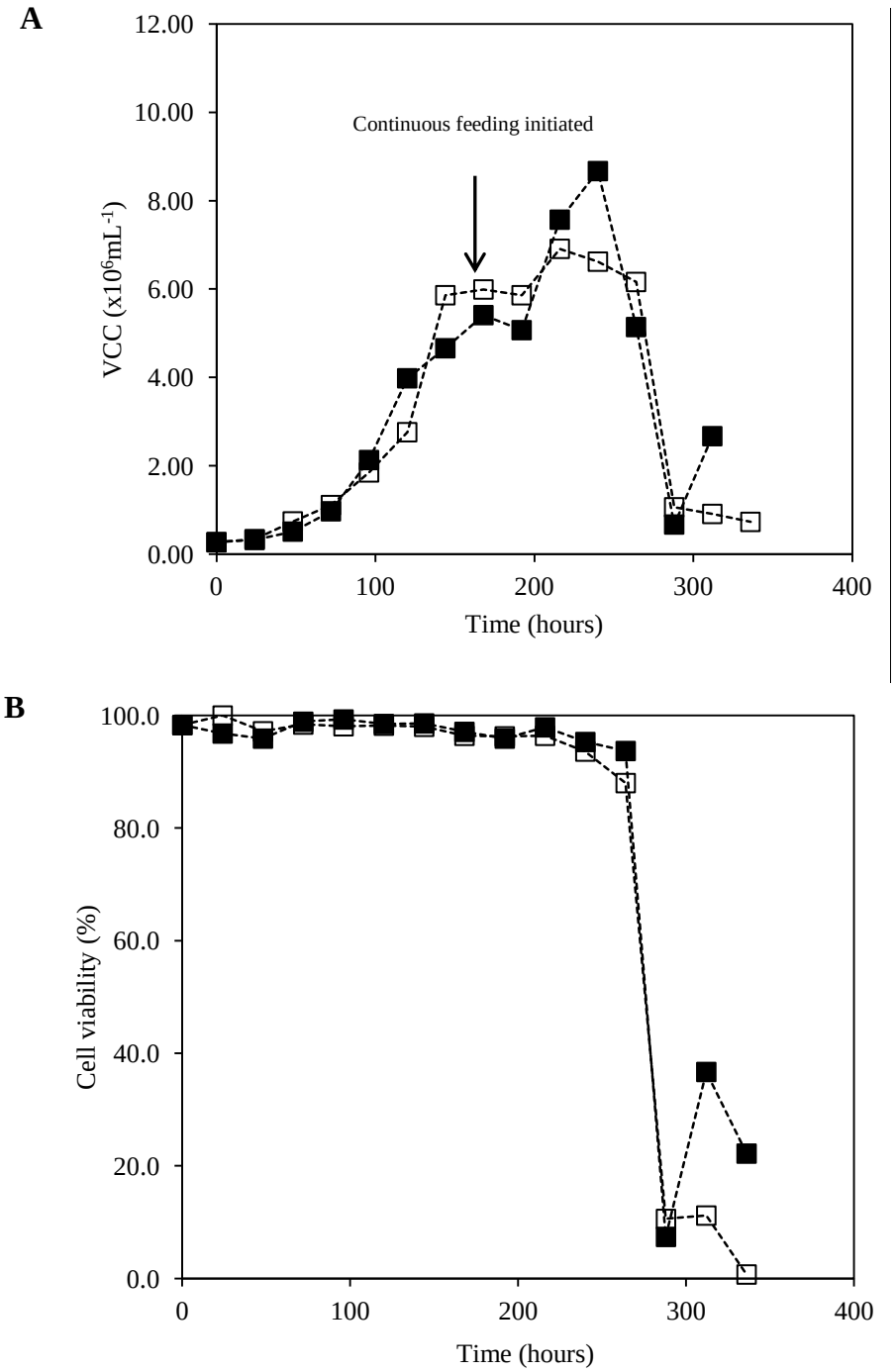

Figure 5.10: CHO growth kinetics for micro-Matrix with control and non-control aeration using continuous feeding: micro-Matrix with control and continuous (■), micro-Matrix with non-control and continuous (□) A: viable cell concentration; B: cells viability. Arrow (↓) represents bolus and continuous feed addition commenced on day 7.

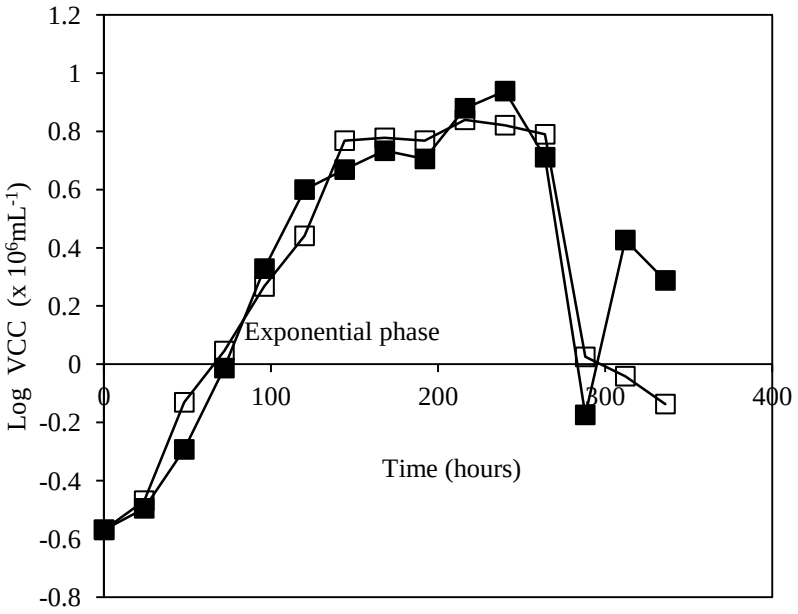

Figure 5.11: Log VCC of CHO growth kinetics for micro-Matrix with control and non-control aeration using continuous feeding: micro-Matrix with control and continuous (■), micro-Matrix with non-control and continuous (□).

Table 5.5: Derived growth parameters of CHO growth kinetics for micro-Matrix with control and non-control aeration using continuous feeding.

Type of reactor	**micro-Matrix (Control)**	**micro-Matrix (Non-control)**
Peak viable cell concentration (x 10^6 cell mL^{-1})	8.67	6.91
CiVC (x 10^8 cell d^{-1} mL^{-1})	3.03	3.01
μmax (h^{-1})	0.018	0.017
IgG antibody titre (gL^{-1})	0.30	0.26
q_P (pg $cell^{-1}$ d^{-1})	4.9	3.7
q_{glc} (pg $cell^{-1}$ d^{-1})	56	50

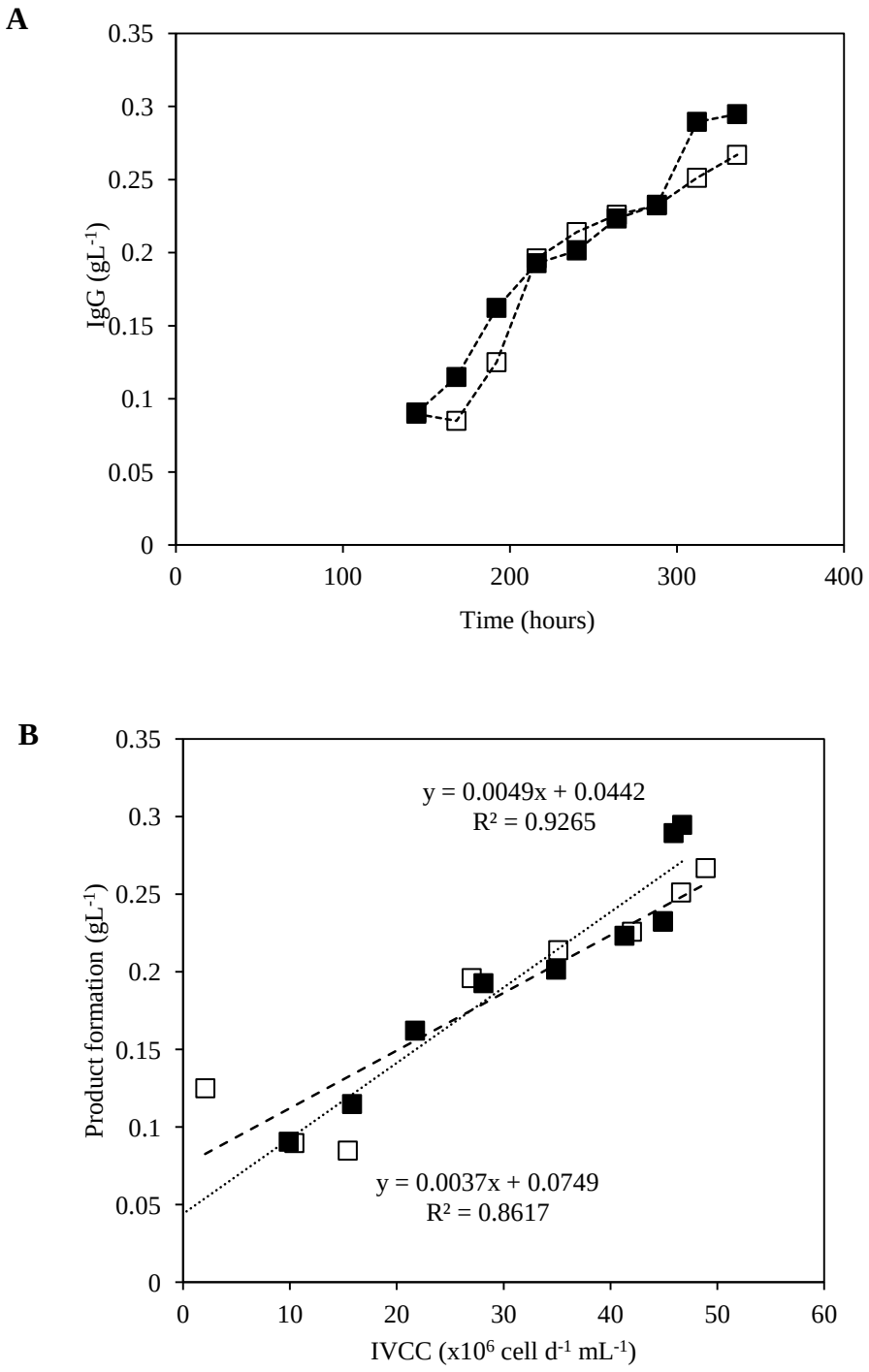

Figure 5.12: A: Antibody production CHO growth kinetics for micro-Matrix with control and non-control aeration using continuous feeding: micro-Matrix with control and continuous (■), micro-Matrix with non-control and continuous (□). B: Comparison plots of product formation vs IVCC with dotted line represents micro-Matrix with control and continuous, and dashed line represents micro-Matrix with non-control and continuous.

5.5.2 Metabolites analysis

The glucose and lactate concentration profiles are shown in Figure 5.13. Glucose concentration (Figure 5.13 A) for control and non-control aeration system showed that the consumption was very similar to the previous bolus addition in Figure 5.4 A. In the exponential phase from 72 hours to 168 hours, the specific glucose consumption rate for control system was 56 pg $cell^{-1}$ d^{-1}, whilst for non-control system it was 50 pg $cell^{-1}$ d^{-1} (Table 5.5). Glucose concentration was observed to keep decreasing until the end of the cultivation and gave an undesirable effect on cell growth and productivity as seen in Figure 5.10 A and 5.12 A. As the glucose concentration started to decrease during exponential phase, lactate concentration in the micro-Matrix started to increase. The lactate concentration in micro-Matrix peaked on 216 hours with 4.5 gL^{-1} for non-control and 4.4 gL^{-1} for control (Figure 5.13 B). However, similar lactate fluctuation was seen in Figure 5.8 B. As discussed in the previous sections, the large fluctuations might be due to the changes in culture parameters (pH, temperature and/or osmolality) and loss of culture volume due to the evaporation (Tsao *et al.*, 2005). Another possible explanation for high lactate might be to the transition of cellular metabolism from glucose to lactate. In animal cell, glucose might be synthesised by lactate via Cori cycle. This phenomenon happens during the initial conversion of lactate through pyruvate, supported by lactate dehydrogenase (LDH) (Tsao *et al.*, 2005). The transition of cellular metabolism has been repeatedly observed in the fed-batch cultures (Zhou *et al.*, 1997). Previously, in Section 4.8.2 we observed the equivalent lactate metabolism shift from production to consumption in the MBR. This is in agreement with findings by Zhou *et al.* (1997) with GS-NS0 cultures cultured in 2 L STR. The increase of lactate concentration is parallel with ammonia accumulation that coincided with cell death phase. Hypothetically, lactate consumed by cells will be converted to pyruvate which will enter the Krebs cycle (Zhou *et al.*, 1997). Once the lactate started being consumed, the cells started to die rapidly (Bibila *et al.*, 1994) as observed in Figure 5.10 A.

The concentration profile of ammonia and glutamate are shown in Figure 5.14. Ammonia concentration in continuous fed cultures shared the same trend as bolus addition where the accumulation possibly started during the growth phase. The ammonia concentration for micro-Matrix (control) and micro-Matrix (non-control) peaked at 7.1 and 6.2 mmol L^{-1} on day 13 respectively (Figure 5.14 A). Notably, the high ammonia concentration might have an effect to the cell growth as reported by (Genzel *et al.*, 2005). On the other hand, glutamate concentrations for control and non-control cultures dropped to very low levels after the continuous feeding commenced (Figure 5.14 B). The low glutamate concentration was also seen in the bolus addition cultures described previously in Section 5.4.2.

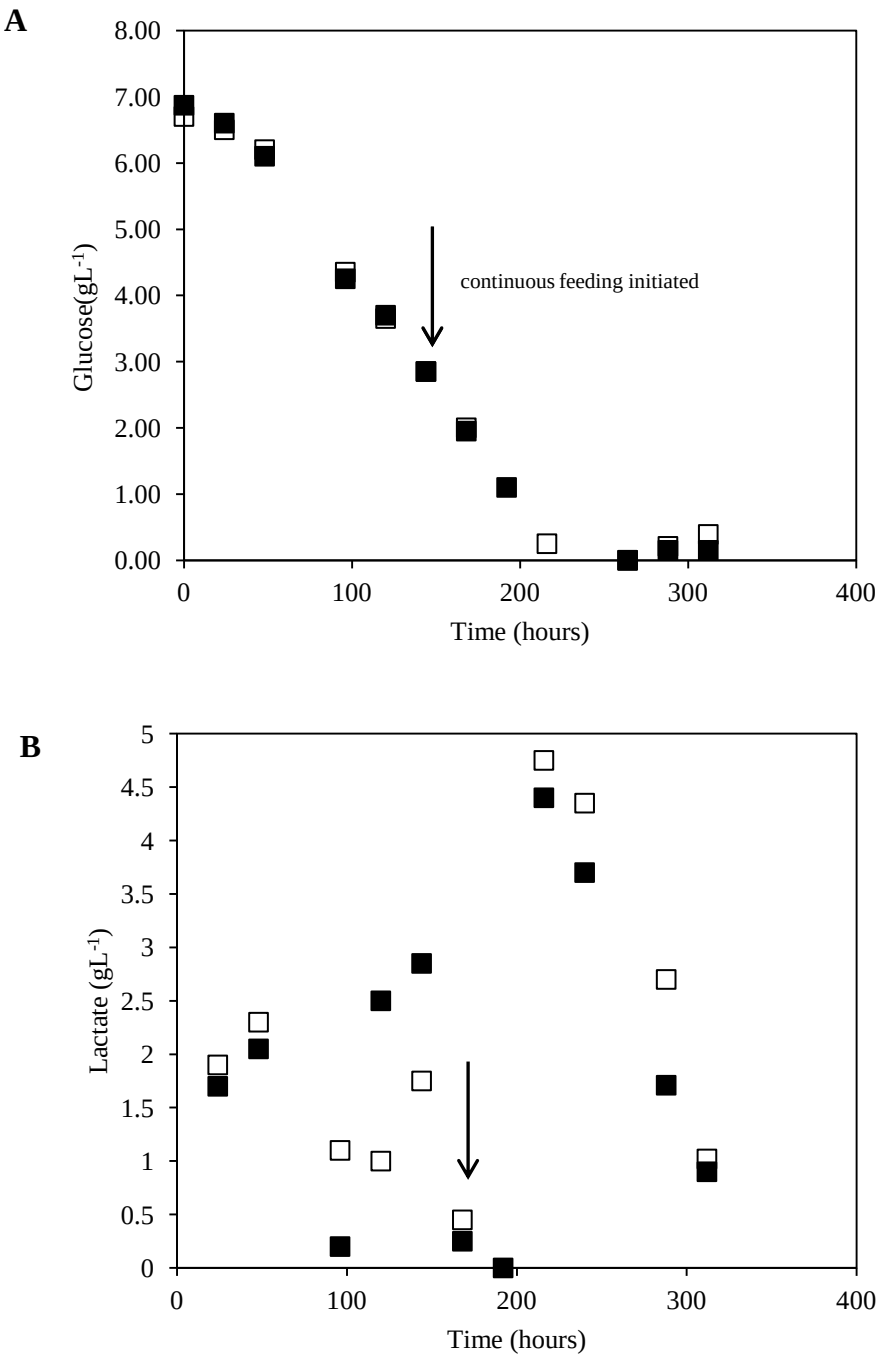

Figure 5.13: CHO metabolites concentration for micro-Matrix with control and non-control aeration using continuous feeding: micro-Matrix with control and continuous (■), micro-Matrix with non-control and continuous (□). A: Glucose concentration, B: Lactate concentration. Arrow (↓) represents continuous feed addition commenced on day 7. Note: Large fluctuation of lactate concentration and missing data points due to the faulty Lac sensor and NOVA during the analysis.

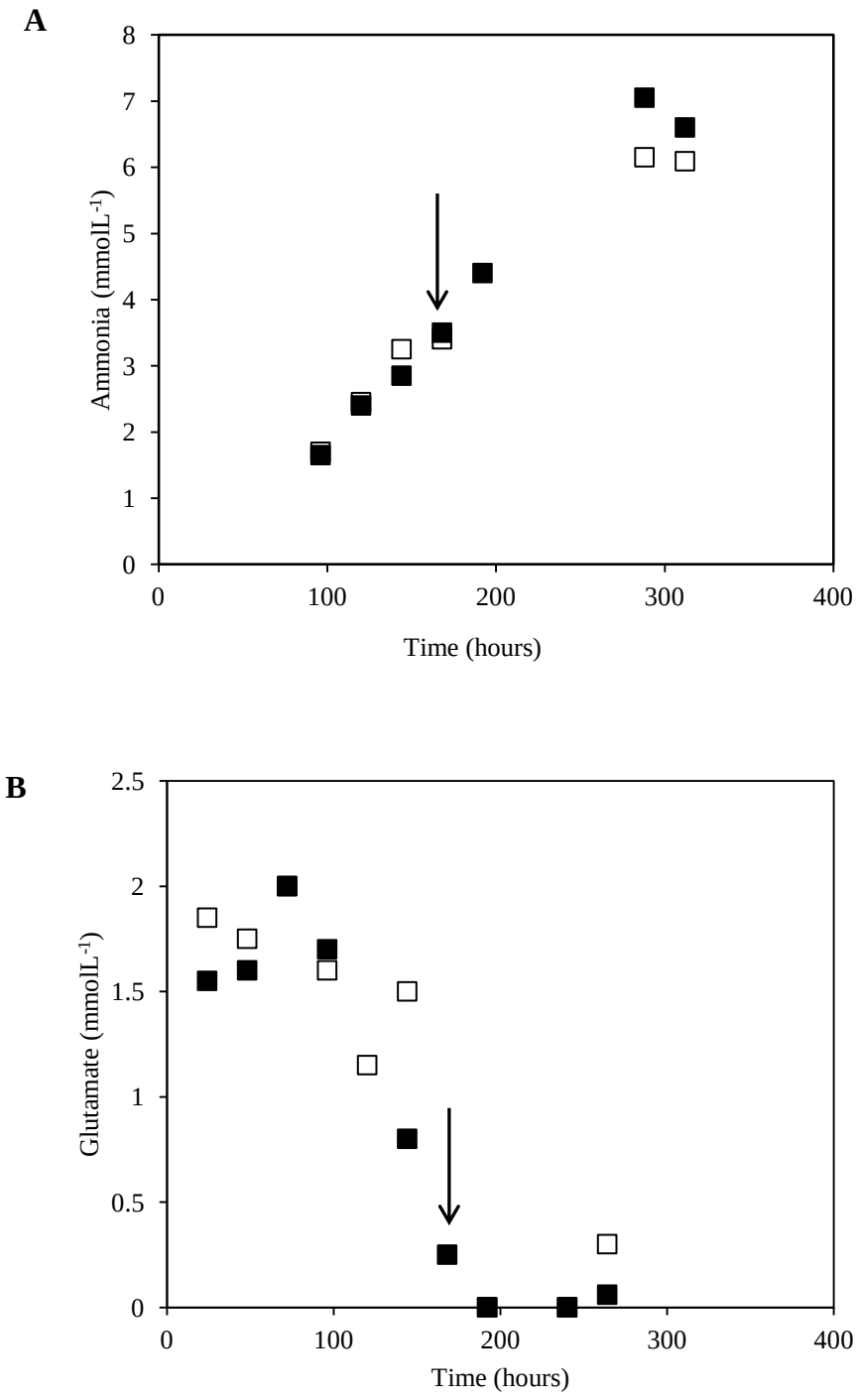

Figure 5.14: CHO metabolites concentration for micro-Matrix with control and non-control aeration using continuous feeding: micro-Matrix with control and continuous (■), micro-Matrix with non-control and continuous (□) and 24-SRW (▲) A: ammonium concentration, B: glutamate concentration. Arrow (↓) represents bolus and continuous feed addition commenced on day 7. Note: missing data points due to the faulty of NOVA during the analysis.

5.6 Fed-batch with continuous feed at matched T_m

In Section 5.2, the comparison of growth kinetics and scale translation from small scale (MTP) and MBR to 5 L STR using bolus addition was investigated. However, continuous feeding strategies were not well established for small scale studies owing to the difficulties for the reactors set-up. Lu *et al.* (2013) demonstrated automated dynamic feeding strategies in 3 L STR using a feeding algorithm. They found that the methods were able to automatically adjust the feed rates according to the cultures demands for glucose and other nutrients. However, comparison studies of mammalian cell cultures with continuous feeding and scale-up from miniature reactors are still limited. Berrios *et al.* (2011) demonstrated the replacement of glucose by mannose for the continuous feeding of CHO cells for production of recombinant tissue plasminogen activator (tPa). The results showed that mannose addition was able to increase the biomass concentration (15 – 20 %), leading to increased productivity by 30 % and reduced specific lactate production by 25 – 35 %. In this section, an investigation of continuous feeding and scale-up between micro-Matrix and MBR is presented. The operating parameters were selected on the basis of matched mixing time of T_m ~ 6 s. From the previous micro-Matrix studies, improvements were made to overcome the problems of low growth rate, poor cell viability and productivity titres. Specifically, the agitation speed was increased to 300 rpm, the fill volume was changed to 2.5 mL and the flow rate of gas mix (95% air and 5 % CO_2) was reduced to 0.1 mL min^{-1}. The reason for changing the agitation speed from 270 rpm to 300 rpm was to increase the specific cell growth rate. The fill volume also was changed from 3.5 mL to 2.5 mL to overcome the issue of medium spillage at the edges of the well. Gas mix flow rate was reduced to overcome the issue of pCO_2 accumulation and dCO_2 toxicity as observed previously in Section 5.4 and 5.5. The MBR agitation speed also was changed from 450 rpm to 420 rpm to match the mixing time of T_m ~ 6 s. Table 5.6 summarised the operating conditions for this study.

Table 5.6: Selected operating conditions for cell culture cultivation between micro-Matrix system and HEL-BioXplore MBR based on matched mixing time.

Reactor	Micro-Matrix (control aeration)	MBR (HEL-BioXplore)
Shaking/Stirring (rpm)	300	420
Aeration system	Headspace with flow rate 0.5 mL min^{-1}	Horseshoe type sparging with flow rate 50 mL min^{-1}
Working volume	2.5 mL	350 mL
pH/DO/Temperature control	Yes	Yes
Feeding strategy	Continuous	Continuous

5.6.1 Growth kinetics and antibody productivity

Figure 5.15 shows the comparison of CHO growth kinetics and viability for micro-Matrix with control of aeration and MBR cultures. Both reactors are using a continuous fed-batch strategy. Viable cell concentration for both reactors peaked after 192 hours and 212 hours for micro-Matrix and MBR correspondingly. The peak viable cell concentrations for micro-Matrix was 11.1 x 10^6 cell mL^{-1}, while the MBR culture reached 9.76 x 10^6 cell mL^{-1}. Furthermore, cell viability percentage also improved in the continuously fed cultures for both reactors. The final viability for MBR on day 14 was almost 70 %, whereas for micro-Matrix culture it was > 90 % on day 11. However, the experiment in micro-Matrix was suddenly stopped due to leakage on the top plate that cover the 24-DWP used in micro-Matrix. As the consequence from the leakage, the top cover was unable to provide a sterile environment for the micro-Matrix, hence the experiment was stopped on day 11. Table 5.7 shows derived growth parameters obtained for both reactors with comparable results. The micro-Matrix culture

exhibited a slightly higher cIVC at 4.43 x 10^8 cell d^{-1} mL^{-1} compared with the MBR (4.09 x 10^8 cell d^{-1} mL^{-1}). Notably, the maximum specific growth rate for micro-Matrix was very similar to that of the MBR as shown in Figure 5.16 and Table 5.7. Both of the reactors have comparable lag, exponential, and stationary phase. The cIVC for the micro-Matrix tremendously improved from previous continuous-fed experiment in Section 5.5 by 30 %. Furthermore, the improvement made to the micro-Matrix system enhanced the titre of CHO cell to 0.50 gL^{-1}, which is slightly better compared to the previous experiment (Figure 5.17 A). It was predicted that the final IgG antibody would be enhanced to 0.80 gL^{-1} if the cultivation would have been continued until day 14. Figure 5.17 B depicts the trend lines to determine the q_p for both reactors. The q_p for both reactors show good comparability with micro-Matrix at 10.5 pg $cell^{-1}$ d^{-1} and MBR with 9.1 pg $cell^{-1}$ d^{-1}.

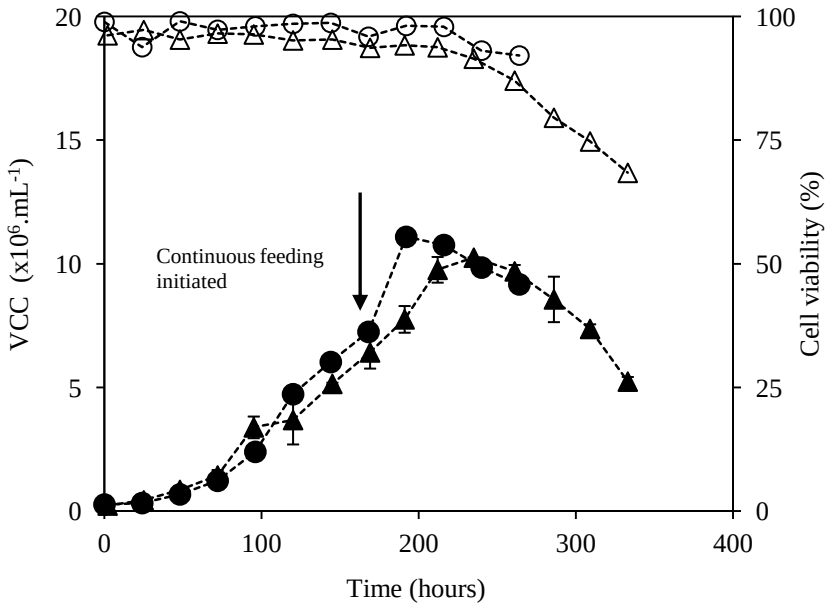

Figure 5.15: CHO growth kinetics in fed-batch culture with continuous feed for two types of reactors micro-Matrix and MBR. The VCC represents micro-Matrix (●) and MBR (▲), while cell viability was represented for micro-Matrix (○) and MBR (Δ) A: viable cell concentration; B: cells viability Arrow (↓) indicated feed addition on day 7. Error bars represent one standard deviation about the mean (n = 2) for MBR. Note: micro-Matrix data until day 11 only due to leakage problem on the top plate cover of the 24-DWP.

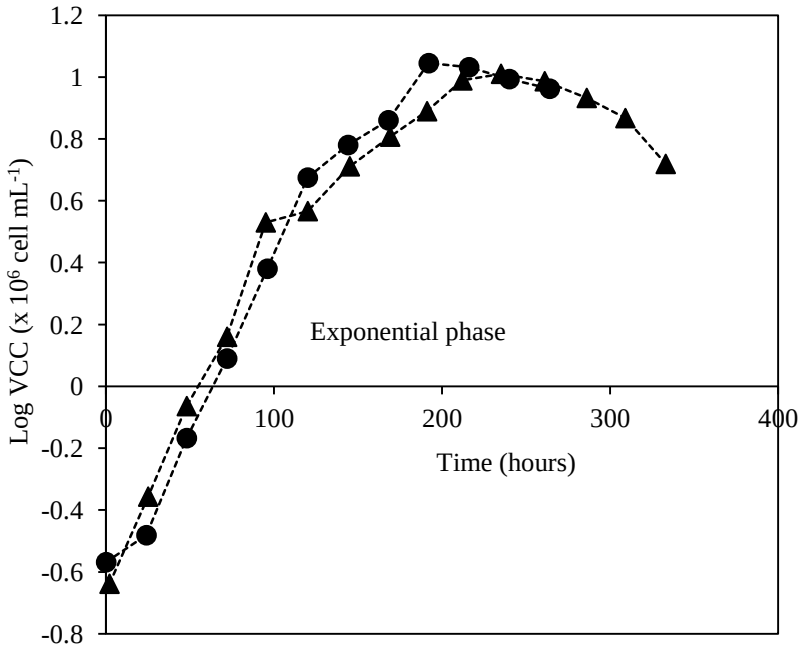

Figure 5.16: Log VCC of CHO growth kinetics in fed-batch culture with continuous feed for two types of reactors; micro-Matrix (●) and MBR (▲).Note: micro-Matrix data until day 11 only due to leakage problem on the top plate cover of the 24-DWP.

Table 5.7: Derived growth parameters obtained from continuous fed batch cultures in micro-Matrix and MBR.

Type of reactor	**micro-Matrix (control)**	**MBR (HEL-BioXplore)**
Peak cell concentration (x 10^6 cell mL^{-1})	11.1	9.76
CiVC (x 10^8 cell d^{-1} mL^{-1})	4.43	4.09
μmax (h^{-1})	0.019	0.020
IgG antibody titre (gL^{-1})	0.50	0.64
q_P (pg $cell^{-1}$ d^{-1})	10.5	9.1
qglc (pg $cell^{-1}$ d^{-1})	58.4	45.7

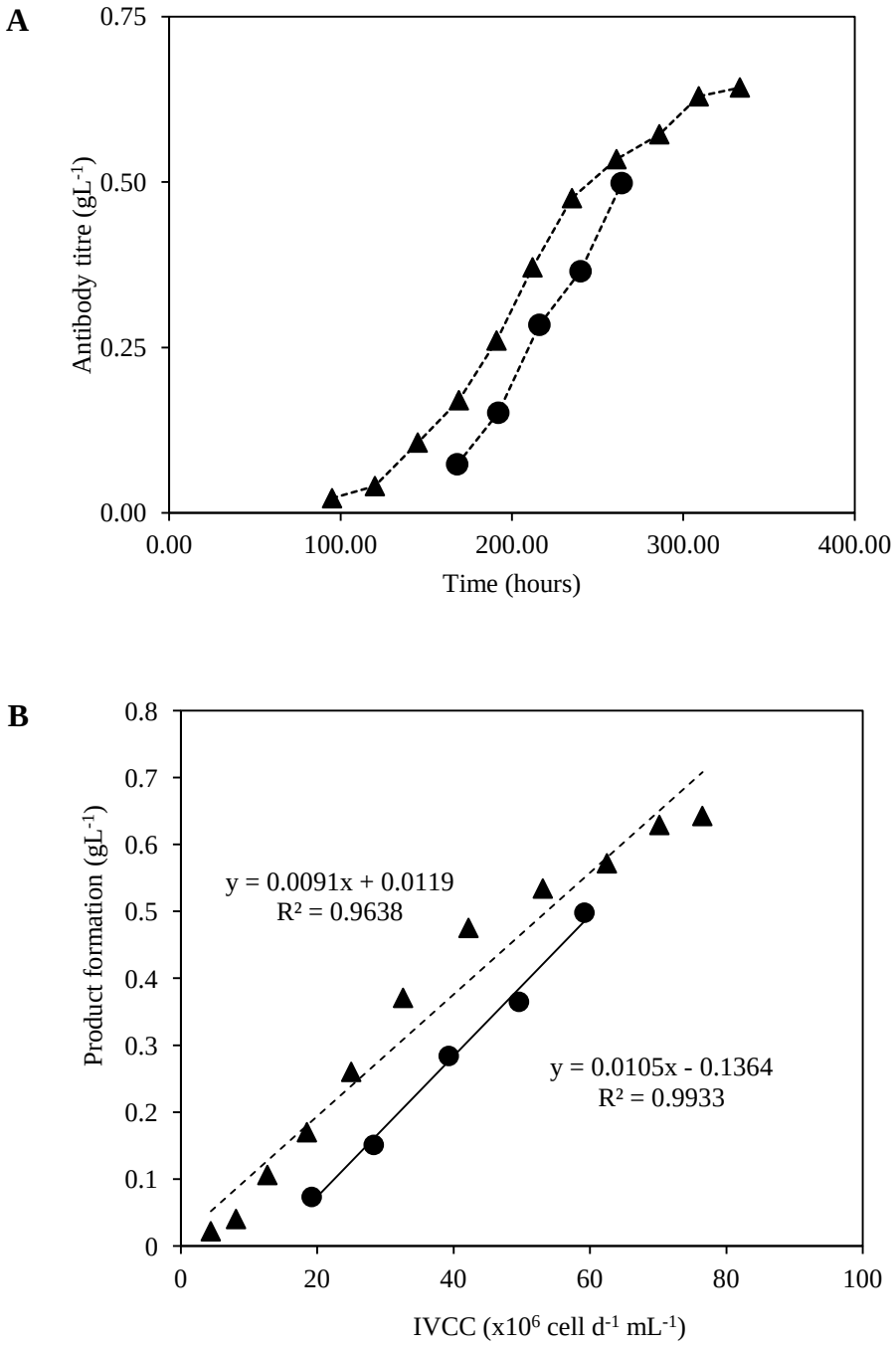

Figure 5.17: A: Antibody production CHO growth kinetics for micro-Matrix and MBR using continuous feeding: micro-Matrix with control and continuous (●), MBR and continuous (▲). B: Comparison plots of product formation vs IVCC with solid line represents micro-Matrix with control and continuous; dashed line represents MBR with continuous. Note: micro-Matrix data until day 11 only due to leakage problem on the top plate cover of the 24-DWP.

5.6.2 Metabolites analysis

The metabolite concentrations (glucose, lactate, ammonia, glutamine and glutamate) were measured using NOVA Flex is shown in Figure 5.18. During the log phase in the cultures, glucose was consumed and partly converted to lactate as shown in Figure 5.18 A and B. After the glucose concentration decreased to at about 2 gL^{-1}, the cultures were supplied with a concentrated feed (supplementary with glucose). The feed added was ~150 gL^{-1} of CD CHO AGT to replenish the nutrients that have been consumed by cells. After the addition, the glucose concentration was analysed and maintained daily around 2 gL^{-1}. The continuous feeding strategy in MBR which largely focused on maintaining cultures at low glucose concentration was able to balance the nutrient demands. Whereas, the micro-Matrix system was able to maintain the glucose level at 0.50 – 1 gL^{-1}. Even though the glucose concentration in the micro-Matrix was quite low compared to the expected level of 2 gL^{-1}, it was sufficient to compensate for nutrient exhaustion in the system, as depicted in Figure 5.15 with viable cell concentration peaked at 11 millions viable cells per mL. Specific glucose consumption rate also shows a 20 % higher consumption in micro-Matrix compared to the MBR cultures (Table 5.7). The higher consumption rate in micro-Matrix might be due to the approximately 10 % higher viable cell concentration shown in Figure 5.15.

High lactate accumulation in culture has long been experienced as the inhibitory factor for mammalian cell growth and recombinant protein production (Zhou *et al.*, 1995; Zhou *et al.*, 1997). Lactate concentrations in the cultures increased after glucose is rapidly consumed in the exponential phase (Figure 5.18 B). Lactate concentration in MBR cultures increased to 1.95 gL^{-1} after 120 hours. Thereafter, lactate was assumed being consumed by cells and then the concentration increase sharply after the continuous feeding commenced. The highest lactate concentration for micro-Matrix and MBR was 2.91 gL^{-1} and 3.83 gL^{-1} respectively. Lactate in the micro-Matrix shows an unstable profile during the course of continuous feeding phase of the culture. The variation in lactate concentration may be due to it being consumed by cells when the level of glucose

is low. This finding corroborates with the work of Ma *et al*. (2009) and Mulukutla *et al.* (2015) regarding the metabolic shift to lactate consumption during low glucose availability in the culture. They added that sometimes in later stage of fed-batch cultivation cell metabolism switches from lactate production to low level of lactate consumption. Additionally, Butler (2005) suggested that lactate production can be reduced by minimising the glucose concentration in the media, particularly during the transition of log to stationary phase. During this phase, cells are actively proliferating and are most productive. He added that low concentration of lactate in culture influence the primary metabolism of cells.

Ammonia is the by-product of glutamine metabolism. Accumulation of ammonia in mammalian cell culture is known to inhibit cell proliferation and protein product quality (Genzel *et al.*, 2005). Ammonia concentrations in the cultures were seen to build up from 0 hour until 120 hours (Figure 5.18 C). The ammonia concentrations at 120 hours was in the range of 2.20 – 2.50 $mmolL^{-1}$ for both cultures. Over the following 24 hours, the analysed ammonia concentration in micro-Matrix reduced to < 2 gL^{-1} before suddenly experienced an increase up to 5.49 $mmolL^{-1}$ after 240 hours. In contrast, ammonia concentration in MBR maintained at 2 gL^{-1} for 300 hours before suddenly it peaked after 336 hours at 3.40 $mmolL^{-1}$. However, the ammonia concentration reported is still low considering the unfavourable concentration would be at of 7 – 10 mM as described by Glacken *et al.* (1983).

Glutamine is an energy source and precursor of anabolic pathways for mammalian cells cultures (Genzel *et al.*, 2005). Generally, mammalian cell media contains 2 – 6 mM glutamine to support metabolism (Genzel *et al.*, 2005). However, for cells with glutamine synthetase (GS) expression system metabolism of glutamine and synthesis of GS enzyme should be in equilibrium and remain unchanged (Zou and Al-Rubeai, 2015). In this study, the glutamine concentration for micro-Matrix might have the similar equilibrium as there was no glutamine produced during the cultivation (Figure 5.18 D). While, inconsistent glutamine concentration for the 14 days cultivation was observed in MBR cultures.

Glutamine was actively produced by cells during exponential phase for 120 hours and peaked at 0.85 $mmolL^{-1}$. Interestingly, before the continuous feeding commenced, glutamine concentration showed a rapid decline. The reduced concentration might be due to the glutamine consumption by cells (Zou and Al-Rubeai, 2015). They added that low glucose concentration might enhance higher glutamine consumption in culture. This is in agreement with Zeng *et al.* (1995) study of mathematical modelling of three modes of cultivation of mammalian cell cultures; batch, fed-batch and continuous. They found that the specific glucose consumption rates in cultures are usually influences by three factors; cell growth, glucose excess and glutamine regulation, while specific glutamine consumption rate was merely due to cell growth and glutamine excess.

Figure 5.18 E depicts the glutamate concentration for both cultures. The glutamate consumption by the cells followed a similar trend as previously described in fed-batch mammalian cell culture. The initial glutamate concentration observed was around 2.0 – 2.5 $mmolL^{-1}$. Glutamate was rapidly consumed by cells during the early proliferation phase from 48 hours until 120 hours. Glutamate concentration in the MBR was maintained in the region of 0.2 $mmolL^{-1}$ for 13 days before it suddenly increased to 0.63 on day 14.

This study has shown that continuous feeding using two different miniature bioreactor geometries has potential to improve CHO cultivation. Furthermore, the continuous feeding show capabilities of supporting the cells with adequate glucose and other nutrients required for energy and cellular metabolism. Advantages of continuous feeding over bolus fed through single intervention not only minimise the contamination issue, but also is less labour intensive for high throughput and parallel MBR systems.

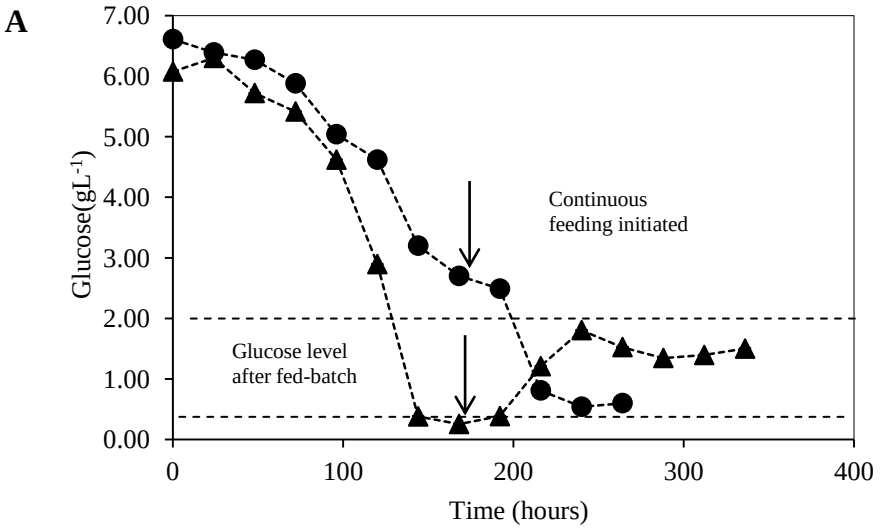
A
Glucose(gL-1)
Continuous
feeding initiated
Glucose level
after fed-batch
Time (hours)

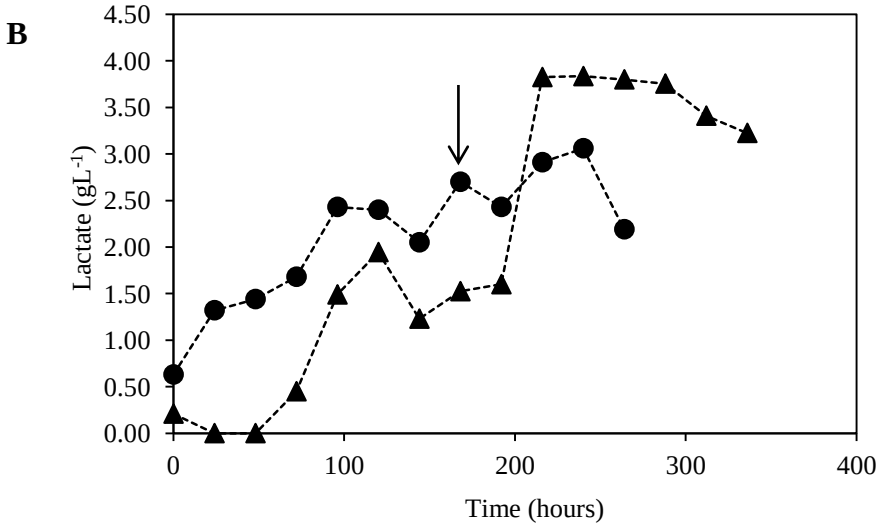
B
Lactate (gL-1)
Time (hours)

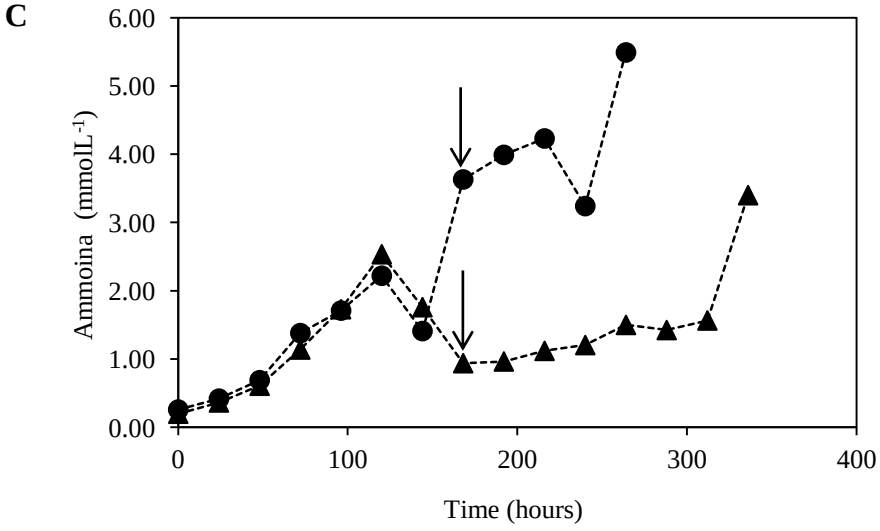
C
Ammoina (mmolL-1)
Time (hours)

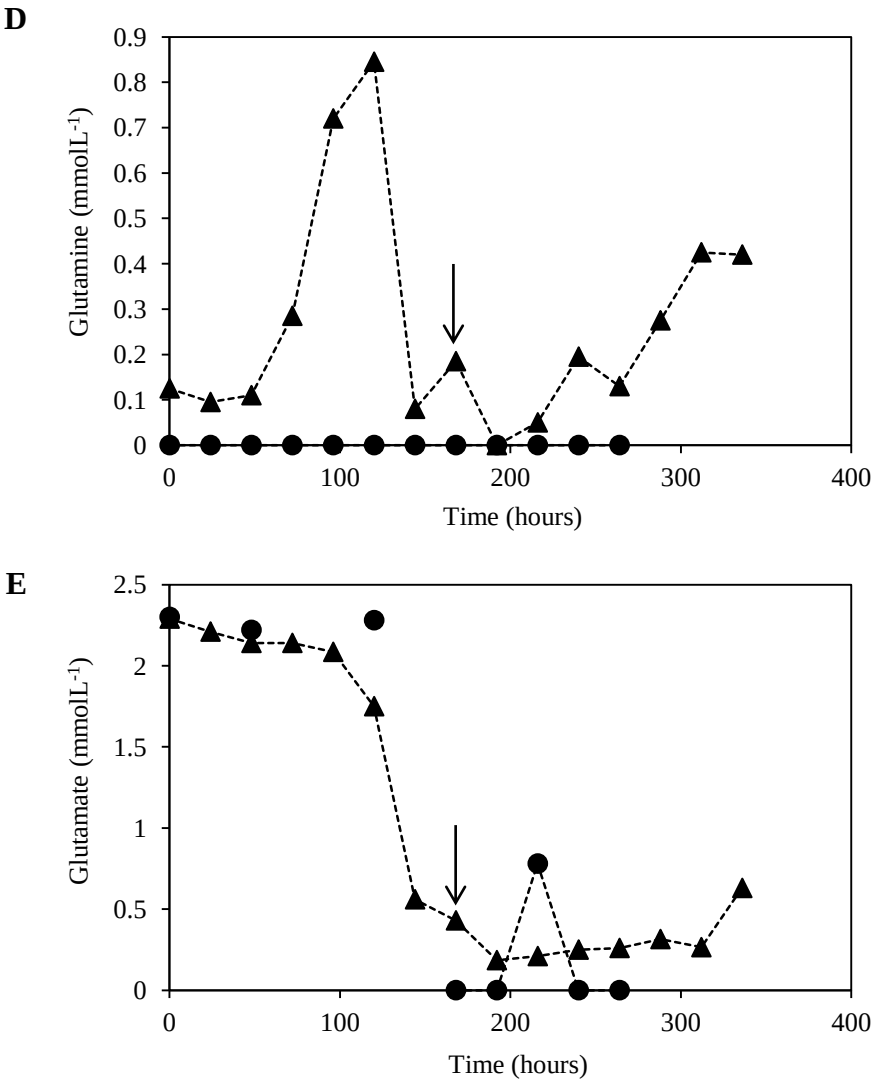

Figure 5.18: CHO metabolites concentration in cultures with continuous feed for two types of reactors; micro-Matrix (●) and MBR (▲). A: glucose concentration, B: lactate concentration. C: ammonia concentration, D: glutamine concentration, E: glutamate concentration. Arrow (↓) indicated feed addition on day 7. Note: micro-Matrix data until day 11 only due to leakage problem on the top plate cover of the 24-DWP.

5.7 Comparison of process parameter control

Process parameter such pH, DO, and temperature in a bioreactor can be measured either on-line, at-line (via connection to calibrated analysers) or off-line (manual intervention by operator) (Li *et al*., 2010). In a controlled bioreactor, monitoring these process parameters for specific set point is essential. Furthermore, these culture process parameters may give significant impacts on the cell growth, metabolism and productivity. Therefore, key process parameters were presented in this section to compare the process capability of the two miniature bioreactors studied in the Section 5.6. The data was from the 24 wells (micro-Matrix), while one MBR (HEL-BioXPlore) with the direct driven impeller and horseshoe type sparger. Additionally, the data reading was logged every 30 seconds for micro-Matrix, while every 60 seconds for MBR.

5.7.1 pH

pH is one of the most vital variables to monitor and control in mammalian cell cultivation. Minor changes in culture pH can significantly impact on cell growth, metabolism and product formation (Li *et al*., 2010). The culture pH in both systems was set at 7.10 with dead band of 0.4 and 0.1 for micro-Matrix and HEL-BioXplore MBR correspondingly. For the first 55 hours, the pH logged for micro-Matrix was 7.00 - 7.35 (Figure 5.19 A). After 60 hours of cultivation, pH was observed dropped in the range 6.90 – 7.15, then gradually increased until 200 hours. Subsequently, after the continuous feeding started on 168 hours, two of the wells show deviation from the set point 7.10 ± 0.4. The pH drift was presumed by the fact that the micro valves on the top plate were not properly opened up during the feeding. The culture in the wells that experience pH drift might not received feed from the system. As consequences, the top plate was found leaked and the experiment in micro-Matrix was stopped on day 11. On contrary, pH in the MBR system was seen very tight on the higher end of the dead band (Figure 5.19 B). pH was logged in the range of 7.15 – 7.20 throughout the cultivation.

A

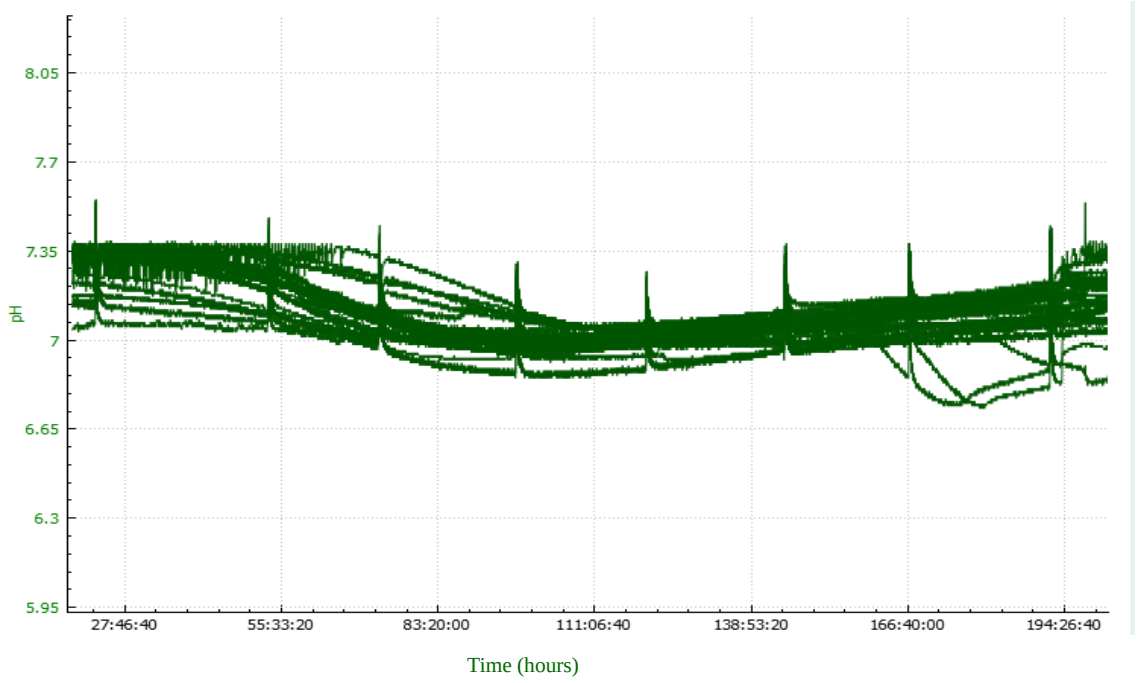

B

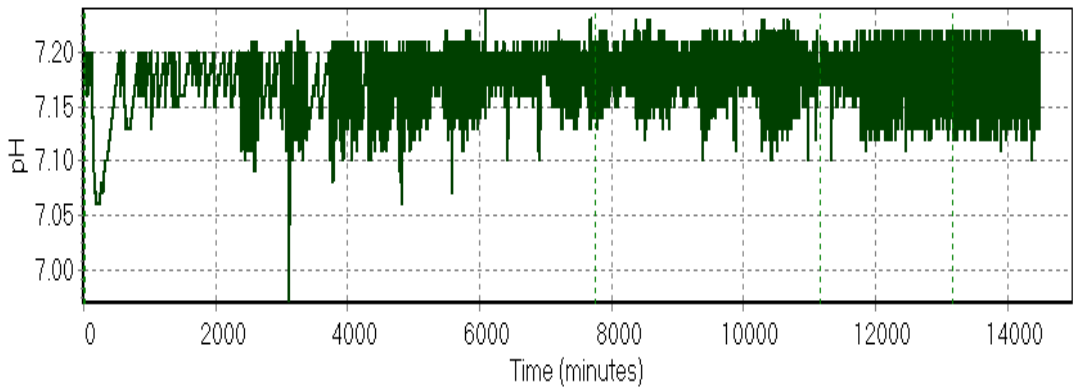

Figure 5.19: pH profiles for the two systems with continuous feeding strategy. A: micro-Matrix system with data logged every 30 seconds B: HEL-BioXplore MBR with data logged every 60 seconds.

5.7.2 Dissolved oxygen

Dissolved oxygen is important parameters controlled in bioreactor to prevent DO limitation, which could lead to cytotoxicity (Li *et al*., 2010). Normally, DO is set at specific point of 20 – 50 % of air saturation. The system was set at 30 % (MBR) and 30 % (micro-Matrix) with dead band of 10 %. The dissolved oxygen profiles for micro-Matrix and MBR showed large variations over the set point. The micro-Matrix DO profiles (Figure 5.20 A) illustrates that air saturation of 80 – 95 % was maintained during the cultivation. The spikes produced during the cultivation might be due to the time taken for the gaseous system to resume back after the system was stopped for sampling. By contrast, the MBR system DO profiles was stable for 100 hours (Figure 5.20 B). The first four days of cultivation, cells are in the lag-log phase where demand for oxygen is very minimal. After these phase, cell enter full exponential phase for proliferation and metabolism which make the demand for oxygen are optimal. This can be seen with the spikes that produced after 100 hours.

5.7.3 Temperature

The temperature profiles for the two systems showed distinctive variation. The temperature control was set at 37°C ± 0.5 for both systems. Figure 5.21 A shows the temperature profiles for the micro-Matrix system over the cultivation period. Based on the data logged every 30 seconds, there are a number of downward and upward spikes for every 24 hours until around 200 hours. Each of the spikes indicated the sampling point, which the micro-Matrix system was stopped for few minutes. During sampling procedure, the micro-Matrix cabinet was opened and the culture was aseptically sampled for analysis. The longer the times taken during sampling mean that a longer time will be needed for the system to continue its operation. By contrast, the temperature profile for the MBR system was very stable over the cultivation period (Figure 5.21 B). The temperature set point was able to maintain within the range of 37°C ± 0.5. Besides that, the minimal spikes found in the logged data were due to the addition of ‘cold’ culture feed. The culture feed was refrigerated to maintain its sterility and nutrients content throughout the continuous feeding strategy. The slight changes of temperature from the continuous feed added might gave these minimal spikes.

A

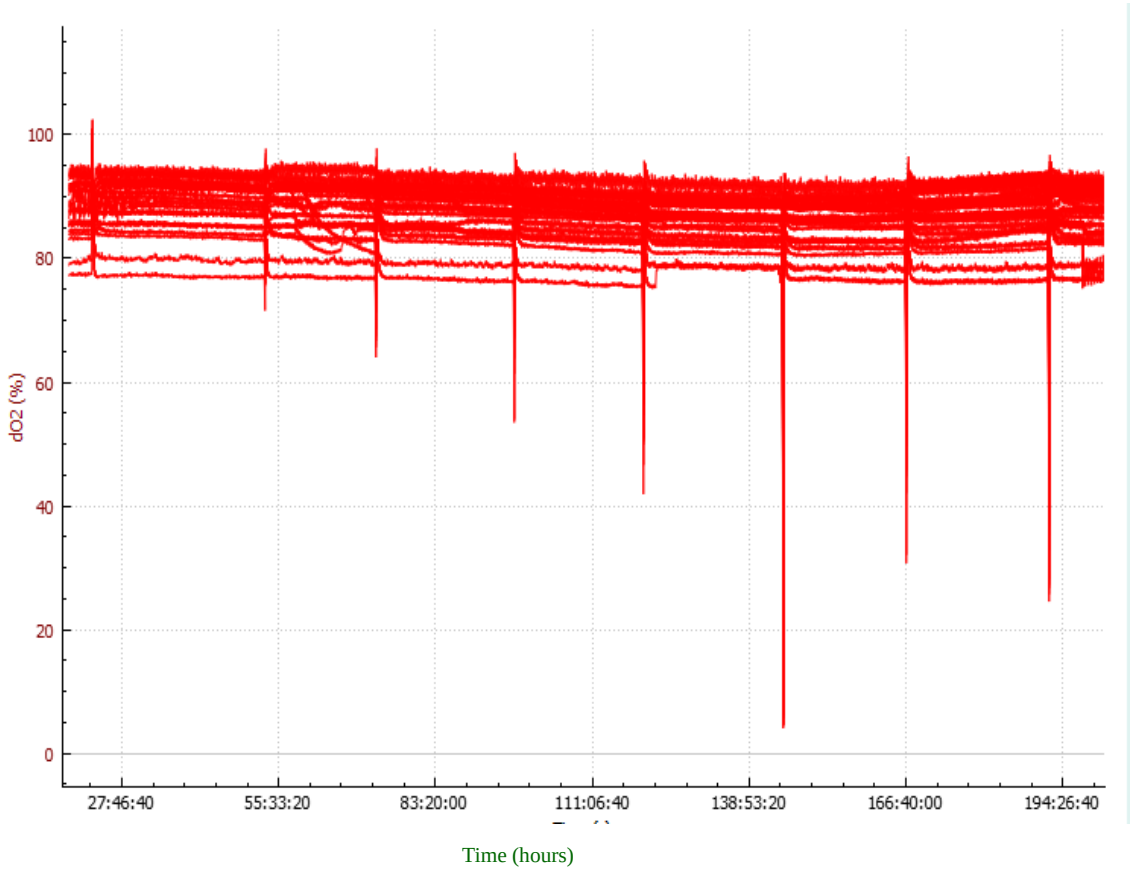

B

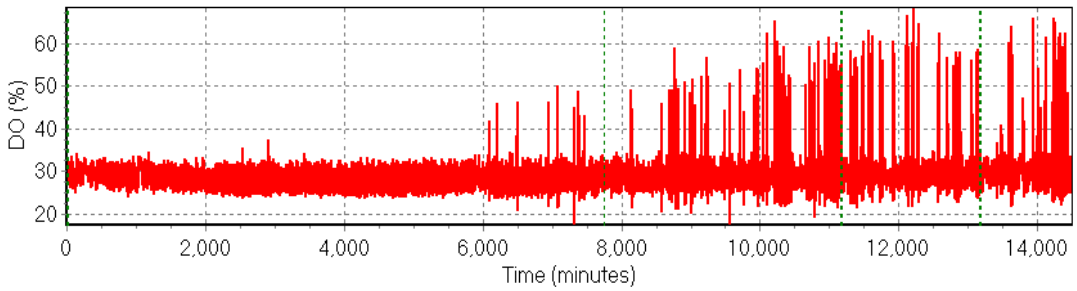

Figure 5.20: DO profiles for the two systems with continuous feeding strategy. A: micro-Matrix system with data logged every 30 seconds B: HEL-BioXplore MBR with data logged every 60 seconds.

A

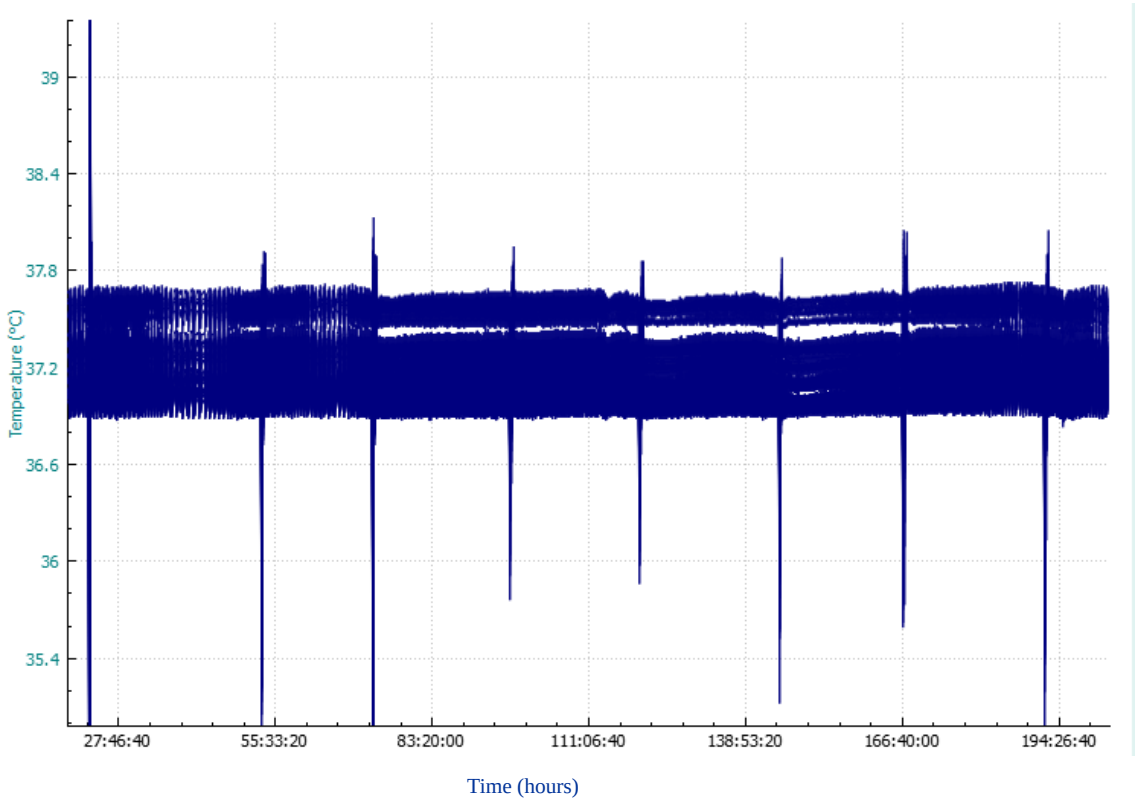

B

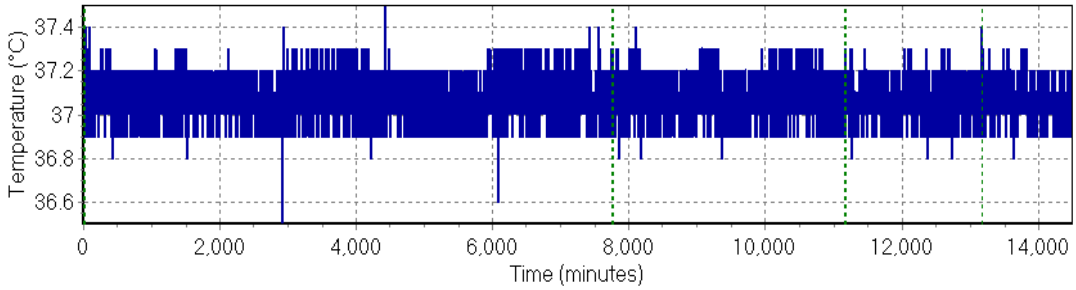

Figure 5.21: Temperature profiles for the two systems with continuous feeding strategy. A: micro-Matrix system with data logged every 30 seconds B: HEL-BioXplore MBR with data logged every 60 seconds.

5.8 Conclusion

This chapter has demonstrated the potential of the microwell based systems and miniature bioreactors for scale translation using matched mixing time as scale translation criteria. Predictive scale-up results achieved in this chapter has provided the basis understanding on performance of different geometries and scales of reactors. Scale comparison cultivations for bolus fed CHO cell cultures were carried out for 24-SRW and miniature bioreactors (MBR) and compared with a standard 5 L STR at matched mixing time of ~6 ± 2 s. The cultivations show that 24-SRW and MBR gave comparable CHO cell growth kinetics with standard 5 L STR. The cell viability data also shows that 24-SRW and MBR systems are able to prolong the viability > 60 % with the bolus addition until the harvest on day 14. All three reactors are able to reach similar product titres with 24-SRW giving the maximum titre of 0.92 gL^{-1}, followed by 5 L STR (0.83 gL^{-1}) and MBR (0.69 gL^{-1}).

In this chapter, a new micro-bioreactor (micro-Matrix) was characterised for its ability to perform a cell culture process. The advantages of the automation system of the micro-Matrix to control automated feed regimes and other engineering parameters were analysed. The systems were studied using a controlled and non-controlled aeration system with either bolus or continuous feeding. Based on the preliminary results, the micro-Matrix with controlled aeration and continuous feeding shows good potential for CHO cell cultivation with peak viable cell concentration of 8.67 x 10^6 cell mL^{-1} and viability > 60 % after 264 hours. However, due to the toxicity of dCO_2 accumulated in the system as discussed in Section 5.4.1 and 5.5.1 that inhibited the cells to maintain good viability and subsequently led to low product yields.

This chapter also indicates the potential of the micro-Matrix with controlled aeration and continuous feeding for scale translation of CHO cell cultivation in comparison with MBR system. The basis of matched mixing time of 6 s was

applied for the scale-up performance. The ability to continuously feed the micro-Matrix and MBR has shown that CHO cell growth kinetics improved tremendously from our previous studies in Section 5.2.1, 5.4.1, 5.5.1. Besides that, several improvements of operating conditions as summarised in Table 5.6 has supported the good results that were achieved in this study. Viable cell concentration for both reactors show good similarity with peak VCC of 11.1 x 10^6 cell mL^{-1} and 9.76 x 10^6 cell mL^{-1} for micro-Matrix and MBR respectively. After 11 days cultivation, both of the system managed to maintain a cell viability of 87 %. The product titre for the MBR was 0.64 gL^{-1} (336 hours), while micro-Matrix was 0.50 gL^{-1} (264 hours). Unfortunately, the micro-Matrix cultivation had to be stopped on day 11 due to the leakage on the top plate that covered the 24-DWP. The experiment was not repeated because of the unavailability of suitable gas filter bars for the top plates. Hence, this preliminary study should be repeated in future for better understanding and ability of the micro-Matrix system for cell culture application.

Chapter 6 Conclusions and Future work

This chapter aims are to review and summarise the key findings of each chapter and provide future work recommendations. Each chapter was evaluated for CHO growth kinetics and IgG formation with different geometries and scales of bioreactors.

6.1 Characterisation of microtitre plates and fed-batch operating strategies

Chapter 3 described the application of microtitre plates in batch and fed-batch operating strategies for CHO growth profiles and antibody productivity. The study in this chapter was built on the work of Silk (2014) who studied extensively different microwell based systems for feasibility of CHO cultivation. The preliminary study was based on selected optimised operating conditions for 24-SRW. Two types of commercial sandwich covers (CR1524 and CR1524a) were evaluated for its performance in batch CHO cultivation. Chinese hamster ovary cells which cultured in 24-SRW showed comparable results for both covers. Both MTPs cultures peak viable cell concentration was 45 % higher compared to a previous study by Silk (2014). The optimised agitation rate of 220 rpm was found suitable for CHO cell cultivation. Besides that, MTP cultured with CR1524a (for slow growing cells) cover has enhanced growth until day 11 with 80 % viability. The lengthened viability also raised the final product titre to 0.86 gL^{-1} in CR1524a. Nonetheless, glucose exhaustion and accumulation of by-products (lactate and ammonia) have inhibited the batch growth and antibody production of CHO cells. Hence, a suitable feeding strategy was employed in the MTP to avoid nutrient limitations.

At the moment, the feeding strategy of CHO cell cultured in MTP is not well established. Only recently, Silk *et al*., (2010) reported that bolus feeding with concentrated glucose for CHO cell cultivation and found that large residual of

glucose had an effect on the culture osmolality. In contrast, Hedge *et al*., (2012) studied glucose feeding achieved using the glucose loaded hydrogel in shake flasks that resulted in a 23 % higher integral viable cell concentration and 89 % lower lactate concentration. The use of diluted glucose solution for bolus feeding and the commercial FeedBead® system for improved fed-batch CHO growth kinetics was studied. The diluted concentrated feed for bolus addition in MTP with CR1524a led to considerably higher viable cell count and viability compared to using FeedBead®. The bolus addition was able to maintain viability of 82.5 %, while using the FeedBead® system the viability decreased to less than 1 %. Notably, fed-batch with bolus addition was able to maintain the average glucose concentration of 2 $gL^{-1}d^{-1}$, in agreement with Barrett *et al*. (2010) and Silk *et al*. (2010). The FeedBead® system was found not to be efficient for the CHO cell cultivation because of the high release rates as described in Section 3.6.1. The high glucose release within short period time (1 – 2 days), lead to large transient increases in nutrient concentrations and gave detrimental effect on cell growth and metabolism (Hegde *et al*., 2012). Therefore, few improvements can be applied in the FeedBead® system for fed-batch strategy in mammalian cells. The release of nutrient from the hydrogel should occur over period of 5 – 7 days to accommodate the long duration of mammalian cell cultivation. Besides that, the release rate of nutrient into the culture should be slower to balance the glucose consumption rate by the slow growing mammalian cells.

6.2 Characterisation of miniaturised stirred bioreactor and evaluation of fed-batch operating strategies

The need to reduce the cost of operation and speed up the process development has enabled companies to develop miniaturised system that have the same key engineering parameters as conventional large scale reactors (Lye *et al*., 2003; Betts and Baganz, 2006). The advantages of small scale systems or miniature reactors are generation of early design data, parallel operation and high throughput (Bareither and Pollard, 2011). The study in Chapter 4 focussed on the evaluation of a commercialised miniature bioreactor system (HEL-BioXplore) for

parallel mammalian cell cultures. The HEL-BioXplore reactor is an MBR with a working volume of approximately 100 – 300 ml that is based on geometry and mechanical similarity to a standard bench scale STR. Gill *et al*., (2008 a,b) reported the MBR performance for microbial cultivation, while Al-Ramadhani, (2015) demonstrated that headspace aeration and suitable feeding strategies for CHO cell cultivation. Design modification to the gas delivery system and continuous feeding strategies were employed in this study. The MBR was fitted with either direct driven impeller or magnetic driven impeller with singular hole impeller or horseshoe type sparger. Before the feasibility of CHO cell cultivation was initiated, a comprehensive engineering characterisation of mixing time, overall volumetric oxygen transfer coefficient and power input was performed.

Mixing time study was conducted experimentally using the pH tracer method. In this study, different types of impeller and gas delivery modes as a function of agitation rate were evaluated. Mixing time obtained in this experiment was comparable with recent literatures for CHO cultivation bioreactor systems (Al-Ramadhani, 2015; Betts, 2015; Silk, 2014). Direct driven impeller with horseshoe sparger achieved the shortest mixing times with averaged measurement ranging from 3.3 – 9.3 s. Since the MBR exhibits a similar geometry as a conventional STR, Nienow (1998) correlation was applied to compare experimental and predicted values. The mixing time obtained for experimental and predicted values was comparable which suggested that the correlation accurately predicted mixing times in the MBR using either impeller system.

Furthermore, the overall volumetric oxygen transfer coefficient was measured experimentally using the static gassing out technique (Wise, 1951). The measured k_La obtained were 5.9 to 12.5 h^{-1} as function of agitation rate ranging from 200 rpm to 500 rpm for two different types of impeller and sparger. The measured k_La values are consistent with studies by Xing *et al*. (2009) and Tissot *et al*. (2012) for k_La values below 15 h^{-1} for the application in mammalian cell cultures. Morevoer, the predicted power input into the MBR was in the range of 1.7 – 54.5 Wm^{-3} as function of impeller system and agitation speed. Unfortunately, the

power input was not measured experimentally due to a broken air bearing dynamometer.

The results from the engineering characterisation studies of the MBR were used to select the operating conditions for CHO cultivation experiments in batch and fed-batch mode. Matched mixing time at 6 s was selected for the magnetic and direct driven impeller giving agitation rates of 400 rpm and 450 rpm respectively. The growth kinetics for both impeller systems in batch mode showed comparable results with direct driven impeller fitted with horseshoe sparger presented the highest viable cell concentration of 7.06 x 10^6 cell mL^{-1} on day 8 and final antibody titre of 0.40 gL^{-1}. The MBR system was further explored for its application in fed-batch mode of CHO cultivation. The suitability of the horseshoe sparger with both impeller system that is magnetic and direct driven was studied. The culture in the reactor with direct driven impeller system attained peak viable cell concentration on day 7 with 8.89 x 10^6 cell mL^{-1}, whilst the culture using in the MBR with magnetic impeller peaked at 7.68 x 10^6 cell mL^{-1}. Bolus feed that was initiated after glucose was depleted able to lengthen the viability of both cultures to >55 % on harvest day. In addition, the improved product formation for both impeller systems was seen in fed-batch mode with 0.84 and 0.73 gL^{-1} for direct driven and magnetic MBR respectively.

6.3 Scale translation between microwell based systems and miniature bioreactors at matched mixing time

Chapter 5 aimed to evaluate the potential of microwell based systems and miniature bioreactors for scale translation using matched mixing time as criterion. Predictive scale-up from small scale reactors to larger scale is vital to determine the scalability of a reactor. Additionally, a successful scale translation of CHO cell cultivation from small scales using different geometry of reactors will provide a better understanding of the reactor performance. The scale comparison was for fed-batch (bolus fed) of CHO cell line based on matched mixing time of 6 s for 24-SRW, miniature bioreactor (MBR) and STR. Initial growth kinetics

depicted that the three reactors gave comparable viable cell concentration with high viability of 60 % after 14 days of culture. The final antibody titres for the three reactors showed that 24-SRW was the highest with 0.92 gL^{-1}, followed by STR (0.83 gL^{-1}) and MBR (0.69 gL^{-1}). Additionally, the specific product formations are equivalent in the range of 9.7 – 12.2 pg cell $^{-1}d^{-1}$. The bolus feed addition commenced on day 7 was able to supply the nutrient consumed in culture and the residual concentration could be maintained in the region of 0.5 – 3 gL^{-1} for all reactors. However, elevated metabolic waste of lactate and ammonia was observed after the addition which could inhibit the cell growth and metabolism.

The micro-Matrix system is an example of an automated system with parallel and high throughput capability that are essential to speed up bioprocess development. In this chapter, a prototype micro-Matrix was characterised for its performance in a cell culture process. The system was evaluated with controlled and non-controlled aeration system using two different feeding strategies (bolus and continuous). Based on the initial results obtained, the micro-Matrix with controlled aeration and continuous feeding shows potential for CHO cell cultivation with peak viable cell of 8.67 x 10^6 cell mL^{-1} and viability > 90 % after 264 hours. However, due to the toxicity of accumulated dCO_2 have inhibited the cell proliferation and hence had a detrimental impact on the cells. The effect of accumulated of CO_2 in reactors has been well documented by other researchers (Gray *et al*., 1996; Kimura and Lee, 1996).

This chapter also described the potential of the micro-Matrix with controlled aeration and continuous feeding for scale translation of CHO cell cultivation in comparison with the MBR system. Besides that, few improvements were done with the micro-Matrix system for scale translation studies as described in Table 5.6. Matched mixing time of 6 s was applied as scale translation criterion. The viable cell concentrations between the two reactor cultures are comparable with micro-Matrix achieving a peak VCC of 11.1 x 10^6 cell mL^{-1} while MBR reached 9.76 x 10^6 cell mL^{-1}. For the first 7 days of cultivation, both systems show good

comparability in terms of cell viability and product formation. The continuous feeding applied to both systems was able to sustain the nutrients depleted in the cultures. Nevertheless, on day 11 the culture in micro-Matrix was abruptly discontinued because of the major leakage on the top plate that covered the 24-DWP. Unfortunately, the experiment could not be repeated due to the severe leakage found in the gas filter bars built-in on the top plate. For this reason, this initial work should be repeated for future work to better determine the capability of micro-Matrix in CHO cell cultivation.

6.4 Overall conclusions

As conclusion, the findings between each of the systems studied (microwell based systems, miniature bioreactors and bench stirred tank reactors) had provided a crucial understanding of the capability of each system for CHO cell growth kinetics and antibody productivity. Based on the predictive scale translation using mixing time as criterion, the three systems have comparable peak viable cell and product concentrations. There was no significant difference between the three systems studied. Bolus feed strategies applied to each of the systems showed that the required glucose level for CHO metabolism at 2 g L^{-1} d^{-1} as reported in literature could be maintained. The antibody productivities obtained are similar with recent studies using microwell systems (Barrett *et al*., 2010; Silk *et al*., 2010), MBR (Al-Ramadhani, 2015), and STR (Velez-Suberbie, 2013). Overall, the small scale bioreactors evaluated have shown a potential as scale-down models which could applied for generation of early bioprocess development data in the biopharmaceuticals industry.

6.5 Future work and recommendations

The work carried out in this study established that small scale reactors with optimised operating conditions have the potential for scale-up to larger scales. The capacity of the microwell based systems and miniature bioreactors to mimic the performance of conventional lab-scale STR (5L) gave fundamental insight into each bioreactor performance. However, there are always few areas that should be scrutinised for future improvement in CHO cell cultivation.

Conventionally, microtitre plate experiments are a manual, labour intensive and time consuming process. The initial proposal for this study to integrate the microtitre plate with a TECAN robotic platform for liquid automation was seen as alternative to speed up the process. In order to perform the automation platform for mammalian cell culture, the unit should maintain high sterility. Hence, the robotic arms should be house in a cabinet (e.g. laminar flow) with temperature control and HEPA unit filter. The unit also could be attached to a shaking incubator for culture cultivation. Furthermore, the robotic system with liquid handling system might be integrated with a flow cytometer for cell quantification and analysis. The integration with robotic arms will reduce the labour intensity of manual feeding in MTP, thus consequently increasing the liquid handling accuracy for sampling, feeding and pH control, thus minimise the contamination risks and time.

The versatility of the HEL-BioXplore^{TM} MBR investigated shows that the system has the potential for predictive scale translation to conventional lab-scale reactors. The variation of impellers and spargers possible with the system provides the basis for further exploration. The possibility of the MBR to run 4, 8 or 16 parallel bioreactors on the same platform makes it an excellent cell culture tools for Quality by Design setting. The development of different feeding strategies and optimisation of operating and environmental conditions might be applied in the DoE approach. By means of the DoE implementation, a series of reproducible results could be generated that would be beneficial in CHO cell cultivation.

Besides that, the application of computational fluid dynamic (CFD) and finite element model (FEM) might give valuable information on the hydrodynamic environment and engineering aspects that are not measureable directly in the vessel. Velez-Suberbie, (2013) described fluid motions and energy dissipation rate measurement in the 5 L STR that can be used to determine the hydrodynamic and shear stress. Furthermore, the experimental values of mixing time and volumetric oxygen transfer coefficient measured might be useful to validate the computational model (Betts, 2015).

Additionally, each of the miniature systems investigated have the potential to perform in early process development and optimisation studies. The microwell based systems (MTP and micro-Matrix) which enable parallelism, reproducibility and high throughput sequences could allow for cell line screening studies as example the selection for high producing clones. Furthermore, these systems could offer optimisation studies for media and feed development. The miniature bioreactors (MBR) investigated could fit in the process characterisation studies where usually bench scale bioreactors have been system of choice. The capability of the systems to run parallel with 4 – 16 reactors and with the implementation of DoE, several key and critical process characterisation studies can be done.

The antibody produced in this study might be evaluated using different downstream processing options to optimise product purification. The method developed within this Department of Biochemical Engineering for microscale cell separation can be used to compare the material harvested at the end of the cultivation. Tait *et al*. (2009) has developed ultra scale down (USD) approaches for centrifugation, whilst Jackson *et al*. (2006) has developed the membrane filtration. Furthermore purification of the antibody product could be accessed using the affinity-based chromatography methods for detail analysis of product quality and quantity. Finally, a generic and robust framework for rapid bioprocess development using small scale bioreactors with combination of downstream process mimics could be established.

6.6 Publication and conferences attended

Book chapters

Mohd Helmi Sani and Frank Baganz, (2012). Miniature Bioreactors for Rapid Bioprocess Development of Mammalian Cell Culture. Jurnal Teknologi, 59(1), pp. 3-4.

Conference

Sani M. H., Kreukniet M., Robinson G., Baganz F. Comparison of feeding strategies for a CHO cell culture process using a single use 24-well miniature bioreactor system (micro-Matrix). Poster for 25th Annual ESACT-UK 2015, Queens Hotel, Leeds, United Kingdom, 7-8 Jan 2015.

Sani M. H., Kreukniet M., Robinson G., Baganz F. Initial evaluation of a single use 24-well miniature bioreactor system (micro-Matrix) applied to fed-batch cultivation of CHO cells. Poster for 11th Annual bioProcess UK Conference, St George Hall, Liverpool, United Kingdom, 25-26 Nov 2014.

Mohd Helmi Sani. CHO cell culture at the micro-bioreactor scale. Oral presentation for Technology Showcase Forum: Micro-bioreactors: the challenges and opportunities for down scale R&D by Applikon Biotechnology UK, Crowne Plaza, London, United Kingdom, 3-4 Nov 2014.

Sani, M.H., Micheletti M., Baganz F. A comparison of two different feeding methods for CHO cell cultures in shaken microtitre plates. Poster for 10th Annual bioProcess UK Conference, BMA House, London, United Kingdom, 3-4 Dec 2013.

Sani M.H., Micheletti M and Baganz F., Rapid Bioprocess Development Using Microwells for Mammalian Cell Culture, Oral Presentation for International Conference on Humanities, Social Sciences, Science and Technology (ICHSST 2012), Cardiff, Wales, 16 July 2012.

REFERENCES

Aggarwal, S. (2014). What's fueling the biotech engine-2012 to 2013. *Nature Biotechnology*, *32*(1), 32-39.

Amanullah, A., Otero, J. M., Mikola, M., Hsu, A., Zhang, J., Aunins, J and Russo, A. P. (2010). Novel micro-bioreactor high throughput technology for cell culture process development: Reproducibility and scalability assessment of fed-batch CHO cultures. *Biotechnology and Bioengineering*, *106* (1), 57-67.

Al-Ramadhani, O. (2015). *Design and characterisation of a parallel miniaturised bioreactor system for mammalian cell culture.* (Ph.D thesis), University College London.

Al-Rubeai, M., Singh, R., Goldman, M., and Emery, A. (1995). Death mechanisms of animal cells in conditions of intensive agitation. *Biotechnology and Bioengineering*, *45*(6), 463-472.

Altamirano, C., Berrios, J., Vergara, M., & Becerra, S. (2013). Advances in improving mammalian cells metabolism for recombinant protein production. *Electronic Journal of Biotechnology*, *16*(3), 10-10.

Altamirano, C., Illanes, A., Becerra, S., Cairó, J. J., and Gòdia, F. (2006). Considerations on the lactate consumption by CHO cells in the presence of galactose. *Journal of Biotechnology*, *125*(4), 547-556.

Altamirano, C., Paredes, C., Cairó, J. J., and Gòdia, F. (2000). Improvement of CHO Cell Culture Medium Formulation: Simultaneous Substitution of Glucose and Glutamine. *Biotechnology Progress*, *16*(1), 69-75.

Altamirano, C., Paredes, C., Illanes, A., Cairó, J. J., and Gòdia, F. (2004). Strategies for fed-batch cultivation of t-PA producing CHO cells: substitution of

glucose and glutamine and rational design of culture medium. *Journal of Biotechnology, 110*(2), 171-179.

Amanullah, A., Buckland, B. C., and Nienow, A. W. (2004). Mixing in the Fermentation and Cell Culture Industries *Handbook of Industrial Mixing* (pp. 1071-1170): John Wiley & Sons, Inc.

Bareither, R., Bargh, N., Oakeshott, R., Watts, K., and Pollard, D. (2013). Automated disposable small scale reactor for high throughput bioprocess development: A proof of concept study. *Biotechnology and Bioengineering, 110*(12), 3126-3138.

Bareither, R., and Pollard, D. (2011). A review of advanced small-scale parallel bioreactor technology for accelerated process development: Current state and future need. *Biotechnology Progress, 27*(1), 2-14.

Barrett, T. A. (2008). *Microwell evaluation of mammalian cell lines for large scale culture.* (Ph.D thesis), University of London.

Barrett, T. A., Wu, A., Zhang, H., Levy, M. S., and Lye, G. J. (2010). Microwell Engineering Characterization for Mammalian Cell Culture Process Development. *Biotechnology and Bioengineering, 105*(2), 260-275.

Berrios, J., Altamirano, C., Osses, N., and Gonzalez, R. (2011). Continuous CHO cell cultures with improved recombinant protein productivity by using mannose as carbon source: Metabolic analysis and scale-up simulation. *Chemical Engineering Science, 66*(11), 2431-2439.

Betts, J. P. J. (2015). *Incorporation of Developability into Cell Line Selection.* (Ph.D thesis). University College London.

Betts, J. I., and Baganz, F. (2006). Miniature bioreactors: current practices and future opportunities. *Microbial Cell Factories, 5*(1), 21.

Betts, J. I., Doig, S. D., and Baganz, F. (2006). Characterization and Application of a Miniature 10 mL Stirred-Tank Bioreactor, Showing Scale-Down Equivalence with a Conventional 7 L Reactor. *Biotechnology Progress, 22*(3), 681-688.

Betts, J. P. J., Warr, S. R. C., Finka, G. B., et al. (2014). Impact of aeration strategies on fed-batch cell culture kinetics in a single-use 24-well miniature bioreactor. *Biochemical Engineering Journal, 82*(0), 105-116.

Bibila, T. A., Ranucci, C. S., Glazomitsky, K., Buckland, C., and Aunins, J. G. (1994). Monoclonal antibody process development using medium concentrates. *Biotechnology Progress, 10*(1), 87-96.

Bibila, T. A., and Robinson, D. K. (1995). In pursuit of the optimal fed-batch process for monoclonal antibody production. *Biotechnology Progress, 11*(1), 1-13.

Birch, J. R., and Racher, A. J. (2006). Antibody production. *Advanced Drug Delivery Reviews, 58*(5–6), 671-685.

Browne, S. M., and Al-Rubeai, M. (2009). Selection Methods for High-Producing Mammalian Cell Lines. Cell Line Development. In Al-Rubeai, M. (Ed.), (Vol. 6, pp. 127-151): Springer Netherlands.

Butler, M., (2005). Animal cell cultures: recent achievements and perspectives in the production of biopharmaceuticals. *Applied Microbiology and Biotechnology, 68*(3), 283-291.

Butler, M., and Meneses-Acosta, A. (2012). Recent advances in technology supporting biopharmaceutical production from mammalian cells. *Applied Microbiology and Biotechnology, 96*(4), 885-894.

Chadd, H. E., and Chamow, S. M. (2001). Therapeutic antibody expression technology. *Current Opinion in Biotechnology, 12*(2), 188-194.

Chatterjee, M., Ge, X., Uplekar, S., et al. (2015). A unique noninvasive approach to monitoring dissolved O2 and CO2 in cell culture. *Biotechnology and Bioengineering, 112*(1), 104-110.

Chee Furng Wong, D., Tin Kam Wong, K., Tang Goh, L., Kiat Heng, C., and Gek Sim Yap, M. (2005). Impact of dynamic online fed-batch strategies on metabolism, productivity and N-glycosylation quality in CHO cell cultures. *Biotechnology and Bioengineering, 89*(2), 164-177.

Chen, P., and Harcum, S. W. (2005). Effects of amino acid additions on ammonium stressed CHO cells. *Journal of Biotechnology, 117*(3), 277-286.

Chisti, Y. (2000). Animal-cell damage in sparged bioreactors. *Trends in Biotechnology, 18*(10), 420-432.

Chisti, Y. (2001). Hydrodynamic Damage to Animal Cells. *Critical Reviews in Biotechnology, 21*(2), 67-110.

Chu, L., and Robinson, D. K. (2001). Industrial choices for protein production by large-scale cell culture. *Current Opinion in Biotechnology, 12*(2), 180-187.

Deshpande, R. R., Wittmann, C., and Heinzle, E. (2004). Microplates with integrated oxygen sensing for medium optimization in animal cell culture. *Cytotechnology, 46*(1), 1-8.

deZengotita, V. M., Abston, L. R., Schmelzer, A. E., Shaw, S., and Miller, W. M. (2002). Selected amino acids protect hybridoma and CHO cells from elevated carbon dioxide and osmolality. *Biotechnology and Bioengineering*, *78*(7), 741-752.

Diao, J. P., Young, L., Zhou, P., and Shuler, M. L. (2008). An actively mixed mini-bioreactor for protein production from suspended animal cells. *Biotechnology and Bioengineering*, *100*(1), 72-81.

Doig, S., Baganz, F., and Lye, G. (2006). High throughput screening and process optimisation. *Basic Biotechnology*. Cambridge: Cambridge University Press.

Doig, S., Diep, A., and Baganz, F. (2005). Characterisation of a novel miniaturised bubble column bioreactor for high throughput cell cultivation. *Biochemical Engineering Journal*, *23*, 97 - 105.

Doran, P. M. (1995). *Bioprocess engineering principles*. GB: Academic Press.

Duetz, W., Ruedi, L., Hermann, R., O'Connor, K., Buchs, J., and Witholt, B. (2000). Methods for intense aeration, growth, storage and replication of bacterial strains in microtiter plates. *Appl Environ Microbiol*, *66*, 2641 - 2646.

Duetz, W. A. (2007). Microtiter plates as mini-bioreactors: miniaturization of fermentation methods. *Trends in Microbiology*, *15*(10), 469-475.

Duetz, W. A., and Witholt, B. (2004). Oxygen transfer by orbital shaking of square vessels and deepwell microtiter plates of various dimensions. *Biochemical Engineering Journal*, *17*(3), 181-185.

Elmahdi, I., Baganz, F., Dixon, K., Harrop, T., Sugden, D., and Lye, G. (2003). pH control in microwell fermentations of S. erythraea CA340: influence on

biomass growth kinetics and erythromycin biosynthesis. *Biochemical Engineering Journal*, *16*, 299 - 310.

Fan, Y., Jimenez Del Val, I., Müller, C., Wagtberg Sen, J., Rasmussen, S. K., Kontoravdi, C., Andersen, M. R. (2015). Amino acid and glucose metabolism in fed-batch CHO cell culture affects antibody production and glycosylation. *Biotechnology and Bioengineering*, *112*(3), 521-535.

Ferreira-Torres, C., Micheletti, M., and Lye, G. J. (2005). Microscale process evaluation of recombinant biocatalyst libraries: application to Baeyer-Villiger monooxygenase catalysed lactone synthesis. *Bioprocess and Biosystems Engineering*, *28*(2), 83-93.

Gagnon, M., Hiller, G., Luan, Y.-T., Kittredge, A., DeFelice, J., and Drapeau, D. (2011). High-End pH-controlled delivery of glucose effectively suppresses lactate accumulation in CHO Fed-batch cultures. *Biotechnology and Bioengineering*, *108*(6), 1328-1337.

Garcia-Ochoa, F., and Gomez, E. (2009). Bioreactor scale-up and oxygen transfer rate in microbial processes: An overview. *Biotechnology Advances*, *27*(2), 153-176.

Ge, X., Hanson, M., Shen, H., et al. (2006). Validation of an optical sensor-based high-throughput bioreactor system for mammalian cell culture. *Journal of Biotechnology*, *122*(3), 293-306.

Genzel, Y., Ritter, J. B., König, S., Alt, R., and Reichl, U. (2005). Substitution of Glutamine by Pyruvate To Reduce Ammonia Formation and Growth Inhibition of Mammalian Cells. *Biotechnology Progress*, *21*(1), 58-69.

Gill, N. K., Appleton, M., Baganz, F., and Lye, G. J. (2008a). Design and characterisation of a miniature stirred bioreactor system for parallel microbial fermentations. *Biochemical Engineering Journal, 39*(1), 164-176.

Gill, N. K., Appleton, M., Baganz, F., and Lye, G. J. (2008b). Quantification of power consumption and oxygen transfer characteristics of a stirred miniature bioreactor for predictive fermentation scale-up. *Biotechnology and Bioengineering, 100*(6), 1144-1155.

Girard, P., Jordan, M., Tsao, M., and Wurm, F. M. (2001). Small-scale bioreactor system for process development and optimization. *Biochemical Engineering Journal, 7*(2), 117-119.

Glacken, M. W., Fleischaker, R. J., and Sinskey, A. J. (1983). Large-scale Production of Mammalian Cells and Their Products: Engineering Principles and Barriers to Scale-up. *Annals of the New York Academy of Sciences, 413*(1), 355-372.

Godoy-Silva, R., Berdugo, C., and Chalmers, J. J. (2010). Aeration, mixing, and hydrodynamics, animal cell bioreactors. *Encyclopedia of Industrial Biotechnology*.

Gray, D., Chen, S., Howarth, W., Inlow, D., and Maiorella, B. (1996). CO2 in large-scale and high-density CHO cell perfusion culture. *Cytotechnology, 22*(1-3), 65-78.

Griffin, T. J., Seth, G., Xie, H., Bandhakavi, S., and Hu, W.-S. (2007). Advancing mammalian cell culture engineering using genome-scale technologies. *Trends in Biotechnology*, 25, (9), pp. 401-408.

Harms, P., Kostov, Y., French, J. A., et al. (2006). Design and performance of a 24-station high throughput microbioreactor. *Biotechnology and Bioengineering, 93*(1), 6-13.

Heath, C., and Kiss, R. (2007). Cell culture process development: advances in process engineering. *Biotechnology Progress, 23*(1), 46-51.

Hegde, S., Pant, T., Pradhan, K., Badiger, M., and Gadgil, M. (2012). Controlled release of nutrients to mammalian cells cultured in shake flasks. *Biotechnology Progress, 28*(1), 188-195.

Hermann, R., Lehmann, M., and Büchs, J. (2003). Characterization of gas–liquid mass transfer phenomena in microtiter plates. *Biotechnology and Bioengineering, 81*(2), 178-186.

Hu, W.-S., and Aunins, J. G. (1997). Large-scale mammalian cell culture. *Current Opinion in Biotechnology, 8*(2), 148-153.

Huang, Y. M., Hu, W., Rustandi, E., Chang, K., Yusuf-Makagiansar, H., and Ryll, T. (2010). Maximizing productivity of CHO cell-based fed-batch culture using chemically defined media conditions and typical manufacturing equipment. *Biotechnology Progress, 26*(5), 1400-1410.

Janeway, C. A. (2001). *Immunobiology : the immune system in health and disease*. (New York): Garland Publishing.

Jayapal, K. P., Wlaschin, K. F., Hu, W., and Yap, M. G. S. (2007). Recombinant protein therapeutics from CHO cells-20 years and counting. *Chemical Engineering Progress*, 103, pp. 40-47.

Jefferis, R. (2007). Antibody therapeutics. *Expert Opinion on Biological Therapy, 7*(9), 1401-1413.

Jeude, M., Dittrich, B., Niederschulte, H., et al. (2006). Fed-batch mode in shake flasks by slow-release technique. *Biotechnology and Bioengineering, 95*, 433 - 445.

Jones. S. D., Castillo, F. J., and Levine, H. L. (2007). Advances in the development of therapeutic monoclonal antibodies. *BioPharm International, 20*(10).

Kelley, B. (2007). Very Large Scale Monoclonal Antibody Purification: The Case for Conventional Unit Operations. *Biotechnology Progress, 23*(5), 995-1008.

Kensy, F., John, G. T., Hofmann, B., and Büchs, J. (2005). Characterisation of operation conditions and online monitoring of physiological culture parameters in shaken 24-well microtiter plates. *Bioprocess and Biosystems Engineering, 28*(2), 75-81.

Kimura, R., and Miller, W. M. (1997). Glycosylation of CHO-Derived Recombinant tPA Produced under Elevated pCO2. *Biotechnology Progress, 13*(3), 311-317.

Kumar, S., Wittmann, C., and Heinzle, E. (2004). Review: Minibioreactors. *Biotechnology Letters, 26*(1), 1-10.

Kuwae, S., Ohda, T., Tamashima, H., Miki, H., & Kobayashi, K. (2005). Development of a fed-batch culture process for enhanced production of recombinant human antithrombin by Chinese hamster ovary cells. *Journal of Bioscience and Bioengineering, 100*(5), 502-510.

Lamping, S., Zhang, H., Allen, B., and Ayazi Shamlou, P. (2003). Design of a prototype miniature bioreactor for high throughput automated bioprocessing. *Chemical Engineering Science, 58*, 747 - 758.

Lao, M. S., and Toth, D. (1997). Effects of ammonium and lactate on growth and metabolism of a recombinant Chinese hamster ovary cell culture. *Biotechnology Progress, 13*(5), 688-691.

Li, F., Vijayasankaran, N., Shen, A., Kiss, R., and Amanullah, A. (2010). Cell culture processes for monoclonal antibody production. *mAbs, 2*(5), 466-479.

Li, J., Wong, C. L., Vijayasankaran, N., Hudson, T., and Amanullah, A. (2012). Feeding lactate for CHO cell culture processes: Impact on culture metabolism and performance. *Biotechnology and Bioengineering, 109*(5), 1173-1186.

Lu, F., Toh, P. C., Burnett, I., et al. (2013). Automated dynamic fed-batch process and media optimization for high productivity cell culture process development. *Biotechnology and Bioengineering, 110*(1), 191-205.

Lye, G. J., Ayazi-Shamlou, P., Baganz, F., Dalby, P. A., and Woodley, J. M. (2003). Accelerated design of bioconversion processes using automated microscale processing techniques. *Trends in Biotechnology, 21*(1), 29-37.

Maier, U., and Buchs, J. (2001). Characterisation of the gas-liquid mass transfer in shaking bioreactors. *Biochemical Engineering Journal, 7*, 99 - 106.

Manns, R. L. (2003). Necessity is the mother of invention: the history of microplates. *Future Drug Discovery, 2003*, 108-112.

Marks, D. (2003). Equipment design considerations for large scale cell culture. *Cytotechnology, 42*(1), 21-33.

Matasci, M., Hacker, D. L., Baldi, L., and Wurm, F. M. (2008). Recombinant therapeutic protein production in cultivated mammalian cells: current status and future prospects. *Drug Discovery Today: Technologies, 5*(2–3), e37-e42.

Micheletti, M., Barrett, T., Doig, S. D., et al. (2006). Fluid mixing in shaken bioreactors: Implications for scale-up predictions from microlitre-scale microbial and mammalian cell cultures. *Chemical Engineering Science, 61*(9), 2939-2949.

Micheletti, M., and Lye, G. J. (2006). Microscale bioprocess optimisation. *Current Opinion in Biotechnology, 17*(6), 611-618.

Mirro, R., and Voll, K. (2009). Which impeller is right for your cell line. *BioProcess Int, 7*(1), 52-58.

Mulukutla, B. C., Yongky, A., Grimm, S., Daoutidis, P., and Hu, W.S. (2015). Multiplicity of Steady States in Glycolysis and Shift of Metabolic State in Cultured Mammalian Cells. *PLoS ONE, 10*(3), e0121561.

Nealon, A. J., O'Kennedy, R. D., Titchener-Hooker, N. J., and Lye, G. J. (2006). Quantification and prediction of jet macro-mixing times in static microwell plates. *Chemical Engineering Science, 61*(15), 4860-4870.

Nienow, A. W., Edwards, M. F., and Harnby, N. (1997). Mixing in the process industries. *Butterworth-Heinemann*.

Nienow, A. (1998). Hydrodynamics of stirred bioreactors. *Applied Mechanics Reviews, 51*(1), 3-32.

Nienow, A. (2006). Reactor Engineering in Large Scale Animal Cell Culture. *Cytotechnology, 50*(1), 9-33.

Nienow, A. (2015). Mass Transfer and Mixing Across the Scales in Animal Cell Culture. In Al-Rubeai, M. (Ed.), *Animal Cell Culture* (Vol. 9, pp. 137-167): Springer International Publishing.

Ozturk, S. S., and Palsson, B. O. (1991). Growth, metabolic, and antibody production kinetics of hybridoma cell culture: 2. Effects of serum concentration, dissolved oxygen concentration, and medium pH in a batch reactor. *Biotechnology Progress, 7*(6), 481-494.

Panula-Perala, J., Siurkus, J., Vasala, A., Wilmanowski, R., Casteleijn, M., and Neubauer, P. (2008). Enzyme controlled glucose auto-delivery for high cell density cultivations in microplates and shake flasks. *Microbial Cell Factories, 7*, 31.

Paredes, C., Prats, E., Cairo, J. J., Azorin, F., Cornudella, L., & Godia, F. (1999). Modification of glucose and glutamine metabolism in hybridoma cells through metabolic engineering. *Cytotechnology*, *30*(1-3), 85-93.

Puck, T. (1985). Development of the Chinese hamster ovary (CHO) cell for use in somatic cell genetics. *Molecular cell genetics*, 37-64.

Puskeiler, R., Kaufmann, K., and Weuster-Botz, D. (2005). Development, parallelization, and automation of a gas-inducing milliliter-scale bioreactor for high-throughput bioprocess design (HTBD). *Biotechnology and Bioengineering, 89*, 512 - 523.

Quek, L.F., Dietmair, S., Kromer, J.O., Nielsen, L.K. (2010). Metabolic flux anaylsis in mammalian cell culture. *Metabolic Engineering*, 12(2), 161-171.

Sheikh, K., Förster, J., and Nielsen, L. K. (2005). Modeling Hybridoma Cell Metabolism Using a Generic Genome-Scale Metabolic Model of Mus musculus. *Biotechnology Progress*, *21*(1), 112-121.

Schröder, M., Matischak, K., & Friedl, P. (2004). Serum-and protein-free media formulations for the Chinese hamster ovary cell line DUKXB11. *Journal of Biotechnology*, *108*(3), 279-292.

Shukla, A. A., and Thömmes, J. (2010). Recent advances in large-scale production of monoclonal antibodies and related proteins. *Trends in Biotechnology, 28*(5), 253-261.

Shuler, M. L., and Kargi, F. (2002). *Bioprocess engineering*: Prentice Hall New York.

Silk, N. J., Denby, S., Lewis, G., et al. (2010). Fed-batch operation of an industrial cell culture process in shaken microwells. *Biotechnology Letters, 32*(1), 73-78.

Silk, N. J. (2014). *High throughput approaches to mammalian cell culture process development.* (Ph.D thesis), University College London.

Takagi, M., Hayashi, H., and Yoshida, T. (2000). The effect of osmolarity on metabolism and morphology in adhesion and suspension chinese hamster ovary cells producing tissue plasminogen activator. *Cytotechnology, 32*(3), 171-179.

Tissot, S., Farhat, M., Hacker, D. L., et al. (2010). Determination of a scale-up factor from mixing time studies in orbitally shaken bioreactors. *Biochemical Engineering Journal, 52*(2–3), 181-186.

Tsao, Y. S., Cardoso, A. G., Condon, R. G. G., et al. (2005). Monitoring Chinese hamster ovary cell culture by the analysis of glucose and lactate metabolism. *Journal of Biotechnology, 118*(3), 316-327.

Van't Riet, K. (1979). Review of measuring methods and results in nonviscous gas-liquid mass transfer in stirred vessels. *Industrial & Engineering Chemistry Process Design and Development, 18*(3), 357-364.

Varley, J., and Birch, J. (1999). Reactor design for large scale suspension animal cell culture. *Cytotechnology, 29*(3), 177-205.

Velez-Suberbie, M. L., Tarrant, R. D. R., Tait, A. S., Spencer, D. I. R., and Bracewell, D. G. (2013). Impact of aeration strategy on CHO cell performance during antibody production. *Biotechnology Progress, 29*(1), 116-126.

Velez Suberbie, L. (2013). *Characterisation of the Bioreactor Environment and its Effect on Mammalian Cell Performance in Suspension Culture during Antibody Production.* (Ph.D thesis), University College London.

Walsh, G. (2014). Biopharmaceutical benchmarks 2014. *Nature Biotechnology, 32*(10), 992-1000.

Warnock, J. N., and Al-Rubeai, M. (2006). Bioreactor systems for the production of biopharmaceuticals from animal cells. *Biotechnology and Applied Biochemistry, 45*(1), 1-12.

Wen, Y. (2009). *Microfluidic and microscale cell cultures for high-throughput cell-based assays and bioprocess development.* (Ph.D thesis), The Ohio State University.

Wise, W. (1951). The measurement of the aeration of culture media. *Journal of general microbiology, 5*(1), 167-177.

Wurm, F. M. (2004). Production of recombinant protein therapeutics in cultivated mammalian cells. *Nature Biotechnology, 22*(11), 1393-1398.

Xing, Z., Kenty, B. M., Li, Z. J., and Lee, S. S. (2009). Scale-up analysis for a CHO cell culture process in large-scale bioreactors. *Biotechnology and Bioengineering, 103*(4), 733-746.

Zeng, A. P., Hu, W. S., & Deckwer, W. D. (1998). Variation of stoichiometric ratios and their correlation for monitoring and control of animal cell cultures.*Biotechnology Progress, 14*(3), 434-441.

Zhang, H., Wang, W., Quan, C., and Fan, S. (2010). Engineering Considerations for Process Development in Mammalian Cell Cultivation. *Current Pharmaceutical Biotechnology, 11*(1), 103-112.

Zhou, W., Rehm, J., Europa, A., and Hu, W.-S. (1997). Alteration of mammalian cell metabolism by dynamic nutrient feeding. *Cytotechnology, 24*(2), 99-108.

Zhou, W., Rehm, J., and Hu, W.-S. (1995). High viable cell concentration fed-batch cultures of hybridoma cells through on-line nutrient feeding. *Biotechnology and Bioengineering, 46*(6), 579-587.

Zhu, M. M., Goyal, A., Rank, D. L., Gupta, S. K., Boom, T. V., and Lee, S. S. (2005). Effects of Elevated pCO2 and Osmolality on Growth of CHO Cells and Production of Antibody-Fusion Protein B1: A Case Study. *Biotechnology Progress, 21*(1), 70-77.

Zou, W., and Al-Rubeai, M. (2015). Understanding central carbon metabolism of rapidly proliferating mammalian cells based on analysis of key enzymatic activities in GS-CHO cell lines. *Biotechnology and Applied Biochemistry*, doi:10.1002/bab.1409.

Appendix

Appendix A1

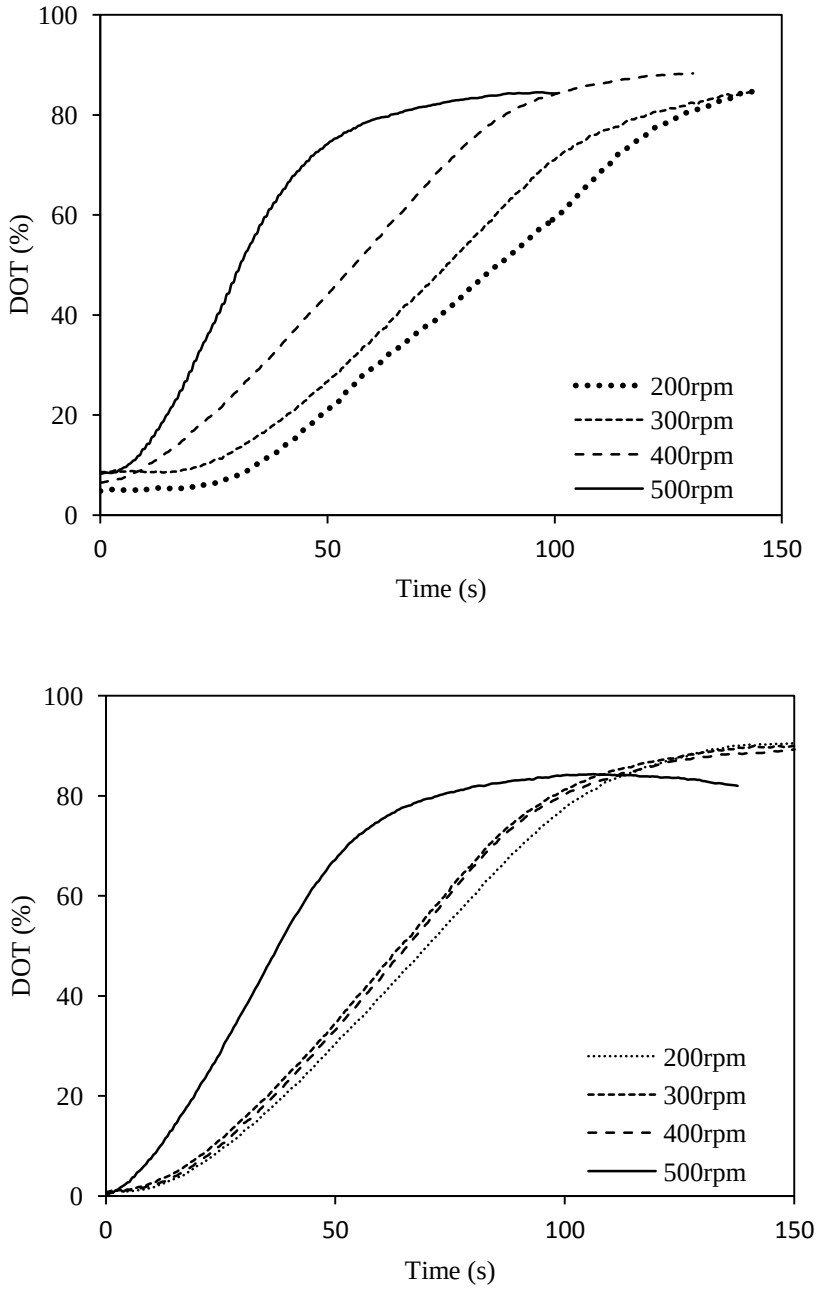

Figure A1: Effect of agitation rate on re-oxygenation of during static gassing out method in MBR with magnetic driven impeller for two different types of sparger A: singular hole sparger, B: horseshoe type sparger.

Appendix A2

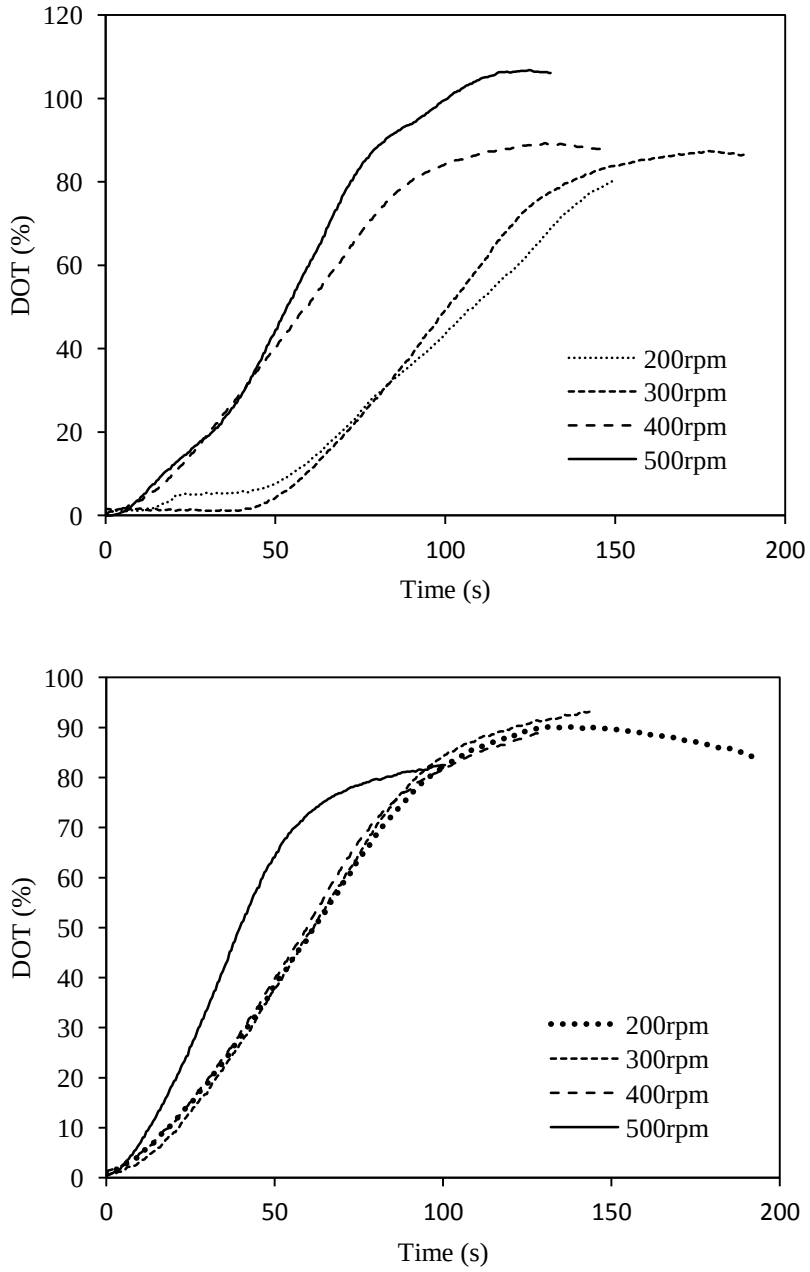

Figure A2: Effect of agitation rate on re-oxygenation of during static gassing out method in MBR for direct driven with two different types of sparger A: singular hole sparger, B: horseshoe type sparger.